SCUOLA NORMALE SUPERIORE

Classe di Scienze

Corso di perfezionamento in

Neuroscienze

32° ciclo

# *'SynActive' – a genetic toolbox to study the connectome and proteome of learning and memory-associated synapses*

Settore Scientifico Disciplinare BIO/09

Candidato
Ajesh Jacob

Relatori

Prof. Antonino Cattaneo

Dr. Marco Mainardi

Anno accademico 2022/23

# Contents

## ABSTRACT

Learning and memory correlate with activity-dependent synaptic plasticity processes at appropriate synaptic circuits. The underlying mechanisms of information storage in the brain are currently investigated at a whole-neuron scale to identify cellular memory engrams i.e., ensembles of neurons whose recruitment and activation are necessary and sufficient for the retrieval of a specific memory. Traditional methods for structural and functional analysis of synapses are not sufficient for investigating which subset of synapses encodes and stores a specific memory in a given neuron. To address this fundamental question, we have developed 'SynActive', a genetic toolbox exploiting regulatory sequences from the *Arc* mRNA and synapse-targeting peptides, that allows the expression of any protein of interest specifically at potentiated synapses. Here I have extended the SynActive toolbox to express the protein of interest, including fluorescent reporters, an affinity purification tag, and an optogenetic actuator specifically at *in vitro* and *in vivo* potentiated spines.

In SynActive-eGRASP, which allows input-specific labeling of potentiated synapses, one split-GFP fragment was expressed constitutively by presynaptic neurons, while the postsynaptic half was synthesized in an activity-dependent fashion at potentiated spines. After extensive validation in cultured neurons, SynActive-eGRASP was employed to map CA3-CA1 synapses potentiated during an associative memory task – contextual fear conditioning. Semi-automated analysis using a custom-made algorithm revealed a spatially nonuniform and clustered distribution of SynActive-eGRASP-positive synapses. SynActive controlled expression of fluorescent reporters- mVenus, and DsRED-E5 labeled dendritic spines undergoing potentiation in primary neuronal cultures. These optimized vectors should facilitate large-scale, possibly brain-wide as well as time-dependent, mapping of potentiated spines. For the proteomic profiling of *in vivo* potentiated spines, SynActive AAVs expressing FLAG-tagged PSD95 was delivered to the mouse hippocampus and the PSD95-interactome was immunoprecipitated from potentiated synapses after contextual fear conditioning. In primary neuronal cultures, photoactivation of channelrhodopsin expressed at potentiated spines via SynActive method induced neuronal spiking. In vivo, this construct can be used to tag memory-specific synapses, and optically activating them might induce memory retrieval.

These novel tools and the initial results they produced provide the first step towards a shift in the study of memory engrams from a cellular to a synaptic resolution. In addition, our quantitative maps of synaptic potentiation in whole brain areas or specific synaptic circuits can be used to refine computational models of neural plasticity. Ongoing experiments are aimed at performing a comparative analysis of synaptic maps obtained in different phases of memory encoding and recall, in both physiological conditions and models of neurodegenerative and neurodevelopmental diseases.

# 1 INTRODUCTION

## 1.1 In search of memory engrams – early attempts

Memory refers to the process by which experiences, and skills acquired by a living organism during its lifetime are encoded, stored, and later retrieved when required. Where and how distinct memories are encoded and stored in the brain is a fundamental question of neuroscience. Richard Semon in the early twentieth century introduced the term 'Engram' to describe the physical representation of memory. He defined engram as "*the enduring though primarily latent modification in the irritable substance produced by a stimulus*" (Semon, 1904, 1921). In other words, engram refers to the long-lasting change that occurs in the brain in response to an event or experience. An engram persists in a dormant state until awaken by re-exposure to parts of the original event i.e., to stimuli that were part of the original encoding set, by a process of "memory retrieval", defined as "ecphory" by Semon (Semon, 1904, 1921).

Even though the engram notion gave a theoretical foundation to the physical nature of memory, proving its existence experimentally has been extremely difficult. In the 1920s, Karl Lashley trained rats in maze navigation tasks to find a food reward and tested for the maze-route memory after ablating portions of cortical area (Lashley, 1963). He hypothesized that if the ablated cortical area contained the engram for maze-route memory, the rats would show performance deficits in the maze upon testing. In contrast with this hypothesis, the performance in the maze only correlated with the amount of cortical tissue removed but not with the location of the lesion (Lashley, 1963). After more than 30 years of research, Lashley concluded that engrams are not localized to a discrete cortical region but rather distributed.

The initial evidence for the existence of engrams was put forward by Scoville and Milner, based on their studies on the patient known to the scientific community as H.M. (Scoville and Milner, 1957). H.M. had suffered from epileptic seizures due to brain damage caused by an accident that occurred in his childhood. To treat his epileptic seizures Scoville surgically removed the medial temporal lobe, which includes the hippocampus. After surgery H.M. recovered from the seizures but was left with severe memory deficits. He failed to form new memories (anterograde amnesia) and was able to recall only distant memories, not recent experiences (graded retrograde amnesia) (Scoville and Milner, 1957). Thus, the case of H.M. provided the first clear

link between memory and the hippocampus. Although H. M's episodic memories were compromised, he retained the ability to learn new motor skills (Scoville and Milner, 1957). Around the same period, neurosurgeon Wilder Penfield serendipitously managed to artificially retrieve an episodic memory in a patient. While performing focal electrical stimulation as a pre-surgery procedure for the removal of an epileptic focus, he observed that stimulating the lateral temporal lobe triggered a vivid recall of random episodic memories in patients (Penfield and Perot, 1963). This provided the first empirical evidence for the notion that the engram for memory is localized in a specific brain region and artificial stimulation of the same brain region was sufficient to reactivate the engram(s) it contained, thus eliciting memory retrieval of the associated memory(ies).

Lashley's studies failed to find the engram likely due to two reasons: i) choice of the memory task and brain area - learning a maze is a complex behavior task that might involve many brain regions and therefore ablation of a single brain area such as cortex is not enough for disrupting the memory; ii) technique for ablation – the thermocautery method used for the ablation was not precise and produced unintended damage to nearby brain areas (Josselyn et al., 2017). Indeed, relooking at the results of Lashley's experiments revealed that in addition to cortical lesions, 21 out of 37 experimental subjects also sustained hippocampal lesions (Milner, 1999). The extent of hippocampal damage in these rats correlated with the size of the lesions on their cortex (Milner, 1999). Likely, the maze-route memory defects observed by Lashley in animals with greater cortical lesions might have occurred due to the ablation of engrams in the hippocampal regions (Josselyn et al., 2017). Indeed, a study by Morris *et al*. had shown that spatial memory was impaired in rats with hippocampal lesions (Morris *et al.*, 1982).

## 1.2 Synaptic plasticity and its role in supporting learning and memory

The idea that learning modifies the strength of connections between neurons was first articulated by Ramon y Cajal in 1894, based on his neuronal anatomical studies (Cajal, 1894). Later, in the mid-twentieth century, Donald Hebb refined this idea into a theoretical model of the functional mechanism of learning. He proposed that synaptic connections between neurons simultaneously activated during learning (called 'cell assemblies' by Hebb) are strengthened to encode the informational content in the brain (Hebb, 1949).

### 1.2.1 Long-term potentiation

The involvement of the activity-dependent modification of the efficiency or strength of synaptic transmission (synaptic plasticity) in learning and memory gained more support when Bliss and Lomo discovered Long-term potentiation (LTP) in the mammalian hippocampus (Bliss and Lømo, 1973). They found that high-frequency (100 Hz for 3-4 s) stimulation (HFS) of perforant path (PP) fibers from the entorhinal cortex (EC) to the dentate gyrus (DG) of the hippocampus produced a rapid and long-lasting increase in the synaptic strength (measured as increased amplitude of both excitatory postsynaptic potentials (EPSPs) and population spike) for periods ranging from 30 min to 10 h. Since its discovery in anaesthetized rabbits, LTP has been found in freely moving animals as well as in hippocampal slices *in vitro* (Bliss and Gardner-Medwin, 1973; Bliss and Collingridge, 1993). In the following sections, (i) what happens during the LTP triggering stimulations, referred to as the induction, and (ii) how are the synapses altered following LTP-induction, i.e., expression, are described using the best-characterized N-methy-D-aspartate receptor (NMDAR)-dependent LTP that occur between CA3 and CA1 pyramidal neurons in the hippocampus.

#### 1.2.1.1 Induction of LTP

The conventional way of inducing LTP is by delivering tetanus (a train of 50-100 stimuli at 100 Hz) to the pathway of interest. In a more physiologically relevant and efficient protocol, theta-burst stimulation (TBS) - several bursts of 4 stimuli at 100 Hz are delivered at an interburst interval of 200 ms, similar to the synchronized firing patterns that occur in the hippocampus during learning (Otto *et al.*, 1991; Bliss and Collingridge, 1993). A weak stimulation (stimulus of low intensity and/or duration), in which only a few afferent fibres were activated, failed to trigger the potentiation indicating the existence of a threshold for LTP-induction and cooperative property of LTP (Figure 4.2a) (McNaughton et al., 1978). However, a weak input can be potentiated if simultaneous tetanus was given in a separate but convergent input – associativity (Figure 4.2a) (Levy and Steward, 1979). LTP is input-specific because the potentiation was induced only in the tetanized pathway; not in the non-activated inputs (Figure 4.2a) (Levy and Steward, 1979). These three properties established LTP as a Hebbian process and can be explained by the two requirements for LTP induction: synaptic stimulation and sufficient depolarization in the postsynaptic neuron at the same time. This induction rule was based on two observations: (i) low

frequency (1 Hz) stimulation (LFS), normally insufficient to potentiate synapses, could produce robust LTP when paired with depolarizing currents injected into the postsynaptic neuron through an intracellular recording electrode; and (ii) preventing depolarization by voltage clamping or hyperpolarizing the postsynaptic neuron blocked the LTP induction by tetanus (Nicoll, 2017).

The neurotransmitter and receptor involved in the LTP induction were determined using highly selective receptor antagonists and agonists. A single stimulus (or normal synaptic transmission) evokes an EPSP mediated by glutamate (neurotransmitter) acting on ionotropic α-amino-3-hydroxy-5-methyl-4-isoxazole propionate receptors (AMPARs) (Figure 4.2b), which can be blocked by antagonists such as 6-cyano-7-nitroquinoxaline-2,3-dione (CNQX) (Bliss and Collingridge, 1993). The other type of glutamate receptor, NMDARs are expressed on the synapses but does not contribute to the normal synaptic response due to the receptor pore blockage by extracellular $Mg^{2+}$ (Figure 4.2b) (Mayer et al., 1984; Nowak et al., 1984). However, they are involved in the induction of LTP, because the application of NMDAR antagonist 2-amino-5-phosphonovaleric acid (AP5) blocked LTP (Collingridge et al., 1983). NMDARs act as molecular coincidence detectors. They are opened to conduct $Ca^{2+}$ only when the postsynaptic membrane is adequately depolarized to expel $Mg^{2+}$ from the channels and at the same time glutamate is available to bind to the receptor (Figure 4.2b) (Mayer et al., 1984; Nowak et al., 1984; Bliss and Collingridge, 1993). Tetanus induces LTP by activating NMDARs (Bliss and Collingridge, 1993). EPSPs mediated by AMPARs (followed by NMDARs) are summated to maintain neuronal depolarization during tetanus (Figure 4.2b) (Bliss and Collingridge, 1993). LTP properties – cooperativity, associativity, and input-specificity can now be explained based on the characteristics of NMDAR. In contrast to tetanus, a weak stimulation does not produce enough depolarization (cooperativity threshold) to remove the $Mg^{2+}$ block and thus fails to induce LTP (Bliss and Collingridge, 1993). Depolarization can spread from a tetanized synapse into its neighboring synapses to enhance the unblocking of NMDARs, which in turn can result in LTP-induction with a weak stimulation (associativity) (Bliss and Collingridge, 1993). The requirement of presynaptic activity for a sufficient concentration of glutamate makes the LTP input-specific (Bliss and Collingridge, 1993).

In an early study, it was found that postsynaptic injection of the $Ca^{2+}$ chelator ethylene glycol tetraacetic acid (EGTA) prevents LTP (Lynch *et al.*, 1983). Unlike AMPARs, NMDARs are $Ca^{2+}$ permeable and their activation during tetanus provided the $Ca^{2+}$ necessary for the induction of LTP

(please see section 1.2.4 for the molecular mechanism) (MacDermott *et al.*, 1986; Ascher and Nowak, 1988).

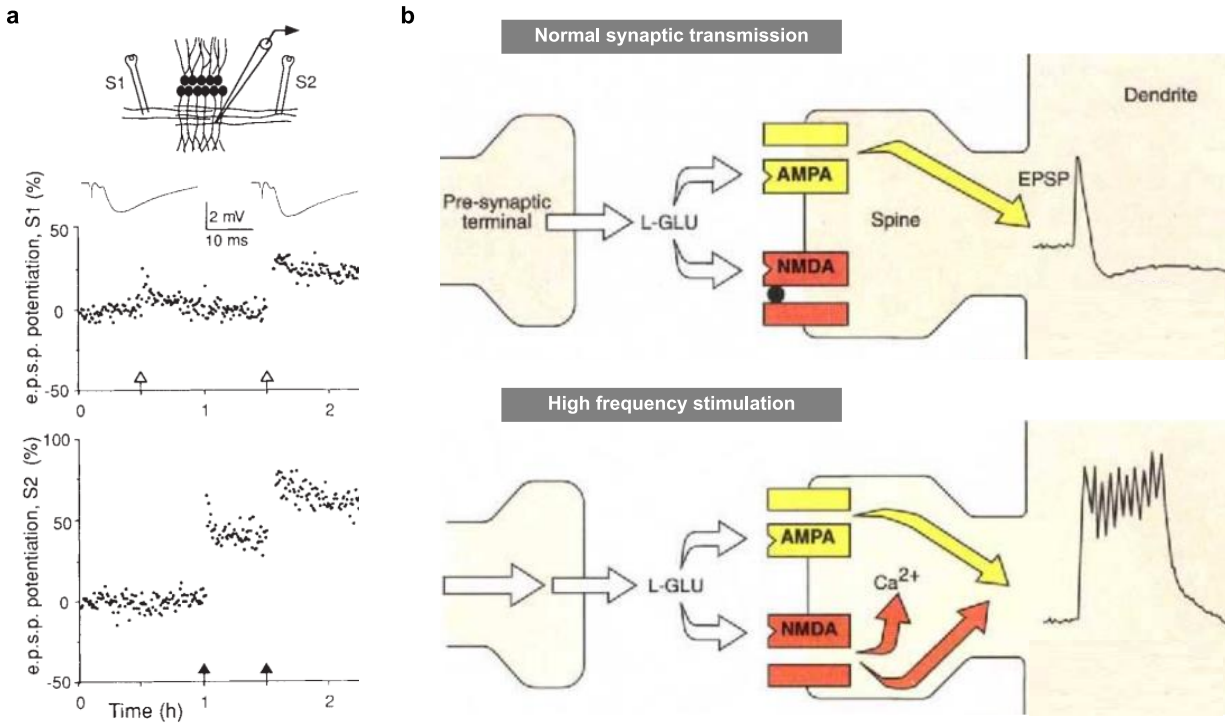


**Figure 1.1 Induction of long-term potentiation.**

(**a**) Demonstration of the properties of long-term potentiation (LTP): cooperativity, input-specificity, and associativity. Pathway S1 receives weak stimulation (open arrows); intensity below the cooperativity threshold for LTP. Strong tetanus (filled arrow) induces LTP in pathway S2, but not in S1. Weak stimulation produces LTP in pathway S1 when paired with strong tetanus in pathway S2. (**b**) During normal synaptic transmission, excitatory postsynaptic potentials EPSPs are mediated by AMPARs and not by NMDARs due to the $Mg^{2+}$ block (*top*). Sustained postsynaptic depolarization by high- frequency stimulation relieves the $Mg^{2+}$ block and permits $Ca^{2+}$ influx through NMDARs (*bottom*). (Adapted from Bliss and Collingridge, 1993).

### 1.2.1.2 Expression of LTP

Dependence on NMDARs made it clear that LTP is induced postsynaptically (Collingridge et al., 1983; MacDermott et al., 1986; Ascher and Nowak, 1988). However, there was a long debate on the site of LTP expression, whether it is a change in postsynaptic sensitivity to glutamate or a change in presynaptic glutamate release. Two important papers published in 1988 highlighted the postsynaptic expression of NMDAR-dependent LTP (Kauer et al., 1988; Muller et al., 1988). By electrophysiological recordings in the presence of glutamate receptor antagonists, they have revealed a selective increase in the AMPAR component of the EPSPs following LTP. Although

NMDARs were required for the induction of LTP, the NMDAR component of the EPSPs was of comparable size in control and potentiated synapses (Kauer et al., 1988; Muller et al., 1988). Almost all subsequent electrophysiological studies confirmed that the enhancement of synaptic transmission associated with LTP is primarily expressed postsynaptically as an increase in AMPAR currents (Nicoll, 2017). The identification of silent synapses in the hippocampus further supported the postsynaptic expression of LTP (Isaac et al., 1995; Liao et al., 1995). Silent synapses are synapses with no functional AMPARs but with NMDARs and can be unsilenced by the insertion of AMPARs during LTP.

LTP expression can be classified into two phases – early phase LTP (E-LTP) and late phase LTP (L-LTP), based on their dependence on protein synthesis (Reymann and Frey, 2007). E-LTP that lasts 1-2 h after the induction of LTP is independent of protein synthesis and relies on existing proteins (Krug et al., 1984; Otani and Abraham, 1989; Frey et al., 1996). However, *de novo* synthesis of mRNAs and proteins is required for the maintenance of LTP beyond a few hours, commonly referred to as late-LTP (L-LTP) (Reymann and Frey, 2007). Protein and mRNA synthesis inhibition using anisomycin and actinomycin D, respectively, impairs L-LTP in the hippocampal slices (Krug et al., 1984; Otani and Abraham, 1989; Frey et al., 1996). (Please see section 1.2.4 for the molecular mechanism of E-LTP and L-LTP).

### 1.2.2 Long-term depression

Long-term depression (LTD) is the counterpart of LTP and is characterized by a long-lasting decrease in synaptic strength. Low-frequency stimulation (LFS, 1 Hz), which activates the postsynaptic neuron below the threshold for LTP, induces LTD in the CA3-CA1 synapses (Dudek and Bear, 1992). Inhibition of NMDARs by AP5 blocked LTD, indicating dependence on NMDARs for LTD induction (Dudek and Bear, 1992). Activation of metabotropic glutamate receptors (mGluRs) by LFS or by the application of mGluR agonist 3,5-dihydroxyphenylglycine (DHPG) can also induce LTD at CA3-CA1 synapses (Collingridge *et al.*, 2010). LTD is mainly expressed postsynaptically as a decrease in AMPAR-mediated synaptic transmission (Collingridge *et al.*, 2010). Anisomycin inhibits the long-term maintenance of LTD (Manahan-Vaughan et al., 2000; Sajikumar and Frey, 2003). This indicates that, like LTP, LTD also has two phases: protein synthesis-independent early-LTD (E-LTD) that lasts up to 3-4 h and de novo protein synthesis-dependent late-LTD (L-LTD) that lasts at least 8h (Sajikumar and Frey, 2003).

### 1.2.3 Structural plasticity

Functional changes in synaptic plasticity are often accompanied by activity-dependent structural remodeling (Figure 1.2b). Modern imaging techniques have made it possible to identify alterations in the morphology and density of dendritic spines following LTP and LTD. Focal induction of potentiation by glutamate uncaging (light-induced repetitive release of caged glutamate, MNI (4-methoxy-7-nitroindolinyl)-glutamate) or by local superfusion of glutamate, induce a rapid and persistent enlargement of stimulated spines (Engert and Bonhoeffer, 1999; Matsuzaki *et al.*, 2004; Govindarajan *et al.*, 2011). AMPAR-mediated synaptic transmission was enhanced in these enlarged spines (Engert and Bonhoeffer, 1999; Matsuzaki *et al.*, 2004; Govindarajan *et al.*, 2011). Indicating input-specificity, unstimulated neighboring spines did not show any structural and functional modifications. At the ultrastructural level, analyzed using electron microscopy, potentiated spines display larger postsynaptic densities (PSDs) and often contain smooth endoplasmic reticulum and polyribosomes (Toni *et al.*, 1999; Harris, 2020). In addition to these spine-specific structural alterations, LTP induces the growth of new spines or filopodia, leading to an increase in spine density (Figure 1.2b) (Engert and Bonhoeffer, 1999; Maletic-Savatic et al., 1999; De Roo et al., 2008). Repetitive confocal imaging reveals selective long-term stabilization of potentiated spines and preferential growth of new spines close to potentiated spines (De Roo et al., 2008). Conversely, LTD-inducing stimulation results in the shrinkage or retraction of the dendritic spines (Figure 1.2b) (Nägerl et al., 2004; Zhou et al., 2004). Although synaptic plasticity-associated structural changes can be observed within a few minutes after the inducing stimulus, its long-term maintenance requires the synthesis of new proteins (Govindarajan *et al.*, 2011). (please see also section 1.2.4 and 1.4).

### 1.2.4 Molecular mechanism of synaptic plasticity

The $Ca^{2+}$ entered through NMDARs during LTP induction triggers a cascade of signaling events that ultimately leads to AMPAR-mediated enhanced synaptic transmission and/or enlargement of dendritic spines. Ca2+ activates calcium/calmodulin-dependent protein kinase II (CaMKII), which is necessary and sufficient for the expression of LTP (Lisman et al., 2012). During E-LTP, activated CaMKII enhances AMPAR-mediated synaptic currents through two processes. First, phosphorylation of AMPAR subunit GluA1 at S831 to increase the average single channel conductance of AMPARs (Figure 1.2a) (Derkach et al., 1999). Second, increase in the

exposure of AMPARs on the synaptic surface (Figure 1.2a) (Kopec *et al.*, 2006; Makino and Malinow, 2009). After LTP induction, CaMKII triggers the insertion of AMPARs at the extrasynaptic membrane, which is then captured at the synapses through the interaction between PSD95 and AMPAR-binding protein stargazin (phosphorylated by CaMKII during LTP) (Makino and Malinow, 2009; Opazo et al., 2010; Lisman et al., 2012). In contrast to LTP, a modest amount of $Ca^{2+}$ entered during NMDAR-dependent LTD activates calcineurin (a protein phosphatase), because of its higher affinity for calcium/calmodulin than CaMKII (Figure 1.2a) (Mulkey et al., 1993; Collingridge et al., 2010). Calcineurin promotes the activation of protein phosphatase 1 (PP1) that dephosphorylates GluA1 at S845 and leads to LTD (Collingridge *et al.*, 2010). In addition, other $Ca^{2+}$-sensitive enzymes activated during LTD trigger the clathrin-mediated endocytosis of AMPARs (Figure 1.2a) (Collingridge *et al.*, 2010). Enlargement of dendritic spines during LTP is associated with the reorganization of the actin cytoskeleton (Fukazawa *et al.*, 2003). Phosphorylation of cofilin promotes F-actin polymerization and is dependent on the activity-dependent expression of Arc (activity-regulated cytoskeleton-associated protein) (Messaoudi *et al.*, 2007).

#### 1.2.4.1 Activity-dependent local translation

Proteins required for the long-term maintenance of LTP are both synthesized locally in the dendritic segments containing stimulated spines and in the somatic compartment. The first evidence for the local translation came from the discovery of polyribosome complexes localized preferentially at the base of the dendritic spines (Steward and Levy, 1982). Subsequent studies have identified more than 30 distinct dendritically localized mRNAs (Steward and Schuman, 2003). Synaptic activation facilitates the transport of mRNAs for activity-regulated cytoskeleton-associated protein (Arc) (please see also section 1.2.5.1 and Figure 1.3), brain-derived neurotrophic factor (BDNF), and tyrosine kinase receptor B (TrkB) into dendrites (Tongiorgi et al., 1997; Steward et al., 1998). mRNAs transported in RNA granules are then released from translation inhibition at stimulated spines (Sutton and Schuman, 2005). The ERK (extracellular signal-regulated kinase)/MAPK (mitogen-activated protein kinase) and PI3K (phosphatidylinositol 3-kinase) signal transduction pathways regulate the activity-dependent translation of dendritically localized mRNAs (Sutton and Schuman, 2005). mTOR (mammalian target of rapamycin) is a signaling molecule critical for the translation and its inhibition by rapamycin blocks L-LTP in the hippocampus (Cammalleri *et al.*, 2003).

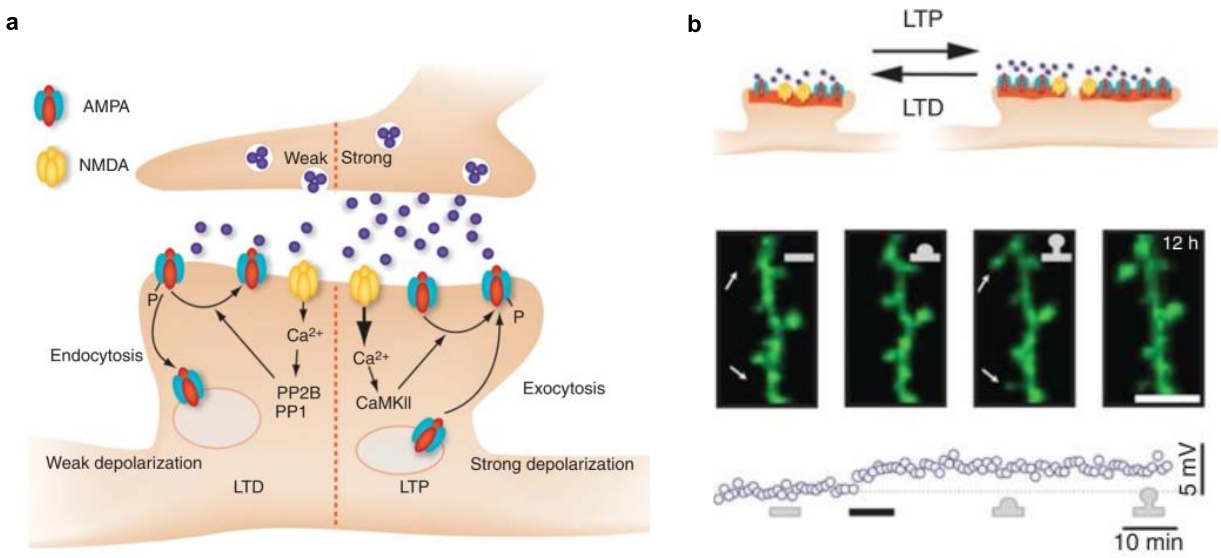


**Figure 1.2 Functional and structural changes associated with synaptic plasticity.**

(**a**) Expression of long-term depression (LTD): a modest amount of $Ca^{2+}$ entered through NMDARs during weak stimulation activates phosphatases that dephosphorylate AMPAR and promote the removal of synaptic AMPARs (*left*). Expression of LTP: strong stimulation activates calcium/calmodulin-dependent protein kinase II (CaMKII), to enhance AMPAR-mediated synaptic currents through phosphorylation of AMPAR and increase in the exposure of AMPARs on the synaptic surface (*right*). (**b**) LTP and LTD cause enlargement and shrinkage of spines, respectively (*top*). LTP promotes spinogenesis and synaptic strength correlates with spine volume (arrow, *bottom*). (Adapted from Luscher and Malenka, 2012).

#### 1.2.4.2 Activity-dependent transcription

LTP declines to baseline after 3 h in isolated dendrites, produced by surgically removing the cell body layer (Frey *et al.*, 1989). Inhibition of transcription using actinomycin D also results in L-LTP impairment (Frey *et al.*, 1996). These results indicate that local translation of pre-existing mRNAs is not sufficient for the long-term maintenance of LTP and require new gene expression. Transgenic animals with a non-functional mutant form of protein *kinase* A (PKA) and c-AMP (cyclic adenosine monophosphate) responsive element binding protein (CREB) show defects in L-LTP, but not in E-LTP (Bourtchuladze *et al.*, 1994; Abel *et al.*, 1997). Activation of PKA, MAPK, and CREB regulates the activity-dependent transcription during L-LTP (Baltaci et al., 2019). The biochemical cascade is as follows - cAMP produced in response to synaptic potentiation-inducing stimulus activates PKA, which in turn phosphorylates CREB (Baltaci et al., 2019). CREB (a transcription factor) binds to CRE (c-AMP responsive element) in the promoter region of their target genes and promotes their expression (please see also section 1.2.5). MAPK (activated by PKA or CaMKII) can also phosphorylate CREB (Baltaci et al., 2019).

#### 1.2.4.3 "Synaptic tagging and capture" (STC) hypothesis

Proteins and mRNAs produced in the cell body in response to synaptic potentiation act specifically at potentiated spines for the long-term expression of LTP. To explain how this is achieved, Frey and Morris came up with the "Synaptic tagging and capture" (STC) hypothesis (Frey and Morris, 1997, 1998; Redondo and Morris, 2011). According to the STC hypothesis, a strong tetanus results in two independent phenomena – setting a synaptic tag specifically at the stimulated synapse (protein synthesis-independent) and producing plasticity-related products (PRPs; protein synthesis-dependent). Only synapses that possess the synaptic tag can capture PRPs to convert E-LTP into L-LTP. Proteins and mRNAs produced in the soma after LTP-inducing stimulation are considered as PRPs.

### 1.2.5 Immediate early genes

Immediate early genes (IEGs) are a pool of genes that are transcribed immediately after the LTP-inducing stimulation (Lanahan and Worley, 1998). They encode for proteins critical for the long-lasting expression of synaptic plasticity and include transcription factors (c-Fos; zinc finger-containing transcription factor 268, zif268), postsynaptic proteins (Arc, also known as activity-regulated gene 3.1, Arg3.1; Homer1a), proteins involved in intracellular signaling (Ras homolog enriched in brain, Rheb), neurotrophins (BDNF), and membrane proteases (tissue-plasminogen activator, tPA) (Lanahan and Worley, 1998; Okuno, 2011). In the sections below, the regulation of IEG expression and function of IEG protein in synaptic plasticity are described using Arc and c-Fos as examples.

#### 1.2.5.1 Arc

The *Arc* mRNA is transcribed rapidly and transiently in neurons following LTP induction (Steward *et al.*, 1998). Two *cis*-acting genomic elements present in the promoter region regulate its activity-dependent transcription. At ~1.4 kb upstream of the transcription start site (TSS), an element consisting of a pair of serum response elements (SREs) that bind serum response factor (SRF) and a 'Zeste-like' factor response element (Figure 1.3) (Pintchovski *et al.*, 2009). A unique element of size 100 bp, termed synaptic activity response element (SARE), is present ~7 kb upstream of the TSS and is necessary and sufficient for the activity-dependent expression of *Arc* (Figure 1.3) (Kawashima *et al.*, 2013). SARE is a cluster of response elements that allow the

binding of the transcription factors CREB, SRF, and myocyte enhancer factor-2 (MEF2) (Kawashima *et al.*, 2013).

After transcription, *Arc* mRNAs are packed into messenger ribonucleoprotein (mRNP) particles and are transported (microtubule-based) to dendrites, a process mediated by two *cis*-acting dendritic targeting elements (DTE) in the *Arc* 3' untranslated region (UTR) and an 11-nucleotide heterogeneous nuclear ribonucleoprotein A2 response element (A2RE) within the Arc coding sequence (Figure 1.3) (Bramham *et al.*, 2010). Within dendrites, *Arc* mRNAs are docked (F-actin-dependent) at regions with recently activated synapses. LTP induction promotes the local translation of *Arc* mRNA through enhanced cap-dependent initiation complex formation, regulated by eukaryotic initiation factor 4E (eIF4E) (Figure 1.3) (Bramham *et al.*, 2010). In addition, cap-independent translation also occurs at internal ribosomal entry sites (IRES) located at the 5' UTR (Bramham *et al.*, 2010). Due to the presence of two introns in the 3' UTR, the *Arc* mRNA is rapidly degraded after translation by the nonsense-mediated RNA decay (NMD) process (Figure 1.3) (Bramham *et al.*, 2010).

Studies using Arc antisense oligodeoxynucleotides (Arc-AS) show that sustained synthesis of Arc (for at least 2-4hr after LTP induction) is necessary for the maintenance of LTP (Messaoudi *et al.*, 2007). L-LTP is accompanied by enlargement of the stimulated spines, which requires phosphorylated cofilin-mediated F-actin stabilization (Fukazawa *et al.*, 2003). Inhibition of Arc by Arc-AS reduces the cofilin phosphorylation and F-actin formation (Messaoudi *et al.*, 2007). Okuno et al. demonstrated that Arc synthesized in response to synaptic activation can be recruited to inactive synapses via interaction with the inactive form of CaMKIIβ - inverse synaptic tagging (Okuno *et al.*, 2012). In inactive synapses Arc promotes the removal of surface AMPARs, resulting in synaptic depression (Okuno *et al.*, 2012). Recently, Arc protein has been attributed to form virus-like capsids that can transfer *Arc* mRNA between neurons (Pastuzyn *et al.*, 2018).

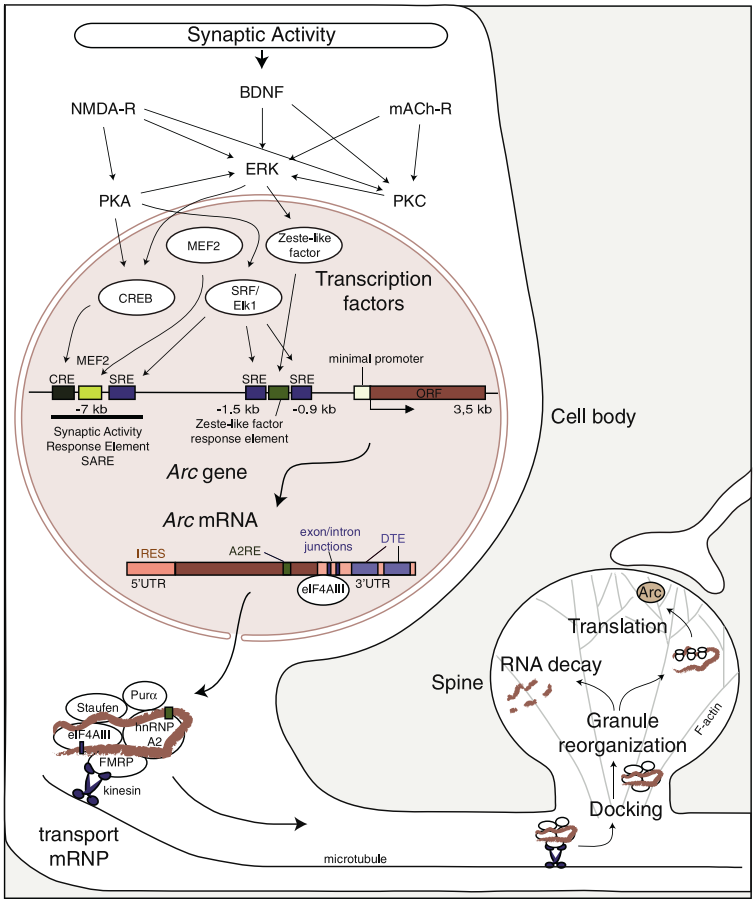


**Figure 1.3 Activity-dependent transcriptional and translational regulation of Arc.**

LTP-inducing stimulation activates the transcription factors CREB, MEF2, and SRF that bind to the regulatory elements in the promoter region to enhance the transcription of *Arc* mRNA. Regulatory elements in the 5' and 3' UTR mediate the dendritic transport and local translation of *Arc* mRNA at potentiated synapses. *Arc* mRNA is rapidly degraded after translation by the nonsense-mediated RNA decay (NMD) process. (Adapted from Bramham *et al.*, 2010).

### 1.2.5.2 c-Fos

The activity-dependent expression of the *c-fos* gene is regulated by two *cis*-acting genomic elements present within its 600-bp promoter sequence (Robertson *et al.*, 1995). A CRE element that binds to CREB, resides close to the TSS of the *c-fos* gene and another regulatory element SRE that binds to SRF is present 250bp upstream from the CRE. c-Fos proteins form heterodimers with Jun family proteins and bind to the activator protein 1 (AP-1) sites in the promoter region of downstream genes to regulate their expression (Okuno, 2011). Central nervous system (CNS) specific c-Fos knock-out (KO) mice display LTP impairment in the CA3-CA1 synapses (Fleischmann *et al.*, 2003).

### 1.2.6 LTP and memory are correlated

LTP possesses certain features that make it a plausible mechanism for learning: i) specificity, LTP is induced only at synapses that are activated by HFS; non-activated neighboring synapses are not potentiated (Levy and Steward, 1979; Govindarajan *et al.*, 2011; Nicoll, 2017); ii) cooperativity, simultaneous activation of multiple inputs are required to produce postsynaptic depolarization sufficient for LTP induction (McNaughton et al., 1978; Govindarajan et al., 2011; Nicoll, 2017); iii) associativity, a weak input, normally insufficient to induce LTP, can potentiate a synapse when paired with a strong input (Levy and Steward, 1979; Govindarajan *et al.*, 2011; Nicoll, 2017). These features are mostly attributed to the behavior of NMDAR, whose activation is dependent on the presence of the ligand glutamate (released by presynaptic activity) as well as the depolarization of the postsynaptic neuron (Nicoll, 2017). Thus, LTP followed the Hebbian plasticity condition.

Since most LTP studies *in vitro* and *in vivo* were based on artificial stimulation of neural tissue, it was not known whether LTP is a physiological phenomenon, and animals used such synaptic plasticity mechanisms for learning and memory. In an initial study, it was found that aged animals displayed deficits in the retention of spatial memory, with a corresponding rapid decay of LTP in the hippocampal synapses (Barnes and McNaughton, 1985). Following this correlational study, Morris et. al provided the first evidence for the causal link between physiological and behavioral changes, by showing that blockade of LTP induction using NMDAR agonist D-AP5, selectively impaired spatial learning in Morris watermaze (MWM) (Box 1.1) (Figure 1.4a) (Morris *et al.*, 1986). Supporting the pharmacological results, targeted genetic ablation of the NMDAR in the CA1 region led to the loss of LTP in the CA3-CA1 synapses and produced severe deficits in spatial learning and contextual fear conditioning (CFC) (Box 1.1) (Tsien et al., 1996; Rampon et al., 2000).

In addition to the experiments described above that interfered with LTP induction, several transgenic mouse lines were created to determine whether disruption of LTP expression affects the acquisition and/or retention of memory. CaMKII is critical for the expression of LTP (Lisman et al., 2012). Mutant mice with no expression of αCaMKII exhibited LTP deficits in the hippocampus and spatial learning impairments in MWM (Silva et al., 1992a, 1992b). Similarly, protein synthesis inhibition by anisomycin (Figure 1.4b), or genetic manipulation to inhibit the activity of plasticity-

related proteins, such as PKA, CREB, Arc, and c-Fos, disrupted L-LTP and caused deficits in spatial and fear memory (Figure 1.4b) (Bourtchuladze *et al.*, 1994; Abel *et al.*, 1997; Fleischmann *et al.*, 2003; Plath *et al.*, 2006).

Not all studies supported the existence of a causal link between synaptic plasticity and memory. In some experiments, animals with significant LTP deficits in the hippocampus exhibited intact hippocampus-dependent memory. Animals displayed only a subtle difference in behavior performance when NMDARs were deleted specifically in CA3 or dentate gyrus (Nakazawa *et al.*, 2002; McHugh *et al.*, 2007). Insertion of AMPARs into the synaptic membrane is critical for the increased synaptic transmission associated with LTP (Nicoll, 2017). Whole brain deletion of AMPAR subunit GluA1 caused deficits in LTP at CA3-CA1 synapses (Reisel *et al.*, 2002). However, these animals displayed normal spatial learning and memory apart from impaired short-term working memory (Reisel *et al.*, 2002).

In an alternative approach, LTP was induced by HFS to the saturation point (the state at which synapses cannot be potentiated further by HFS), prior to the onset of behavior training. This should impair learning since the synapses are already saturated and cannot undergo a further round of learning-induced potentiation. Repeated high-frequency stimulation of the perforant path saturated LTP in the DG and impaired spatial learning in Barnes maze and MWM (McNaughton *et al.*, 1986; Castro *et al.*, 1989; Moser *et al.*, 1998). Similar learning impairments were observed for associative tasks such as eyelid conditioning, following LTP saturation at CA3-CA1 synapses (Gruart et al., 2006). Conversely, time-dependent occlusion of LTP by electrical stimulation was observed in the hippocampus, following the learning of behavior tasks including MWM and inhibitory avoidance (IA) (Box 1.1) (Figure 1.4d) (Whitlock *et al.*, 2006; Habib *et al.*, 2014; Pavlowsky *et al.*, 2017).

*In vivo* electrophysiological recordings were employed to detect whether learning of behavioral tasks also induced LTP. While theoretically simple, this was 'searching for the needle in a haystack' problem, given that a single neuron receives thousands of synaptic inputs and only a small subset of synapses among sparsely distributed neurons are thought to be responsible for memory storage (McNaughton and Morris, 1987; Megías *et al.*, 2001). In 1997, two groups independently identified increased synaptic strength (mediated by AMPARs) in the lateral amygdala of rodents that had undergone auditory fear conditioning (Box 1.1) (McKernan and Shinnick-Gallagher, 1997; Rogan et al., 1997). Later, Mark Bear's group provided the first

convincing evidence for learning-induced synaptic change in the hippocampus. To increase the likelihood of detecting LTP, they conducted multi-electrode array recordings in the CA1 region, before and after a one-trial IA training (Whitlock *et al.*, 2006). Among the 44 electrodes (from 6 animals), 12 electrodes showed >10% field EPSP enhancement after the behavioral training and occluded subsequent HFS-induced LTP (Figure 1.4c, d) (Whitlock *et al.*, 2006). Confirming the electrophysiology results, LTP biomarkers, such as phosphorylation of the GluA1 AMPAR subunit at Ser831 and increased synaptic localization of AMPARs, were found to be present after IA training (Whitlock *et al.*, 2006). Further electrophysiological studies using other forms of behavioral tasks such as eyelid conditioning, MWM, and active avoidance learning, lend additional support to the existence of learning-induced LTP in the hippocampus (Gruart et al., 2006; Habib et al., 2014; Pavlowsky et al., 2017).

Memories are hypothesized to be stored as a specific pattern of synaptic strengths in the neural network (Marr D, 1971; McNaughton and Morris, 1987). Manipulation of such a pattern should disrupt the information content and impair memory retrieval (McNaughton *et al.*, 1986). To test this, Brun *et al*. trained rodents in MWM and subsequently induced LTP in DG by repeated HFS of the perforant path (Brun *et al.*, 2001). Following HFS, animals failed to show any preference for the platform region during the retention test, suggesting HFS-induced disruption of spatial memory. In an study by Nabavi et al., optogenetic stimulation was used to manipulate the synaptic strength in a network known to be critical for fear conditioning (Figure 1.4e) (Nabavi *et al.*, 2014). In the conventional auditory fear conditioning paradigm, an associative fear memory is created by pairing a foot shock with a tone, resulting in a conditioned response (freezing) to the tone. In the modified version, Nabavi et al. paired a foot shock with optogenetic activation of auditory inputs from the auditory cortex and medial geniculate nucleus expressing channelrhodopsin2 (ChR2) to the lateral amygdala. During the recall test, animals displayed the conditioned response – reduced lever pressing in response to light. Induction of optical-LTD (aimed to reverse the learning-induced LTP) the day before the recall test impaired the conditioned response, indicating the inactivation of fear memory. However, animals displayed a recovery in conditioned response when an additional optical-LTP was induced following optical-LTD.

**Box1.1 Some behavioral paradigms to study learning and memory**

Morris water maze

An animal is placed in a circular pool of water and required to locate a hidden escape platform. After repeated training, the animal learns to swim to the platform with a more direct swim path and decreasing escape latencies. In the probe trial to test spatial learning, the platform is removed from the pool, and the animal is allowed to swim for a few minutes. A well-trained animal will spend more time in the quadrant of the pool where the platform was present during the training. (Morris *et al.*, 1986).

Contextual fear conditioning

In contextual fear conditioning, a foot shock (unconditioned stimulus, US) is delivered to an animal placed in a particular context (conditioned stimulus, CS). The animal associates foot shock with the context and demonstrates a freezing behavior – an absence of movement (conditioned response, CR) when returned to the same context. (Maren and Fanselow, 1996).

Auditory fear conditioning

Auditory fear conditioning is similar to contextual fear conditioning, except a tone (conditioned stimulus, CS) is played during the delivery of foot shock. The animal associates foot shock with the tone and demonstrates freezing on a second exposure to the tone. (Romanski and LeDoux, 1992).

Inhibitory avoidance

When an animal is placed in a brightly lit compartment of the test box, by its habit moves to the adjacent dark, where it receives a foot shock. In the test phase, the animal avoids entering the dark compartment if it has learned the task. (Gold, 1986; McGaugh and Roozendaal, 2009).

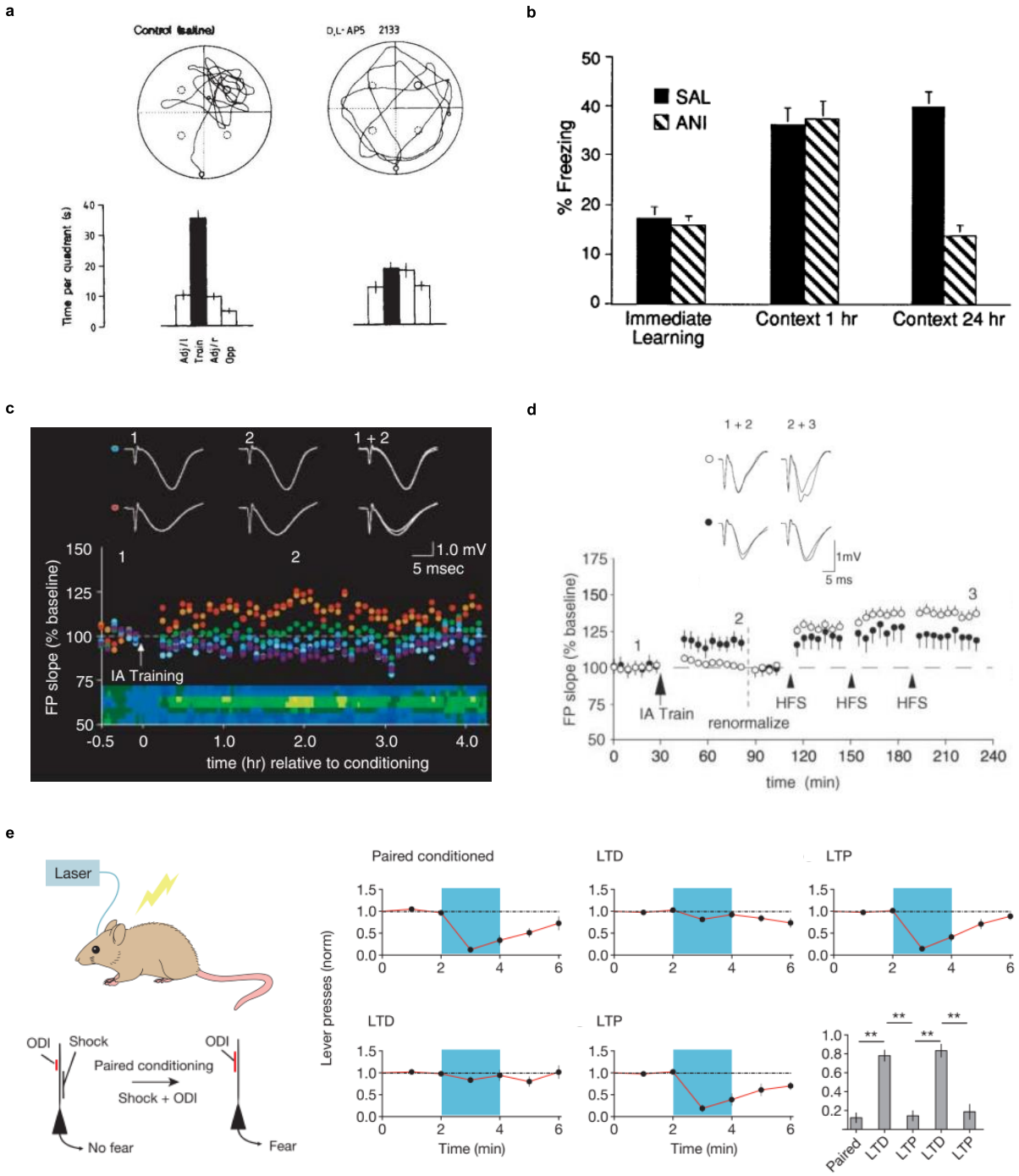


**Figure 1.4 Empirical evidence for synaptic plasticity and memory.**

(**a**) Blockade of LTP induction using NMDAR agonist D-AP5 impairs spatial learning in Morris water maze (adapted from Morris *et al.*, 1986). (**b**) Protein synthesis inhibitor anisomycin that blocks L-LTP disrupts long-term memory of contextual fear conditioning (adapted from Bourtchuladze *et al.*, 1994). (**c, d**) In CA1, inhibitory avoidance training increases field potentials on some electrodes of a multi-electrode array, (**c**) and occludes subsequent HFS-induced LTP (**d**) (adapted from Whitlock *et al.*, 2006). (**e**) Mice conditioned with optogenetic stimulation-shock pairings display conditioned response (CR, lack of lever press) to optogenetic stimulation. Optical induction of LTD aimed to reverse the training-induced LTP results in the loss of CR, whereas an additional round of optical-LTP reinstates the CR (adapted from Nabavi *et al.*, 2014).

## 1.3 The modern era of engram research

Earlier studies have identified broad brain regions that support memories. Both in animals and patients, hippocampal lesions impair the retrieval of episodic memories (Scoville and Milner, 1957; Morris *et al.*, 1982; Squire, 2004). In contrast, electrical stimulation of the hippocampus triggers the reactivation of the memory (Penfield and Perot, 1963). Although they were able to localize a memory at an anatomical level, these experiments did not pinpoint the neuronal subpopulation(s) that encode the memory. This is currently addressed by relying on immediate early genes to identify neurons that are activated by learning and memory tasks (please see sections 1.3.1, and 1.3.2 below for the details) (Han et al., 2007; Reijmers et al., 2007; Liu et al., 2012). These studies have led to elaborating the current definition for cellular memory engrams, engram cells/neurons which refers to neurons that are: (i) activated by a learning task, (ii) had undergone learning-induced physical or chemical changes, and (iii) reactivated by stimuli (or a subset of it) present during the learning. Consequently, engram cell reactivation should result in memory retrieval, visualized in laboratory models as the expression of a typical behavioral response associated with the memory-induced task (e.g., freezing behavior in the case of fear conditioning) (Tonegawa *et al.*, 2015; Josselyn and Tonegawa, 2020). Based on the experimental strategies and the criteria used, studies evaluating the existence of engram neurons can be classified as observational, loss-of-function, and gain-of-function.

### 1.3.1 Observational studies

Observational studies are usually correlative and are designed to detect the population of neurons that were active and had undergone enduring changes during encoding and/or recall. Due to the wide and sparse distribution of engram neurons, it is extremely difficult to identify them using conventional electrophysiology methods (Whitlock *et al.*, 2006). The discovery of immediate early genes (IEGs), a group of genes that are rapidly and transiently induced by

neuronal activity, made it possible to label the neurons activated during the learning or recall of a specific memory (putative engram neurons) (Minatohara et al., 2016). Methods that use IEG RNAs or proteins to detect putative engram neurons rely on three characteristics of IEG. First, IEG expression is low under basal activity conditions, but synaptic plasticity-inducing stimuli or experience dramatically increase IEG expression in neurons within minutes (Guzowski *et al.*, 2001). Second, both the protein and mRNA levels of IEG return to baseline within a few hours after the behavior (Guzowski *et al.*, 2001). Third, IEGs code for proteins including regulatory transcription factors, and scaffolding proteins that are crucial for translating a temporally limited stimulus into long-lasting cellular and synaptic changes required for the maintenance of memories (Guzowski, 2002).

#### 1.3.1.1 IEG staining

In 1987, two groups independently identified *c-fos* (regulatory transcription factor) as an IEG, with mRNA levels reaching maximum at 60 min post seizure induction (a protocol which leads to an increase in synaptic transmission efficiency) and returning to baseline in 180 min (Dragunow and Robertson, 1987; Morgan *et al.*, 1987). Following this discovery, studies used staining of brain slices with antibodies against c-Fos to map neurons that were active during a short time window (1–2 h) following specific stimuli. For instance, mice exposed to contextual fear conditioning showed a significantly higher density of c-Fos positive nuclei in CA1 than the control mice exposed to context or shock only, both after the learning and recall (Figure 1.5a) (Milanovic *et al.*, 1998). Although c-Fos staining reliably labelled neurons that were active during the behavior, it was difficult to classify them as engrams and to establish their relationship with the specific memory of fear conditioning since other sources of activation, such as stress, motor activity, novelty, or other processes that accompany the behavioral response could not be ruled out (Guzowski *et al.*, 2005).

*Arc* is an IEG coding for a cytoskeletal protein found in dendrites and essential for LTP maintenance (please see section 1.2.5.1) (Guzowski, 2002). *Arc* mRNA is detected as intranuclear foci, sites of transcription at the genomic alleles, within 2 min of neuronal activation and by 30 minutes *Arc* mRNA moves from the nucleus to accumulate in the cytoplasm. Exploiting the time-dependent subcellular localization of *Arc* mRNA, an IEG imaging method termed cellular compartment analysis of temporal activity by fluorescent in-situ hybridization (catFISH), was developed to label the neuronal populations activated at two different time points (Figure 1.5b)

(Guzowski *et al.*, 1999). The advantage of catFISH over c-Fos staining is it permits an intra-subject comparison of neuronal activity at two different time points. Indeed, when animals were sequentially exposed to two different environmental contexts, *Arc* catFISH identified that approximately 40% of CA1 neurons were activated in each environment, consistent with electrophysiological studies (Guzowski *et al.*, 1999). Neurons activated in both contexts could be detected by the presence of *Arc* mRNA as both cytoplasmic and internuclear foci. A high similarity between the two contexts led to a higher fraction of $Arc^+$ neurons showing both intranuclear and cytoplasmic foci (90%) than when rats were exposed to two distinct environments (16%) (Guzowski *et al.*, 1999). These double-labeled neurons might be engram neurons supporting context memory. However, the correlative nature of this study did not allow to obtain conclusive evidence in this regard.

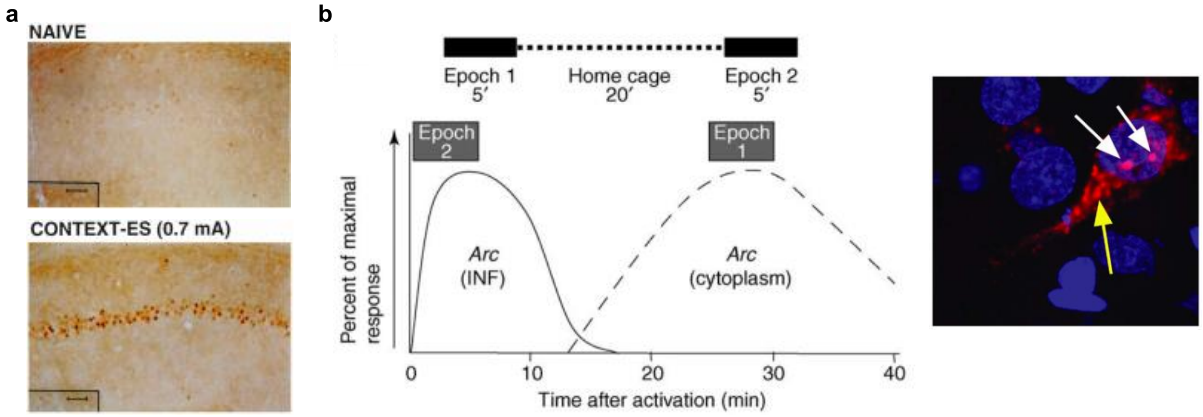


**Figure 1.5 Immediate early gene staining to map active neurons.**

(**a**) c-Fos staining; the density of $c\text{-}Fos^+$ cells in the CA1 area of the hippocampus is higher in contextual fear-conditioned mice compared to naïve animals (adapted from Milanovic *et al.*, 1998). (**b**) Approximate time course of *Arc* mRNA expression and localization in a two-context exposure (epoch 1 and 2) experiment (*left*). *Arc* catFISH (cellular compartment analysis of temporal activity by fluorescent in-situ hybridization) identifies neurons activated during epoch 1 (first context exposure) and epoch 2 (second context exposure) by the localization of *Arc* mRNA as cytoplasmic and intranuclear foci, respectively (*right*) (adapted from Guzowski *et al.*, 2005).

### 1.3.1.2 Putative engram capture strategies

IEG mRNA and protein levels return to baseline within a short period after the induction (Guzowski *et al.*, 2001). As a result, the IEG labeling methods described above cannot be used to observe putative engrams after a long time interval has elapsed since the memory encoding or recall phases. To overcome this temporal limitation, putative engram capture strategies that exploit the IEG promoters have been developed to tag the neurons activated during an event for a

prolonged time (Mayford and Reijmers, 2015). These genetically labelled putative engram neurons can then be analyzed by imaging or electrophysiology of the corresponding brain slices (Ryan et al., 2015; Kitamura et al., 2017; Tonegawa et al., 2018).

The Mayford group generated a transgenic mouse line - TetTag mouse, that carries two transgenes - i) *c-fos* promoter driving the expression of tetracycline transactivator (tTA) and ii) gene of interest (e.g. *lacZ* gene (encodes for β-Galactosidase), green fluorescent protein (GFP)) under the control of tetracycline responsive element (TRE) promoter (Figure 1.6a) (Reijmers *et al.*, 2007). tTA is a transcription factor that can be regulated with the tetracycline derivative, doxycycline (Dox). Dox inhibits the binding of tTA to the TRE promoter and blocks the gene of interest expression driven by the TRE promoter. In TetTag mice, tTA is continuously expressed in activated neurons and genetic tagging of memory specific putative engram neurons is achieved by removing Dox from the animal diet, to open a time window where *lacZ* expression is induced in activated neurons (Figure 1.6a). Reijmers *et al*. used *lacZ* expression and immunolabeling for the endogenous IEG ZIF268 to label the neurons activated during learning and recall, respectively (Reijmers *et al.*, 2007). They found that, in the basolateral amygdala (BLA), 12% of neurons (significantly above chance level) activated during the learning of a fear-conditioning task were also reactivated during the retrieval, suggesting these neurons could be a putative engram for the fear memory (Reijmers *et al.*, 2007). Furthermore, the number of reactivated neurons in the amygdala correlated positively with the amount of freezing (the behavioral expression of the fear memory). Like in the amygdala, neurons in the hippocampus and cortex that were active during learning were also reactivated during memory retrieval (Figure 1.6b) (Ramirez *et al.*, 2013; Tayler *et al.*, 2013).

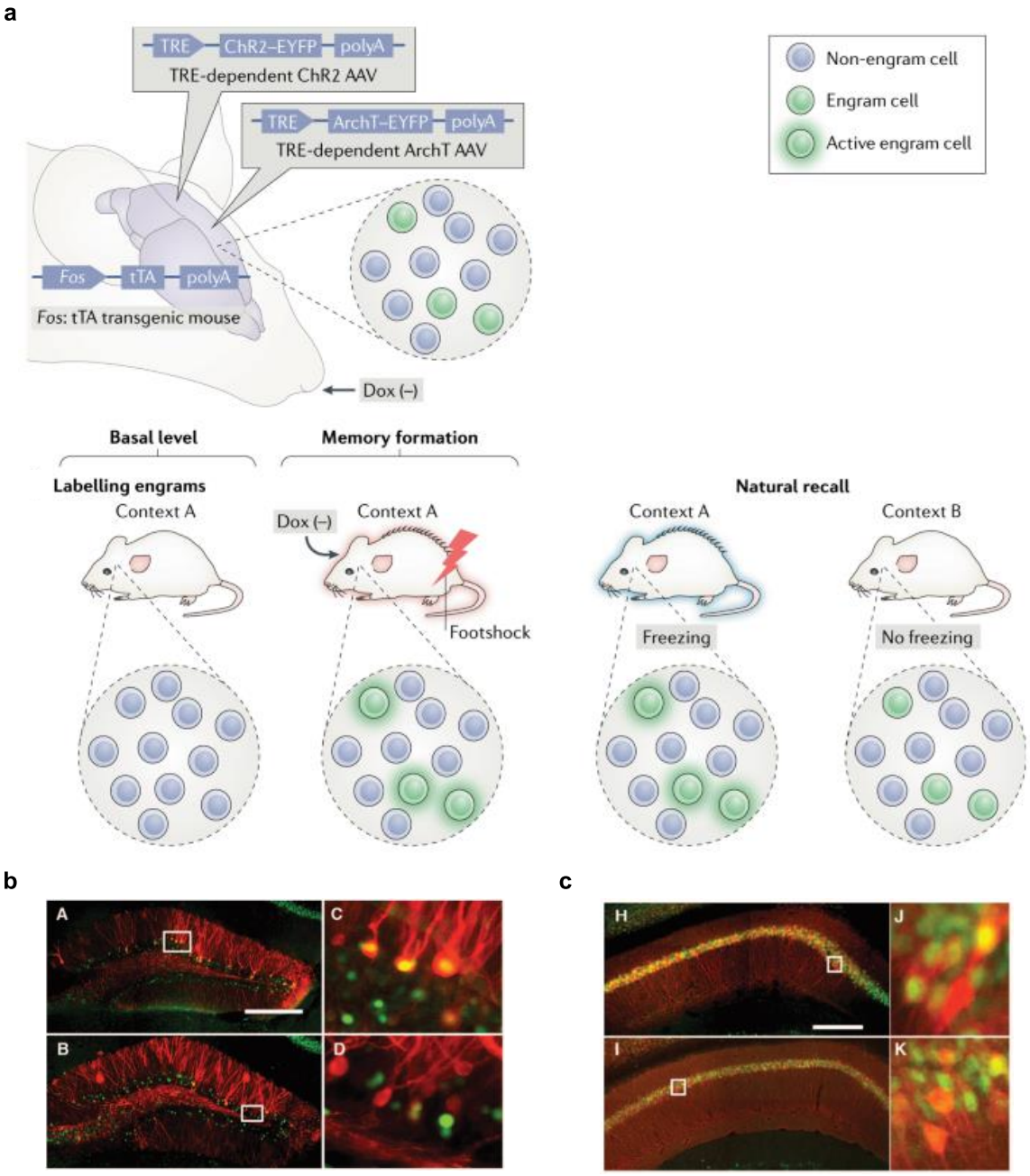


**Figure 1.6 Activity-dependent neuron labelling using TetTag.**

(**a**) Schematics showing the TetTag tool. TetTag mouse carries two transgenes - i) *c-fos* promoter driving the expression of tetracycline transactivator (tTA) and ii) gene of interest (e.g., yellow fluorescent protein, YFP) under the control of tetracycline responsive element (TRE) promoter. tTA is continuously expressed in activated neurons and genetic tagging of memory-specific putative engram neurons is achieved by removing Dox from the animal's diet, to open a time window where YFP expression is induced in activated neurons. (Adapted from Tonegawa et al., 2018). (**b, c**) In the dentate gyrus (**b**) and CA1 region (**c**) of the hippocampus, mCherry (red) expressed using the TetTag approach labels neurons activated during a novel context exposure. After 24 h, exposure to the same context (*top*), but not to a different context (*bottom*) reactivates the mCherry+ neurons. Reactivated neurons (green) are labelled using, c-Fos staining. (Adapted from Ramirez et al., 2013).

Although the TetTag mouse enabled to achieve prolonged tagging of neurons activated in response to specific *in vivo* stimuli, the expression of the protein tag was transient, and it eventually disappeared owing to protein degradation. To obtain permanent genetic access to the neuronal ensemble that was activated by a learning experience, a new approach termed targeted recombination in active populations (TRAP) was introduced. TRAP utilizes two transgenes – i) *c-fos* or *Arc* promoter driving the expression of tamoxifen (TM) - dependent Cre recombinase, $CreER^{T2}$, and ii) effector construct containing loxP-flanked coding region and controlled by a constitutively active promoter (Figure 1.7a). $CreER^{T2}$ is expressed only in activated neurons and becomes active only if tamoxifen has been administered to the transgene-bearing mouse. Thus, recombination and long-term expression of the protein of interest occurs only in neurons activated during a specific time window (Figure 1.7a, b) (Guenthner *et al.*, 2013; Denny *et al.*, 2014). In agreement with TetTag results, TRAP demonstrated that a small percentage of neurons active in the DG and CA3 during encoding were also active during recall (Figure 1.7b) (Denny *et al.*, 2014). As the tagging is permanent, TRAP opens the possibility to examine the tagged neurons even after a long period, such as during testing for memory retrieval weeks after the encoding. On the contrary, the time window available for retrieval in catFISH and TetTag was a few minutes and days, respectively (Guzowski *et al.*, 2005; Mayford and Reijmers, 2015).

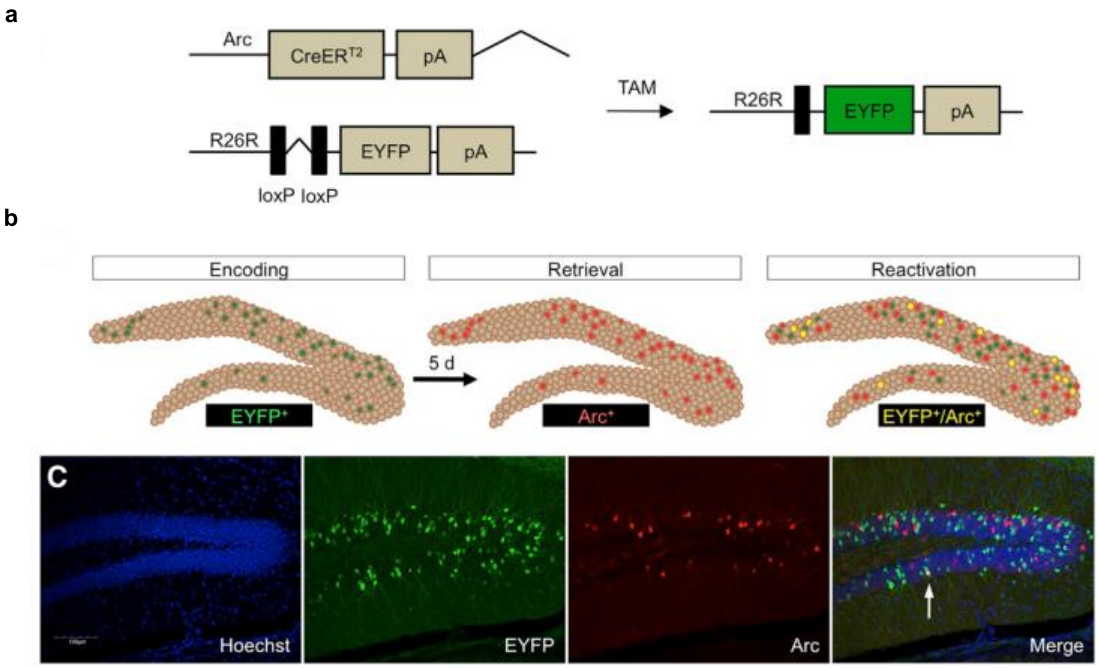


**Figure 1.7 TRAP permanently labels activated neurons**

(**a**) Schematics showing the targeted recombination in active populations (TRAP) method. TRAP utilizes two transgenes – i) *c-fos* or *Arc* promoter driving the expression of tamoxifen (TM) - dependent Cre recombinase, CreER$^{T2}$, and ii) effector construct containing loxP-flanked coding region (e.g., EYFP) and controlled by a constitutively active promoter. Active neurons express CreER$^{T2}$, but Cre-mediated recombination and expression of EYFP occur only in neurons activated during a time window controlled by TM administration. (**b**) Representative images showing EYFP$^+$ and Arc$^+$ neurons in the dentate gyrus, activated during encoding and retrieval of a memory, respectively. (Adapted from Denny et al., 2014).

Both TetTag and TRAP identified that the overlap of neurons activated during the encoding and recall of an experience was above the chance level. However, these neurons represent a remarkably low fraction of the total number of reporter-expressing neurons. This could be due to the over-tagging of active neurons caused by the presence of Dox or TM for hours to days preceding the actual behavioral event, which lasts only for a few minutes. This indicates that engram neurons that support long-term memory encoding are just a subset of these tagged neurons. Different IEG promoters may tag different populations of neurons with different roles in memory. For instance, Fos and Npas4 IEGs tag neuronal ensembles within the DG with memory generalization and discrimination function, respectively (Sun *et al.*, 2020).

### 1.3.2 Engram manipulation

Observational studies cannot establish a causal link between neurons labelled during learning and the behavioral expression of a given memory. To demonstrate that neurons tagged during the encoding phase of a memory belong to an engram, it must be shown that their activity is necessary and/or sufficient for the behavioral expression of that memory. The following sections describe the gain-of-function and loss-of-function studies that address the sufficiency and necessary criteria of engrams, respectively.

#### 1.3.2.1 Gain-of-function studies

Naturally, memory retrieval occurs in an animal when it gets exposed to the cues that were present during the corresponding learning process. Earlier studies by Penfield and colleagues demonstrate that electrical stimulation of certain parts of the lateral temporal cortex can elicit recall of episodic memories in patients (Penfield and Perot, 1963). This suggests the possibility of artificially eliciting the memory in the absence of a retrieval cue. By combining optogenetics or chemogenetics with activity-dependent expression using IEG promoters, neurons activated during learning can now be precisely stimulated at later time points to induce memory expression in the absence of any retrieval cue (Figure 1.8a).

Using TetTag mice, Liu et al. expressed the excitatory channelrhodpsin2 (ChR2) in an ensemble of DG neurons that were active during contextual fear conditioning (Figure 1.8a) (Liu *et al.*, 2012). Interestingly, photostimulation of ChR2-expressing neurons elicited freezing behavior in a neutral context that had never been paired with a foot shock (Figure 1.8c) (Liu *et al.*, 2012). On the other hand, photostimulation of ChR2-expressing neurons that were recruited during exposure to a neutral context did not induce freezing in mice that had undergone fear conditioning in a different context (Liu *et al.*, 2012). As an alternative to light-gated opsins, Designer Receptors Exclusively Activated by Designer Drugs (DREADDs), can be used for sustained activation or inhibition of neurons using the synthetic ligand clozapine-N-oxide (CNO). Yiu et al. expressed the excitatory DREADD hM3Dq in a subpopulation of lateral amygdala (LA) neurons and activated them by CNO administration immediately before auditory fear conditioning. In analogy with light-induced activation, subsequent activation of hM3Dq expressing neurons by CNO administration induced freezing in a novel context (Yiu *et al.*, 2014). These results suggest that the tagged neurons are a part of the engram supporting the fear memory and are sufficient for memory retrieval.

Although both optogenetics and chemogenetics can be used to control the activity of neurons, they have their advantages and limitations. Optogenetics provides high temporal resolution, as the activation and deactivation of receptors (ChR2) are controlled by the presence and absence of light of appropriate wavelength (470 nm for ChR2) (Vlasov et al., 2018). On the contrary, activation of DREADDs is slow and prolonged in chemogenetics because of the delay in drugs reaching the target and the presence of the drug until gets cleared by the body (Vlasov et al., 2018). This can result in the activation of neurons for longer periods. Chemogenetics is suitable for the activation of target cells in multiple brain regions as the ligand can diffuse throughout the brain. With optogenetics, only the ChR2-expressing cells below the fibers can be directly activated, which is beneficial if brain area-specific manipulation is the goal.

In a study by Ramirez *et. al*., ChR2 was expressed in DG neurons activated during exposure to a neutral context using the TetTag system. Subsequently, these labelled neurons were photoactivated while the mice experienced fear conditioning in another context (Ramirez *et al.*, 2013). When exposed to the neutral context again, mice displayed freezing behavior even though they had never been shocked in this context. This indicates the creation of an artificial memory, where mice associated the neutral context with the foot shock. In a similar study, ChR2 was expressed in the hippocampal neurons activated by neutral context and the basolateral amygdala neurons activated by the foot shock. After photoactivation of these two populations of ChR2-expressing neurons, mice displayed freezing in the neutral context, suggesting the formation of a false associative memory (Ohkawa *et al.*, 2015).

Although stimulation of putative engram neurons by both optogenetics and chemogenetics led to the expression of the memory (e.g., freezing in contextual fear conditioning), the magnitude of the behavioral response was smaller than the response elicited by the natural retrieval cues (Liu *et al.*, 2012; Yiu *et al.*, 2014). One possible reason is that, unlike natural recall, artificial reactivation of putative engram neurons does not recapitulate the precise spatiotemporal activity pattern that was present at the encoding. Using chemogenetics, it has been shown recently that simultaneous reactivation of putative engram neurons in multiple brain regions can induce memory expression (freezing) close to the levels induced by natural recall (Roy et al., 2022).

Memory is thought to be distributed across multiple brain regions (Wheeler *et al.*, 2013; Roy *et al.*, 2022). However, focal reactivation of putative engram neurons in a single area was sufficient

to induce the retrieval of memory (Liu *et al.*, 2012; Yiu *et al.*, 2014). This suggests that engram neurons are functionally connected and reactivation of a sufficient number of putative engram neurons might induce a broader pattern of reactivation across the entire engram, eventually resulting in behavior expression of the memory. Supporting this hypothesis, Roy et. al has recently demonstrated that optogenetic reactivation of putative engram neurons in the CA1 or BLA activates putative engram neurons in the other brain areas (Roy et al., 2022). Moreover, putative engrams in a few brain regions such as the entorhinal cortex (EC) and periaqueductal gray (PAG) are activated both by the CA1 and BLA putative engram reactivation. These areas might serve as 'hubs' that can exert greater influence on the expression of the memory.

#### 1.3.2.2 Loss-of-function studies

Loss-of-function studies address the necessity criteria by examining whether eliminating or inhibiting the tagged neurons impairs memory recall (Figure 1.8b). CREB is a transcription factor activated by synaptic potentiation and is essential for the maintenance of LTP as well as memory formation (please see section 1.2.4) (Bourtchuladze et al., 1994; Baltaci et al., 2019). An initial study by Han et. al demonstrates that lateral amygdala neurons with higher expression of CREB during auditory fear conditioning are more likely to be reactivated than their neighbors during recall (Han *et al.*, 2007). To selectively ablate putative engram neurons, the diphtheria toxin receptor (DTR) was expressed in CREB-overexpressing neurons by including Cre recombinase in the CREB expression cassette and using transgenic mice with loxP-flanked DTR. Injection of DT induces apoptosis in DTR-expressing neurons. Mice showed high levels of freezing to the auditory cue when initially tested for intact fear memory. However, the deletion of the CREB-overexpressing neurons (but not a similar number of random LA neurons) blocked the subsequent expression of the fear memory (Han *et al.*, 2009). The freezing impairment was not due to performance deficit, as the mice were able to relearn the task normally post-ablation. Similarly, reversibly inactivating the allocated neurons with the *Drosophila* allatostatin G-protein-coupled receptor (AlstR)/ligand system, minutes before the recall test impaired memory expression (Zhou *et al.*, 2009).

Apart from expressing a transgene for visualizing the activated neurons, TetTag and TRAP mice can be exploited to drive the expression of transgenes that allow physiological manipulations at later time points. Using the TRAP approach, Denny et al. expressed Archaerhodopsin (ArchT), in the ensemble of neurons that were active during the acquisition of a contextual fear memory

(Denny *et al.*, 2014). ArchT is a light-driven outward proton pump, that allows the rapid and transient silencing of expressing neurons in response to photostimulation (593.5 nm) (Han *et al.*, 2011). Optogenetic inhibition of ArchT$^{+}$ neurons in the DG or CA3 prevented the expression of the fear memory during the recall test (Figure 1.8d) (Denny *et al.*, 2014). In a related study using the TetTag system, optical silencing of the tagged CA1 neurons impaired memory retrieval (Tanaka *et al.*, 2014). Interestingly, the reactivation of putative engram neurons in the cortex and amygdala was also found to be compromised by the silencing of putative engram neurons in the hippocampus, suggesting network connectivity between engram neurons in different brain regions (Tanaka *et al.*, 2014). The memory impairment induced by neuronal silencing was evident even days or weeks after the training, which indicates the stable encoding of memory in the putative engram neurons (Denny *et al.*, 2014; Tanaka *et al.*, 2014).

Although engram neurons were thought to be distributed across multiple brain regions, silencing only a subset of the putative engram neurons in a single brain region (such as the LA or hippocampal subfields – CA1, CA3, or DG) was sufficient to impair the memory expression (Han *et al.*, 2009; Denny *et al.*, 2014; Tanaka *et al.*, 2014). These findings indicate that engram neurons in certain brain regions may act as a hub and can have a more prominent role than others in the expression of memory. For instance, hippocampal putative engram neurons are indispensable for the expression of recently acquired memories and become silent (not activated by recall) with time (Kitamura et al., 2017; Tonegawa et al., 2018). On the contrary, putative engram neurons in the cortex exert more influence on the expression of remote memory (Kitamura et al., 2017; Tonegawa et al., 2018). BLA is essential for both recent and remote memory expression (Kitamura et al., 2017; Tonegawa et al., 2018).

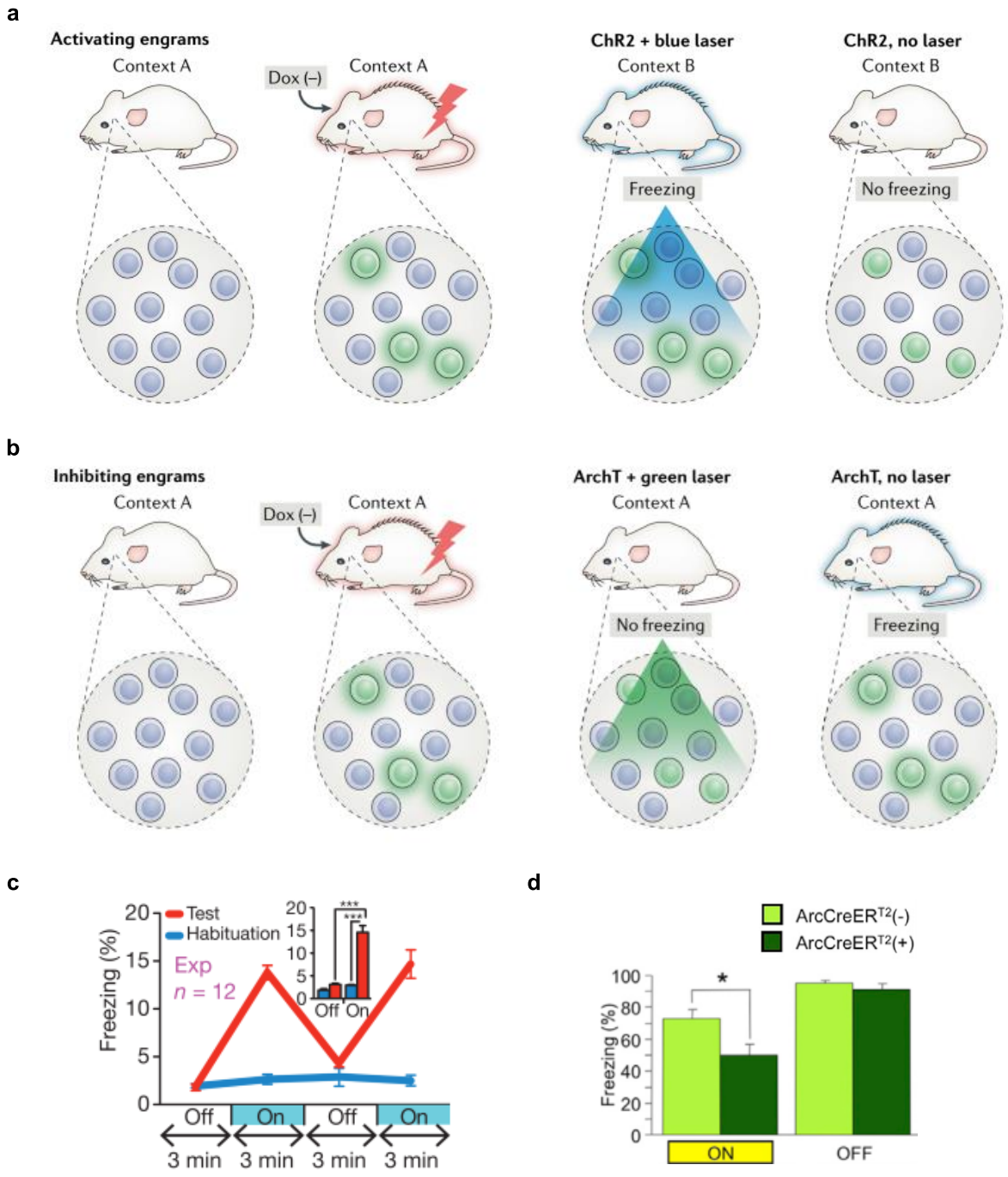


**Figure 1.8 Manipulation of putative engram neurons affects memory retrieval**

(**a, c**) Gain-of-function: Using TetTag approach (please see section 1.3.1.2 and Figure 1.6), neurons activated during contextual fear conditioning (green) are tagged with channelrhodopsin2 (ChR2). Reactivation of ChR2-expressing neurons in the dentate gyrus by photostimulation induces freezing response in a neutral context, thus demonstrating their sufficiency for memory retrieval. (Adapted from Tonegawa et al., 2018 (**a**); Liu et al., 2012 (**b**)) (**b**, **d**) Loss-of-function: Using TRAP approach (please see section 1.3.1.2 and Figure 1.7), neurons activated during contextual fear conditioning (green) are tagged with archaerhodopsin (ArchT). Photoinhibition of ArchT-expresing neurons in the dentate gyrus reduces freezing response in the conditioning context, thus demonstrating their necessity for memory retrieval. (Adapted from Tonegawa et al., 2018 (**b**); Denny et al., 2014 (**d**)).

## 1.4 Synaptic plasticity and memory engrams

Collectively, the studies discussed in section 1.2.6 provide evidence for the correlation between activity-dependent synaptic plasticity processes such as LTP or LTD and memory. However, the underlying mechanisms of information storage in the brain are currently investigated at a whole-neuron scale (please see section 0 above) to identify cellular memory engrams i.e., ensembles of neurons whose recruitment and activation are necessary and sufficient for the retrieval of a specific memory. Although successful, they are limited with cellular level resolution and cannot identify the subset of synapses that have undergone learning-induced synaptic plasticity. *In vivo* electrophysiological recordings have detected learning-induced changes in synaptic strength in the amygdala (McKernan and Shinnick-Gallagher, 1997; Rogan et al., 1997) and hippocampus (Gruart et al., 2006; Whitlock et al., 2006; Habib et al., 2014; Pavlowsky et al., 2017). Precise identification of synapses undergoing learning-induced synaptic plasticity is limited by the electrophysiology technique. This is because the field potentials obtained from recording electrodes are the summed activity of many neurons around the electrode. However, electrophysiological recordings of a single neuron could be obtained by using microelectrode(s) or patch-clamp (hard to perform *in vivo).* Extracellular recordings can also be performed with multi-channel silicon probes to detect single neuron activity *in vivo* (Spalletti *et al.*, 2017)**.** The sections below discuss several tools that are available now to examine the structural and/or functional changes associated with synaptic plasticity up to the single synapse resolution.

### 1.4.1 Structural plasticity of dendritic spines

#### 1.4.1.1 Ultrastructural studies

Since the 1950s, transmission electron microscopy (TEM) has been used by researchers to gain insight into the structure and composition of synapses at the nanometer scale. Serial-section electron microscopy (ssEM) of brain samples followed by 3D reconstruction allows studying the variations in the size, shape, and subcellular composition (including endosomes, polyribosomes,

and smooth endoplasmic reticulum) of synapses associated with learning or undergoing plastic changes such as LTP (Bailey, Kandel and Harris, 2015).

Early EM studies analyzing ultrastructural synaptic plasticity relied on the induction of LTP in hippocampal slices by tetanic or theta burst stimulation. The synapse number and morphology were altered in the DG but remained unchanged in the CA1, 1-2 h following tetanic stimulation in the perforant pathway and Schaffer collaterals, respectively (Fifková and van Harreveld, 1977; Sorra and Harris, 1998). When LTP was induced using a theta-burst stimulation (TBS), that resembles the endogenous neuronal firing patterns in the hippocampus, rapid synaptogenesis followed by a reduction in the small spine number was observed in the CA1 (**Error! Reference source not found.**a) (Bourne and Harris, 2011). Interestingly, the lower density of small spines was counterbalanced by the enlargement of the existing excitatory synapses, thus keeping the total surface area constant (**Error! Reference source not found.**a) (Bourne and Harris, 2011). Enlargement and clustering of synapses observed following LTP have shown to be dependent on the local availability of resources such as smooth endoplasmic reticulum, polyribosomes, and endosomes, that regulate $Ca^{2+}$ levels, local protein synthesis and trafficking of proteins and lipids (Harris, 2020).

ssEM can be used to examine the structural changes complementing the functional synaptic change associated with learning. Memory is proposed to be stored in enlarged spines, while small spines possess the capacity to store new information. Supporting this hypothesis, auditory fear conditioning increased the number of large synapses with a spine apparatus (a specialized form of smooth endoplasmic reticulum found in a subpopulation of dendritic spines), thus enhancing the amount of stable connectivity (**Error! Reference source not found.**b) (Ostroff *et al.*, 2010). The frequency of polyribosomes (the sites of protein synthesis) and multivesicular bodies (organelles for protein degradation) was also found to be elevated in the dendrites of fear-conditioned mice (Ostroff *et al.*, 2010).

Although EM identified ultrastructural synaptic correlates of plasticity, it was not possible to know which synapses were active during learning and whether the dendrite segment used for 3D reconstruction belonged to an engram or a non-engram neuron. Since EM analysis can only be performed on fixed tissue, it cannot determine whether enlarged spines were formed *de novo* or

from existing spines. Other caveats of EM are small sample sizes and limited whole-cell reconstruction.

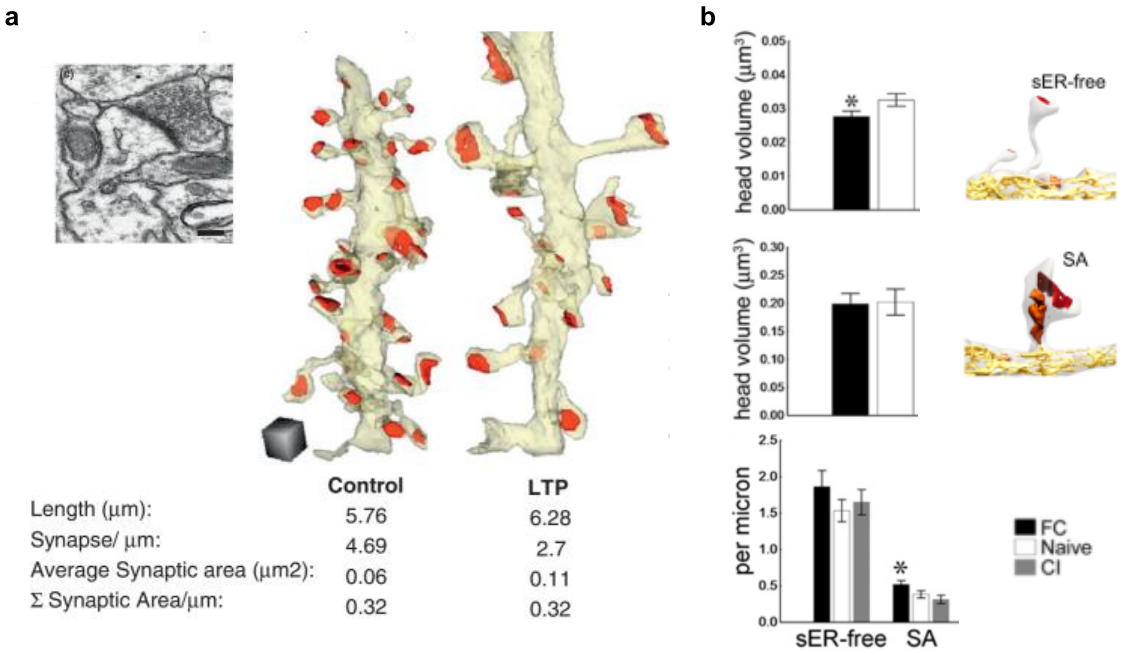


**Figure 1.9Ultrastructural analysis using electron microscopy.**
(**a**) LTP induction via TBS increases the spine volume of CA1 neurons in mature hippocampal slices (adapted from Bourne and Harris, 2011). (**b**) Fear conditioning (FC) increases the density of spines with spine apparatus (SA; reflects larger and stable synapses) in the lateral amygdala (adapted from Ostroff *et al.*, 2010).

1.4.1.2 Dendritic spine imaging using fluorescence microscopy.

Although EM provided accurate measures of synapses, 3D reconstruction was time-consuming and possible only for short dendrite stretches. To visualize spines along the entire dendritic tree, confocal microscopy was employed to acquire images of neurons filled with fluorescent dyes (delivered by glass microelectrodes) (Trommald and Jensen, 1995). Using time-lapse imaging of dye-filled neurons, it was found that the LTP induction resulted in the emergence of new spines in the CA1 dendrite segments closer to the stimulation area (Engert and Bonhoeffer, 1999). Supporting the *in vitro* data, an increase in spine density was observed in the hippocampal CA1 basal dendrites following spatial training in a complex environment (Moser et al., 1994).

Genetic expression of fluorescent proteins (such as GFP) was an improvement over dye-based techniques. It became possible to image a large number of neurons at multiple time points,

allowing the detection of spine genesis or deletion or morphometric changes induced by learning or LTP stimulation. In line with previous results, a rapid and persistent enlargement of stimulated spines or an increase in their number was observed following LTP induction (**Error! Reference source not found.**a) (Maletic-Savatic, 1999; Matsuzaki *et al.*, 2004). These LTP-associated structural changes were input-specific, as there was no significant expansion of spines close to a stimulated spine or new spine formation in dendritic segments far from the stimulation area (Maletic-Savatic, 1999; Matsuzaki *et al.*, 2004). Repetitive confocal imaging on hippocampal slices found that LTP promotes selective long-term stabilization of activated spines, as well as preferential growth of new spines in the nearby dendritic region (De Roo et al., 2008).

Combining transcranial two-photon imaging with transgenic mice sparsely expressing yellow fluorescent protein (YFP) in cortical neurons, two independent studies found that motor skill learning promoted rapid (within an hour) spine formation in layer V pyramidal neurons in the motor cortex (Xu et al., 2009; Yang et al., 2009). Interestingly, a small fraction of the newly formed spines persisted for months and correlated with memory expression, suggesting stable synaptic connections as the physical substrate of long-term memories (**Error! Reference source not found.**b) (Xu et al., 2009; Yang et al., 2009).

Studies expressing fluorescent proteins in a random set of neurons in a given brain area did not distinguish between engram and non-engram neurons. With the current putative engram capture technologies discussed above (section 1.3.1.2), it is now possible to examine synaptic structural changes specifically in putative engram neurons that were active during learning and memory recall. In a recent study, neurons activated during contextual fear conditioning in the DG were labelled with ChR2-mCherry, expressed using the TetTag approach (Figure 1.6) (Ryan *et al.*, 2015). Subsequently, structural plasticity was examined in both putative engram (ChR2-mCherry-poisitive) and non-engram (ChR2-mCherry-negative) neurons, by filling neurons with biocytin (Ryan *et al.*, 2015). Putative engram neurons showed higher spine density than non-engram neurons (**Error! Reference source not found.**c). Administration of the protein synthesis inhibitor anisomycin immediately after learning abolished both synaptic changes and memory retrieval (**Error! Reference source not found.**c) (Ryan *et al.*, 2015). This study provides direct proof for the existence of learning-induced structural plasticity necessary for the storage and subsequent retrieval of the corresponding memory (Ryan *et al.*, 2015).

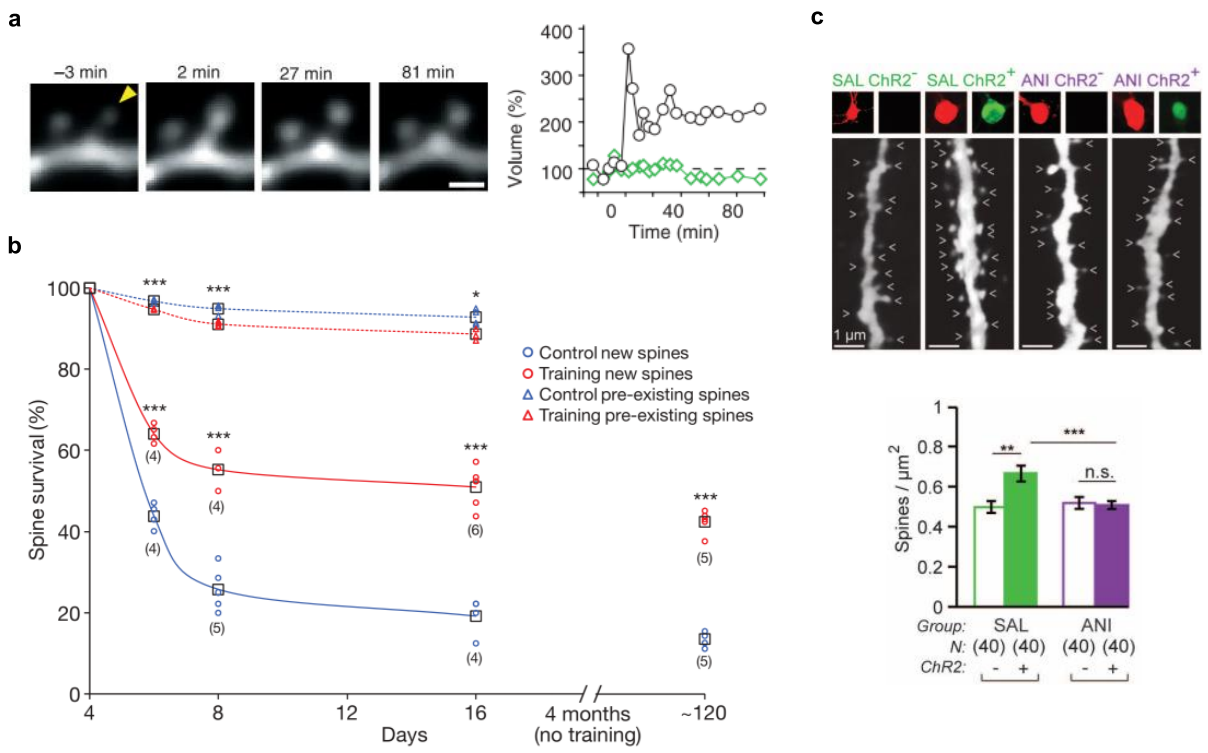


**Figure 1.10 Fluorescence imaging to examine structural potentiation.**

(**a**) LTP induction causes a rapid and long-lasting increase in spine volume; Time-lapse images (*left*) and estimated spine-head volume (*right*) of a potentiated (black) and a neighboring (green) dendritic spine on a CA1 neuron expressing GFP. (Adapted from Matsuzaki *et al.*, 2004). (**b**) Motor skill learning stabilizes newly formed spines in the motor cortex (adapted from Xu *et al.*, 2009). (**c**) In the dentate gyrus, neurons activated during contextual fear conditioning (ChR2$^+$; labelled using TetTag approach (section 1.3.1.2 and Figure 1.6)) show protein-synthesis dependent increase in spine density (adapted from Ryan *et al.*, 2015).

### 1.4.2 Functional plasticity of dendritic spines

Structural imaging has established a relationship between spine enlargement and spinogenesis following LTP induction or learning (Maletic-Savatic, 1999; Matsuzaki *et al.*, 2004; Ryan *et al.*, 2015). The following step consisted in demonstrating whether (i) newly formed spines are functionally active and integrated into the circuit and (ii) enlarged spines have a correlative enhanced synaptic transmission. To overcome the insufficient resolution of electrophysiology-based functional connectivity and plasticity analyses, newer methods that use genetics and confocal microscopy have been introduced to study learning-associated functional changes at the single-spine resolution.

#### 1.4.2.1 Calcium sensors

Synaptic stimulation evokes postsynaptic intracellular $Ca^{2+}$ concentration changes that result from $Ca^{2+}$ entry through ligand-gated calcium channels (*e.g.*, NMDA) and voltage-gated calcium channels (VGCCs), and $Ca^{2+}$ release from internal stores (Ross, 2012). The strength of synaptic transmission at single synapses can be assessed by imaging the changes in amplitude (postsynaptic origin) and probability of occurrence (presynaptic origin) of evoked postsynaptic $Ca^{2+}$ transients (EPSCaTs) (Emptage *et al.*, 2003). The relative intracellular $Ca^{2+}$ levels and their change over time can be detected via synthetic calcium indicators (*e.g.*, Fluo-5F, Oregon Green BAPTA (OGB)-1)) or through genetically encoded calcium indicator (GECI, *e.g.*, GCaMP). Synthetic calcium indicators are generally delivered to neurons via cell permeabilization by patch clamp, limiting *in vivo* usage. In contrast, GECIs are less invasive (generally delivered via viruses) and allow selective labelling of neuronal cell types. GCaMP is a recombinant protein consisting of circularly permutated green fluorescent protein (cpGFP), calcium-binding protein calmodulin (CaM), and CaM-interacting M13 peptide (Nakai et al., 2001). Because calcium-binding induces conformational changes in CaM/M13, modulating the solvent access and $pK_a$ of the chromophore inside the cpGFP β-barrel, an increase in the local $Ca^{2+}$ levels can be detected as an increase in GFP fluorescence. Calcium indicators combined with two-photon microscopy allow the investigation of neuronal activity at individual spines with a temporal resolution of a few milliseconds (Chen *et al.*, 2013).

To identify whether LTP-induced structural changes are associated with a functional change, several studies have employed calcium indicators. EPSCaT amplitude and frequency at stimulus-responsive spines increased following LTP, with a direct correlation with the electrophysiological recording of EPSPs amplitude at the soma (Figure 1.11a) (Emptage *et al.*, 2003; Wiegert *et al.*, 2018). Spines that expanded post-LTP exhibited a large rapid $Ca^{2+}$ transient in response to a single presynaptic stimulus (Lang *et al.*, 2004). Furthermore, stimulus-evoked $Ca^{2+}$ currents were detected in the new spines generated after LTP induction, suggesting their functional incorporation into the existing neuronal circuit (De Roo et al., 2011). Repetitive imaging of GCaMP-expressing neurons in hippocampal slice cultures identified that EPSCaT amplitude and frequency as well as the spine head volume return to baseline 24 h after LTP induction, probably by homeostatic mechanisms (Wiegert *et al.*, 2018). However, these spines were more likely to persist compared

to non-stimulated spines, thus supporting the concept that memory can be stored in long-lasting synapses (Wiegert *et al.*, 2018).

*In vivo*, calcium imaging has been successfully employed in the somatosensory, auditory, and visual cortices to examine synaptic responses to sensory stimuli (Figure 1.11b) (Jia *et al.*, 2010; Chen *et al.*, 2011; Varga *et al.*, 2011). Two-photon microscopy is required to study $Ca^{2+}$ dynamics at the spine-level resolution, for which the animal head has to remain immobile. This constraint of head fixation makes $Ca^{2+}$ imaging challenging in classical learning paradigms such as contextual fear conditioning and Morris water maze, which require free movement (can be partially overcome by the implementation of the trackball and virtual reality). Furthermore, since calcium events are transient, simultaneous visualization of multiple spines from multiple dendrites or neurons is limited. Recently, head-mounted miniature microscopes with cellular resolution have been used to visualize GCaMP activity in putative engram and non-engram neurons in the CA1 region (Ghandour *et al.*, 2019). Putative engram neurons displayed higher repetitive activity during learning of a novel context and a subset of them with synchronous activity reactivated during both sleep and subsequent memory retrieval (Ghandour *et al.*, 2019). Further development of miniature microscopes to achieve a higher resolution would allow studying the physiological nature of individual synapses in a putative engram neuron.

Calcium-modulated photoactivatable ratiometric integrator (CaMPARI) is complementary approach to GCaMPs (Fosque *et al.*, 2015). CaMPARI undergoes an irreversible green-to-red chromophore conversion upon violet light illumination and binding of calcium (Fosque *et al.*, 2015). Thus, a lasting 'snapshot' of neuronal activity can be generated by defining the time window of photoconversion. Since photoconverted proteins remain in the cell for a longer time than the stimulus, continuous live monitoring is not essential. After photoconversion the tissue can be fixed and imaged for photoconverted proteins, allowing the post-hoc analysis of the neuronal activity in a relatively large volume of tissue with single spine resolution. CaMPARI fused either to presynaptic protein synaptophysin or to an intrabody against the postsynaptic protein PSD95 marks a small subset of synapses that were active during the illumination both *in vitro* and *in vivo* (Figure 1.11c) (Perez-Alvarez *et al.*, 2020). However, analysis of learning associated synaptic changes using CaMPARI remains challenging, because of the reduced signal-to-noise ratio, rapid protein turnover, and possibility of tissue damage by 405 nm light illumination required for photoconversion.

.

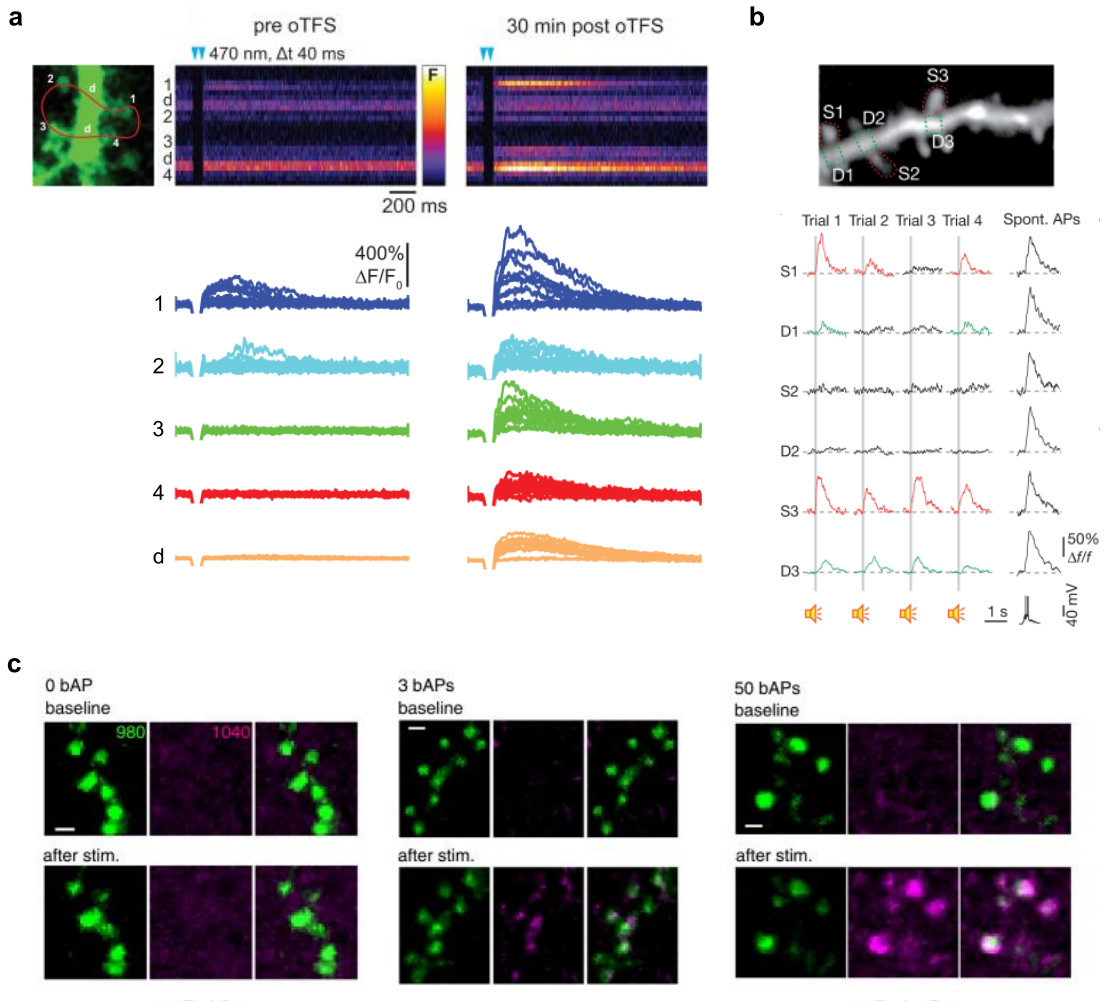


**Figure 1.11 Detection of synaptic activity using calcium sensors.**

(**a**) GCaMP detects an increase in synaptic response following LTP in hippocampal slices. The traces of GCaMP6s-fluorescence from the spines and dendritic shafts during test stimulation before (pre oTFS) and 30 after (30 min post oTFS) induction of LTP are shown in the figure panel (adapted from Wiegert *et al.*, 2018). (**b**) *In vivo* detection of auditory-stimulation-evoked $Ca^{2+}$ transients in the auditory cortex via GCaMP (adapted from Chen *et al.*, 2011). (**c**) Imaging synaptic activity using calcium-modulated photoactivatable ratiometric integrator (CaMPARI) fused to synaptic proteins. CaMPARI undergoes an irreversible green-to-red (represented as green and magenta) chromophore conversion upon illumination with a 405 nm laser and calcium binding. (Adapted from Perez-Alvarez *et al.*, 2020).

### 1.4.2.2 GluA1 labelling

The initial enhancement of synaptic transmission associated with LTP is mediated by the diffusion and accumulation of AMPARs on the postsynaptic membrane (Huganir and Nicoll, 2013). Tagging AMPAR subunits with a fluorescent protein and monitoring their membrane trafficking allows the identification of synapses undergoing functional plasticity. In an initial

study, Shi et. al. fused GFP to the AMPAR subunit GluA1 and observed rapid delivery of GluA1-GFP into the dendritic spines following LTP induction by tetanic stimulation (Shi *et al.*, 1999). Later, using the TetTag approach, Matsuo *et al*. expressed GluA1-GFP selectively in CA1 neurons that were active during the contextual fear conditioning (Matsuo et al., 2008). After 24 h, these newly synthesized AMPARs were present only in about 50% of the spines of putative engram neurons and were preferentially localized in stable mushroom spines (Figure 1.12a) (Matsuo et al., 2008)

GluA1-GFP did not distinguish between the synaptic membrane-bound receptors and the intracellularly localized receptors. To selectively visualize functionally active AMPARs inserted in the plasma membrane, super-ecliptic-pHluorin (SEP) was fused to the N-terminus of AMPAR subunits GluA1 or GluA2. SEP is a pH-sensitive version of GFP that is brightly fluorescent at the neutral pH of extracellular space but quenched in acidic environments of the secretory and endocytic vesicle pathways (Miesenböck et al., 1998). Surface expression of GluA1 and GluA2 at spines increased after chemical induction of synaptic potentiation in organotypic hippocampal slices, either by bath application of glycine or by glutamate uncaging at single spines (Kopec, 2006; Makino and Malinow, 2009; Patterson et al., 2010). Initial incorporation of AMPARs into the synapse was mediated by lateral diffusion of preexisting AMPARs on the spine surface, followed by the exocytosis of new AMPARs to the surface of stimulated spines or nearby dendritic segments spines (Kopec, 2006; Makino and Malinow, 2009; Patterson et al., 2010). *In vivo*, SEP-GluA1 has been used to study functional synaptic plasticity associated with sensory experiences in the mouse barrel cortex. Longitudinal imaging of AMPAR levels at individual synapses of a neuron identified a significant and long-lasting increase in surface GluA1 intensity in both spines and surrounding dendritic shafts following whisker stimulation (Figure 1.12b) (Makino and Malinow, 2011; Zhang *et al.*, 2015). Interestingly, potentiated synapses with increased SEP-GluA1 intensity were clustered after whisker stimulation (Makino and Malinow, 2011).

Although successful in tracking potentiated synapses associated with sensory experience, SEP-GluA1 has not been used yet to study learning-associated synaptic plasticity in cortical or in deep subcortical structures such as the hippocampus, probably owing to the requirement of sophisticated imaging techniques and analysis. Initial studies using SEP-GluA1 relied on overexpression of exogenous receptors, which might result in protein mistargeting and dysregulation. A transgenic knock-in mouse expressing endogenous GluA1 tagged with SEP was recently developed. This

new model does not have impairments in synaptic function, plasticity, or behavior and could be used for future studies on single-synapse potentiation (Graves *et al.*, 2021).

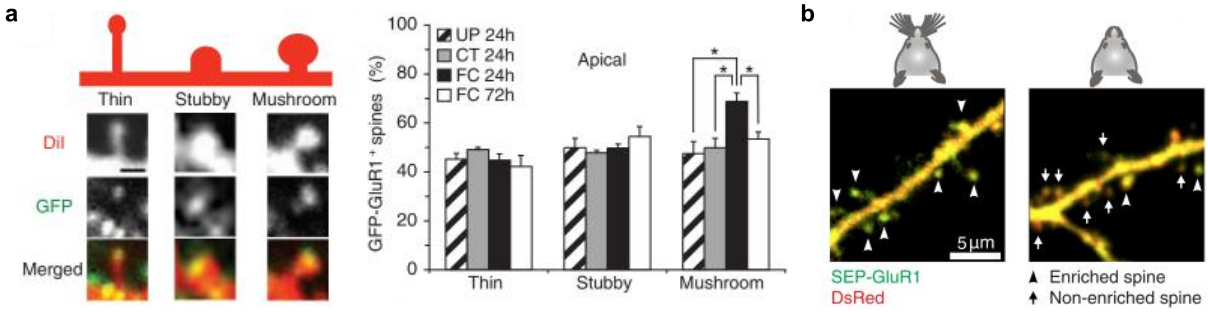


**Figure 1.12 AMPARs tagged with fluorescent proteins labels early potentiated synapses.**

(**a**) In the CA1 neurons activated during contextual fear conditioning, GFP tagged AMPAR GluA1 subunit is enriched in mushroom spines (stable spines with larger volume) (adapted from Matsuo et al., 2008). (**b**) SEP-GluA1 (super-ecliptic-pHluorin fused to AMPAR GluA1 subunit) detects dendritic spine that had undergone early potentiation in the barrel cortex after whisker stimulation (adapted from Makino and Malinow, 2011).

### 1.4.2.3 CaMKII sensor

CaMKII is known to be necessary and sufficient for the induction of LTP (Lisman et al., 2012). Förster resonance energy transfer (FRET)-based CaMKIIα sensor, Camuiα was developed to measure the activation of CaMKII at potentiated spines (Lee *et al.*, 2009). In the green- Camuiα variant, a donor-acceptor pair consisting of monomeric enhanced GFP (mEGFP) and REACh (yellow fluorescent protein variant) was fused to the C and N terminus of CaMKIIα, respectively. Synaptic activation changes the conformation of CaMKIIα to an open state, thereby increasing the distance between the donor-acceptor pair, which in turn decreases FRET and leads to higher emission in the GFP channel. FRET is measured using fluorescence lifetime imaging microscopy (FLIM), which is insensitive to the concentration of fluorophores but depends on its local micro-environment. In hippocampal slices, induction of LTP by glutamate uncaging rapidly increased the fluorescence lifetime of green-Camuiα specifically in stimulated spines, leaving the dendritic shaft and adjacent spines unaffected (Figure 1.13). The intensity of green-Camuiα signal correlated with structural potentiation i.e., spine enlargement. While the method proved useful in studying potentiated spines *in vitro*, its application to study learning-associated synapses still has to be tested.

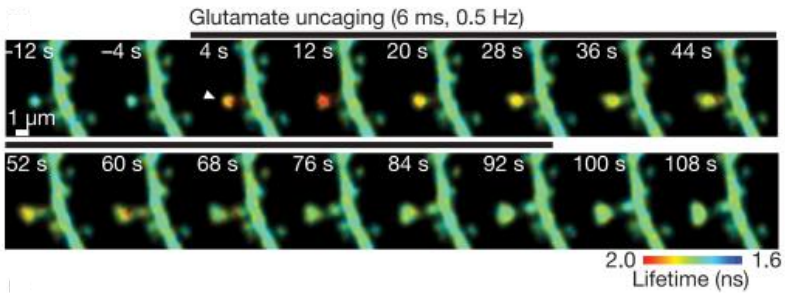


**Figure 1.13 CaMKII sensor detects potentiated spines.**

In hippocampal slices, LTP-induction increases the fluorescence lifetime of Förster resonance energy transfer (FRET)-based CaMKIIα sensor, Camuiα specifically in stimulated spines (adapted from Lee *et al.*, 2009).

### 1.4.3 Mapping synaptic connectivity

Since most excitatory synapses are formed on the dendritic spines of a postsynaptic neuron, synaptic strength is traditionally analyzed as a change in the shape, number, and distribution of dendritic spines, as described in the above sections. However, not all spines might form a functional synapse. Synaptic connectivity can be determined by counting the dendritic spines proximal to a presynaptic axon through neuronal reconstruction from TEM data and found that only a small fraction (~0.2) of intersections between axons and spines correspond to synapses (Mishchenko *et al.*, 2010). Although powerful, EM analysis is labor-intensive and faster methods involving fluorescence-based synapse labelling have been introduced to accelerate synaptic connectivity analyses. A functional synapse can be identified by the colocalization (or close apposition) of presynaptic and postsynaptic proteins, labelled via antibodies or genetically tagged by fusion with fluorescent proteins (Ahmari and Smith, 2002). However, unambiguous identification of synaptic partners is not possible with this method in brain areas where many synapses coexist, such as the mammalian cortex with more than 100,000 synapses/mm$^3$ (Binzegger et al., 2004).

#### 1.4.3.1 GFP Reconstitution Across Synaptic Partners (GRASP)

GRASP was introduced for the *bona fide* identification of synaptic connectivity even in brain areas with high synapse density. This tool is based on splitting GFP into two parts which are independently expressed in separate gene constructs and are stable, but unable to fluoresce (Cabantous et al., 2005). Strikingly, if the two parts are close enough, full GFP can be reconstituted, and fluorescence emission is restored. Of note, the radius of interaction for GFP

reconstitution is in the order of around 20 nm and matches the size of the synaptic cleft (Figure 1.14a) (Feinberg *et al.*, 2008; Kim *et al.*, 2011). More in detail, one fragment of the split-GFP includes strands 1-10 of the GFP β-barrel structure, consisting of the initial 214 residues. The remaining 16 residues (215-230), which make up the 11$^{th}$ strand, are contained in the second fragment. (Feinberg *et al*. 2008; Kim *et al.*, 2011). GRASP labels existing synapses without causing spurious synapse formation or inappropriate reconstitution at non-synaptic regions (Feinberg *et al.*, 2008; Kim *et al.*, 2011).

The *in vivo* feasibility and accuracy of GRASP were initially established in *Caenorhabditis elegans*, which has the advantage of a well-defined synaptic connectome (Feinberg *et al.*, 2008), to be later adapted to more complex systems, such as the mouse. mGRASP (Figure 1.14a), optimized for mammalian synapse detection, revealed spatially non-uniform and clustered synaptic connectivity patterns for the excitatory CA3 input to CA1 pyramidal neurons in the hippocampus (Kim *et al.*, 2011; Druckmann *et al.*, 2014). Such connectivity patterns are thought to be effective in generating dendritic spikes, thereby enhancing synaptic plasticity and storage capacity (Poirazi et al., 2003).

The great advantage of GRASP is that the synaptic connectivity between two specific populations of neurons can be examined by restricting (genetically or spatially) the expression of individual GRASP components to the corresponding neurons (Kim *et al.*, 2011; Choi *et al.*, 2018). Recently, Choi et.al exploited a dual-eGRASP system (GRASP in two different colors) to study the CA3-CA1 synaptic connectivity among cFos-expressing putative engram and non-engram neurons (Figure 1.14b) (Choi *et al.*, 2018). Yellow eGRASP and Cyan eGRASP labelled the synapses formed between CA1 neurons and putative engram or non-engram CA3 neurons. Selective expression of yellow eGRASP components in putative engram neurons of the CA3 and CA1 regions was achieved through the *c-fos* promoter and Tet-ON system. Cyan GRASP was expressed in a non-activity-restricted fashion by Cre-dependent recombination under the control of the CaMKII promoter. The eGRASP system identified a significant increase in the number and size of spines on putative CA1 engram cells receiving input from putative CA3 engram cells 48 h after contextual fear conditioning (Choi *et al.*, 2018). This learning-associated enhanced synaptic connectivity between putative engram neurons correlated with memory strength, emphasizing the importance of connectivity between engram neurons for memory formation.

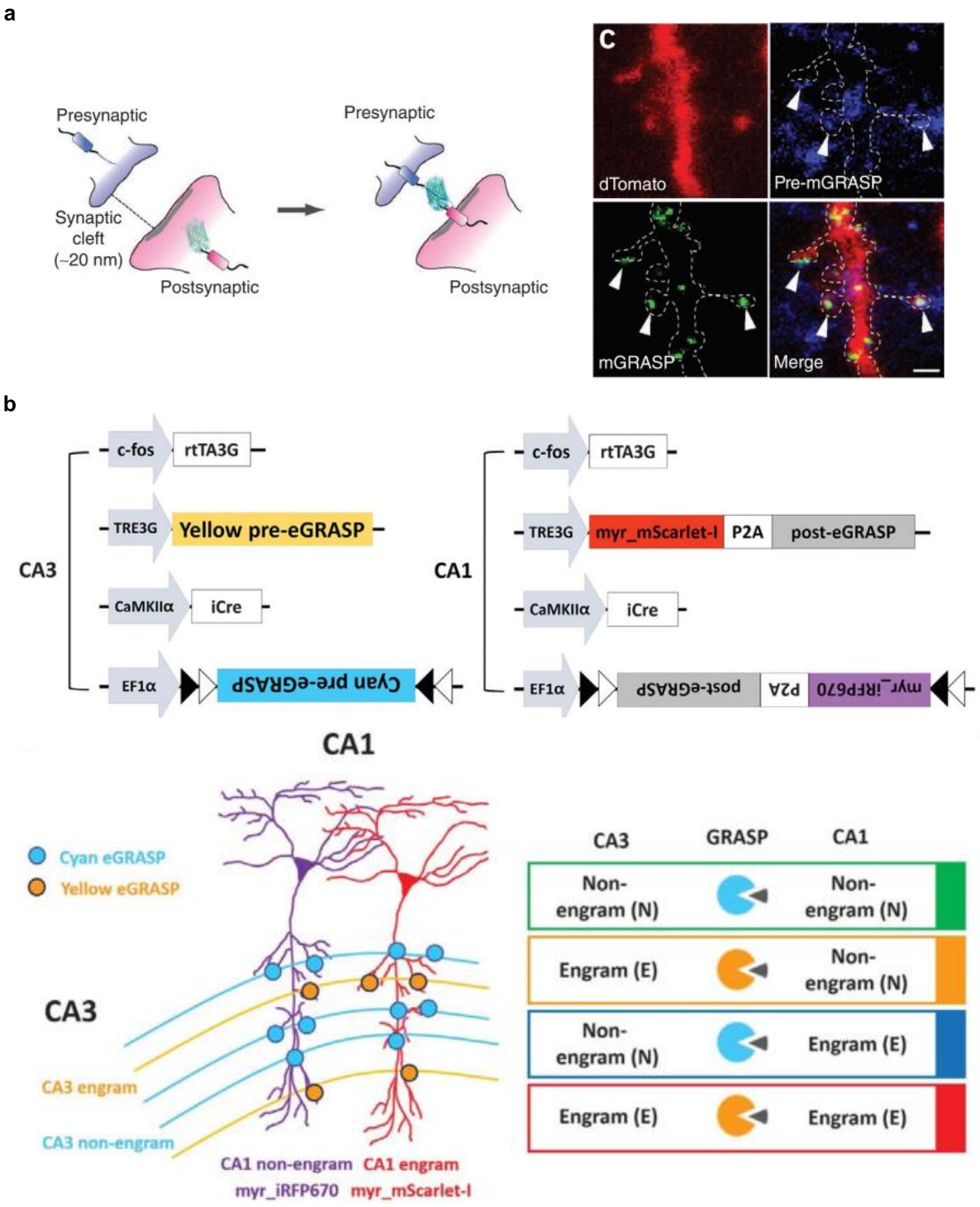


**Figure 1.14 GRASP enables mapping synaptic connectivity.**

(**a**) GRASP (GFP Reconstitution Across Synaptic Partners) expresses split-GFP components separately in presynaptic and postsynaptic neurons, and a full GFP is reconstituted at the synapses. mammalian optimized GRASP (green) detects synapses between CA3 (blue) and CA1 (red) neurons in the mouse hippocampus (adapted from Kim *et al.*, 2011). (**b**) dual-eGRASP system (GRASP in two different colors)

labels the CA3-CA1 synapses among c-Fos-expressing putative engram (yellow) and non-engram neurons (cyan) (adapted from Choi et al. 2018).

### 1.4.4 Synapse manipulation

Observational studies using the tools explained in the above section established a correlation between synaptic plasticity and memory. However, to prove that the synapses modified during learning are indeed the core substrate of memory, it must be shown that the functional alteration of those synapses will interfere with memory expression. Artificial activation of the subset of synapses that were potentiated during learning should be sufficient to induce the recall of the corresponding memory. On the contrary, ablation or reducing the synaptic efficiency of memory-associated synapses should delete or inhibit memory expression. With the advent of optogenetics and chemogenetics, putative engram manipulation at the level of neurons could be achieved (Josselyn and Tonegawa, 2020). However, an engram neuron can support multiple memories at different synaptic locations (Abdou *et al.*, 2018). So, we need new tools for synapse-specific manipulation that modulate only the memory associated with those synapses, without disturbing the identity and storage of others (Hayashi-Takagi *et al.*, 2015).

Hayashi-Takagi *et.al* introduced a genetic tool that allows to tag and delete potentiated synapses (Hayashi-Takagi *et al.*, 2015). Exploiting the activity dependency of *Arc* promoter and *Arc* UTRs, and synaptic localization of truncated PSD95 (PDZ1,2 deleted PSD95), a photoactivatable version of Rac1 protein (AS-PaRac1) was expressed in the potentiated spines (Figure 1.15a). Since prolonged activation of Rac1 is known to induce spine shrinkage, potentiated spines can be permanently deleted by optical activation of AS-PaRac1 (Figure 1.15b) (Luo *et al.*, 1996; Hayashi-Takagi *et al.*, 2015). Hayashi-Takagi *et.al* tagged the potentiated spines in the motor cortex with AS-PaRac1 when the animals were undergoing training on a beam task. Deletion of labelled spines by optical activation of AS-PaRac1 impaired performance (latency to fall in beam/rotarod) in the beam task, but not in the rotarod task (Figure 1.15c) (Hayashi-Takagi *et al.*, 2015).

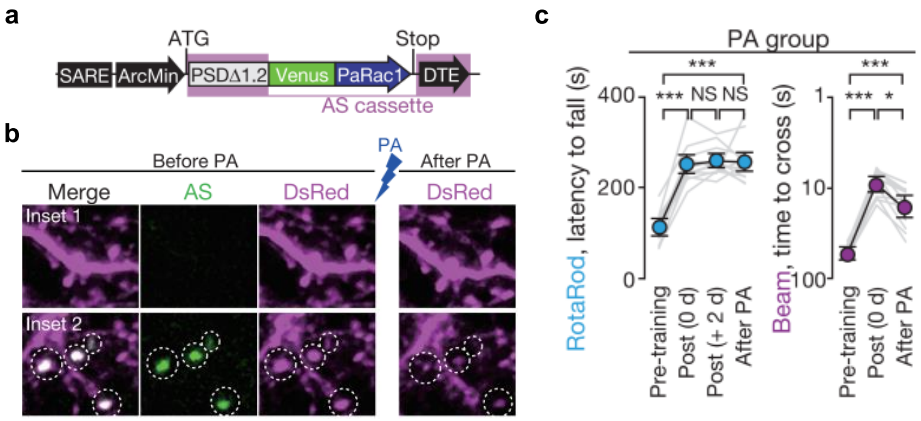


**Figure 1.15 Optical erasure of learning-induced potentiated synapses.**

(**a**) Diagram of AS-PaRac1 construct that expresses a photoactivatable version of Rac1 (PaRac1) selectively in potentiated spines. SARE-ArcMin and DTE regulate activity-dependent expression, and PSDΔ1.2 (PDZ1,2 deleted PSD95) promotes synaptic localization. (**b**) Photoactivation of PaRac1 selectively deletes AS-PaRac1-positive spines (green) in the motor cortex, tagged during motor task training. (**c**) Optical erasure of beam task-evoked potentiated spines impairs the performance (latency to fall in beam/rotarod) in beam task, but not in rotarod task. (Adapted from Hayashi-Takagi *et al.*, 2015).

Recently, we developed a novel genetic tool termed 'SynActive', that allows genetic labeling of synapses potentiated during a short time window (Figure 1.16a) (Gobbo *et al.*, 2017; Gobbo and Cattaneo, 2020). SynActive is based on 3 elements: 1) the doxycycline-dependent TRE promoter, 2) 5' and 3' UTRs (untranslated regions) extracted from the *Arc* mRNA, and 3) an optional synapse localization signal. These elements are used to drive and control the expression of any protein of interest, including fluorescent reporters and optogenetic actuators. TRE-mediated transcription requires the binding of the tetracycline-dependent transactivator (tTA). Use of the normal or reverse (rtTA) tTA variants determines the effect of doxycycline (Dox) administration on transcriptional activation (TetOFF or TetON, respectively). In addition to regulation of the time window for SynActive expression using Dox, specific promoters restrict the expression of (r)tTA to specific cell populations. The *Arc* mRNA is known to be transported into the dendrites with the help of Dendrite Targeting Elements (DTEs) of the 3' UTR and locally translated in response to synaptic activity using IRES (internal ribosome entry site) – like activity of 5'UTR and translation regulation by 3'UTR (please see section 1.2.5.1 and Figure 1.3) (Steward *et al.*, 2015). Thus, by including 5' and 3' UTR of Arc, the translation of SynActive-controlled proteins can be restricted to dendritic segments close to a potentiated synapse. As the local translation typically occurs at the foot of the spine, a synapse localization signal (such as PSD-95 PDZ domain binding peptide

ETQV and NMDAR C terminal sequence SIESDV, referred to as SYNtag) can be employed to target the newly translated protein at the potentiated spine head. This sequence is not necessary if proteins (or their fragments) natively localized at synapses are expressed under SynActive control.

We exploited the SynActive method to express channelrhodopsin2 tagged with mCherry and SYNtag (SA-ChR) selectively at potentiated spines (Gobbo *et al.*, 2017). In primary neuron cultures, SA-ChR expression (visualized using mCherry) was significantly increased in response to chemically induced LTP and decreased when NMDARs were inhibited by D-AP5. SA-ChR-positive spines were indeed potentiated, as they correlated with a rise in spine volume and surface AMPAR (labeled using SEP-GluA1). Interestingly, when LTP was induced focally by glutamate uncaging, SA-ChR labelled only stimulated spines and not the neighboring ones, suggesting input specificity. *In vivo*, SA-ChR (visualized using mCherry) labelled potentiated spines in the hippocampal CA1 and DG, following a novel context exposure (Figure 1.16b) (Gobbo *et al.*, 2017). SA-ChR-positive spines were closer to each other and showed a clustered distribution along the dendrites.

ChR expressed selectively at the potentiated spines using SynActive was functional and can be optically activated to drive synaptic currents as well as global neuronal activation (Gobbo *et al.*, 2017). By performing learning in the presence of dox, it is possible to tag the spines potentiated during the encoding phase with SA-ChR. If these tagged synapses support the storage of the memory, their optical activation at later time points should be sufficient to induce memory retrieval.

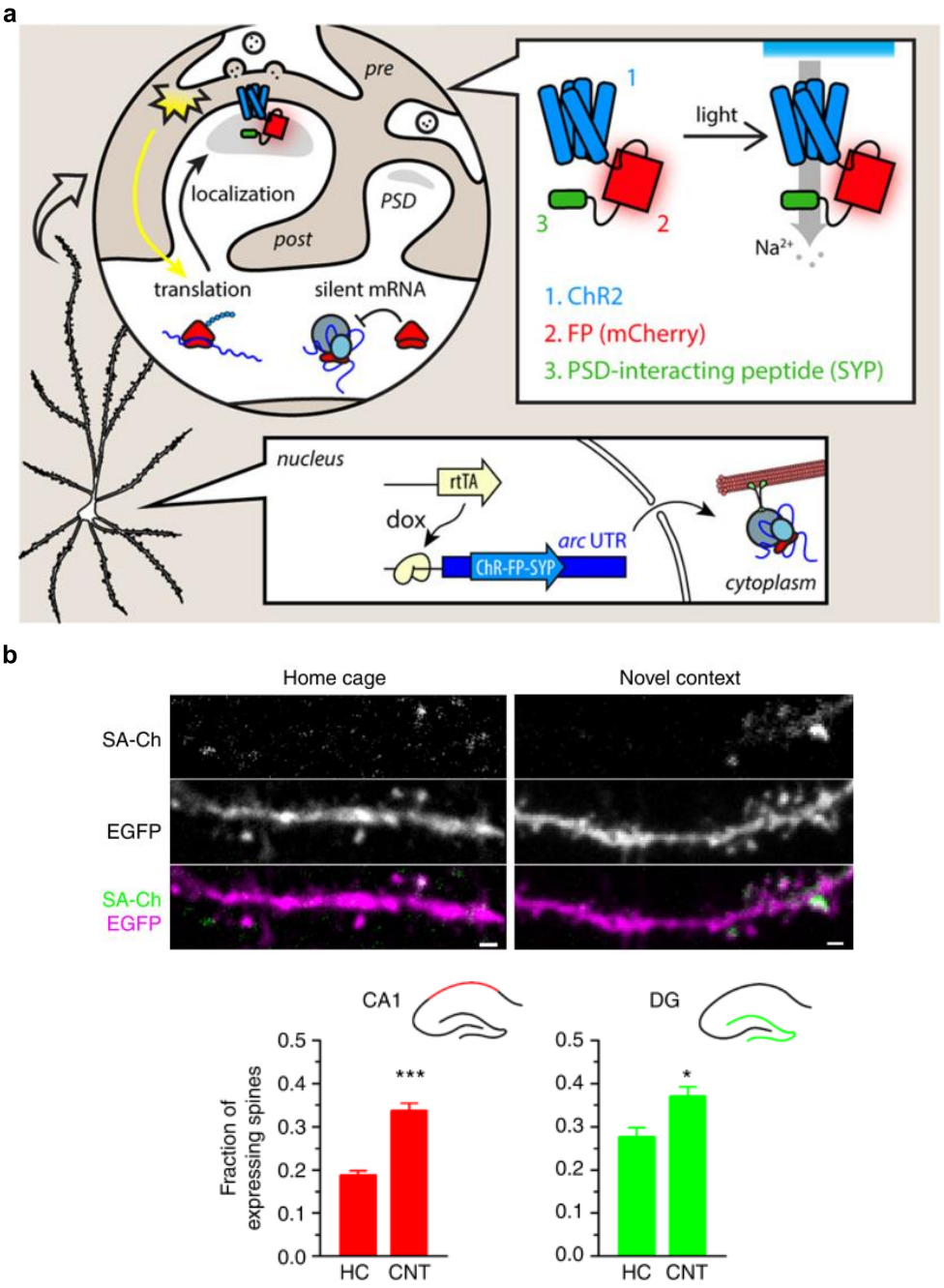


## Figure 1.16 SynActive to tag and activate potentiated spines.

(**a**) Schematics showing the activity-dependent expression of SynActive. Doxycycline induces the synthesis of SynActive mRNAs carrying the coding sequence (eg. Channelrhodopsin2 (ChR2) fused to mCherry (FP) and PSD interacting peptide (SYP)) and *Arc* 5' and 3' untranslated regions (UTRs). SynActive mRNAs are then transported to dendrites and translated in response to synaptic potentiation. SYP facilitates ChR2 enrichment at potentiated synapses, visualized via FP. (Adapted from Gobbo and Cattaneo 2020). (**b**) Compared to home cage (HC) animals, novel context exposure (CNT) increases the density of SynActive-positive potentiated spines (SA-Ch) in CA1 and DG regions of the hippocampus (adapted from Gobbo *et al*. 2017).

## 1.5 Systems consolidation and synaptic plasticity

The representation of a memory in the brain network can undergo time-dependent reorganization, a process referred to as system consolidation (Frankland and Bontempi, 2005). In rodents, pharmacological or optogenetic inhibition of the hippocampus during memory retrieval impairs recall of recent, but not remote memories (Tonegawa et. al., 2018). On the contrary, retrieval of remote but not recent memory was impaired by the inactivation of the medial prefrontal cortex (mPFC) or anterior cingulate cortex (ACC) (Tonegawa et. al., 2018). This suggests that episodic memories initially encoded in the hippocampus are transferred to a more stable memory in the cortical regions over time. Recently, the immediate early gene-based putative engram capture strategies have been used to study the nature and dynamics of neurons activated during the encoding phase at recent and remote time points (Kitamura et al., 2017;). mPFC neurons tagged during the learning were reactivated only at remote recall and their spine density increased with time, indicating rapid generation of putative engram neurons in mPFC during learning and their functional maturation with time. Hippocampal neurons tagged during the learning showed an opposite pattern; they were reactivated only at recent recall and their spine density decreased with time to become silent.

Although synaptic plasticty and memory are correlated, how it links to the systems consolidation is not very clear. Using a novel optogenetic tool to selectively erase LTP within a defined time window Goto *et. al.* have identified distinct plasticity events that underline the early phase of memory consolidation (Goto *et al.*, 2021). The first round of hippocampal LTP, which occurs immediately after learning, establishes the selectivity of neuronal firing to the shock context in a fear conditioning paradigm. Synchronous neuronal activity induced by the second round of hippocampal LTP during sleep further stabilizes the memory in the activated neurons. A third wave of LTP occurring in the ACC during sleep the following day facilitates system consolidation. Further development in the experimental techniques will improve our understanding of the cellular mechanism of systems consolidation.

## 2 AIMS OF THE PRESENT THESIS

Synaptic plasticity is essential for the encoding of new information and its subsequent retrieval at later time points. This has been substantiated by studies that showed pharmacological or genetic interference of synaptic plasticity resulted in memory impairment (Morris *et al.*, 1986; Silva *et al.*, 1992; Tsien *et al.*, 1996; Takeuchi *et al.*, 2014; Dringenberg 2020). Synaptic plasticity mechanisms such as LTP are characterized by an increase in synaptic efficiency, which requires protein synthesis for persistent expression and involves immediate early genes (IEGs) (Baltaci *et al.*, 2019). Current experimental strategies utilize IEGs to tag and manipulate neurons activated during learning and to classify them as part of cellular memory engrams (Josselyn and Tonegawa 2020). Although successful, they are limited with cellular level resolution and cannot identify the subset of synapses that have undergone learning-induced synaptic plasticity. Techniques commonly used *in vitro* to study the structural and functional properties of individual synapses are not suitable for investigating synapses specifically associated with a memory.

My Ph.D. thesis is aimed at exploiting 'SynActive' to investigate which subset of synapses out of the many thousands received by any given neuron is responsible for representing memory elements. The specific objectives are as follows:

**Aim 1**: Develop 'SynActive-eGRASP' to label synapses potentiated following a learning task in a circuit-specific fashion.

We have so far successfully employed SynActive to label spines potentiated in response to LTP induction *in vitro* and novel context exposure *in vivo* (Gobbo *et al.*, 2017; Gobbo and Cattaneo 2020). However, the identity of the presynaptic neuron forming synapses with potentiated spines was not known. GRASP reliably labels synaptic contacts in the mammalian brain and has been recently used to study the connectivity between putative engram neurons in CA3 and CA1 (Kim *et al.*, 2011; Choi *et al.*, 2018). Thus, I sought to combine SynActive and GRASP to investigate the properties and distribution of potentiated synapses between two specific neuronal populations.

**Aim 2**: For brain-wide mapping of potentiated spines, improve the synaptic localization of fluorescent proteins expressed using SynActive. As an extension, to label two rounds of synaptic potentiation (e.g., encoding and recall) modify SynActive to express fluorescent proteins that change the emission spectra over time (e.g., DsRED-E5).

**Aim 3**: Proteomic studies that tried to obtain learning associated changes in synaptic protein pool had technical drawbacks since they included both potentiated and non-potentiated synapses for analysis (Kähne *et al*. 2012; Rao-Ruiz *et al*. 2015; Dieterich and Kreutz 2016). To overcome this limitation, I designed a construct to express PSD95 (a major scaffolding protein of excitatory synapses) tagged with FLAG specifically at *in vivo* potentiated spines using SynActive. Subsequent affinity purification of PSD95-FLAG should allow characterization of the potentiation-specific protein content of synapses.

**Aim 4**. Reactivation of potentiated spines could be achieved, in principle, by expressing Channelrhodopsin specifically at potentiated spines using SynActive and optically activating them at later time points. We found that the photocurrents produced at potentiated spines were too low for affecting neuronal spiking, which would make it very unlikely to have any effect on memory recall (Gobbo *et al*. 2017). To circumvent this issue, I worked on generating SynActive constructs carrying Channelrhodopsin variants with higher photocurrents and faster kinetics.

# 3 MATERIALS AND METHODS

## 3.1 Gene Constructs

Constitutive (Const)-post-eGRASP (Addgene 111584) was previously described in (Choi *et al.*, 2018). SynActive-post-eGRASP was constructed by sequentially cloning the third-generation TRE promoter (TRE3g), activity-regulated cytoskeleton-associated protein *(Arc)* 5' untranslated region (UTR), myristoylated(myr)-mScarlet-P2A-post-eGRASP, *Arc* 3' UTR and short poly(A) signal (spA) into the parental AAV plasmid pAAV-human synapsin promoter(hSyn)-EGFP-WPRE-pA (Addgene 50465), between inverted terminal repeats (ITRs). Sequences of TRE3g, 5'*Arc* UTR and 3'*Arc* UTR are as described in (Gobbo *et al.*, 2017). myr-mScarlet-P2A-post-eGRASP was PCR amplified from the Const-post-eGRASP plasmid. spA (consisting of the upstream sequence element and full late polyadenylation signal sequence of SV40) was derived from pAAV-CW3SL-EGFP (Addgene 61463). To insert pre-eGRASP in the pAAV backbone (pAAV-TRE3g-preGRASP-WPRE-pA), hSyn-EGFP in the parental plasmid was replaced with TRE3g and preGRASP (amplified from Addgene 111598). Const-cyan-pre-eGRASP and Const-yellow-pre-eGRASP contained GFP1-10 mutant versions described in (Choi *et al.*, 2018)(Addgene 111586, 111587). All pre-eGRASP constructs used p32 (SPSYSPPPPP) as the Abl SH3-binding peptide. (Alternative version of pre-eGRASP containing Abl SH3-binding peptide with low binding affinity, p30 (APTKPPPLPP) exists)

To obtain PSD95Δ (i.e., rat PSD95 (NM_019621) deleted of the portion comprised within 250-993 bp (corresponding to AA 84-331) as described in (Hayashi-Takagi *et al.*, 2015), mutagenesis followed by PCR amplification and stitching was performed on FU-dio PSD95-mCherry-W (Addgene 73919). SynActive-PSD95Δ-mVenus was generated by inserting PSDΔ in frame with Venus and HA tag, between the *Arc* 5' and 3' UTRs of the SynActive plasmid.

DsRED-E5 was amplified from the plasmid ESARE-DsRED-E5 (a gift from CM Alberini, New York University). The synaptic tagging oligopeptide (SYNtag) described in (Gobbo *et al.*, 2017) was attached to its C-terminus by overhang PCR. To construct SynActive-DsRED-E5, DsRED-E5-SYNtag was cloned in between the *Arc* 5' and 3' UTRs of the SynActive plasmid. Similarly, SynActive-ChR2XXM-mVenus was generated by inserting channelrhodopsin2-XXM (Scholz *et al.*, 2017) fused to mVenus.

The SynActive-PSD95-FLAG construct consists of the ESARE promoter, mouse PSD95, TAP tag, *Arc* 3' UTR and spA, flanked by ITRs. The synthetic ESARE promoter described in (Kawashima *et al.*, 2013) was constructed by synthesizing SARE-ArcMin promoter as gBlocks Gene fragment (Integrated DNA Technologies) and multiplexing the SARE enhancer fragment (-6793 to -6690; +1 denotes the transcription initiation site) to obtain 5×SARE-ArcMin. The mouse PSD95 coding sequence was amplified from PSD95-TS: YSOG1 (Addgene 42226). The TAP tag (Histidine affinity tag (HAT), TEV protease, and FLAG) sequence described in (Fernández *et al.*, 2009) was synthesized as gBlock Gene fragment (Integrated DNA Technologies). To create Const-PSD95-FLAG, EGFP from the parental pAAV-hSyn-EGFP plasmid was replaced with mouse PSD95-TAP.

"Filler" constructs were generated by cloning rtTA-P2A and a fluorescent protein (tdTomato, mTurquoise2, Chronos-mScarlet-I, Chronos-EGFP) inbetween hSyn promoter and WPRE of the parental AAV plasmid. To yield rtTA-P2A, rtTA2S-M2 was amplified from the plasmid described in (Gobbo *et al.*, 2017) and P2A sequence was attached to its C-Terminus by overhang PCR. For constructing filler with IRES, rTA and IRES-tdTomato were used.

(Please see also Appendix for sequences of the constructs)

### 3.2 Cell culture

Primary neuronal cultures were established as described previously (Gobbo *et al.*, 2017). Briefly, hippocampi and cortices were micro dissected from P0 B6/129 mice and cut into small pieces in ice cold $Ca^{2+}$-free Hank's balanced salt solution (HBSS) supplemented with 1% penicillin-streptomycin. Pooled hippocampi or cortices from 4-6 mice were then digested in 0.1% trypsin (Gibco), incubated in 37°C water bath for 20min with occasional agitation. To inactivate trypsin an equal volume of Dulbecco's modified Eagle's medium (DMEM, Euroclone®) with 10% fetal bovine serum (FBS, Euroclone®) and 20 μg/ml DNase (Sigma-Aldrich®) was added and triturated with 10 ml plastic pipettes. Dissociated neurons were pelleted by centrifugation at 1000 rpm for 5 min, followed by resuspension in neuron plating medium (Neurobasal-A medium (Gibco) supplemented with 4.5 g/L D-glucose (Sigma-Aldrich®), 10% FBS (Euroclone®), 2% B27 (Gibco), 1% L-glutamine, 1 mM sodium pyruvate, 12.5 μM glutamate (Sigma-Aldrich®). Neurons were plated on 13 mm glass coverslips coated with Poly-D-Lysine (PDL, Sigma-Aldrich®) and placed on the bottom of 24-well plates, at a seeding density of $1\times10^5$ hippocampal

cells or $1.5\times10^5$ cortical cells per well. All cell culture plates were kept at 37°C, 5% $CO_2$ in a humidified incubator until the end of experiments. The day of plating was considered as day-in-vitro (DIV) 0. From DIV1, neurons were maintained in neuron culture medium (Neurobasal-A medium (Gibco) supplemented with 2% B27 (Gibco), 1% L-glutamine, 10 µg/ml gentamicin (Gibco), 12.5 µM glutamate (Sigma-Aldrich®; added only for the first change) with 150 µl/well medium refreshed every 2-3 days. To inhibit the proliferation of glial cells, 1-β-D-arabinofuranosylcytosine (Ara-C; Sigma-Aldrich®) to a final concentration of 2.5 µM was added to the wells on DIV2. Neurons were either transfected with Lipofectamine 2000 (Invitrogen) on DIV3 or infected with AAVs on DIV8. All experiments were done on mature neurons aged DIV14-16. If required, doxycycline (Sigma-Aldrich®, final concentration 1 µg/ml) was added to cultures the evening before the experiment. All procedures for primary neuronal culture were approved by the Italian Ministry of Health and was conducted in compliance with the European guidelines on the use of animals for research.

### 3.3 Transfection

Primary neuronal cultures were transfected using Lipofectamine 2000 (Invitrogen) according to the manufacturer instructions. The protocol followed for a well in a 24-well plate is as follows. The conditioned medium was collected from the well and neurons were washed with warm HBSS containing 2 mM $CaCl_2$ and 1 mM $MgCl_2$. Neurons were then placed back in the incubator after adding 400 µl of fresh neuron culture medium. For *in vitro* SynActive-eGRASP experiments, two separate transfection mixes were prepared: (A) Const-pre-eGRASP (0.5 µg) and tdTomato filler (0.5 µg) diluted in Opti-MEM (Gibco) to 25 µl, mixed with Lipofectamine2000 (1.5 µl) diluted in Opti-MEM to 25 µl. (B) SynActive-post-eGRASP or Const-post-eGRASP (0.5 µg) and mTurquoise2 filler (0.5 µg) diluted in Opti-MEM to 25 µl, mixed with Lipofectamine 2000 (1.5 µl) diluted in Opti-MEM to 25 µl. After incubation at room temperature for 5min, each transfection mix was separately added to same well, with incubation lasting for 2.5 h at 37°C. Finally, the transfection mix-containing medium was replaced with conditioned medium (350 µl) and fresh neuronal growth medium (150 µl). (Please see also Figure 4.2Figure 4.2).

For experiments using only one component of eGRASP (Figure 4.3), transfection mix without the eGRASP component contained 1 µg of filler. To optically activate neurons, Chronos-mScarlet-I filler was used in the transfection mix (A) instead of tdTomato filler. For AMPAR and NMDAR

enrichment experiments (Figure 4.10), mTurquoise2 filler and tdTomato filler was used along with the pre-synaptic and postsynaptic GRASP component, respectively. The combination of constructs used for SynActive-eGRASP color variants are: (A) Const-Yellow-pre-eGRASP and tdTomato filler, (B) SynActive-post-eGRASP and mTurquoise2 filler; (A) Const-Cyan-pre-eGRASP and Chronos-EGFP filler, (B) SynActive-post-eGRASP and tdTomato filler ().

Single transfection mix - SynActive-DsRED-E5 (1 µg) and mTurquoise2 filler (1µg) diluted in Opti-MEM to 50 µl and mixed with Lipofectamine 2000 (3 µl) diluted in Opti-MEM to 50 µl, was used for experiments described in (Figure 4.22). SynActive-ChR2XXM-mVenus was transfected using calcium phosphate as described in Gobbo *et al*. 2017.

### 3.4 Infection

On DIV8, the conditioned medium (150 µl/well) was replaced with fresh neuron culture medium (150 µl/well) containing AAVs (serotype 2/5) for SynActive-PSD95Δ-mVenus ($10^9$ viral genomes (vg)/well) and tdTomato filler (hSyn-rtTA-IRES-tdTomato, $10^9$ vg/well). Routine partial media change was performed every 2-3 days. For *in vitro* proteomics experiments AAVs used were SynActive-PSD95-FLAG ($10^9$ vg/well) or Const-PSD95-FLAG ($10^9$ vg/well). AAVs were generated by the AAV Vector Unit at the International Centre for Genetic Engineering and Biotechnology (ICGEB) Trieste following a protocol as previously described (Arsic *et al.*, 2003).

### 3.5 Treatments

Glycine-mediated chemical LTP (Gly-cLTP) was induced in cultured hippocampal neurons as described in Lu et al. (2001). Briefly, conditioned medium was collected, and the neurons were initially incubated in extracellular solution (ECS, pH 7.4, containing 140 mM NaCl, 1.3 mM $CaCl_2$, 5 mM KCl, 25 mM HEPES, 33 mM D-glucose, 0.5 µM tetrodotoxin (TTX, Tocris BioSciences), 1 µM strychnine (Sigma-Aldrich®) and 50 µM picrotoxin (PTX, Tocris BioSciences) at 37°C for 30 min. The solution was then replaced with ECS containing 200 µM Glycine (Sigma-Aldrich®) to induce LTP. After 3 min, the solution was switched back to normal ECS and neurons were incubated at 37°C for another 30 min. Finally, ECS was removed, and conditioned medium aspirated at the beginning of the experiment was added back to each well. The neurons then remained in the 37°C incubator until fixation at 24 h post Gly-cLTP (6, 24 or 48 h for SynActive-DsRED-E5 time course experiment; Figure 4.23). In the experiments to block

NMDAR-mediated LTP, D-2-amino-5-phosphonovaleric acid (D-AP5, Sigma-Aldrich®, final concentration 50 µM) was added to the cultures along with doxycycline and fixed after 36 h. In the optoLTP control experiments, 0.5 µM TTX was added along with the D-AP5. For KCl-induced depolarization, neurons were placed in conditioned media containing 10 mM KCl and fixed after 90 min. See also (Figure 4.2) for treatments timelines.

### 3.6 Fixation

After 2 washes with warm HBSS containing 2 mM $CaCl_2$ and 1 mM $MgCl_2$, 4% Paraformaldehyde in PBS was added to neuronal cultures and incubated at room temperature for 10 min. Then, neurons were washed thrice in PBS and once in water. Glass coverslips with fixed neurons were then mounted directly or after immunofluorescence using Fluoroshield with DAPI (Sigma-Aldrich®) or Vectashield antifade (Vector Laboratories) mounting media.

### 3.7 Immunofluorescence

After fixation, neurons expressing SynActive-eGRASP or Const-eGRASP were permeabilized in 0.1% Triton X-100, 2.5% bovine serum albumin (BSA) PBS for 7 min, followed by five washes with PBS and blocking in 5% BSA PBS for 1 h. Neurons were then incubated with primary antibodies in 2.5% BSA PBS for 2-3 h at room temperature. The primary antibodies used were: mouse monoclonal PSD95 antibody (Synaptic Systems 124011, 1:500), mouse monoclonal Synaptophysin1 antibody (Synaptic Systems 101011, 1:500), rabbit monoclonal GluA1 antibody (Cell signaling 13185, 1:500) and rabbit polyclonal GluN2A/B antibody (Synaptic Systems 244003, 1:500). After washing thrice with PBS, neurons were incubated with secondary antibodies, anti-rabbit-647 (Invitrogen) or anti-mouse-647 (Invitrogen), in 2.5% BSA PBS for 1 h at room temperature. Neurons were finally washed thrice in PBS and once in water and mounted.

For the proteomics experiment, primary antibodies used were- anti-FLAG (rabbit, 1:1600, Cell Signaling 14793) and anti-MAP2 (mouse, 1:2000, abcam ab5392), and secondary antibodies used were anti-rabbit-488 (Invitrogen) and anti-mouse-555 (Invitrogen).

### 3.8 Optogenetics

For inducing LTP by optogenetics, conventional electrically induced TBS protocol was adapted to optogenetic stimulation (optoLTP; 12 bursts of 4 blue (470-nm) light pulses delivered

at 100Hz, separated by 200ms, and repeated 3 times with an interval of 10s) (Testa *et al.*, 2019). The light pulses were delivered using a 470-nm light-emitting diode (LED, Thorlabs), connected to a DC2200 LED driver (Thorlabs) and Digidata 1322A digitizer (Molecular Devices), and controlled via Clampfit 10.7 (Molecular Devices). During optoLTP neuronal cultures remained in ECS without TTX.

For patch-clamp recordings, coverslips containing the neuronal cultures were transferred to a submerged chamber continuously perfused with Tyrode's solution containing (in mM): NaCl 150, KCl 4, $MgCl_2$ 1, $CaCl_2$ 4, D-glucose 10, and HEPES 10 (pH 7.4) with NaOH at 32°C saturated with O2 (Siano *et al.*, 2019). Borosilicate glass pipettes were pulled with a P-97 puller (Sutter, CA) to a resistance of 5–6 MΩ when filled with an internal solution containing (in mM): K-gluconate 145, $MgCl_2$ 2, HEPES 10, EGTA 0.1, Mg-ATP 2.5, Na-GTP 0.25 and phosphocreatine 5 (pH 7.35) with KOH. Excitatory postsynaptic currents (EPSCs) evoked with short pulses of 470-nm light were recorded while holding the neuron at a command potential of – 70 mV. Neurons were held at 0 mV during optoLTP. Data were acquired using a MultiClamp 700A amplifier, connected to a Digidata 1322A digitizer (Molecular Devices), and analyzed using Clampfit (Molecular Devices).

### 3.9 Microscopy

Z-stack images (1024 x 1024 pixels, 8-bit, 0.4 µm z-step) of neuron cultures expressing SynActive-eGRASP were acquired with a Leica TCS SP2 confocal microscope using an oil objective (HCX PL APO 63×/1.4 numerical aperture (NA)). To avoid spectral crosstalking, sequential illumination with 488 nm (emission range 500-550 nm), 543 nm (emission range 555-700 nm) and 458 nm (emission range 465-495 nm) was used for eGRASP, tdTomato (+ mScarlet-1) and mTurquoise2, respectively. SynActive-eGRASP images in Figure 4.9 Figure 4.10 were acquired with Leica TCS SP5 (oil objective - HCX PL FLUOTAR 100.0×/1.3 NA) and Zeiss LSM 800 (oil objective - Plan-Apochromat 63×/1.4 NA DIC M27) confocal microscopes.

SynActive-DsRED-E5 images were acquired with a Leica TCS SP2 confocal microscope. The emission and excitation settings for green, red, and blue channels were same as those used for SynActive-eGRASP. For high-magnification images of SynActive-DsRED-E5, a Zeiss LSM 800 confocal microscope (in Airy Scan mode) was used with laser lines set to 561 nm, 488 nm and 405 nm for DsRED-E5-red, DsRED-E5-green and tag-BFP, respectively. SynActive-PSD95Δ-

mVenus and SynActive-ChR2XXM-mVenus images were acquired with a Leica TCS SP5 confocal microscope.

### 3.10 Image analysis

Signal overlap or apposition of a presynaptic tdTomato axon with a postsynaptic mTurquoise2 dendrite was considered as a synapse. For each experimental condition, the number of synapses in a neuron was counted manually using ImageJ cell counter plugin and calculated the percentage of synapses with a Const-/SynActive-eGRASP signal. Neurons with less than 10 synapses were excluded from the analysis. For colocalization analysis, intensity profile of a line ROI drawn from the spine head to the dendritic shaft was obtained from a maximum intensity projection image. Intensity profile was then normalized by subtracting the minimum intensity and dividing by the intensity range. To obtain the final representative plot, the normalized intensity profiles from all synapses were averaged at each distance, after aligning based on the maximum green intensity. To calculate percentage of colocalization, number of Const-/SynActive-eGRASP puncta overlapped with PSD95 (or in close apposition to synaptophysin) was normalized to the total number of Const-/SynActive-eGRASP puncta. For AMPAR and NMDAR enrichment analysis, circular ROIs of radius approximately equal to the spine head were drawn over the spines with Const-/SynActive-eGRASP signal. Background subtracted integrated AMPAR (or NMDAR) intensity was then calculated for each ROI. Background intensities were obtained from the spine ROIs translated in x/y to a nearby region. Volume of a spine was calculated using the formula, $\frac{4}{3}\pi r^3$, where $r$ is the radius of the corresponding spine ROI.

For time-course analysis of SynActive-DsRED-E5 analysis, ROIs were drawn over all spines of a neuron. Spines with red and green average intensity 2 times greater than the average background was considered as positive for red and green SynActive-DsRED-E5, respectively. Background subtracted average intensity of SynActive- DsRED-E5-positive spines was used for the intensity plot in (Figure 4.23).

For representative images shown in the figures, maximum intensity projection of acquired confocal images were cropped, background subtracted (rolling ball algorithm) and intensity linearly adjusted using ImageJ.

### 3.11 Stereotaxic surgery

C57BL/6J mice (2-4 months old males/females) were anaesthetized with intraperitoneal injection of ketamine (100mg/kg)/xylazine (10mg/kg) solution and positioned in a stereotaxic apparatus. During all the procedures animal body temperature was maintained constant at 36°C using a closed loop temperature control system (Harvard apparatus). After making an incision on the head, a craniotomy was performed using a dental drill at stereotaxic coordinates: Right CA3 (anteroposterior (AP) -1.75 mm relative to bregma, mediolateral (ML) 2.35 mm relative to bregma, and dorsoventral (DV) -1.675 mm below the brain surface) and Left CA1 (AP -1.80 mm, ML -1.5 mm, DV -1.3 mm). 0.5 µl of viral suspension was then injected into the target region at a rate of 0.1 µl/min, using a heat-pulled glass micropipette (BLAUBRAND® intraMARK) attached to a CellTram 4r Oil (Eppendorf) manual microinjector. The viral suspensions contained: right CA3 - Const-pre-eGRASP ($0.95 \times 10^9$ viral genomes (vg)/µl) and mTurquoise2 filler ($3.05 \times 10^9$ vg/µl); left CA1 - SynActive-post-eGRASP ($1.52 \times 10^9$ vg/µl) and tdTomato filler ($0.74 \times 10^9$ vg/µl). All AAVs used for the injection belonged to the 2/PHP.eB serotype and were produced by InnovaVector (Naples) from our endotoxin-free pAAV plasmid MaxiPreps. To prevent backflow of the injected viral suspension, the micropipette stayed in place for another 10 min after injection and was slowly retracted. Following cleaning and suturing of the wound, animals were allowed to recover from anesthesia, then placed back to their home cages. Postoperative analgesia was obtained with oral treatment with paracetamol (100 mg/kg) for 3-5 days.

For proteomics experiments, 2-months-old C57BL/6J male mice were used and 1µl of viral suspension containing SynActive-PSD95-FLAG (AAV2/5, $5.4 \times 10^8$ vg/µl) or Const-PSD95-FLAG (AAV2/5, $4.7 \times 10^8$ vg/µl) was bilaterally injected into hippocampal CA1 (AP: -2.0 mm, ML ±1.9 mm, DV -1.4 mm).

### 3.12 Contextual fear conditioning

All behavioral experiments were performed 3-4 weeks after AAV injection. Mice were initially habituated to the fear conditioning chamber (Ugo Basile), composed of a Perspex box with electrified grid floor, with patterned stimuli attached to the walls to provide context information, housed inside a box of internal size – 39 × 47 × 48 cm. During the habituation session, following a 30-min acclimatization in the experimentation room, each mouse was introduced in the fear

conditioning chamber and allowed to explore it for 5 min. Two hours after the habituation, 150 µl of 10 mg/ml doxycycline solution dissolved in saline was delivered by intraperitoneal injection. Mice were fear-conditioned 24 h after the habituation. An additional dose of doxycycline was injected 2 h before the conditioning session. During the conditioning session, each mouse was kept in the conditioning chamber and seven 0.5 mA foot shocks of 1 s duration with 25 s inter-shock interval were delivered for a total duration of 3min, followed by an additional 2 min of permanence in the apparatus. Freezing behavior was automatically measured during the entire 5 min session. After fear conditioning, mice were returned to their home cage. Histological fixation via transcardial perfusion was performed 24 h later for SynActive-eGRASP analysis. The home cage group of mice was not exposed to habituation and fear conditioning but received two doses of doxycycline and was perfused analogously to fear conditioned mice. Mice belonging to the "No-doxycycline" group were exposed to fear conditioning in the absence of doxycycline. As a positive control, strong neural activity was induced with a low dose of the proconvulsant kainic acid (5 mg/kg), administered intraperitoneally 2 h after the second doxycycline injection.

Mice injected with SynActive-PSD95-FLAG, were sacrificed 3hr after the fear conditioning by cervical dislocation and fresh hippocampal tissue were harvested for immunoprecipitation and western blot analysis. Mice that received Const-PSD95-FLAG remained in home cage until the sacrifice and tissue harvest. Both groups of animals did not receive doxycycline.

### 3.13 Preparation of fixed brain section and confocal imaging

24 h after contextual fear conditioning, mice were overdosed with choral hydrate and transcardially perfused (using peristaltic pump (Gilson) at the rate of 18.5 ml/min) with PBS followed by 4% paraformaldehyde (PFA) in 0.1 M Phosphate buffer (PB, pH 7.4) to fix the tissue. Brains were then extracted, post-fixed in 4% PFA overnight at 4°C and cryoprotected in 30% sucrose in PB 0.1 M for at least three days at 4°C. Coronal sections (80µm) were cut with a sliding microtome (Leica SM2010 R Sliding Microtome) and mounted using VectaShield.

The hippocampal CA1 region was imaged with a Leica TCS SP2 confocal microscope (HCX PL APO 63×/1.4 NA oil objective, 2× digital zoom). The 8-bit z-stack images had a voxel size of 0.116 µm × 0.116 µm × 0.396 µm. The acquisition parameters were as in section 3.9. To cover the *strata oriens, pyramidale, radiatum* and *lacunosum-moleculare* of the CA1 region, 4 images with 10-20% overlap were sequentially acquired from each brain slice. High-resolution images of

SynActive-eGRASP shown in (Figure4.15) were acquired with Zeiss LSM 800 confocal microscope using Plan-Apochromat 63x/1.4 NA oil DIC M27 objective with 5-fold digital zoom. Image shown in (Figure4.12b) was acquired with Leica TCS SP2 confocal microscope using the objective HC PL APO 20.0x0.70 NA IMM UV.

### 3.14 Immunoprecipitation and Western blotting

For each sample, hippocampi from 2-3 animals injected with AAVs for SynActive-PSD95-FLAG (or Const-PSD95-FLAG) and underwent contextual fear conditioning (or remained in home cage) were homogenized in cold DOC buffer (500 µl/animal) (50 mM Tris pH 9.0, 1% sodium deoxycholate, 50 mM NaF, 1mM $Na_3VO_4$, 20 µM ZnCl, 1 tablet/10ml Complete Mini Protease Inhibitor Cocktail (Sigma) and 1 tablet/10ml PhosSTOP phosphatase inhibitor (Roche). After a 1 h incubation on ice, the extracts were clarified by centrifugation at 13,000g for 30 min at 4°C followed by incubation with Anti-FLAG M2 paramagnetic beads (Sigma M8823) (50 µl/animal) for 2 h at 4°C with constant agitation. The beads were washed thrice in DOC buffer without deoxycholate, and immunoprecipitated proteins were eluted from the beads by heating in elution buffer (50 µl/animal) (4% SDS, 100mM Tris-HCl pH 8.0) for 10 min at 90°C. The total protein concentration in the samples was quantified using Pierce™ BCA Protein Assay Kit (Thermo Scientific) according to manufacturer instructions.

Samples (2-10 µg) were subjected to SDS-PAGE on 10% house-made gels, transferred to Amersham Protran 0.45 NC nitrocellulose membrane (GE Healthcare Life science). After blocking in 5% skimmed milk (Bio-Rad) for 1 h, blots were incubated with primary antibodies overnight at 4°C with constant agitation. Blots were then washed thrice in TBST (Tris-buffered saline, 0.1% Tween 20) and incubated with horseradish peroxidase (HRP)-conjugated secondary antibodies for 1 hr at room temperature with agitation. The primary and secondary antibodies used were: mouse monoclonal anti-FLAG M2 antibody (1:1000, Sigma F1804), rabbit polyclonal GluN2A/B antibody (1:1000, Synaptic Systems 244003), rabbit monoclonal GluA1 antibody (1:1000, Cell signaling 13185), goat polyclonal CaMKII antibody (1:500, Thermofisher PA5-19128), rabbit monoclonal Arc antibody (1:1000, Cell signaling 65650), rabbit monoclonal S6 antibody (1:1000, Cell signaling 2217), rabbit polyclonal Histone H3 antibody (1:1000, Abcam 1791), mouse IgGk BP-HRP (1:2000, Santa Cruz 516102), mouse anti-rabbit IgG-HRP (1:2000, Santa Cruz 2357), mouse anti-goat IgG-HRP (1:2000, Santa Cruz 2354). Following three washes in TBST,

chemiluminescence signals from HRP were detetected using SuperSignal West Femto Maximum Sensitivity Substrate (Thermo Scientific) and ChemiDoc MP Imaging system (Biorad).

For the analysis, the optical density of the bands of interest was normalized to the optical density of either the corresponding band in the blot for the IP input material or of the bait protein PSD95-FLAG. Normalized values were further normalized to the average of Const-PSD95-FLAG, in each blot.

## *3.15* SynActive-eGRASP image analysis *in vivo*

### 3.15.1 Image stitching

Prior to analysis, overlapping confocal images were stitched together to form a single image, using the BigSticher software package available in ImageJ (Hörl et al. 2019). In the pre-alignment step, the relative positions of the image tiles were specified either by loading locations from a tile configuration file or by manually translating the images in the BigDataViewer window. The image tiles were then aligned automatically using a translation model based on the pixel intensities and fused to create a single 16 bit-image for each channel. Using a radius value greater than the largest object in the image (100 pixels for tdTomato, 10 pixels for mTurquoise2 and SynActive-eGRASP), rolling ball background subtraction (ImageJ plugin) was performed on all z-slices of each channel (Sternberg 1983). Finally, after converting to 8-bit, the 3 channels were merged to create a single z-stack image of RGB format and saved as a Tiff image. The three channels Red (R), green (G) and blue (B) channels corresponded to tdTomato, SynActive-eGRASP and mTurquoise2, respectively.

### 3.15.2 Tracing of dendritic segments

neuTube software was used for manually tracing the dendritic segments from the stitched images of the hippocampal CA1 region (Feng *et al.*, 2015). Each trace is a digital reconstruction of the dendritic morphology, saved in SWC format that consists of node number, type, 3D coordinates, diameter and parent node number (Cannon et al. 1998). A trace was obtained by connecting the nodes of appropriate diameter rightly positioned in x, y, and z on the dendritic segment. Before saving the trace in SWC format, node type was changed to 0 for all nodes. Using Vaa3D software, traces were then resampled with a step length of 1 to contain maximum possible number of tree nodes and sorted to keep the parent node most proximal to the stratum radiatum as

the root node - the first node in the tree (Iascone et al. 2020). Finally, the type of the root node was changed to 1 if it was soma or 5 otherwise. Dendrites in the stratum radiatum with at least one nearby SynActive-eGRASP was chosen for tracing and 4-12 such traces were made from each slice.

### 3.15.3 SynActive-eGRASP analysis

All the SynActive-eGRASP analysis were performed using custom-written codes in MATLAB. Initially green (SynActive-eGRASP) and blue (mTurquoise2) channels of the stitched images were loaded in the program, and the pixel intensity values were corrected for photo beaching in z-direction by multiplying with a bleach ratio, $\frac{\bar{I}_{max}}{\bar{I}_z}$ (*Miura et al*., 2020). The corrected pixel value,

$$I'_z(x,y) = \frac{\bar{I}_{max}}{\bar{I}_z} * I_z(x,y)$$

where $\bar{I}_z$ is the average blue intensity calculated for each z-slice and $\bar{I}_{max}$ is the maximum of $\bar{I}_z$ values. For the puncta detection, images were masked around each trace with a cuboid of 31 × 31 × 9 pixels (corresponding to 3.596 µm, 3.596 µm, and 3.564 µm in x, y and z respectively). SynActive-eGRASP signals from potentiated CA3-CA1 synapses and mTurquoise2 signals from CA3 presynaptic boutons were automatically detected using the puncta detection algorithms described in (Feng *et al*., 2012). The values for the puncta detection parameters $I_{min}$, $V_{max}$, and $V_{min}$ were empirically determined based on the criterion that false positives (image noise, over segmented puncta) and negatives (under segmented puncta) should be low. $V_{min}$ values used for SynActive-eGRASP and mTurquoise2 were 25 pixels and 50 pixels, respectively. $V_{max}$ was 115 pixels for both. For mTurquoise2, $I_{min}$ varied between the images, whereas $I_{min}$ = 30 was used for SynActive-eGRASP in almost all images. Finally, over segmentation errors were manually corrected by joining or deleting (only for mTurquois2) the detected puncta.

A SynActive-eGRASP puncta was considered as a true positive if the Euclidean distance between its centroid and the centroid of its nearest neighbor mTurquoise2 puncta was less than 2µm. For each trace, SynActive-eGRASP colocalized with mTurquoise2 was calculated as the percentage of true positives among the SynActive-eGRASP puncta detected. SynActive-eGRASP density and proportion was calculated by dividing the number of SynActive-eGRASP puncta by

pathlength of the dendritic trace (measured using neuTube) and number of mTurquoise2 puncta, respectively. The ratio of number of mTurquoise2 puncta to the dendritic trace pathlength gave the CA3-CA1 synapse density. To calculate SynActive-eGRASP puncta volume, number of voxels in a punctum was multiplied with the voxel volume (0.116 µm × 0.116 µm × 0.396 µm). For the plots shown in (figure4.18-20), values per mouse was obtained by averaging the values from all traces belonging to the mouse.

For distribution analysis along the *stratum radiatum*, mTurquoise2 puncta was initially mapped to the closest node in the dendritic trace. SynActive-eGRASP puncta was then mapped to the trace node of their colocalized mTurquoise2 puncta. This results in two groups of traces nodes – 1) nodes with mTurquoise2 puncta only and 2) nodes with both mTurquoise2 and SynActive-eGRASP puncta. The relative position ($d_i$) of the trace node in the stratum radiatum was calculated as,

$$d_i = \frac{y_i - y_{min}}{y_{max} - y_{min}} * 100$$

where $y_i$, $y_{min}$ and $y_{max}$ represents the y-coordinate of mapped node $i$, stratum radiatum starting level and stratum radiatum ending level, respectively. The nodes were then binned (bin width 10% approximately equal to 20µm of stratum radiatum) according to their $d_i$ values. For distribution analysis, the percentage of SynActive-eGRASP nodes (normalized to mTurquoise2 nodes) was calculated in each bin. To obtain the density, number of mTurquoise2 nodes in a bin was divided by pathlength of the trace in the bin. Volume of SynActive-eGRASP puncta in each bin was averaged for volume distribution analysis.

For clustering analysis, SynActive-eGRASP puncta were mapped directly to the closest node in the dendritic trace and calculated the pathlength from the branching node (root node if the trace was not branched). This reduced the spatial dimension from 3D (x,y,z) to 1D (pathlength). Pathlength was calculated by iterative summation of the Euclidean distance between two adjacent nodes starting from SynActive-eGRASP node and ending in branching node. Distance between one SynActive-eGRASP node to other SynActive-eGRASP nodes in the branch was calculated as the difference between their corresponding pathlength from the branch. Minimum of these distances gave its nearest neighbor distance (d). Clustering analysis was performed using the MATLAB function - *dbscan* with parameters, input matrix - SynActive-eGRASP node pathlength

from the branch, epsilon neighborhood – median $d_{CFC}$ and minimum number of points – 3 (Ester *et al*. 1996). This defined a 'cluster' as an ensemble of three or more SynActive-eGRASP-positive puncta with the nearest neighbor distance value lower than the median nearest neighbor distance values in the HC group (median $d_{HC}$, 1.08 µm) (Figure 4.20b). Cluster density is the number of clusters in a trace normalized to its total pathlength.

## 3.16 Statistical Analysis

Statistical analysis was performed with GraphPad Prism 8. Student's *t*-test (two-tailed) was used for comparing the means of two samples. The distribution of data was evaluated using two-sample Kolmogorov-Smirnov test. For multiple comparisons, one-way or two-way ANOVA followed by Tukey's or Bonferroni tests were performed. For all statistical tests significance was set at $\alpha$=0.05. All information, including the number of samples in each group and the statistical significance obtained can be found in the legends. Data were represented as mean ± standard error of the mean (SEM) for all bar graphs.

# 4 RESULTS

## 4.1 Design and *in vitro* testing of SynActive-eGRASP

### 4.1.1 Design of SynActive-eGRASP constructs

GFP reconstitution across synaptic partners (GRASP), based on the self-complementation of GFP fragments expressed on the surface of presynaptic and postsynaptic membranes, is currently used to reliably detect synapses in worms, flies, and mammals (Figure 4.1a) (Feinberg *et al.*, 2008; Gordon and Scott, 2009; Kim *et al.*, 2011). To identify the synapses between two specific neuronal populations that had undergone potentiation of reciprocal excitatory glutamatergic connections, I combined GRASP with the SynActive strategy (Gobbo *et al.*, 2017). Among the different variants of GRASP, I chose enhanced GRASP (eGRASP) because it exhibits increased GRASP signal intensity compared to mGRASP (Choi *et al.*, 2018). The signal improvement of eGRASP has been achieved by introducing (i) a weakly interacting p32 peptide (dissociation constant, $K_d$ = 1.8 µM – low interaction strength) and Abl SH3 domain in the individual GRASP components that facilitates GFP reconstitution, and (ii) a mutation in the GFP-β barrel strand 1-10 ($GFP_{1-10}$ fragment) that enhances GFP fluorescence (Figure 4.1b) (Choi *et al.*, 2018). Briefly, the presynaptic eGRASP component (pre-eGRASP) contains an IgGκ signal peptide, mutant GFP-β barrel strand 1-10 (residues 1-214), $(GGS)_{x3}$ linker, an Abl SH3 binding peptide (p32, SPSYSPPPPP), $(GGGS)_{x2}$ linker and stalk, transmembrane and intracellular domain of rat neurexin1β (NRXN1β) (residues 290-468) (Figure 4.1b) (Choi *et al.*, 2018). The first 289 residues of the NRXN1β were deleted to avoid interaction with postsynaptic neuroligin, whereas the C-terminus (residues 414–468) containing the PDZ-binding motif were retained for proper intracellular trafficking and presynaptic targeting (Kim *et al.*, 2011). The postsynaptic GRASP component (post-eGRASP) contains an IgGκ signal peptide, an Abl SH3 domain, $(GGGS)_{x2}$ linker, mutant GFP-β barrel strand 11 (residues 215-230), $(GGGS)_{x2}$ linker and stalk, transmembrane and intracellular domain of mouse neuroligin1 (NLGN1) (residues 627-839) (Figure 4.1b) (Choi *et al.*, 2018). The first 626 amino acids (AAs) and the last 4 AAs, corresponding to the NLGN1 presynaptic neurexin-interacting domain and the PDZ-binding sequence, respectively, were removed to prevent undesired synapse formation and recruitment of receptors and scaffolding proteins (Kim *et al.*, 2011).

To label potentiated synapses, I generated SynActive-post-eGRASP to restrict post-eGRASP expression only to the potentiated spines in an activity-dependent manner by flanking the coding sequence with the 5' and 3' untranslated regions (UTRs) of the activity-regulated cytoskeleton-associated protein (Arc) mRNA (Figure 4.1c). To facilitate the identification of dendritic segments showing the punctate and sparse signal of SynActive-eGRASP, a membrane-targeted mScarlet-I (myristoylated mScarlet-I, myr_mScarlet-I; a red fluorescent protein) was fused to the N-terminus of post-eGRASP via self-cleavable P2A peptide (Figure 4.1c) (Liu *et al.*, 2017). Since mScarlet-I is between the *Arc* UTRs but not fused to any postsynaptic proteins or peptides, it is expected to be expressed only in active neurons and targeted to both dendritic and synaptic membranes via myristoylation (Figure 4.1c). In addition, I adapted the Const-pre-eGRASP construct, which expresses pre-GRASP at all presynaptic sites irrespective of neuronal activity (Figure 4.1c). The term 'SynActive-eGRASP' will be used when SynActive-post-eGRASP and Const-pre-eGRASP constructs are used together to detect potentiated synapses belonging to specific pre-postsynaptic contacts. Use of Const-post-eGRASP that expresses post-eGRASP at all spines along with Const-pre-eGRASP will be referred to as 'Const-eGRASP' (Figure 4.1d).

To achieve temporal control on SynActive-eGRASP expression, I exploited the Tet-On system. Both pre- and post-eGRASP constructs were under the control of tetracycline-responsive element (TRE3g) promoter. The reverse tetracycline transactivator (rtTA) under the human synapsin (hSyn) promoter was expressed *in trans* by a second construct, which I named "filler". In the presence of doxycycline (Dox), rtTA will bind to its target TRE3g and drive the translation of eGRASP constructs (Figure 4.1c, d). To visualize the morphology of presynaptic and postsynaptic neurons, tdTomato or mTurquoise2 were fused to the C-terminus of the rtTA via a self-cleavable P2A peptide (Figure 4.1c, d).

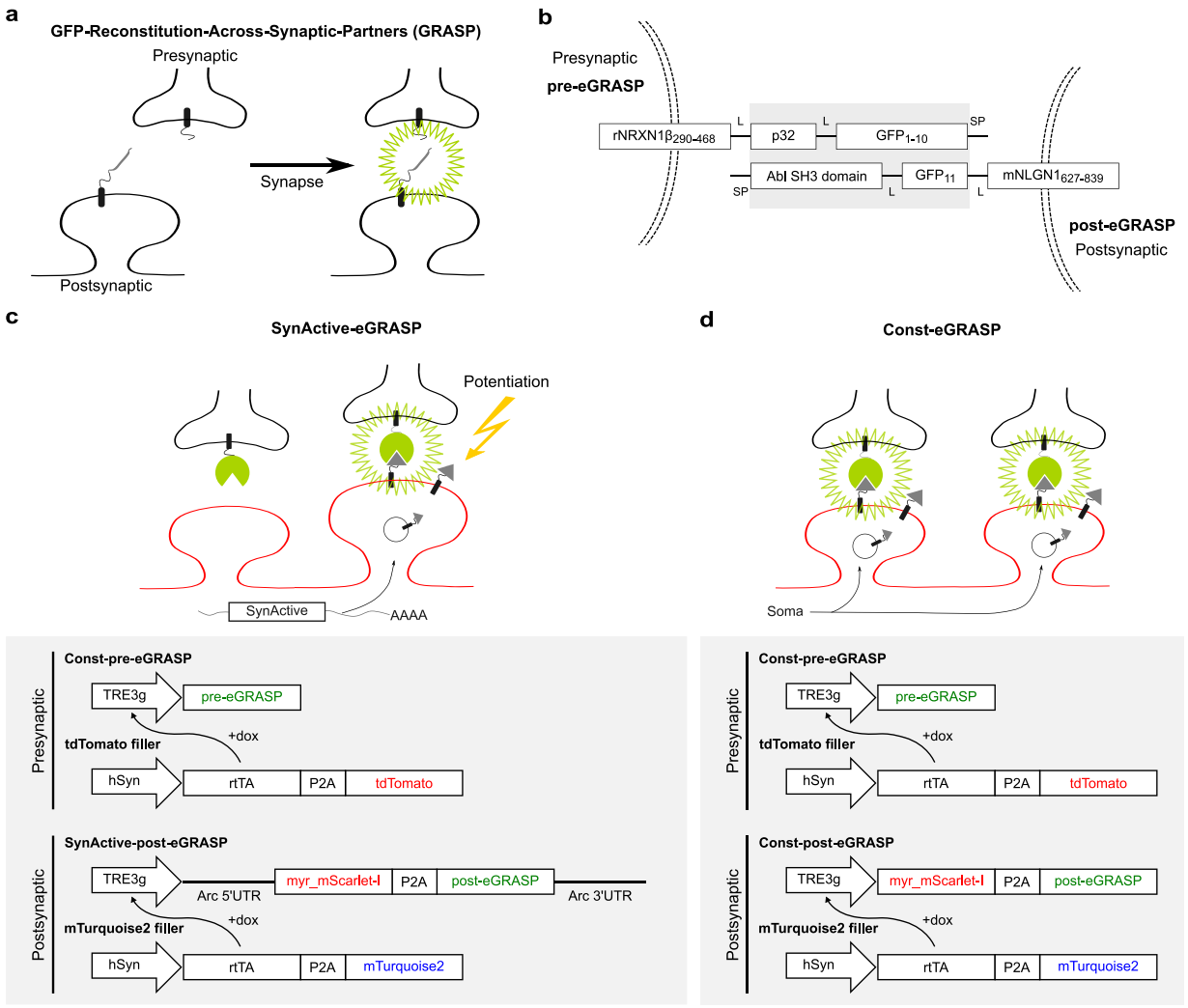


**Figure 4.1 SynActive-eGRASP constructs and their functions.**

(**a**) Schematic illustration of GFP reconstitution in the synaptic cleft. (**b**) Diagram of pre- and post-eGRASP. Signal peptide (SP), GFP fragment ($GFP_{1-10}$ or $GFP_{11}$), SH3 binding peptide (p32), linkers (L). (**c**) Schematic illustration of GFP reconstitution between post-eGRASP and pre-eGRASP expressed at potentiated spines and all presynaptic terminals, respectively (*top*). SynActive-eGRASP constructs used (*bottom*). (**d**) Schematic illustration of GFP reconstitution between post-eGRASP and pre-eGRASP expressed at all spines and presynaptic terminals, respectively (*top*). Const-eGRASP constructs used (*bottom*).

### 4.1.2 Chemical induction of LTP promotes SynActive-eGRASP expression.

Initially, I examined the expression and functional assembly of SynActive-eGRASP at potentiated synapses in primary hippocampal cultures. To achieve expression of individual SynActive-eGRASP components in two separate neuronal populations, I transfected neuronal cultures as described in section methods 3.3 (Figure 4.2a, b). Briefly, two separate transfection mixes were initially prepared: (A) Const-pre-eGRASP and tdTomato filler mixed with

Lipofectamine2000 and (B) SynActive-post-eGRASP or Const-post-eGRASP and mTurquoise2 filler mixed with Lipofectamine 2000. Each transfection mix was then added sequentially to neurons in the same well and incubated for a few hours. It was expected that a small number of neurons will be randomly transfected with either transfection mix A or B, resulting in a co-culture of neurons expressing pre-eGRASP (red) or post-eGRASP (blue) (Figure 4.2 b). Sparse labelling of random neurons with either mTurquoise2 or tdTomato expression appeared in the days following transfection (Figure 4.2c, d). Owing to the co-transfection of each SynActive-eGRASP component with a specific filler construct, I considered mTurquoise2 and tdTomato neurons as postsynaptic and presynaptic neurons, respectively.

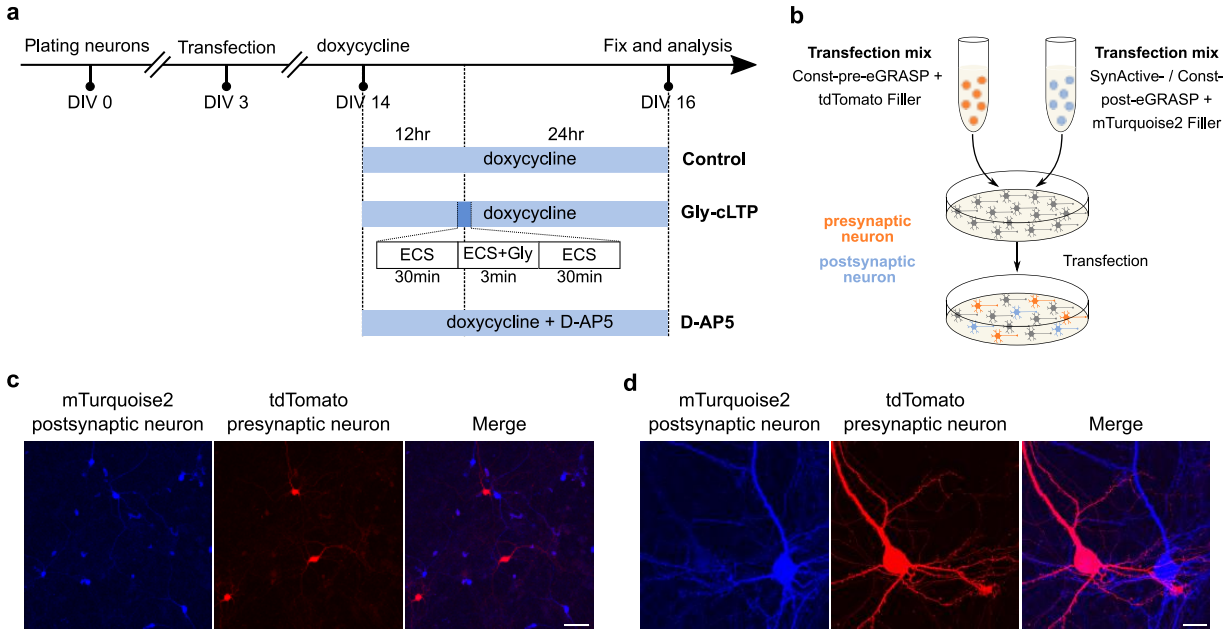


**Figure 4.2 *In vitro* experimental timeline and protocols**

(**a**) Schematic of experimental timeline and protocols to chemically modulate the neuronal activity in primary neuron culture. (**b**) Transfection strategy to achieve co-culture of the distinct neuronal population with pre-GRASP (red) and post-eGRASP (blue) expression. (**c**) Low and (**d**) High magnification images of neuron culture showing sparse labelling of random neurons with either mTurquoise2 (postsynaptic neuron) or tdTomato (presynaptic) expression. Scale bar, 100 µm (**c**) and 20 µm (**d**).

Bath application of the NMDAR coagonist Glycine has been demonstrated to induce long-term-potentiation (LTP) selectively and reliably at synapses, where NMDARs were stimulated by the spontaneous release of glutamate from presynaptic terminals (Lu *et al.*, 2001). Twenty-four hours following the induction of Glycine-mediated chemical LTP (Gly-cLTP) in the presence of Dox, a weak red fluorescence along the dendritic membrane of mTurquoise2-postitive

postsynaptic neurons was detected in addition to the strong red fluorescence from tdTomato-positive presynaptic axons (Figure 4.2a; Figure 4.3a, b). This signal originated from membrane-targeted mScarlet-I (fused to the post-eGRASP) and confirmed the presence of SynActive-post-eGRASP construct in mTurquoise2-positive neurons. GFP-positive puncta, generated from the trans-synaptic reconstitution of SynActive-eGRASP, were detected only in a subset of intersections between mTurquoise2-positive dendrites and tdTomato-positive axons (Figure 4.3a, b). Relative to control neurons that received only Dox, Gly-cLTP-treated neurons had a significantly higher number of SynActive-eGRASP-positive synapses (Figure 4.3a, b, c). In contrast, the blockade of LTP using D-2-amino-5-phosphonovaleric acid (D-AP5) decreased the fraction of SynActive-eGRASP-positive synapses (Figure 4.3a, b, c). These results show that the expression of SynActive-eGRASP is activity-dependent, and labels potentiated synapses.

To verify that the variability in the number of SynActive-eGRASP-positive synapses under different conditions was indeed caused by the restricted expression of SynActive-post-eGRASP at the potentiated spines rather than by potential changes in Const-pre-eGRASP availability, I analyzed the response of Const-eGRASP. Since post-eGRASP was expressed constitutively at all spines of a mTuquoise2-positive neuron, the availability of pre-GRASP at the presynaptic terminal can be indirectly assayed by the presence of GFP fluorescence at the synapses (Figure 4.1d). I found that neither LTP induction nor NMDAR blockade with D-AP5 affected the number of GFP-positive puncta in cultures expressing Const-eGRASP, thus demonstrating the expected activity-independent expression of Const-pre-eGRASP (Figure 4.3a, b, c).

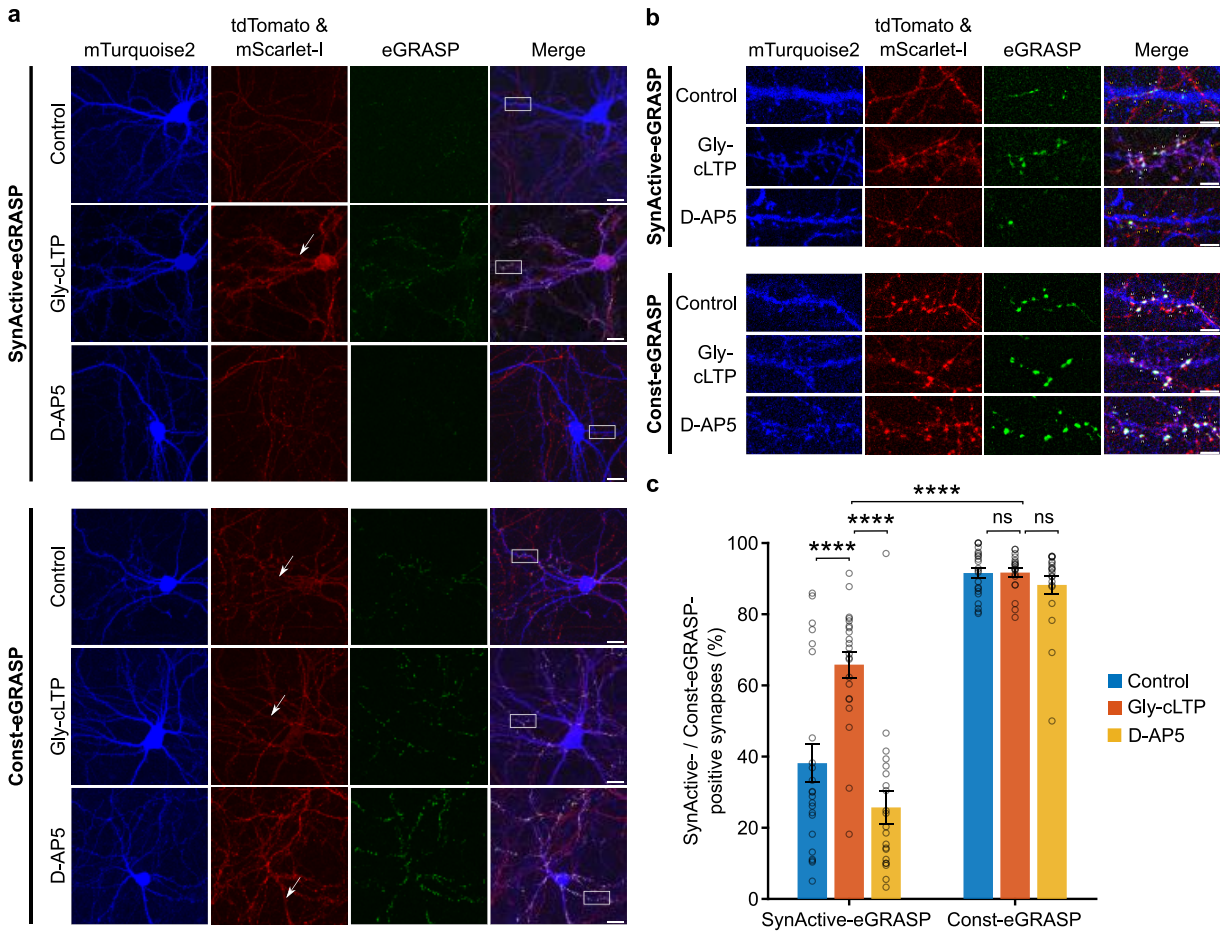


**Figure 4.3 SynActive-eGRASP expression is activity-dependent.**

**(a)** Representative images of SynActive-eGRASP (green) (top) and Const-eGRASP expression (green) (bottom) in different experimental conditions - doxycycline (Dox) alone (control), Glycine-mediated chemical LTP (Gly-cLTP) in the presence of Dox, and blockade of LTP using D-2-amino-5-phosphonovaleric acid (D-AP5). Postsynaptic and presynaptic neurons were visualized by mTurquoise2 (blue) and tdTomato (red), respectively. Weak red fluorescence along the mTurquoise2-positive dendrites corresponded to myristoylated mScarlet-I (white arrow) expressed together with post-eGRASP. Scale bar, 20 µm. (**b**) Magnified views of boxes in **a**. GFP-positive puncta were detected at intersections between mTurquoise2-positive dendrites and tdTomato-positive axons (white arrowheads). Not all putative synapses (i.e., tdTomato-mTurquoise2 intersections) expressed SynActive-eGRASP (yellow arrowheads). Scale bar, 5 µm (**c**) Gly-cLTP increased the number of SynActive-eGRASP-positive synapses compared to control and D-AP5, while Const-eGRASP was expressed in virtually all synaptic contacts, regardless of the experimental condition. (SynActive-eGRASP: control n=23, Gly-cLTP n=22, D-AP5 n=21 neurons from 4 independent experimental replicates; Const-eGRASP: control n=22, Gly-cLTP n=20, AP5 n=20 neurons from 5 independent experimental replicates; ANOVA-2, Group × Treatment interaction, $p<0.0001$, followed by Tukey post hoc test, ****$p<0.0001$; ns, nonsignificant).

Next, I examined whether the green fluorescence visualized at the intersections between mTurquoise2 postsynaptic dendrites and tdTomato presynaptic axons was a *bona fide* signal from trans-synaptic reconstitution of eGRASP. In both SynActive-eGRASP- and Const-eGRASP-

transfected cultures, green fluorescence (as well as mScarlet-I in postsynaptic neurons) was not detected following Gly-cLTP induction when I omitted to trigger the expression of post-eGRASP and pre-eGRASP components, i.e. when I did not add Dox (Figure 4.4a, b). Similarly, a complete absence of green fluorescence was observed when post-eGRASP was expressed in the absence of pre-eGRASP or vice-versa (Figure 4.5a, b). In both SynActive-eGRASP- and Const-eGRASP-transfected cultures, I found a small number of neurons showing perinuclear green fluorescence, as well as green puncta along mTurquoise2-positive postsynaptic dendrites even in the absence of a tdTomato presynaptic neuron (Figure 4.6a, b). These neurons might have taken both the post-eGRASP and pre-eGRASP components during transfection, resulting in non-synaptic GFP reconstitution within the same neuron.

Taken together, these data demonstrate that (i) SynActive-eGRASP is doxycycline-inducible and potentiation-dependent and that ii) the trans-synaptic SynActive-eGRASP signal requires expression of both post-eGRASP and pre-eGRASP components from separated neurons.

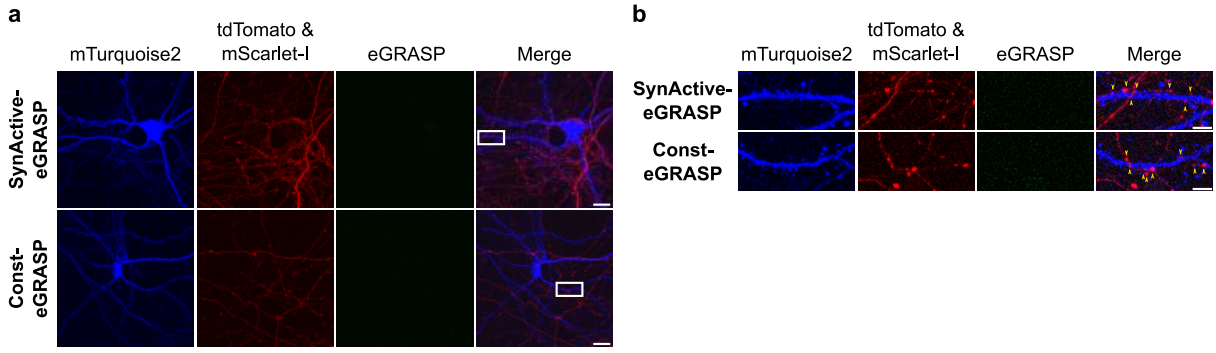


**Figure 4.4 SynActive-eGRASP expression is doxycycline-inducible.**

(**a**) SynActive-eGRASP- and Const-eGRASP-transfected cultures showed no green fluorescence in the absence of doxycycline (i.e., not triggering the expression of post-eGRASP and pre-eGRASP components). Scale bar, 20 µm (**b**) Magnified views of boxes in **a** showing synapse between mTurquoise2-positive dendrites and tdTomato-positive axons without GFP-positive puncta (yellow arrowheads). Scale bar, 5 µm.

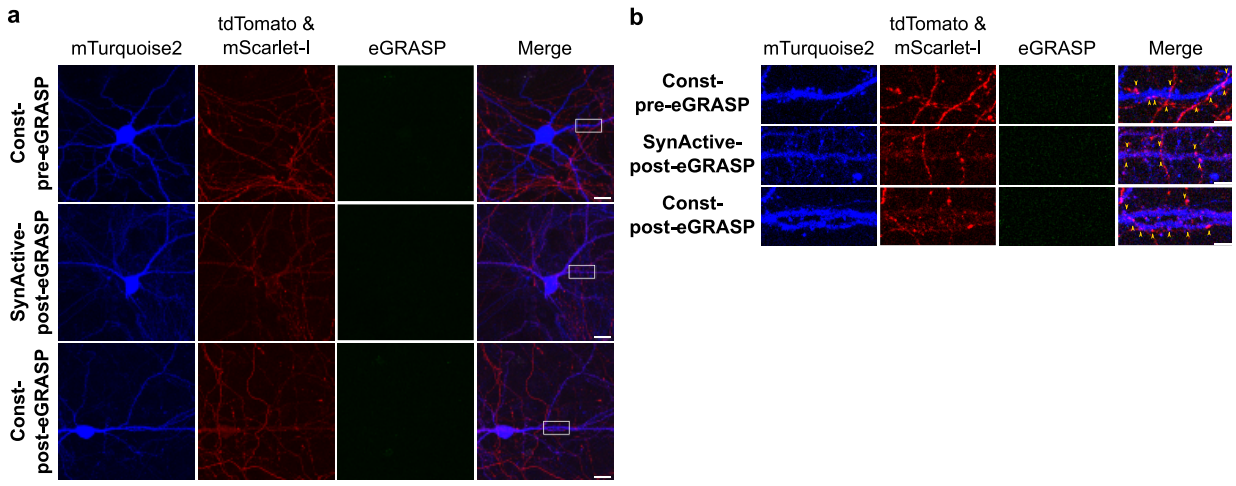


**Figure 4.5 SynActive-eGRASP requires both pre- and postsynaptic components.**

(**a**) No visible green fluorescence when only one component was expressed. Scale bar, 20µm (**b**) Magnified views of boxes in **a** showing synapse between mTurquoise2 dendrites and tdTomato axons without SynActive/Const-eGRASP (yellow arrowheads). Scale bar, 5µm.

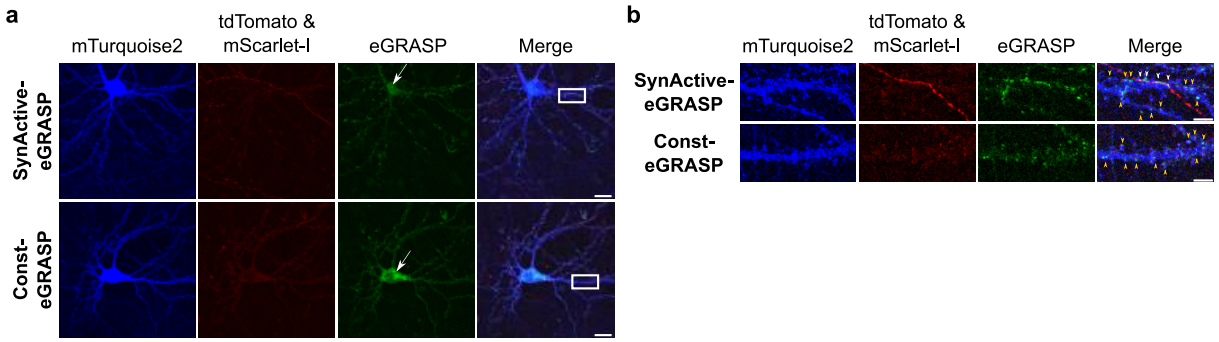


**Figure 4.6 Spurious GFP reconstitution due to co-expression of pre-eGRASP and post--eGRASP in the same neuron.**

(**a**) Representative images of neurons (likely expressing both pre-eGRASP and post-eGRASP) with perinuclear green fluorescence (white arrow). Scale bar, 20 µm. (**b**) Magnified views of boxes in **a** showing green puncta at mTurquoise2-positive spines with (white arrowheads) or without (yellow arrowheads) a nearby tdTomato-positive axon. Scale bar, 5 µm.

### 4.1.3 Expression of SynActive-eGRASP using optogenetically induced LTP

To determine whether an alternative LTP induction protocol can induce SynActive-eGRASP expression, presynaptic neurons were transfected with a filler construct that expresses mScarlet-I tagged channelrhodopsin (Chronos) (Figure 4.7a). Chronos is a channelrhodopsin variant with

faster kinetics and high blue-light (470-nm) sensitivity, that can drive precise and repeated spiking up to 100 Hz, mimicking natural neuronal network activity (Klapoetke *et al.*, 2014; Ronzitti *et al.*, 2017). Initially, neurons were transfected with Chronos-mScarlet-I filler alone to verify that photostimulation of neurons could trigger light-induced ionic currents. To photoactivate Chronos-expressing presynaptic neurons, an optical fiber connected to a 470-nm LED light source was placed directly below the neuron culture dish to achieve wide-field illumination (Figure 4.7b).

Electrical theta-burst stimulation (TBS) induces LTP reliably and efficiently in brain slices (Larson and Munkácsy, 2015; Testa *et al.*, 2019). Since neuronal firing rates up to 100 Hz can be optically evoked in Chronos-expressing neurons, I adapted the conventional electrically induced TBS protocol to optogenetic stimulation (optoLTP; 12 bursts of 4 blue light pulses delivered at 100Hz, separated by 200ms, and repeated 3 times with an interval of 10s) (Figure 4.7c) (Ronzitti *et al.*, 2017; Testa *et al.*, 2019). To examine whether this optoLTP stimulation protocol could efficiently induce potentiation, a Chronos-mScarlet-I-negative postsynaptic neuron was patch-clamped and recorded the optically evoked excitatory postsynaptic currents (EPSCs). These neurons showed time-matched photocurrents in response to a test stimulus (short pulse of light) suggesting that they received direct inputs from a nearby Chronos-mScarlet-I-positive presynaptic neuron. A gradual increase in the amplitude of EPSC in response to a test stimulus was observed following optoLTP stimulation, indicating functional potentiation of synaptic transmission (Figure 4.7d). Given the preliminary nature of this experiment, with a very low number of neurons tested (n=2), no statistical analysis was performed. This test was aimed at verifying that light-induced activation of post-synaptic neuron connected to a Chronos-mScarlet-I-positive presynaptic neuron. Future experiments will address this aspect in a more systematic and formal manner.

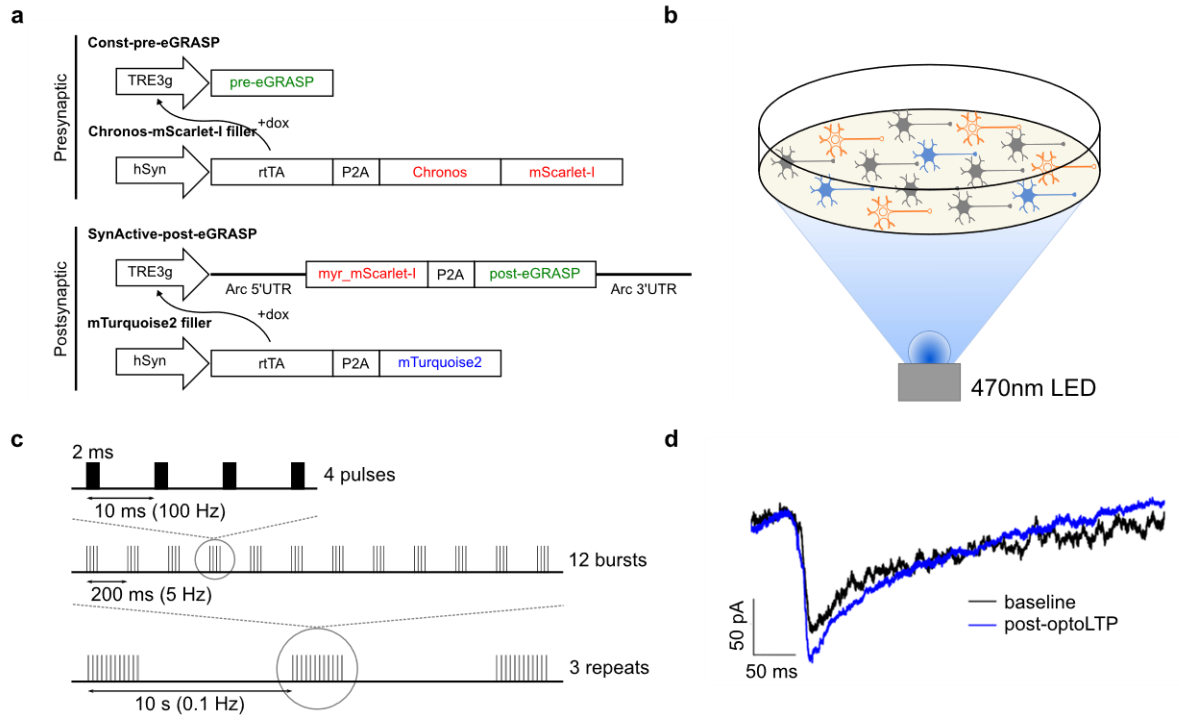


**Figure 4.7 Optogenetic LTP induction in neuronal cultures transfected with SynActive-eGRASP and Chronos channelrhodopsin.**

(**a**) Constructs used for optogenetic LTP induction experiments. Presynaptic filler construct includes channelrhodopsin (Chronos-mScarlet-I). (**b**) Schematic illustration showing photoactivation of Chronos-mScarlet-I-positive presynaptic neurons by 470-nm light illumination. (**c**) Diagram of optically delivered Theta-burst stimulation (optoLTP) (**d**) Representative patch-clamp traces from a Chronos-mScarlet-I-negative postsynaptic neuron receiving inputs from a nearby Chronos-mScarlet-I-positive presynaptic neuron. The difference between the excitatory postsynaptic currents (EPSCs) in response to a test stimulus (short pulse of light) before (baseline, black) and 2 min after (post-optoLTP, blue) optoLTP induction indicates functional potentiation of synaptic transmission.

Next, I examined whether opto-LTP induction could result in SynActive-eGRASP expression at potentiated synapses from Chronos-mScarlet-I-positive neurons. To do that, Const-pre-eGRASP and SynActive-post-eGRASP were expressed along with Chronos-mScarlet-I filler and mTurquoise2 filler, respectively (Figure 4.7a). Interestingly, 24 h after opto-LTP stimulation, GFP-positive puncta were detected along mTurquoise2-positive postsynaptic dendrites at intersections with Chronos-mScarlet-I-positive axons (Figure 4.8a, b). The abundance of SynActive-eGRASP synapses increased significantly following optoLTP stimulation, an effect that was hindered by TTX (tetrodotoxin; $Na^+$ channel blocker) and D-AP5

treatment (Figure 4.8a, b, c). These findings indicate that the expression of SynActive-eGRASP is sensitive to the induction of synaptic potentiation via optoLTP.

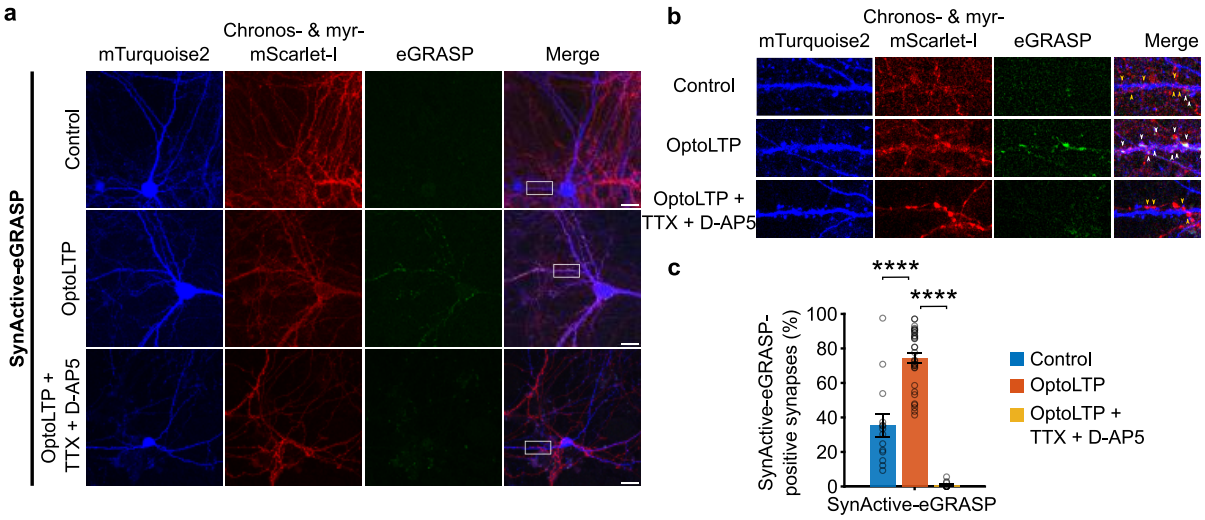


**Figure 4.8 Optically induced LTP triggers SynActive-eGRASP expression.**

(**a**) Representative images showing SynActive-eGRASP (green) expression under the conditions: no optical stimulation (control), optically induced LTP (optoLTP), or optically induced LTP in the presence of TTX (tetrodotoxin) and D-AP5 (opto-LTP + TTX + D-AP5). Scale bar, 20 µm. (**b**) Magnified views of boxes in **a**. SynActive-eGRASP-positive puncta (white arrowheads) were detected at synapses between mTurquoise2-positive dendrites (blue) and Chronos-mScarlet-I-positive axons (red). The density of SynActive-eGRASP-positive synapses was increased after optoLTP, while SynActive-eGRASP-negative synapses (yellow arrowheads) were more frequent in control and optoLTP + TTX + D-AP5 conditions. Scale bar, 5 µm. (**c**) Quantification of the percentage of SynActive-eGRASP-positive synapses with respect to the total number of synaptic contacts. (SynActive-eGRASP: control n=14, optoLTP n=33, optoLTP + TTX + D-AP5 n=11 neurons from 2 independent experimental replicates; ANOVA-1 $p<0.0001$, followed by Tukey's post hoc test, ****$p<0.0001$).

### 4.1.4 SynActive-eGRASP labels potentiated excitatory synapses.

To confirm that the SynActive-eGRASP-containing intersections between tdTomato-positive axons and mTurquoise2-positive spines are actual synapses rather than simple appositions or overlappings among neurites, I analyzed the colocalization of SynActive-eGRASP puncta with selected synaptic proteins, which were visualized via immunolabeling. SynActive-eGRASP puncta were (i) in close apposition to synaptophysin, a marker of mature presynaptic boutons, (Figure 4.9a, b, c) (ii) overlapped with PSD95, which labels excitatory postsynapses (Figure 4.9d, e, f). SynActive-eGRASP and Const-eGRASP exhibited similar colocalization patterns, (Figure

4.9a-f). These results indicate that SynActive-eGRASP- (as well as Const-eGRASP-) -labelled synapses are excitatory.

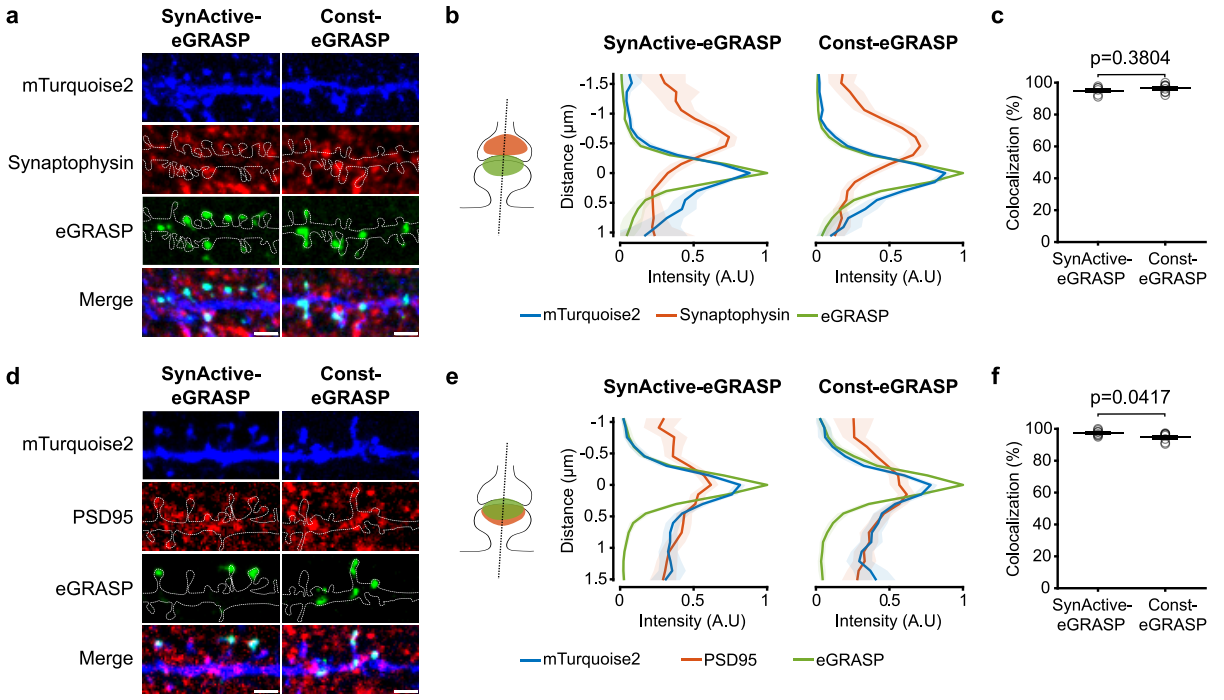


**Figure 4.9 SynActive-eGRASP puncta colocalize with presynaptic and post-synaptic proteins of excitatory synapses.**

(**a, b**) Representative images (**a**) and intensity line scan plots (**b**) showing SynActive- and Const-eGRASP (green) localization at dendritic spine heads (blue), in close apposition to presynaptic synaptophysin (red). Scale bar, 2 µm (**a**). Line scan plot (**b**) is shown as mean intensity and 95% confidence interval for the mean at each distance. (SynActive-eGRASP: n=856 spines from 2 coverslips, Const-eGRASP: n=1204 spines from 2 coverslips). (**c**) No significant difference in the percentage of SynActive- and Const-eGRASP spines colocalizing with synaptophysin. (SynActive-eGRASP: n=6 neurons from 2 coverslips), Const-eGRASP: n=8 neurons from 2 coverslips); Student's *t*-test, p=0.3804). (**d, e**) Representative images (**d**) and intensity line scan plots (**e**) show an overlap between SynActive- and Const-eGRASP (green) with the postsynaptic PSD95 (red). Scale bar, 2 µm. (SynActive-eGRASP: n=1177 spines from 2 coverslips, Const-eGRASP: n=840 spines from 2 coverslips). (**f**) The percentage of SynActive- and Const-eGRASP-positive spines colocalizing with PSD95 are similar. (SynActive-eGRASP: n=8 neurons from 2 coverslips, Const-eGRASP: n=8 neurons from 2 coverslips; Student's *t*-test, p=0.0417).

NMDAR-mediated LTP increases synaptic strength via membrane insertion of AMPARs stored in intracellular vesicles, followed by newly synthesized units (Makino and Malinow, 2009; Lisman et al., 2012). The AMPAR subunit GluA1 has been demonstrated to be selectively incorporated and retained in structurally potentiated mushroom spines, even 24 h after learning (Matsuo et al., 2008). To determine whether GluA1 receptor subunits are enriched in SynActive-eGRASP-positive synapses with respect to non-potentiated synapses, I performed immunolabeling

for GluA1 on neurons fixed 24 h after Gly-cLTP, followed by the analysis of fluorescence intensity and quantification of spine volume. Here, the tdTomato filler was used to label post-eGRASP-expressing neurons. In this way, the combined red fluorescence from soluble tdTomato and the membrane-targeted mScarlet-I facilitated dendritic spine visualization and volume measurement (Figure 4.10a). Const-eGRASP was used as a control to determine synaptic potentiation-independent GluA1 expression. Twenty-four hours after Gly-cLTP, GluA1 was detectable at dendritic spines, in both SynActive- and Const-eGRASP-transfected neurons (Figure 4.10a). However, SynActive-eGRASP-positive spines exhibited significantly higher GluA1 intensity compared to Const-eGRASP-positive spines (Figure 4.10b). Approximately 67% of SynActive-GRASP-positive spines had GluA1 levels higher than the median GluA1 level calculated in Const-eGRASP-positive spines (Figure 4.10b). In addition, SynActive-eGRASP-positive spines had a significantly larger volume than Const-eGRASP-positive spines (Figure 4.10b, d).

Although induction of LTP requires NMDARs, the NMDAR component of the EPSPs was found to be of comparable size in control and potentiated synapses (Kauer et al., 1988; Muller et al., 1988). In hippocampal slice cultures, chemical induction of LTP produces a small decrease (GluN2B) or no change (GluN2A) in the NMDAR subunits (Kopec *et al.*, 2006). To examine whether the receptor enrichment at SynActive-eGRASP spines is specific to AMPARs, SynActive-eGRASP or Const-eGRASP transfected neurons were immunolabeled with antibodies against the NMDAR subunits GluN2A and GluN2B (GluN2A/B). In contrast to GluA1, 24 h after Gly-cLTP induction, GluN2A/B intensity levels were similar between SynActive-eGRASP-positive spines and Const-eGRASP-positive spines (Figure 4.10c, d). Thus, I could conclude that SynActive-eGRASP labels synapses displaying upregulation of GluA1 and structural potentiation (i.e. increase of spine volume).

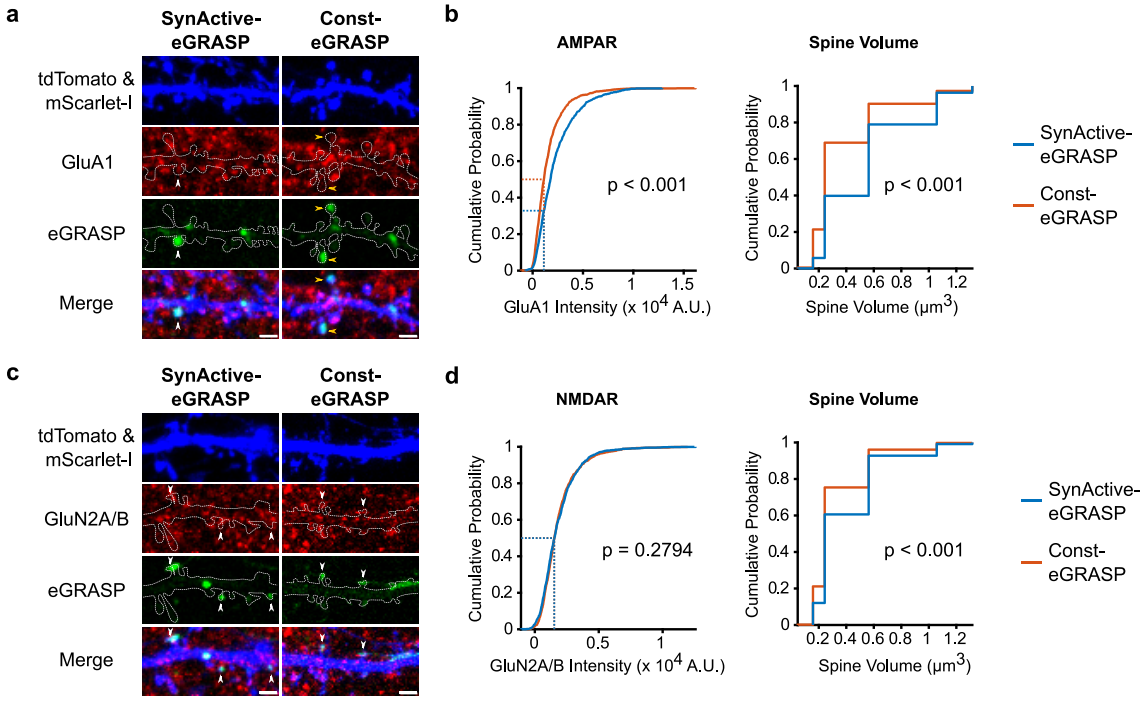


**Figure 4.10 SynActive-eGRASP-positive dendritic spines show a higher content of GluA1 and a larger volume.**

(**a**) The AMPAR subunit GluA1 was detected in SynActive-eGRASP-positive synapses (white arrowhead) and Const-eGRASP-positive synapses (yellow arrowhead). Scale bar, 2 µm. (**b**) Cumulative distributions for quantification of fluorescence intensity, showing that SynActive-eGRASP-positive synapses (blue curve) had significantly higher integrated GluA1 intensity (*left*, Kolmogorov-Smirnov test, $p=6.68 \times 10^{-23}$) and spine volume (*right*, Kolmogorov-Smirnov test, $p=9.71 \times 10^{-45}$) than Const-eGRASP-positive synapses. (SynActive-eGRASP: n=1163, Const-eGRASP: n=1220 spines from 2 independent experimental replicates) (**c, d**) Cumulative distributions for quantification of fluorescence intensity, showing no significant difference in GluN2A/B levels between SynActive-eGRASP-positive synapses and Const-eGRASP-positive synapses (white arrowheads in **c**; **d** *left*, Kolmogorov-Smirnov test, p=0.2794). Analysis of spines showing GluN2A/B-immunoreactivity and GFP-positive puncta confirmed a larger volume for SynActive-eGRASP-positive synapses in comparison to Const-SA-eGRASP-positive synapses (**d** *right*, Kolmogorov-Smirnov test, $p=6.26 \times 10^{-14}$). Scale bar, 2 µm. (SynActive-eGRASP: n=1259, Const-eGRASP: n=1608 spines from 2 independent experimental replicates).

### 4.1.5 Expanding the SynActive-eGRASP palette with color variants

Postsynaptic neurons receive input from multiple presynaptic neurons of distinct cell types or origins. For instance, the CA1 receives input from both the CA3 and entorhinal cortex (EC) (Kajiwara *et al.*, 2008). Recently, GRASP has been extended to obtain reconstituted GFP variants emitting in the cyan, yellow, or red channels by introducing mutations in the $GFP_{1-10}$ fragment, that allowed labelling of various subsets of synapses within the same neuron with different colors (Macpherson *et al.*, 2015; Choi *et al.*, 2018; Feng *et al.*, 2019). SynActive-Cyan-eGRASP and

SynActive-Yellow-eGRASP were developed by modifying the Const-pre-eGRASP construct with the $GFP_{1-10}$ mutants for cyan and yellow (Choi *et al.*, 2018). Then, the functionality of SynActive-eGRASP color variants at potentiated synapses was assessed by transfecting primary hippocampal cultures either with SynActive-Cyan-eGRASP or SynActive-Yellow-eGRASP. The combinations of SynActive-eGRASP and filler constructs that I developed and validated are listed in Table 4.1. Puncta of cyan and yellow fluorescence were observed along dendrites expressing SynActive-post-eGRASP, demonstrating reconstitution of GFP variants at synaptic contacts with Const-Cyan-eGRASP- or Const-Yellow-eGRASP-expressing presynaptic neuron (Figure 4.11a, b).

**Table 4.1 Constructs used for SynActive-Yellow/Cyan-eGRASP experiments.**

| | Presynaptic neurons | Postsynaptic neurons |
|---|---|---|
| **SynActive-Yellow-eGRASP** | Const-Yellow-pre-eGRASP<br>tdTomato Filler | SynActive-post-eGRASP<br>mTurquoise2 Filler |
| **SynActive-Cyan-eGRASP** | Const-Cyan-pre-eGRASP<br>Chronos-EGFP Filler | SynActive-post-eGRASP<br>tdTomato Filler |

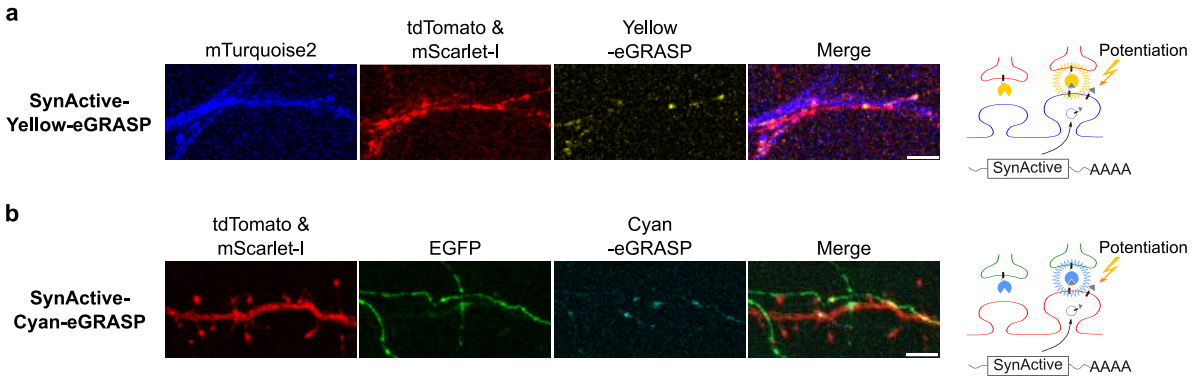


**Figure 4.11 Multicolor labelling of potentiated synapses with SynActive-eGRASP spectral variants.**

(**a**) Representative images (*left*) and schematic (*right*) of SynActive-Yellow-eGRASP (yellow) expression at potentiated synapses between mTurquoise2-positive (blue) postsynaptic neurons and tdTomato-positive (red) presynaptic neurons. Scale bar, 5 µm. (**b**) Representative images (*left*) and schematic (*right*) of SynActive-Cyan-eGRASP (cyan) expression at potentiated synapses between tdTomato-positive (red) postsynaptic neurons and EGFP-positive (green) presynaptic neurons. Scale bar, 5 µm.

## 4.2 Exploiting SynActive-eGRASP to map circuit-specific learning-related synaptic potentiation *in vivo*.

### 4.2.1 SynActive-eGRASP labels CA3-CA1 synapses potentiated by associative learning.

After extensive *in vitro* validation, described in the preceding paragraphs, I used SynActive-eGRASP to detect neuronal circuit-specific potentiated synapses associated with a learned behavioral task. To this aim, I prepared a series of adeno-associated viruses (AAVs) driving the expression of the SynActive-eGRASP and filler constructs (see list of AAVs in Figure 4.12a).

CA3 synapses onto CA1 neurons (CA3-CA1) have been shown to be potentiated after behavioral paradigms such as inhibitory avoidance and contextual fear conditioning (CFC) (Whitlock *et al.*, 2006; Choi *et al.*, 2018). The CA1 postsynaptic field receives presynaptic inputs from both the ipsilateral and the contralateral CA3 hippocampal fields (Finnerty and Jefferys, 1993; Kim *et al.*, 2011; Choi *et al.*, 2018). To map the distribution of CFC-associated potentiated CA3-CA1 synapses, adult mice (2-4 months) were injected with the AAVs (Serotype with PHP.eB capsid and AAV2 inverted terminal repeats (ITRs); Chan *et al.*, 2017) for the transduction of SynActive-eGRASP and filler constructs (Figure 4.12a, c). To avoid the occurrence of spurious reconstituted GFP fluorescence caused by the expression of both components in the same neuron (Figure 4.6), the AAV cocktail of SynActive-post-eGRASP and tdTomato (red fluorophore) filler was injected in the left CA1 region (Figure 4.12a), while an AAV cocktail of Const-pre-eGRASP and mTurquoise2 (cyan fluorophore) filler was injected in the right CA3 region (Figure 4.12a). After Dox administration, mice were subjected to CFC. Histological fixation was performed 24 h later, in line with SynActive-eGRASP expression time in primary neurons (Figure 4.3; Figure 4.12c).

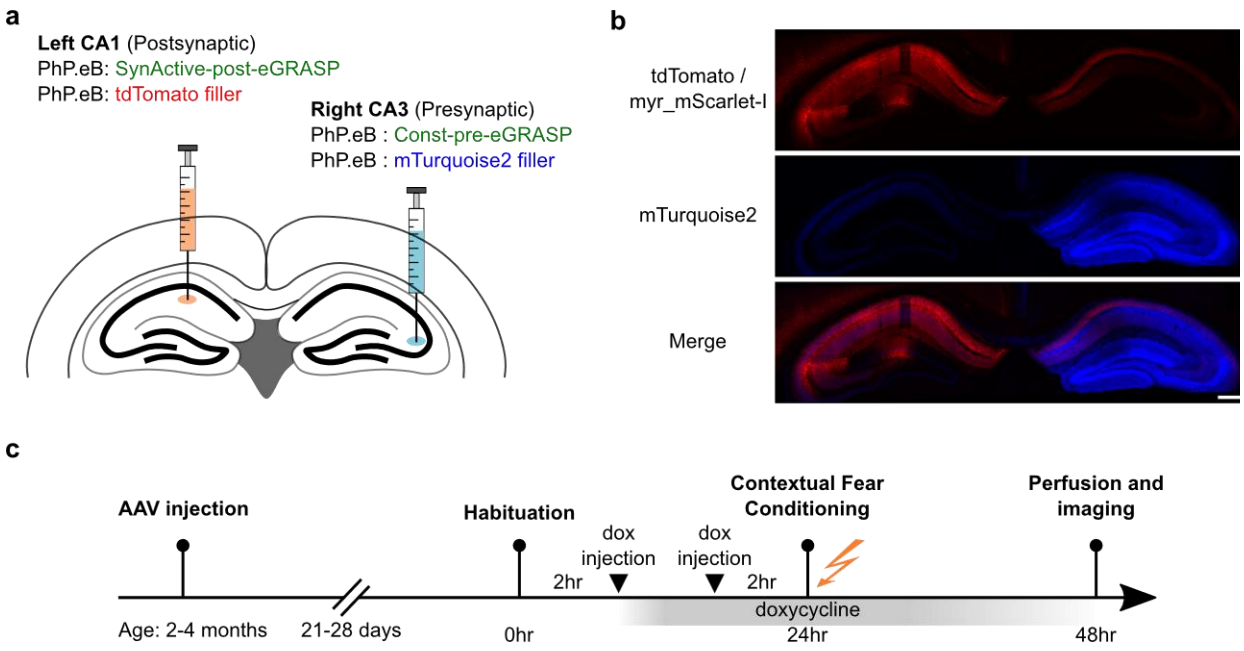


**Figure 4.12 SynActive-eGRASP injection schema and experiment timeline**

(**a**) Schematic illustration of SynActive-eGRASP injections in the mouse hippocampus to label potentiated CA3-CA1 synapses. (**b**) Neurons in the left CA1 and right CA3 expressed tdTomato (red) and mTurquoise2 (blue), respectively. Axons from left CA1 (red) and right CA3 (blue) were visible in the CA1 region of the contralateral hemisphere. (**c**) Experiment timeline.

I observed dense labelling of CA1 and contralateral CA3 neurons with tdTomato and mTurquoise2, respectively (Figure 4.12b). In agreement with the CA3 anatomical connectivity (Amaral and Lavenex, 2007; Kim *et al.*, 2011), mTurquoise2-positive axons projecting from the left CA3 region were present in the *strata oriens* and *radiatum* of the contralateral CA1 region (Figure 4.13; Figure 4.14a, b, c). Consistently, bright, and punctate GFP fluorescence (i.e., corresponding to SynActive-eGRASP) could be detected along the tdTomato-positive dendrites (Figure 4.13; Figure 4.14a, b, c; Figure 4.15). Interestingly, the number of SynActive-eGRASP puncta appeared to be larger in hippocampal sections from mice exposed to CFC in comparison to mice that had been left in their home cage (HC) (Figure 4.13a, b; Figure 4.14a, b, c). On the other hand, induction of massive neuronal hyperactivity (Steward *et al.*, 1998; Farris *et al.*, 2014) via kainic acid injection resulted in the highest density of SynActive-eGRASP puncta along CA1 dendrites (Figure 4.13c; Figure 4.14a, b, c). High-magnification images showed bright green puncta at dendritic spine heads of tdTomato-positive CA1 dendrites apposed to mTurquoise2-positive axons (Figure 4.15). Of note, no SynActive-eGRASP expression was detected in the absence of Dox, confirming Tet-ON regulated expression (Figure 4.13d; Figure 4.14a, b, c).

In the CA1 *stratum lacunosum-moleculare*, known to receive input from the EC but not from the CA3 (Amaral and Lavenex, 2007), I observed neither mTurquoise2-positive CA3 axons nor SynActive-eGRASP puncta, further supporting the specificity of SynActive-eGRASP in labelling CA3-CA1 synapses (Figure 4.13; Figure 4.14d). Unlike the *stratum lacunosum-moleculare*, a faint punctate green fluorescence was present in the *stratum pyramidale* (present even in the absence of Dox with intensity comparable to +Dox conditions, Figure 4.13d), which did not derive from SynActive-eGRASP, as mTurquoise2-positive CA3 axons were not evident in this hippocampal layer (Figure 4.13; Figure 4.14e), but could be rather caused by somatic lipofuscin autofluorescence (Economo *et al.*, 2016).

These *ex vivo* imaging findings indicate that (i) CA3-CA1 potentiated synapses can be labelled with SynActive-eGRASP with a very favorable signal-to-noise ratio following a learning task, (ii) the labelling intensity of potentiated CA3-CA1 synapses with SynActive-eGRASP reflects the degree of synaptic potentiation induced by progressively stronger stimuli, i.e., home cage < CFC < kainic acid and (iii) SynActive-eGRASP labels potentiated CA3-CA1 synapses during a time-window defined by doxycycline administration. This method sets the basis for performing a systematic atlasing of the subregional location and cellular and subcellular distributions of potentiated synapses following specific learning tasks.

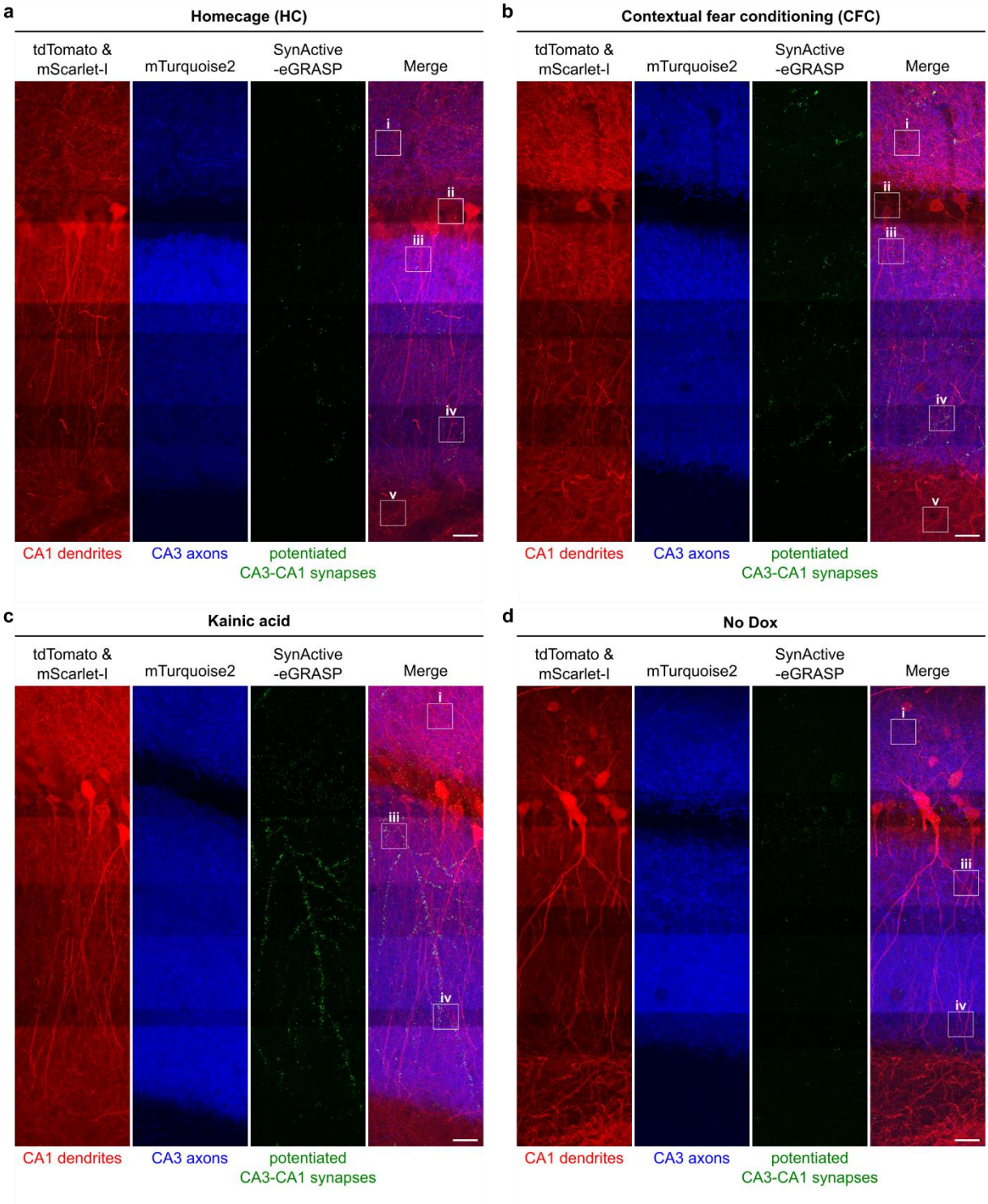


**Figure 4.13 SynActive-eGRASP labels *in vivo* potentiated CA3-CA1 synapses**

Representative confocal microscopy images of the left hippocampal CA1 region from a mouse (**a**) kept in its home cage (HC), (**b**) exposed to contextual fear conditioning (CFC), (**c**) subjected to kainic acid injection, and (**d**) exposed to CFC in the absence of doxycycline (no Dox). Scale bar, 20 µm.

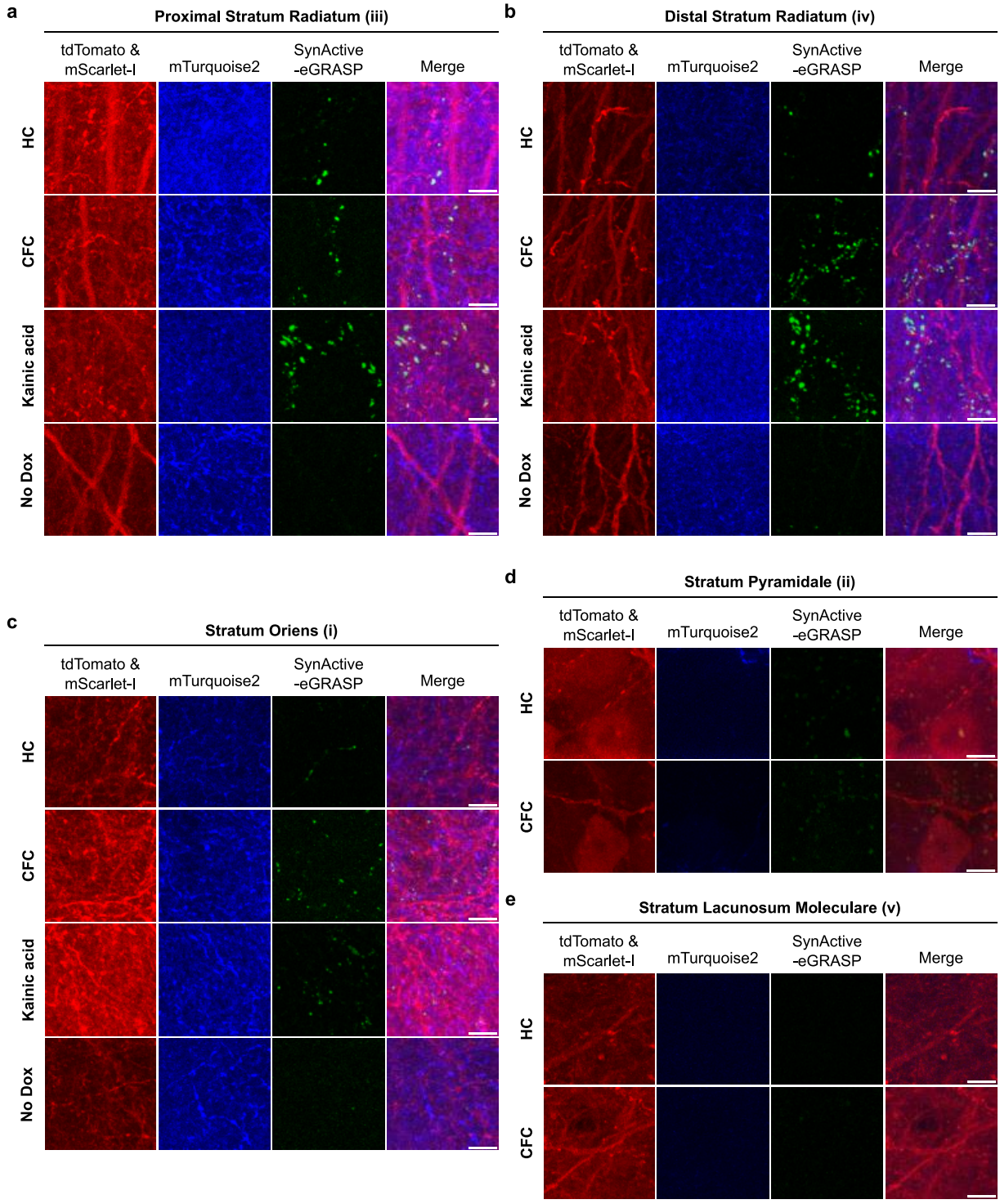

**Figure 4.14 High-magnification images showing SynActive-eGRASP expression in CA1 *strata.***

Magnified views of boxes in Figure 4.13. (**a-c**) *strata radiatum* (**a, b**) and *oriens* (**c**) showing expression of mTurquoise2-positive CA3 axons (blue) and SynActive-eGRASP-positive puncta (green) along the tdTomato-positive CA1 dendrites (red). Scale bar, 5 µm. No SynActive-eGRASP-positive puncta in *strata pyramidale* (**d**) and *lacunosum-moleculare* (**e**), as mTurquoise2-positive CA3 axons were not evident in these hippocampal layers. Scale bar, 5 µm.

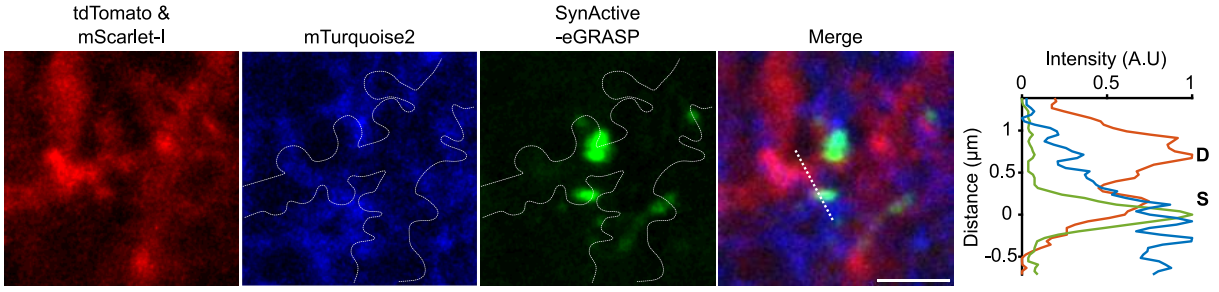


**Figure 4.15 SynActive-eGRASP expression is localized at contacts between CA3 axons and CA1 dendrites.**

High-magnification images (*left*) and a representative intensity line scan plot (*right*) of a tdTomato-positive CA1 dendrite (red) with SynActive-eGRASP-positive puncta (green) in the spine head and a close-by mTurquoise2-positive CA3 axon (blue). D - dendrite, S – spine. Scale bar, 2 µm.

### 4.2.2 Automatic detection of SynActive-eGRASP-positive puncta

To investigate the spatial distribution of potentiated CA3-CA1 synapses, I developed a pipeline for semi-automated detection and analysis of GFP-positive puncta. To restrict puncta detection and analysis to a well-identified dendritic segment of interest, I masked the confocal image around the dendritic trace created using neuTube and Vaa3D (Figure 4.16a, b) (Peng *et al.*, 2014; Feng *et al.*, 2015; Iascone *et al.*, 2020). Then, dendritic segments belonging to the *stratum radiatum* were manually traced (Figure 4.16 b). SynActive-eGRASP-positive puncta in the CA1 *stratum radiatum* had a wide range of sizes and overlapped each other (Figure 4.16c). Although mTurquoise2-positive CA3 axons and SynActive-eGRASP-positive puncta were evident also in the *stratum oriens*, puncta detection and analysis were not performed due to thin dendritic diameter and dense labelling that impeded accurate tracing (Figure 4.14c). An improved version of the filler construct that allows strong expression of fluorescent proteins in a sparse population of neurons is required to overcome this difficulty.

Efficient computational methods have been successfully implemented to accurately detect and segment mGRASP-labelled synapses in 3D (Feng *et al*., 2012; Kim *et al*., 2011). To automatically identify individual SynActive-eGRASP-positive puncta, I adapted the puncta detection algorithms described in Feng *et.al.* (2012). After preprocessing the images by masking around the trace as described above, I applied global thresholding to binarize the image. Voxels with SynActive-eGRASP intensity greater than an intensity threshold value (will be referred to as $I_{min}$) were considered foreground voxels (Figure 4.16a, c). Thresholding resulted in many isolated aggregates of connected foreground voxels and an aggregate was considered as an individual SynActive-eGRASP puncta if its voxel count was less than the voxel threshold $V_{max}$ (defined as the maximum number of voxels a punctum can contain) (Figure 4.16c). When larger aggregates corresponding to multiple overlapping puncta were found, these were segmented for assigning sub-aggregates of voxels to individual puncta through the watershed algorithm (Figure 4.16a, c). The watershed algorithm identifies individual puncta with a clear bright center from an aggregate (Feng *et al.*, 2012). When the watershed was ineffective in segmentation, Variational Bayesian Gaussian Mixture Models (VBGMMs)-based modeling of puncta as 3D gaussian distributions (assuming a bright center and a convex shape) were applied (Feng *et al.*, 2012). To avoid over-segmentation caused by outliers and noise and to estimate the correct number and location of the puncta, VBGMMs were refined by mean-shift and post-processing merge (Feng *et al.*, 2012). In Figure 4.16c, yellow arrows show aggregates that were segmented by watershed and mean-shift regulated VBGMMs to identify individual SynActive-eGRASP-positive puncta, marked in different colors and white circles.

To prevent incorrect identification of image noise constituted by random high-intensity pixels as SynActive-eGRASP-positive puncta, I adopted a size threshold (Figure 4.16c, d). Since noise puncta are generally smaller than genuine GFP puncta, including filtering based on the voxel count removed them during the final proof-editing step (Figure 4.16d, white arrow). Occasionally, over-segmentation errors were observed when puncta had saturated pixels and elongated shape (Figure 4.16d, yellow arrow). In the proof-reading step, these puncta were manually merged with the assistance of 3D visualization via neuTube.

The accuracy of the puncta detection algorithm is highly dependent on the initial parameters – intensity threshold for image binarization, $I_{min}$ and voxel count threshold for segmentation, $V_{max}$. High $I_{min}$ values result in not detecting voxels with low intensity of SynActive-eGRASP, which

can increase the likelihood of missing a complete punctum (false negatives) or an inaccurate description of the shape, size, and position of a punctum (Figure 4.16e, left). On the contrary, low $I_{min}$ values pick the image noise and create false positives or overestimate puncta size (Figure 4.16e, right). For accurate detection of SynActive-eGRASP puncta, I used $I_{min}$ as the intensity at which almost all voxels with SynActive-eGRASP signal were considered as foreground upon visual inspection (30 in most of the images) (Figure 4.16e, middle). $V_{max}$ determines whether a voxel aggregate must be segmented by watershed and/or mean-shift regulated VBGMMs algorithms to identify individual SynActive-eGRASP puncta. Under-segmentation errors (multiple puncta wrongly counted as a single big punctum) and puncta shrinkage (caused by voxel removal following over-segmentation) were observed at high and low $V_{max}$ values, respectively (Figure 4.16f). After trial and error, I fixed $V_{max}$ as 115, which resulted in accurate segmentation in SynActive-eGRASP confocal images captured at 0.116 µm ×0.116 µm ×0.396 µm voxel size (Figure 4.16f, middle).

3D reconstructions from serial section electron microscopy (EM) have shown that presynaptic boutons (axonal regions with presynaptic vesicles that form synapses with postsynaptic dendritic spines) are thicker than the shaft in CA3 axons (Shepherd and Harris, 1998; Bourne *et al*., 2013). Confirming the literature, I found enlarged presynaptic boutons along mTurquoise2-positive CA3 axons that were approximately ellipsoid in shape (Figure 4.17a). Interestingly, mTurquoise2 intensity was higher in presynaptic boutons than in parent axonal shafts (Figure 4.17a). To automatically identify the mTurquoise2-positive CA3 boutons surrounding a tdTomato CA1 dendrite, I performed puncta detection on the mTurquoise2 image masked around the trace (Figure 4.17a). False positives arising from axonal shafts and over-segmentation of boutons were then corrected during the prof-reading steps (Figure 4.17a).

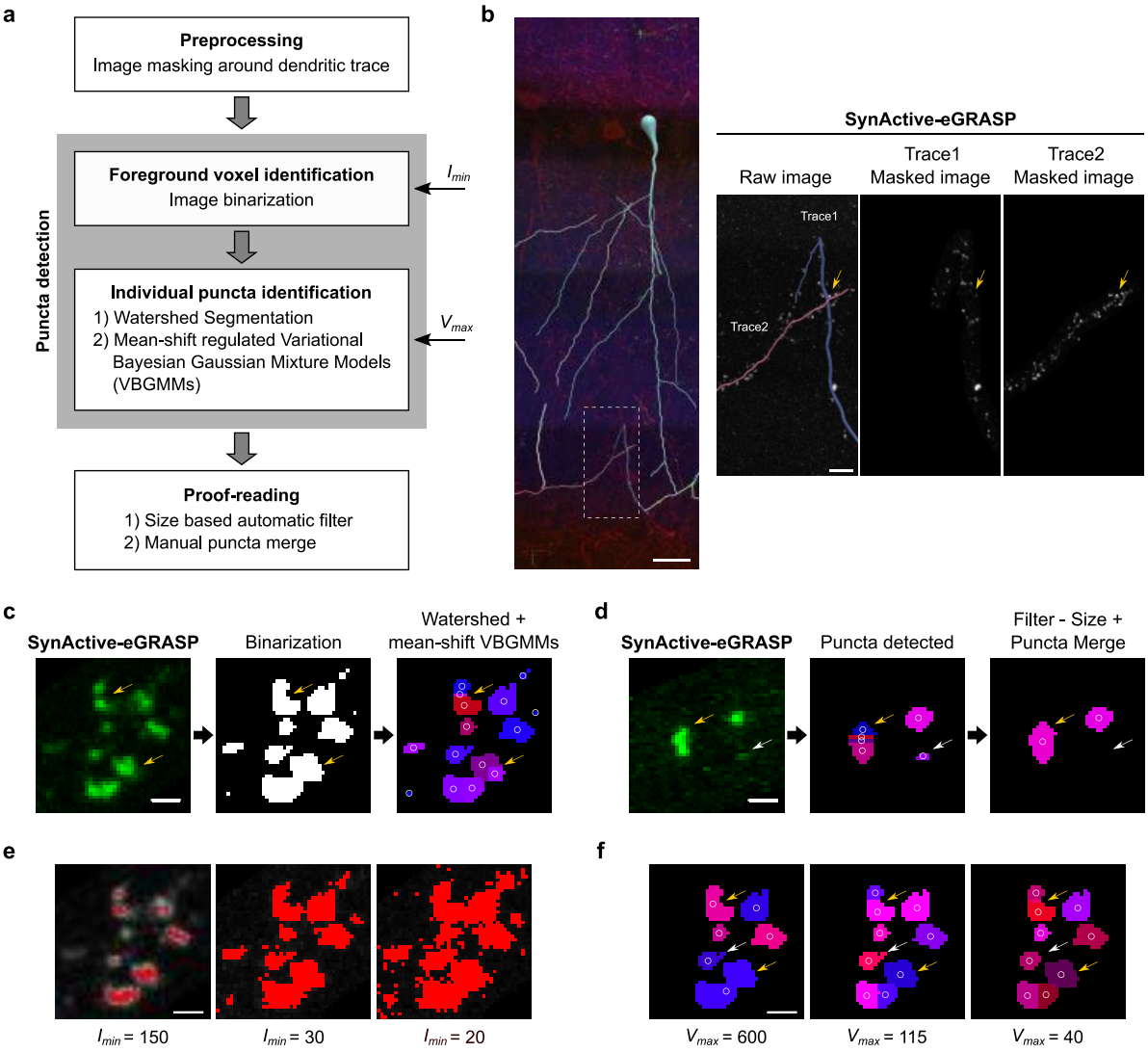


## Figure 4.16 Semi-Automated detection of SynActive-eGRASP puncta

(**a**) Diagram outlining the puncta detection process. (**b**) Confocal image of CA1 region from a CFC mouse, superimposed with traces of dendrites showing SynActive-eGRASP signal (green) (*left*). SynActive-eGRASP image masked around traces 1 or 2 (*right*). The yellow arrow (*right*) refers to a region where SynActive-eGRASP signal belonging to two traces overlapped in the z-stack image. Scale bar, 20 µm (*left*) and 5 µm (*right*). (**c**) Aggregates of foreground voxels (voxels with SynActive-eGRASP intensity greater than $I_{min}$) identified after image binarization (*middle*). Larger aggregates with voxel count greater than $V_{max}$ (yellow arrow) were segmented by watershed and/or mean-shift regulated VBGMMs. Individual SynActive-eGRASP-positive puncta identified after segmentation are marked in different colors and white circles denote their centers (*right*). Scale bar, 1 µm. (**d**) Puncta detection results after proof-reading. Small puncta were removed by size-based filtering (white arrow) and the over-segmentation error was corrected by manual puncta merge (yellow arrow). Scale bar, 1 µm. (**e**) Foreground voxels (red) identified with high (*left*), optimum (*middle*), and low (*right*) $I_{min}$ values. Scale bar, 1 µm. (**f**) Individual SynActive-eGRASP-positive puncta identified after segmentation and size-based filtering are marked in different colors and white circles. Under segmentation (yellow arrow) and puncta shrinkage (white arrow) were observed with high (*left*) and low (*right*) $V_{max}$ values, respectively. Scale bar, 1 µm.

To determine whether automatically identified SynActive-eGRASP-positive puncta were a genuine signal, I analyzed their colocalization with mTurquoise2-positive CA3 boutons. A SynActive-eGRASP-positive punctum and mTurquoise2-positive CA3 bouton were considered to be colocalized if the Euclidean distance between their centroids was less than 2 µm (Figure 4.17b, c). I found that 92% and 95% of SynActive-eGRASP puncta colocalized with a mTurquoise2 puncta in HC and CFC mice, respectively (Figure 4.17c). This suggests that the puncta detection algorithms accurately identified SynActive-eGRASP-positive potentiated CA3-CA1 synapses.

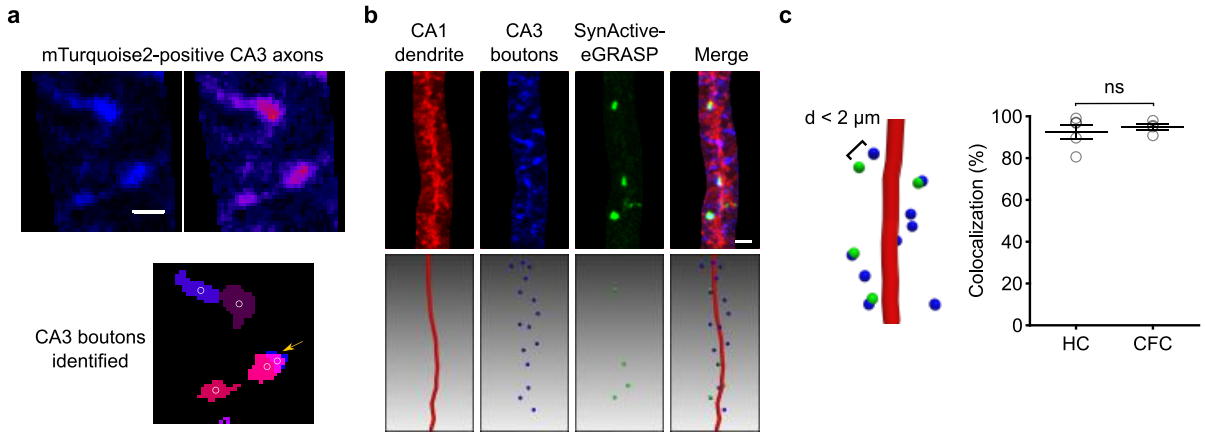


**Figure 4.17 SynActive-eGRASP colocalizes with mTurquoise2-positive CA3 axonal boutons.**

(**a**) Representative images of mTurquoise2-positive CA3 axons with thicker and brighter presynaptic boutons (*top left*, raw image, *top right*, fire lookup table (LUT)). Individual mTurquoise2-positive CA3 boutons identified by semi-automatic puncta detection are shown in different colors and white circles denote their centers (*bottom*). The yellow arrow denotes an over-segmented bouton which was corrected by manual puncta merge during the proof-reading step. Scale bar, 1 µm. (**b**) Representative masked images (*top row*), and the corresponding tdTomato-positive CA1 dendritic trace (red), detected mTurquoise2-positive CA3 boutons (blue) and SynActive-eGRASP-positive puncta (green) (*bottom row*). (**c**) 3D visualization (*left*) and quantification (*right*) of SynActive-eGRASP-positive puncta colocalization with mTurquoise2-positive CA3 boutons (distance between the puncta centroids, d < 2 µm). (HC n=5, CFC n=4 mice from 3 independent experimental replicates; Student's *t*-test, p=0.6056; ns, non-significant).

### 4.2.3 CA3-CA1 potentiated synapse connectivity increases after contextual fear conditioning.

Next, I used this semi-automated detection method to examine the data on the relative strength of CA3-CA1 synapses labelled by SynActive-eGRASP-positive puncta and mTurquoise2-positive

CA3 boutons. Compared to HC mice, CFC mice had significantly higher density (normalized with respect to dendritic trace length; HC 0.19±0.02 puncta/µm, CFC 0.36±0.07 puncta/µm) and percentage (normalized with respect to the total number of mTurquoise2-positive CA3 boutons in the same dendritic segment) (HC 9.47±0.93%, CFC 19.52±3.42%) of SynActive-eGRASP-positive puncta (Figure 4.18a). In contrast, mTurquoise2-positive CA3 bouton density was comparable between the two groups (Figure 4.18b). This indicates that the increased density of SynActive-eGRASP-positive puncta observed in mice exposed to CFC with respect to HC controls was not caused by inter-mouse fluctuations in infection efficiency and the associated pre-eGRASP expression. Interestingly, I observed a high variation in SynActive-eGRASP density among individual dendritic traces from a single CFC mouse (Figure 4.18c). This suggests that a specific memory is not uniformly distributed among neurons, and neurons with a high density of potentiated synapses might encode more information than others.

mGRASP puncta size has been shown to correlate with synaptic strength estimations via mEPSC measurements (Song *et al*., 2018). I found considerable variation in the volume of SynActive-eGRASP-positive puncta (pooled from dendritic segments in different locations along the *stratum radiatum*), with a significant trend towards higher volume in CFC mice than in HC mice (HC 0.61±0.06 $\mu m^3$, CFC 0.91± 0.22 $\mu m^3$) (Figure 4.18d). These analyses show that a strengthening of CA3-CA1 connectivity via synaptic potentiation accompanies the learning of contextual fear conditioning.

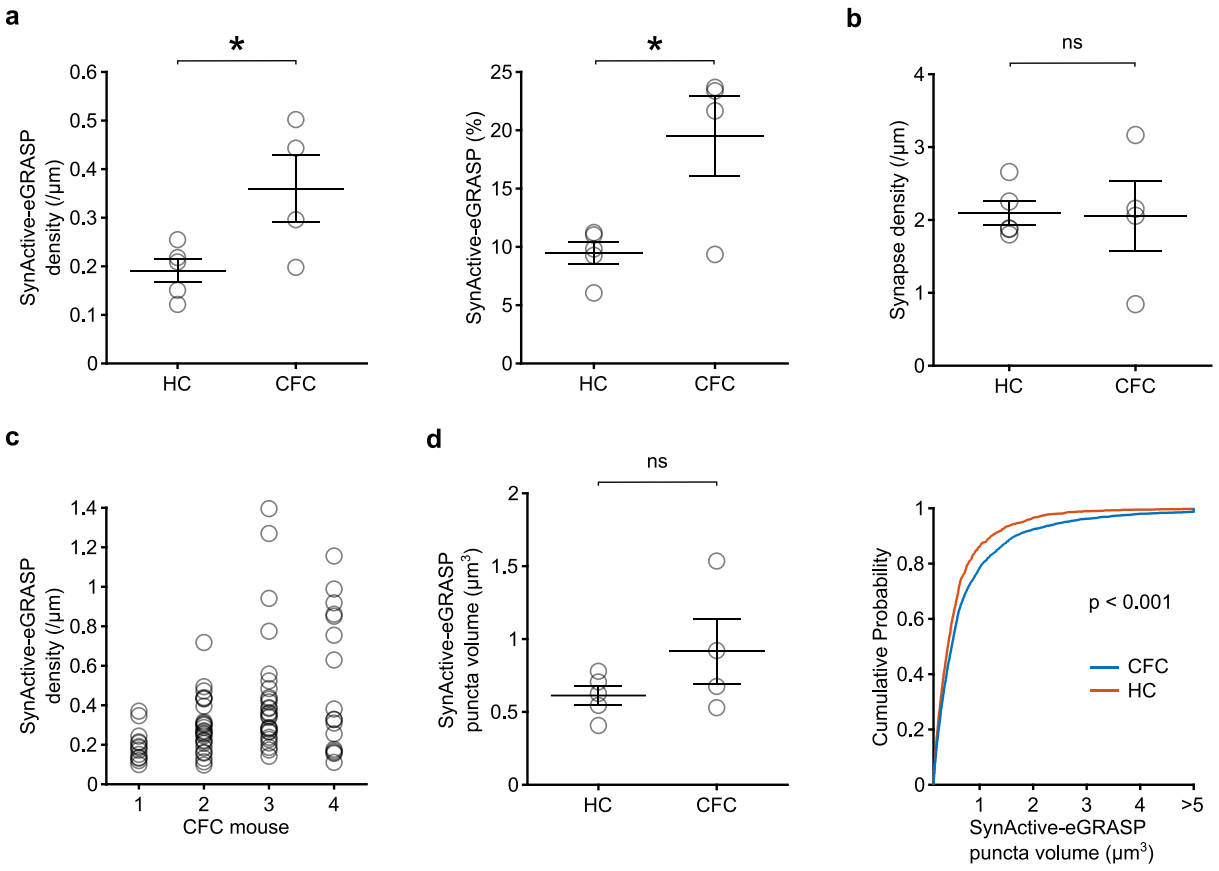


**Figure 4.18 Increased density of CA3-CA1 potentiated synapses after CFC.**

(**a**) The number of SynActive-eGRASP puncta normalized with respect to dendritic trace length (density) (*left*) or total number of mTurquoise2-positive CA3 boutons in the same dendritic segment (*right*) is higher in CFC mice compared to HC mice. (HC n=5, CFC n=4 mice from 3 independent experimental replicates; Student's *t*-test, *p<0.05). (**b**) No significant difference in the density of mTurquoise2-positive CA3 boutons between the CFC and HC groups. Each data point represents a mouse. (HC n=5, CFC n=4 mice from 3 independent experimental replicates; Student's *t*-test, p=0.9339, ns, non-significant). (**c**) Intraindividual variability in the density of SynActive-eGRASP-positive potentiated synapses among dendritic segments. Each data point represents a dendritic trace (**d**) Plots showing a trend towards higher SynActive-eGRASP-positive puncta volume in CFC mice compared to HC mice. (*Left:* HC n=5, CFC n= 4 mice from 3 independent experimental replicates; Student's *t*-test, p=0.1898, ns, non-significant; *right*: HC n=1840, CFC n=4023 SynActive-eGRASP-positive puncta from 3 independent experimental replicates; Kolmogorov-Smirnov test, $p=1.10 \times 10^{-9}$).

### 4.2.4 Distribution of SynActive-eGRASP-positive potentiated synapses along the CA1 *stratum radiatum*

Inhibition of EC-CA1 synaptic transmission by tetanus toxin light chain (TeTX) expression impairs learning of a fear conditioning task in mice (Suh *et al.*, 2011). In hippocampal slices,

activation of EC inputs in the *stratum lacunosum moleculare* facilitates potentiation at CA3-CA1 synapses in the *stratum radiatum* synapses (heterosynaptic potentiation) (Dudman *et al.*, 2007). To examine whether CA3-CA1 synapses closer to the EC-CA1 synapses are more likely to be potentiated than proximal synapses during CFC, I examined the distribution of SynActive-eGRASP-positive puncta along the *stratum radiatum.* Images of this hippocampal layer were divided into 10 equal parts (16-18 µm bin width) and counted percentage (normalized to the number of mTurquoise2-positive CA3 boutons) of SynActive-eGRASP-positive puncta in each dendritic territory (Figure 4.19a).

The mTurquoise2-positive CA3 bouton density was relatively low in the more distal and proximal extremities of the *stratum radiatum*, but there was no significant difference between the CFC and HC groups (Figure 4.19b). In contrast, the percentage of SynActive-eGRASP-positive synapses was greater in CFC compared to HC at all levels across the *stratum radiatum* (Figure 4.19c). Interestingly, I found an increasing trend in the percentage of SynActive-eGRASP-positive synapses from the proximal to distal *stratum radiatum* (Figure 4.19c). The volume of SynActive-eGRASP-positive synapses showed a similar trend (Figure 4.19d). These findings are preliminary, and the number of animals has to be increased for statistical analysis.

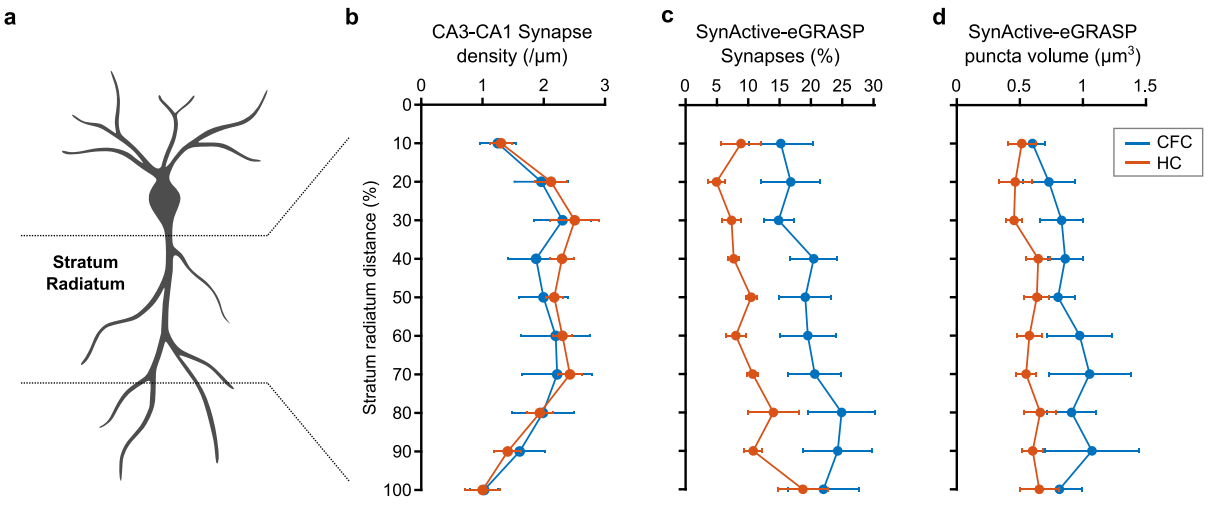


**Figure 4.19 SynActive-eGRASP is non-uniformly distributed along the *stratum radiatum*.**

(**a**) Schematic of CA1 pyramidal neuron with the analyzed region *stratum radiatum* marked. (**b, c, d**) Preliminary plots showing the distribution of mTurquoise2-positive CA3 bouton density (**b**), Percentage

of SynActive-eGRASP-positive synapses normalized to mTurquoise2-positive CA3 bouton density (**c**), and SynActive-eGRASP-positive puncta volume (**d**) along the *stratum radiatum*. (HC n=5, CFC n= 4 mice from 3 independent experimental replicates; HC n=1840, CFC n=4023 SynActive-eGRASP-positive puncta; preliminary data).

### 4.2.1 Clustering of potentiated CA3-CA1 synapses after associative learning.

Adjacent spines with synchronous activity and/or receiving inputs from the same presynaptic neuronal population were frequently found to be clustered within the dendrites (Druckmann et al., 2014; Kleindienst et al., 2011; Takahashi et al., 2012). Theoretical models suggest that synaptic clustering can increase the computational power of dendrites by nonlinear synaptic integration and action potential generation (Kastellakis and Poirazi, 2019). To examine whether potentiated CA3-CA1 synapses are clustered, I calculated the nearest neighbor distance (d), defined as the pathlength along the dendritic trace between two adjacent SynActive-eGRASP-positive puncta (Figure 4.20a). In CFC mice, the distribution of nearest neighbor distance was found to be shifted to shorter values compared to HC animals, suggesting the grouping of potentiated CA3-CA1 synapses (Figure 4.20a).

To further characterize this aspect, I defined a 'cluster' as an ensemble of three or more SynActive-eGRASP-positive puncta with the nearest neighbor distance value lower than the median nearest neighbor distance values in the HC group (median $d_{HC}$, 1.08 µm) (Figure 4.20b). The median value was used instead of the mean because the nearest neighbor distance values were not normally distributed (Shapiro-Wilk test, $p<0.0001$) in the HC group. To perform clustering, I used the DBSCAN (Density-Based Spatial Clustering of Applications with Noise) algorithm in MATLAB (Ester et al. 1996). Median $d_{HC}$ was used as the epsilon neighborhood parameter of the DBSCAN that defines the maximum distance between two points in a cluster and the minimum number of points required to form a cluster was set to 3.

I found that mice exposed to CFC had a higher percentage of SynActive-eGRASP-positive synapses belonging to clusters compared to HC controls (32% and 17%, respectively; Figure 4.20c). Similarly, dendritic segments from CFC mice had a significantly higher number of clusters than HC mice (Figure 4.20b, d). The cumulative distribution of cluster size (i.e., the number of SynActive-eGRASP-positive puncta contained in each cluster) of CFC mice showed a significant shift towards higher values in comparison to HC mice (Figure 4.20e). Of note, no significant

difference between the volume of clustered and of isolated SynActive-eGRASP-positive puncta was found. Anyways, both clustered and isolated potentiated synapses remained larger in CFC mice than in HC controls (preliminary, the number of animals has to be increased for statistical analysis). (Figure 4.20f). These findings may indicate that learning promotes the clustering of potentiated CA3 synapses onto CA1 dendritic segments.

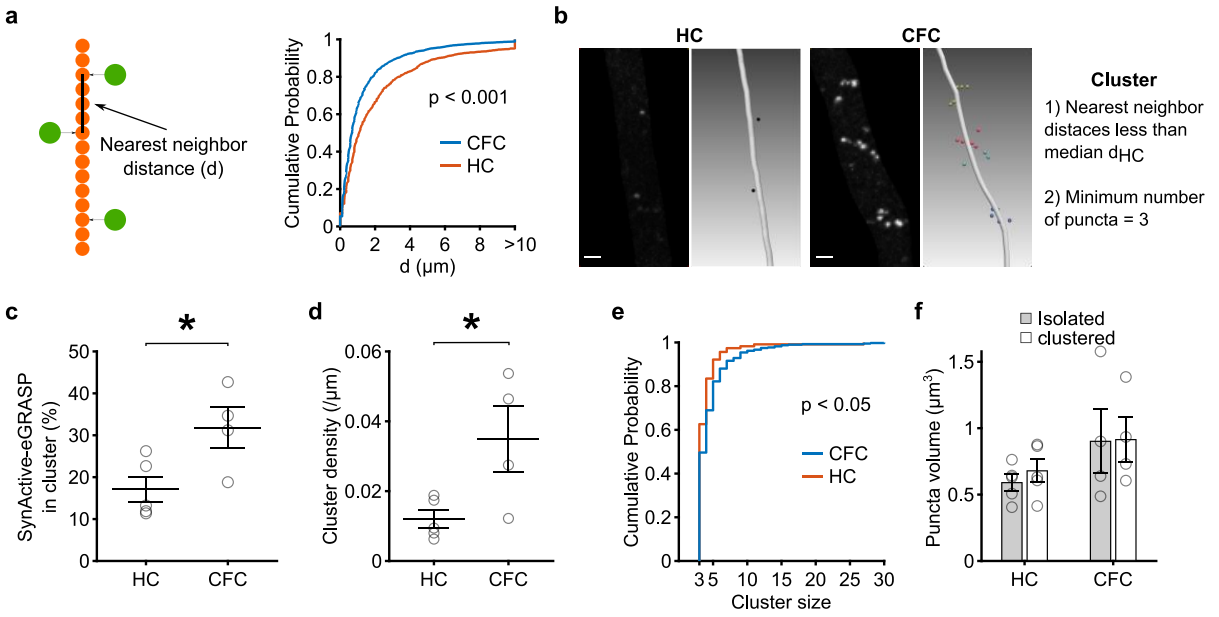


**Figure 4.20 SynActive-eGRASP synapses are clustered in CFC mice.**

**(**a) Graphical representation (*left*) and cumulative distribution (*right*) of pathlength along a dendritic trace between two adjacent SynActive-eGRASP puncta (Nearest neighbor distance, d), which was significantly smaller in CFC mice with respect to HC controls (HC n=1823, CFC n=4011 SynActive-eGRASP-positive puncta from 3 independent experimental replicates; Kolmogorov-Smirnov test, $p=5.83 \times 10^{-33}$). (**b**) Representative images and 3D visualization of SynActive-eGRASP-positive puncta in HC and CFC mice. Non-clustered puncta are in black. Puncta in clusters are color-coded and each color corresponds to a cluster. Scale bar, 2 µm. (**c**, **d**) The percentage of SynActive-eGRASP-positive puncta that belonged to cluster (**c)** and the number of clusters normalized to the dendritic trace length (**d**) was significantly higher in CFC mice compared to HC controls. (HC n=5, CFC n= 4 mice from 3 independent experimental replicates; Student's *t*-test, *p < 0.05). (**e**) Cumulative distribution of cluster size (i.e., number of SynActive-eGRASP synapses contained in each cluster), which was significantly larger in CFC mice than HC controls. (HC n=115, CFC n=393 clusters of SynActive-eGRASP-positive puncta from 3 independent experimental replicates; Kolmogorov-Smirnov test, p=0.0422). (**f**) Plot showing the volume of clustered and isolated SynActive-eGRASP-positive puncta in HC and CFC. (HC n=5, CFC n= 4 mice from 3 independent experimental replicates; preliminary data).

## 4.3 Further expanding the SynActive toolbox for mapping, characterizing and manipulating potentiated synapses.

The biological principle on which the SynActive strategy is based -- namely local translation triggered by synaptic potentiation, occurring close or into a potentiated spine, followed by import of the locally translated reporter protein into the potentiated spine – allows, in principle, the expression of any reporter or actuator at excitatory potentiated postsynaptic dendritic spines. These include fluorescent proteins and optogenetic proteins (Gobbo *et al.*, 2017; Gobbo and Cattaneo, 2020) and split reporters for transsynaptic tracing (this thesis). In this Section, I will describe the design, construction, and validation (and in some cases initial exploitation) of vectors for different applications of the SynActive experimental strategy. In particular, I will describe vectors for i) the optimization of large-scale mapping of learning-related potentiated synapses, ii) the labeling of two temporally sequential and distinct rounds of synaptic potentiation, iii) the proteomic characterization of learning-related potentiated synapses and iv) the functional investigation of the necessity and sufficiency of putative synaptic engrams.

### 4.3.1 SynActive for brain-wide mapping of potentiated spines

In Gobbo *et. al*., SynActive was successfully implemented via *in utero* electroporation to label potentiated spines in a neuron associated with a novel context via expressing Channelrhodopsin fused to red fluorescent protein mCherry and to SYNtag (SA-Ch) (please see section 1.4.4). Here, I sought to (i) improve the protein-moiety for synaptic localization of SynActive reporters into the dendritic spines and (ii) facilitate their *in vivo* delivery. To this end, I took inspiration from Hayashi-Takagi *et al.* (2015) and created SynActive-PSD95Δ-Venus. This construct contains a truncated rat PSD95 (PDZ1 and PDZ2 domains deleted to avoid overexpression artifacts and to avoid the possibility of unwanted dominant negative effects) fused to the yellow fluorescent protein mVenus and to the HA peptide tag, which I cloned in between the *Arc* 5’ and 3’ UTR and under the control of the TRE promoter (Figure 4.21a). To target the newly translated protein at the potentiated spine head, this construct employs a synaptic protein (PSD95) rather than a synapse localization signal (PSD-95 PDZ domain binding peptide ETQV and NMDAR C terminal sequence SIESDV, referred to as SYNtag in Gobbo *et al*., 2017). In keeping with the general approach, I adopted for controlling the time window of SynActive expression, a second construct was employed to express rtTA, along with the tdTomato fluorescent protein under the control of

the human synapsin (hSyn) promoter. TdTomato acts as a filler to visualize the complete morphology of infected neurons (Figure 4.21a).

Initially, I infected primary hippocampal cultures with SynActive-PSD95Δ-mVenus packaged in AAV5 to examine activity-dependent expression and labelling of potentiated spines. Compared to control neurons that received only Dox, a strong mVenus signal enriched at dendritic spine heads was observed 90 min after KCl treatment to depolarize neurons and lower the threshold for potentiation (Figure 4.21b, c). Perisomatic fluorescence, likely from the translation of a non-dendritically/synaptically targeted SynActive mRNAs (Gobbo *et al.*, 2017), was present in transduced neuronal cultures.

This optimized vector system should facilitate large-scale, possibly brain-wide, mapping of potentiated spines.

### 4.3.2 Employing SynActive to label two rounds of synaptic potentiation.

Although synaptic plasticity has been shown to be correlated with learning and memory (please see section 1.2.6), whether the same set of synapses is involved in encoding and recall is not known. Experimental tools to address this fundamental question are lacking and need to be developed. To this end, I developed SynActive-DsRED-E5, to label in two different colors synapses that have undergone potentiation at two distinct time points. DsRED-E5 is a slowly maturing fluorescent protein that changes its emission spectra from green to red over time (Figure 4.22a) (Terskikh *et al.*, 2000). Similar to other SynActive constructs described in the above sections, DsRED-E5 fused to SYNtag was cloned in between the *Arc* 5’ and 3’UTRs. Using SynActive-DsRED-E5, spines potentiated at two different time points, (e.g., memory encoding and recall) can be identified by the presence of red and green fluorescence, respectively (Figure 4.22b). Moreover, synapses expressing DsRED-E5 in both immature and mature forms (i.e., green and red) would have undergone potentiation at both time points (Figure 4.22b).

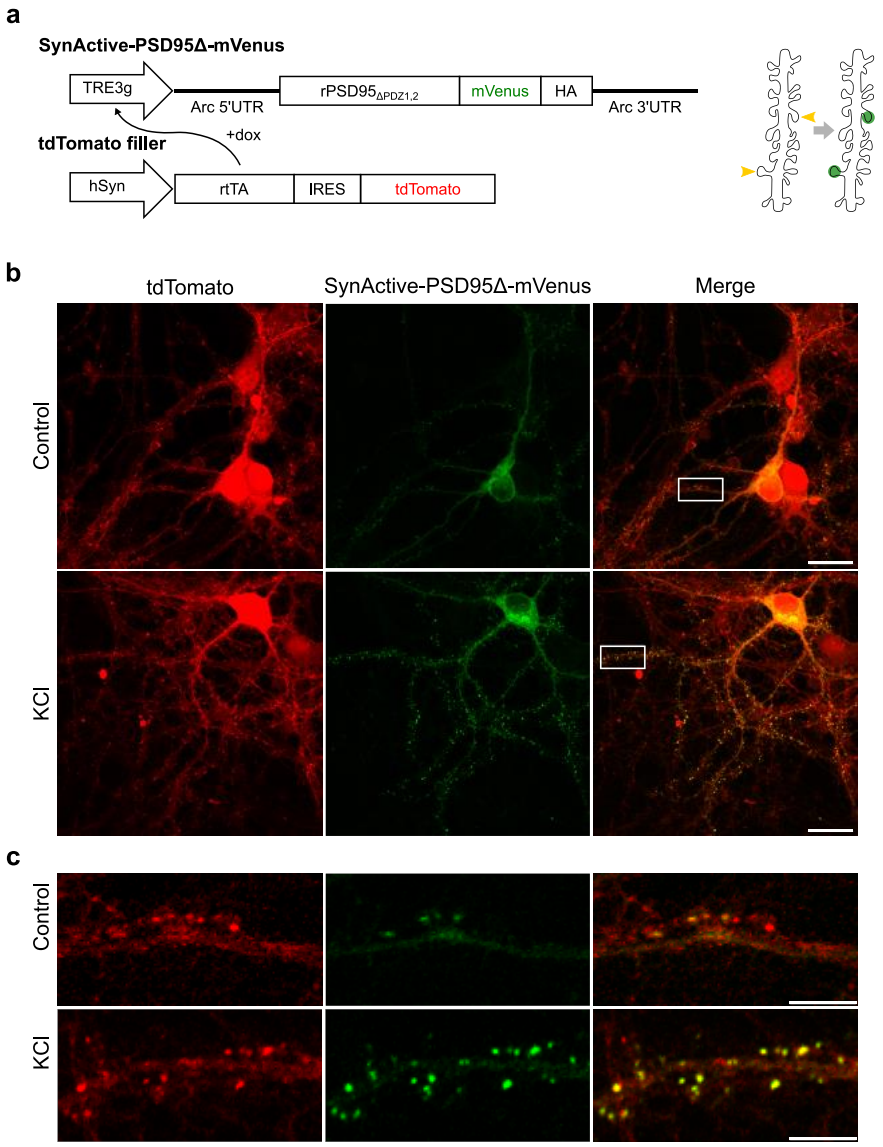


**Figure 4.21 SynActive-PSD95Δ-mVenus labels potentiated spines in cultured primary hippocampal neurons.**

(**a**) Diagram of the SynActive-PSD95Δ-mVenus construct (*left*). Schematic shows labelling of potentiated spines (green) by SynActive-PSDΔ-mVenus (*right*). (**b**) KCl treatment to depolarize neurons and lower the threshold for potentiation promotes enrichment of SynActive-PSD95Δ-mVenus (green) at dendritic spines, visualized via tdTomato expression (red). Scale bar, 20 µm. (**c**) Magnified views of boxes in **b**. Scale bar, 5 µm.

To examine potentiation-dependent labeling of dendritic spines, I transfected primary hippocampal neurons with SynActive-DsRED-E5 and mTurquoise2 filler constructs and analyzed the expression pattern under different conditions. Bright red and green fluorescence were evident

in neurons 24 h after the induction of Gly-cLTP in the presence of Dox (Figure 4.22c, d). No apparent red and green fluorescence was present in the conditions (i) Dox alone (control), (ii) no Dox, (iii) LTP blockade with D-AP5 (Figure 4.22c, d). Spines with red fluorescence were most often also positive for green fluorescence, indicating 24 h as an intermediate timepoint where the timer reporter DsRED-E5 was present as both its remote (red) and recent (green) forms (Figure 4.22c, d). Only a subset of spines displayed both red and green forms of DsRED-E5 after Gly-cLTP. Figure 4.22e shows a representative image (*left*) and an intensity line scan plot (*right*) through two spines, with and without the expression of both red and green forms of DsRED-E5 after Gly-cLTP (S2 and S1 respectively).

To determine the temporal evolution of DsRED-E5 emission spectra at potentiated spines, I fixed transfected neurons at various time points after Gly-cLTP. At 6h post-Gly-cLTP, both green and red fluorescence spines were very weakly labelled (Figure 4.23a, b). The signal improved over time, with evident green and red fluorescence spines both at 24 h and 48 h time points (Figure 4.23a, b). The greater increase of the red+green spines, with respect to the percentage of red-only spines, suggests the initially ongoing contribution of newly potentiated spines (that would lead to the local translation of the green form of DsRED-E5). In keeping with the progressive maturation of DsRED-E5 from green to red, the percentage of spines with both red and green fluorescence showed a decreasing trend from 24 h to 48 h (Figure 4.23c). However, no apparent increase in the number of spines showing only red fluorescence was detected at 48 h (Figure 4.23c). This could be because of DsRED-E5 degradation, or spine turnover that results in the removal of SynActive-DsRED-E5-positive spines. These results demonstrate activity-dependent expression and temporal evolution of SynActive-DsRED-E5. The very low number of green-only spines at 6 hours (after which it decreases) may indicate that recently potentiated spines (labelled in the first 1-2 hours following Gly-cLTP) might have already made their transition to red).

Following these single-round LTP experiments, further *in vitro* experiments involving two rounds of LTP induction are required to validate whether SynActive-DsRED-E5 can reliably label synapses potentiated at two-time points in two different colors.

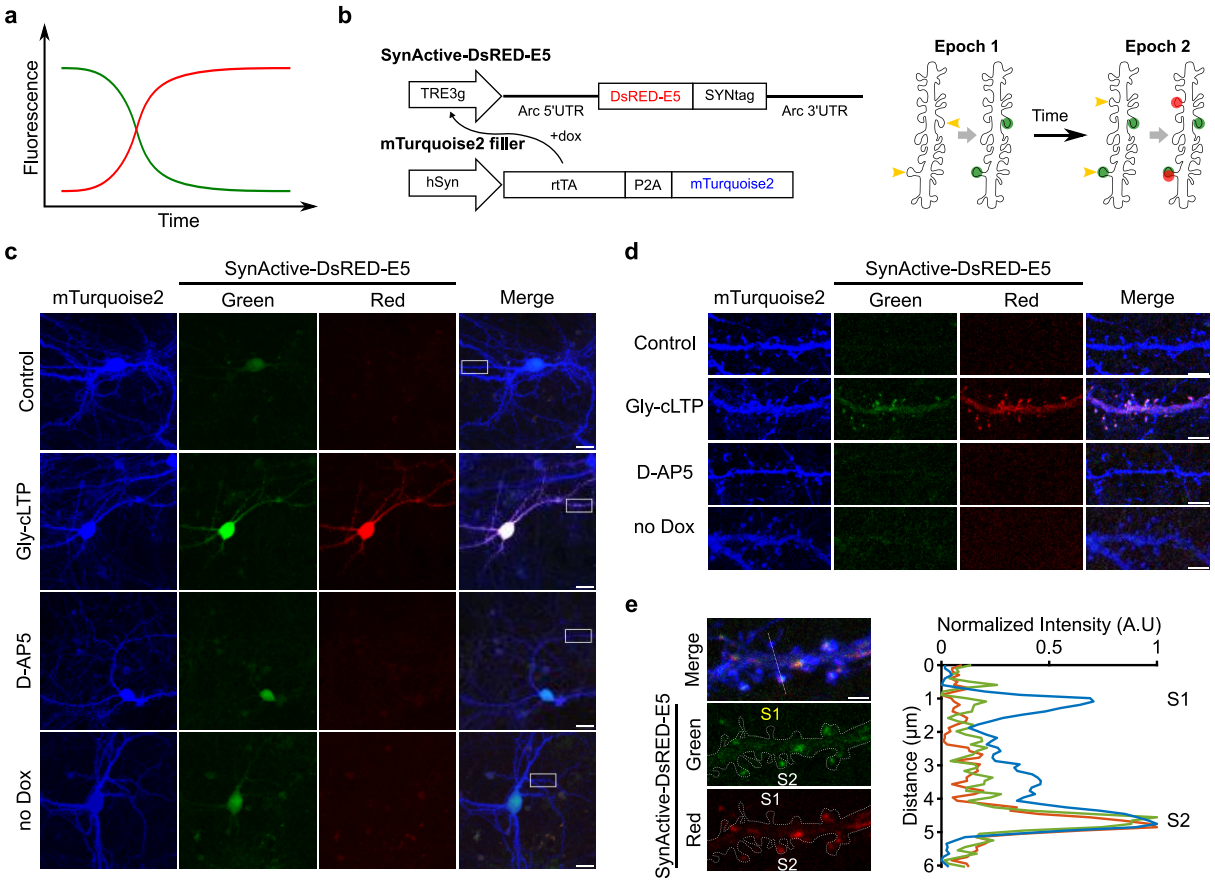


## Figure 4.22 Expression of DsRED-E5 under SynActive control.

(**a**) Schematic plot showing the time course of DsRED-E5 maturation-dependent spectral shift. Early after expression, DsRED-E5 is in the immature, green-emitting state, followed by maturation to the red-emitting state. (**b**) SynActive-DsRED-E5 constructs (*left*) and the cartoon showing how SynActive-DsRED-E5 can tag spines potentiated at remote (red) and recent (green) time points (right). (**c, d**) SynActive-DsRED-E5 (green, red) was evident in mTurquoise2-positive neurons (blue) 24 h after the induction of Gly-cLTP in the presence of Dox; but not in Dox alone (control), no Dox, and (iii) LTP blockade with D-AP5 conditions. Magnified views of the boxes in **c** are shown in **d**. Scale bars, 20 µm (**c**), 5 µm (**d**). (**e**) Representative images (*left*) and intensity line scan plot (*right*) showing that only a subset of spines (blue) displayed both red and green forms of DsRED-E5 after Gly-cLTP. S2 and S1 denote spines with and without the expression of DsRED-E5, respectively. Scale bar, 2 µm.

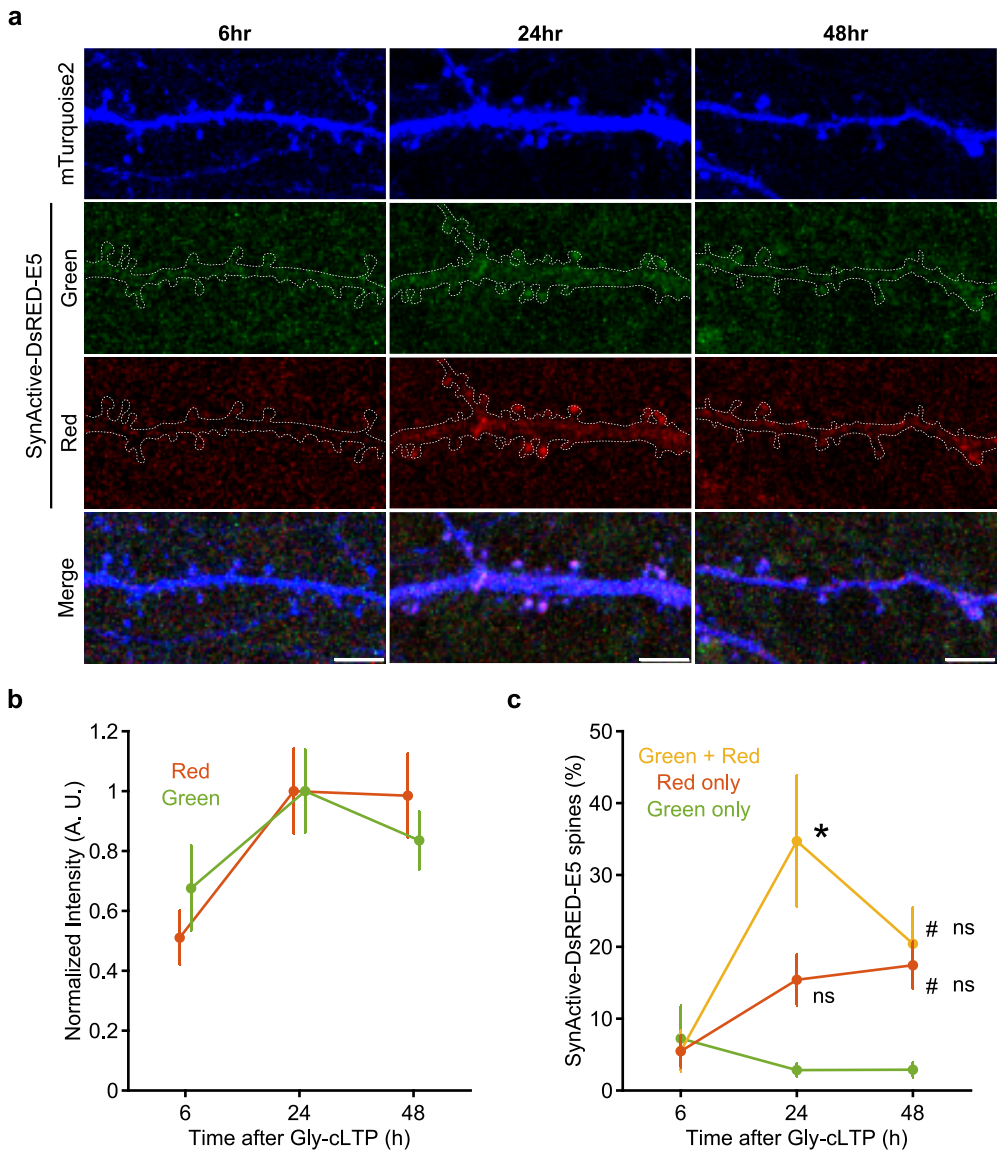


**Figure 4.23 Temporal profile of SynActive-DsRED-E5 expression after Gly-cLTP.**

(**a**) SynActive-DsRED-E5 expression at 6, 24 and 48 h after Gly-cLTP. Scale bar, 5 µm. (**b, c**) Normalized intensity (**b**) and percent of spines (**c**) with green and red forms of DsRED-E5 at 6, 24 and 48 h after Gly-cLTP. (6 h n=7, 24 h n=13, 48 h n=16 neurons from 3 independent experimental replicates; **b,** ANOVA-2 repeated measures test, Time × DsRED-E5 form interaction, ns, nonsignificant ; **c,** ANOVA-2 repeated measures test, Time × DsRED-E5 form interaction, $p<0.05$, followed by Tukey post hoc test, 6 h versus 24 h, *$p<0.05$ (yellow line), ns, nonsignificant (red line) ; 6 h versus 48 h, #$p<0.05$ (yellow and red line) ; 24 h versus 48 h, ns, nonsignificant (yellow and red line)).

### 4.3.3 Characterizing the potentiation-specific protein content of synapses using SynActive-PSD95-FLAG

The formation of memory is associated with long-lasting changes in the strength of synaptic transmission that depend on the rearrangement and trafficking of existing proteins and on *de novo* synthesis (Mayford *et al*., 2012). In addition to the classical studies that examined individual proteins, proteomics approaches have identified several proteins that were up- or down-regulated at the synapses following learning (Dieterich and Kreutz, 2016; Kähne *et al*., 2012; Rao-Ruiz *et al*., 2015). However, these proteomics data should be interpreted cautiously, as samples consisted of synaptic membrane fractions coming from total neural tissue lysates. Towards a more specific isolation of synaptic proteins at a proteomic scale, Fernandez *et. al.* generated a knock-in mouse line to characterize the synaptic interactome of the multi-connected protein hub PSD95, by creating a knock-in gene encoding a fusion protein in which the tandem affinity purification (TAP) tag (composed of a poly-histidine affinity (HAT) tag and the 3x FLAG tag, separated by tobacco etch virus (TEV) protease cleavage site) is C-Terminally fused to PSD95 (Fernández *et al*., 2009). This approach allowed the characterization of the general interactome of PSD95 using immunoprecipitation coupled with mass spectrometry. However, the resulting PSD95 protein interactome database refers to a heterogeneous set of synapses and while offering a powerful reference dataset, does not provide proteomic information on the protein composition of potentiated synapses. Since only a small proportion of synapses were supposed to potentiate and encode memory (Dieterich and Kreutz, 2016), these potentiated synapses would be significantly "diluted" if no specific tagging is performed to isolate them from the bulk of all synapses.

Towards the generation of a potentiation-specific proteomic tag, I reasoned that the proteomic reporter FLAG-tagged PSD95, used by Fernandez *et al.* (2009) to generate their PSD95interactome dataset, could be placed under the control of SynActive to gain insight into the potentiated synapse proteomics (Figure 4.24a). This was achieved by cloning PSD95-FLAG flanked by *Arc* 5' and 3' UTRs under the control of the activity-dependent ESARE synthetic promoter (construct will be referred to as SynActive-PSD95-FLAG) (Figure 4.24a) (Kawashima *et al.* 2013). In addition, to attain a general proteome of the excitatory spines, I generated a second construct to express PSD95-FLAG constitutively at all synapses under the control of the

constitutive hSyn (human Synapsin) promoter (will be referred to as Const-PSD95-FLAG) (Figure 4.24a).

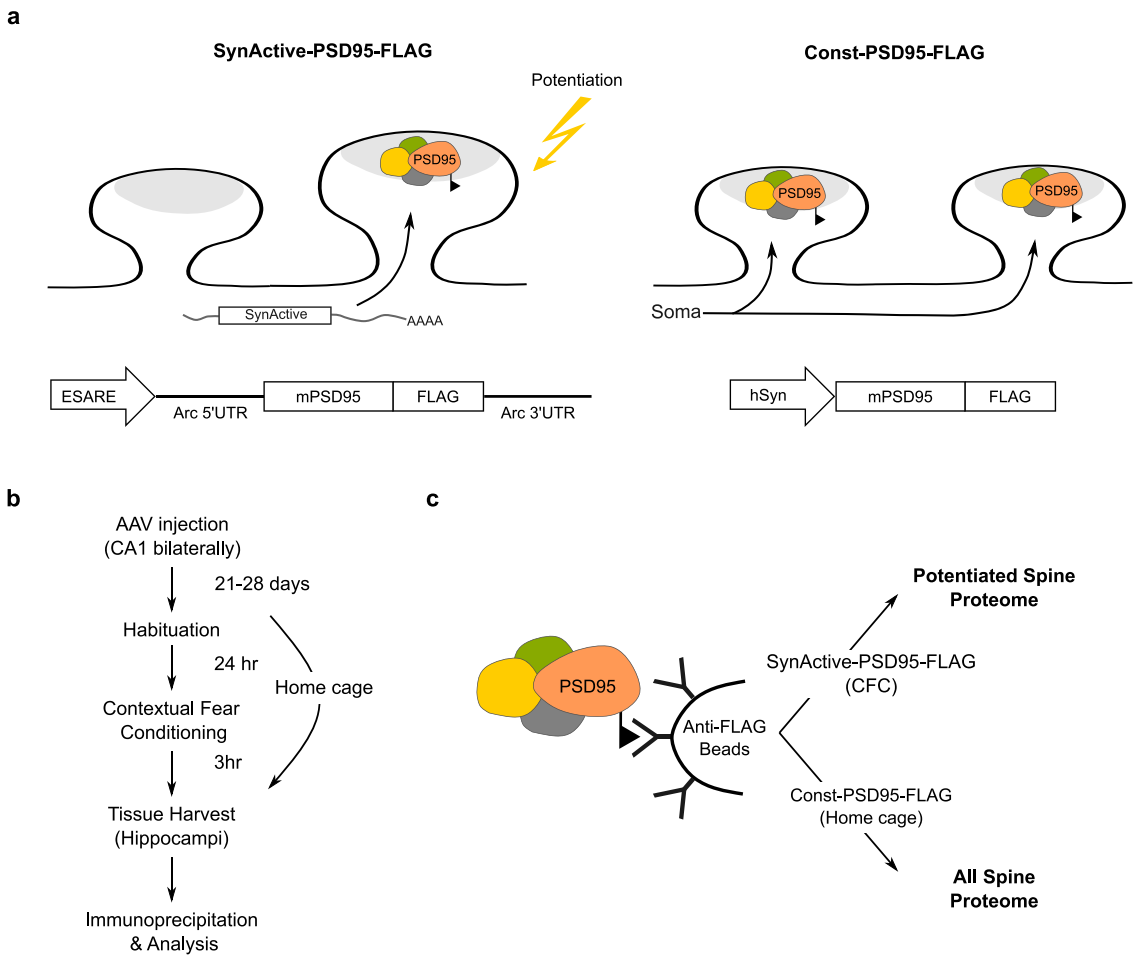


**Figure 4.24 Potentiated spine-specific affinity purification of PSD95 and its interactors.**

(**a**) Schematic illustration of SynActive-PSD95-FLAG and Const-PSD95-FLAG expression at potentiated synapses and all synapses, respectively. PSD95-interacting proteins are shown as dark grey, yellow and green objects close to PSD95 (orange) with the FLAG tag (**b**) *In vivo* experimental timeline for affinity purification of PSD95 and its interactors. (**c**) Immunoprecipitation of SynActive-PSD95-FLAG with anti-FLAG coated beads yields potentiated spine proteome, whereas Const-PSD95-FLAG yields all spine proteome.

Initially the expression pattern of SynActive- and Const-PSD95-FLAG were analyzed in primary hippocampal cultures. Neurons infected with SynActive-PSD95-FLAG AAVs displayed an increased density of FLAG-positive puncta following Gly-cLTP, in comparison to non-treated control neurons (Figure 4.25). In contrast no significant difference in FLAG-positive puncta was observed between Gly-cLTP and control, in neurons infected with Const-PSD95-FLAG AAVs

(Figure 4.25). The density of FLAG-positive puncta was lower in SynActive-PSD95-FLAG infected neurons than Const-PSD95-FLAG infected neurons. These results provide *in vitro* evidence for the activity dependent expression of SynActive-PSD95-FLAG and labelling of potentiated spines.

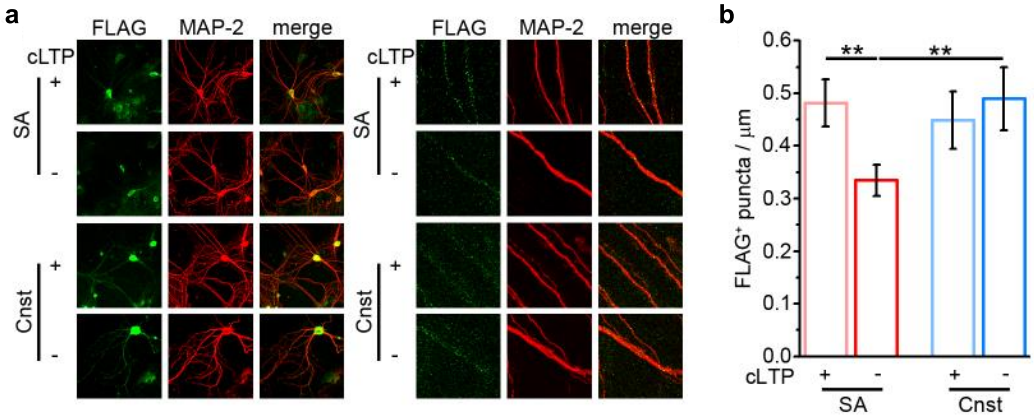


**Figure 4.25 SynActive-PSD95-FLAG expression is activity-dependent in primary neuron cultures.**

**a**) Representative low- (*left*) and high- (*right*) magnification images showing the expression of SynActive-PSD95-FLAG (SA) and Const-PSD95-FLAG (Cnst) in MAP2-positive neurons following glycine mediated LTP induction (cLTP). **b**) Quantification of FLAG-positive puncta reveals a significant increase in the density after Gly-cLTP in SA, but not in Cnst. (SA: +cLTP n=11, -cLTP n=13, neurons; Cnst: +cLTP n=11, -cLTP n=8, neurons; ANOVA-2, followed by Tukey post hoc test, **p<0.01).

To obtain the potentiation-specific interactome of PSD95, AAVs of SynActive-PSD95-FLAG were bilaterally injected into the CA1 region of adult mice (2 months) (Figure 4.24b). Then, activity-dependent synaptic potentiation was triggered by CFC and fresh hippocampal tissue was harvested 3 h later. Mice that received Const-PSD95-FLAG AAVs remained in the home cage till the tissue dissection (Figure 4.24b). Hippocampi from different animals (2 and 3 mice for Const-PSD95-FLAG and SynActive-PSD95-FLAG, respectively) were pooled together and immunoprecipitation of PSD95-FLAG was performed with anti-FLAG M2 paramagnetic beads (Figure 4.24c). To obtain sufficient material after immunoprecipitation, I chose not to perform a two-step tandem affinity purification via TEV protease cleavage of the FLAG tag to expose the HAT tag, because of the high loss of proteins after the multiple rounds of washing and precipitation required by the second round of purification in this protocol. The price paid by a somewhat reduced

purity is well compensated by the reduced losses of the specific proteins, given the high biological precision of the expressed proteomic bait selectively at potentiated synapses.

To check the quality of the immunoprecipitated proteins (IP), I performed western blot analysis of proteins affinity purified from hippocampal tissues. When blots were probed with anti-FLAG, a band close to $M_w$ of 100 kDa $M_w$ that corresponds to the PSD95-FLAG bait was detected in the input and IP samples from both groups - Const-PSD95-FLAG and SynActive-PSD95-FLAG (**Error! Reference source not found.**a). Compared to Const-PSD95-FLAG, the amount of PSD-FLAG was lower in the SynActive-PSD95-FLAG, as expected from its predicted expression only in a subset of the overall spines. A lower proportion of N-terminal truncated PSD95 is known to exist in the synapses and was detected in our western blots as an additional band close to $M_w$ of 75 kDa groups (**Error! Reference source not found.**a) (Xu *et al.*, 2008). Histone 3 (H3) was not present in the IP samples from both groups, indicating the absence of nuclear contaminants (**Error! Reference source not found.**b).

Next, I probed the blots with antibodies specific for some known direct or indirect PSD95 interactors involved in synaptic potentiation, such as NMDAR subunits GluN2A and GluN2B (GluN2A/B), calcium-calmodulin-dependent kinase II (CaMKII) subunits α and β, AMPAR subunit GluA1, activity-regulated cytoskeleton-associated protein (Arc), and ribosomal protein S6 (**Error! Reference source not found.**c) (Bramham *et al.*, 2010; Lisman *et al.*, 2012; Luscher and Malenka, 2012). The western blots were normalized with respect to the PSD95-FLAG bait. PSD95 interactors detected in the IP samples were lower in the SynActive-PSD95-FLAG group in comparison to Const-PSD95-FLAG. This was in line with the expression of PSD95-FLAG (**Error! Reference source not found.**a) and indicates that PSD95 interactors are retrieved from the small subset of synapses undergoing potentiation in SynActive-PSD95-FLAG expressing mice. However, the ratio of each of the tested target proteins, with respect to the bait protein PSD95-FLAG was significantly higher in the IP samples from mice expressing SynActive-PSD95-FLAG compared to Const-PSD95-FLAG. This indicates stronger interaction and enrichment of these individually tested PSD95 interactors in potentiated spines (**Error! Reference source not found.**d).

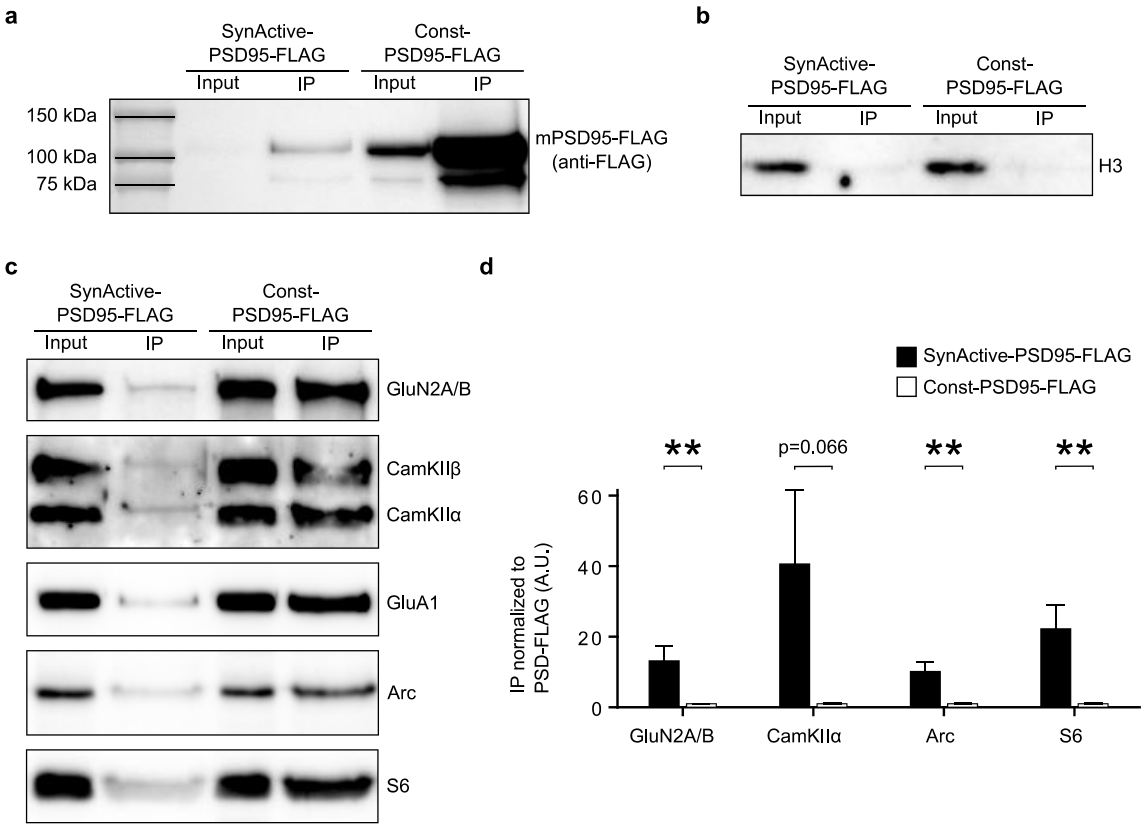


**Figure 4.26 Immunoprecipitation using SynActive- and Const-PSD95-FLAG recovers known interactors of PSD-95**

Protein extracts from hippocampal tissues harvested from mice expressing SynActive-PSD95-FLAG or Const-PSD95-FLAG were processed for immunoprecipitation using anti-FLAG-coated paramagnetic beads (IP) and compared with the corresponding input material (input). (**a**, **b**) Western blot images showing enrichment of PSD95-FLAG (**a**) and absence of nuclear contaminant (i.e., Histone3, H3) (**b**) in IP samples from both groups. (**c**) Affinity purification of PSD95-FLAG retrieves known PSD95 interactors. (**d**) Normalization of signal intensity on PSD95-FLAG IP bait reveals that GluN2A/B, CaMKIIα, Arc and S6 show increased interaction with PSD95 in samples from mice expressing SynActive-PSD95-FLAG compared to Const-PSD95-FLAG. (SynActive-PSD95-FLAG: GluN2A/B n=10, CamKIIα n=5, Arc n=7, S6 n=7 samples; Const-PSD95-FLAG: GluN2A/B n=13, CamKIIα n=6, Arc n=8, S6 n=8 samples; Student's *t*-test, **p<0.01).

These experiments demonstrated that PSD95 and its interactors can be purified and identified selectively from *in vivo* potentiated synapses. Label-free tandem mass spectrometry analysis of IP samples from mice expressing SynActive- and Const-PSD95-FLAG is currently under progress to characterize the changes in the PSD95-interactome by learning-induced synaptic plasticity.

### 4.3.4 Memory retrieval by photoactivation of potentiated spines.

To establish whether SynActive-labelled synapses represent synaptic memory engrams, one should demonstrate that they are necessary and/or sufficient for the behavioral expression of that specific memory. The sufficiency criteria can be addressed by expressing channelrhodopsin specifically at potentiated spines using SynActive and optically reactivating them at later time points to induce the expression of memory (Figure 4.27a). We previously demonstrated that Channelrhodopsin (ChR) can be selectively expressed at potentiated synapses and functionally reactivated by light in primary neurons (Gobbo *et al.,* 2017). However, the photocurrents produced by the opening of ChR at potentiated spines, in response to short pulses of the light stimulus were lower, possibly too low for affecting neuronal spiking (Gobbo *et al.,* 2017). This would make memory recall by selective potentiated-synapse reactivation quite unlikely. To circumvent this issue, I decided to express under the SynActive strategy, a more powerful excitatory optogenetic channel. I, therefore generated SynActive-ChR2XXM-mVenus construct, carrying a channelrhodopsin variant - ChR2XXM with higher photocurrents. ChR2XXM (extra high expression and medium open state) indicates the D156H mutant of channelrhodopsin, which has been reported to display higher expression and larger photocurrents than the wildtype in *Xenopus* oocytes and *Drosophila* neurons (Scholz *et al*., 2017). Similar to other SynActive constructs described in the above sections, ChR2XXM fused to mVenus and SYNtag was cloned in between the *Arc* 5' and 3'UTRs, under the control of the TRE3g promoter (Figure 4.27a).

Primary neuronal cultures were transfected with SynActive-ChR2XXM-mVenus and tdTomato filler (hSyn-rtTA-IRES-tdTomato). Confocal microscopy showed enrichment of SynActive-ChR2XXM-mVenus at dendritic spines following KCl-induced depolarization (Figure 4.27b, c). On the other hand, SynActive-XXM-Venus expression was very low in the control conditions represented by – (i) Dox only, (ii) KCl-treatment without Dox (KCl only), (iii) No Dox and No KCl. (Figure 4.27b, c), thus confirming doxycycline-dependent transcription and activity-dependent expression.

Following the imaging data, we performed a functional assessment of the synaptically expressed SynActive-ChR2XXM-mVenus. Patch clamp recording showed photocurrents and spikes in response to 470-nm light stimulation (Figure 4.28a, b), demonstrating that the Channelrhodopsin ChR2XXM expressed from the SynActive-ChR2XXM-mVenus vector is

functional. Preliminary analysis on patch-clamp recordings obtained from a small number of neurons showed that both whole-cell photocurrents and the number of spikes were higher in KCl-treated neurons in comparison to the control conditions (Figure 4.28a, b). These imaging and electrophysiology results demonstrate activity-dependent expression of SynActive-ChR2XXM-mVenus in primary neuron cultures. *In vivo* validation of SynActive-ChR2XXM-mVenus is currently under investigation in our lab.

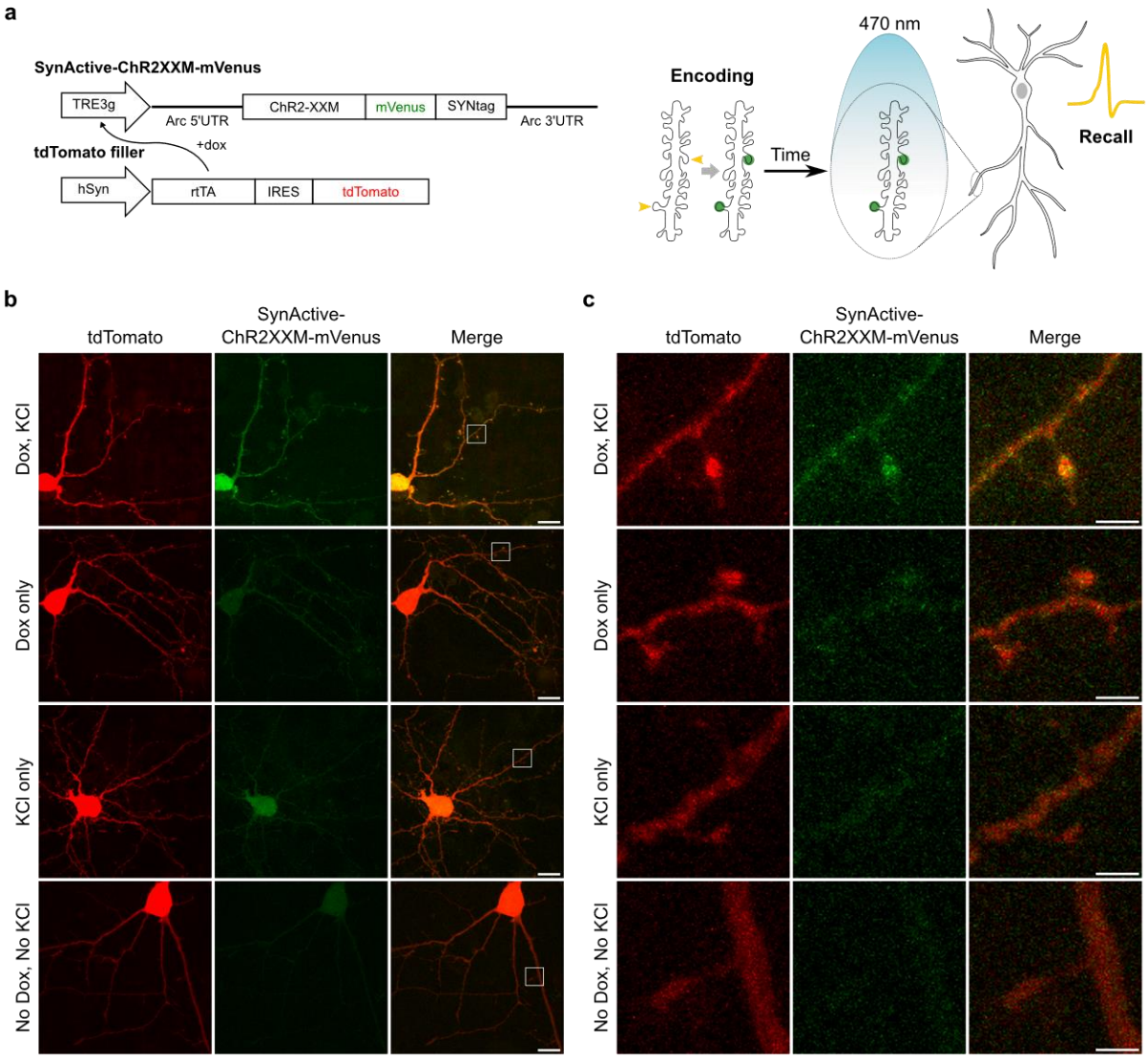


**Figure 4.27 Expression of SynActive-ChR2XXM-mVenus in primary neuronal cultures.**

(**a**) SynActive-XXM-Venus constructs (*left*) and schematic of labelling of potentiated spines with SynActive-ChR2XXM-mVenus to demonstrate the existence of synaptic memory engrams (*right*) -

activation of SynActive-ChR2XXM-mVenus expressed at potentiated spines by 470-nm light stimulation induces neuronal spiking and leads to memory retrieval. (**b)** Expression of SynActive-ChR2XXM-mVenus (green) after KCl-induced depolarization in the presence of Dox (Dox, KCl) and in the control conditions – (i) Dox only, (ii) KCl-treatment without Dox (KCl only), (iii) No Dox and No KCl. Neurons were visualized via tdTomato expression (red). Scale bar, 10 µm. (**c**) Magnified views of boxes in **b**. Scale bar, 2 µm.

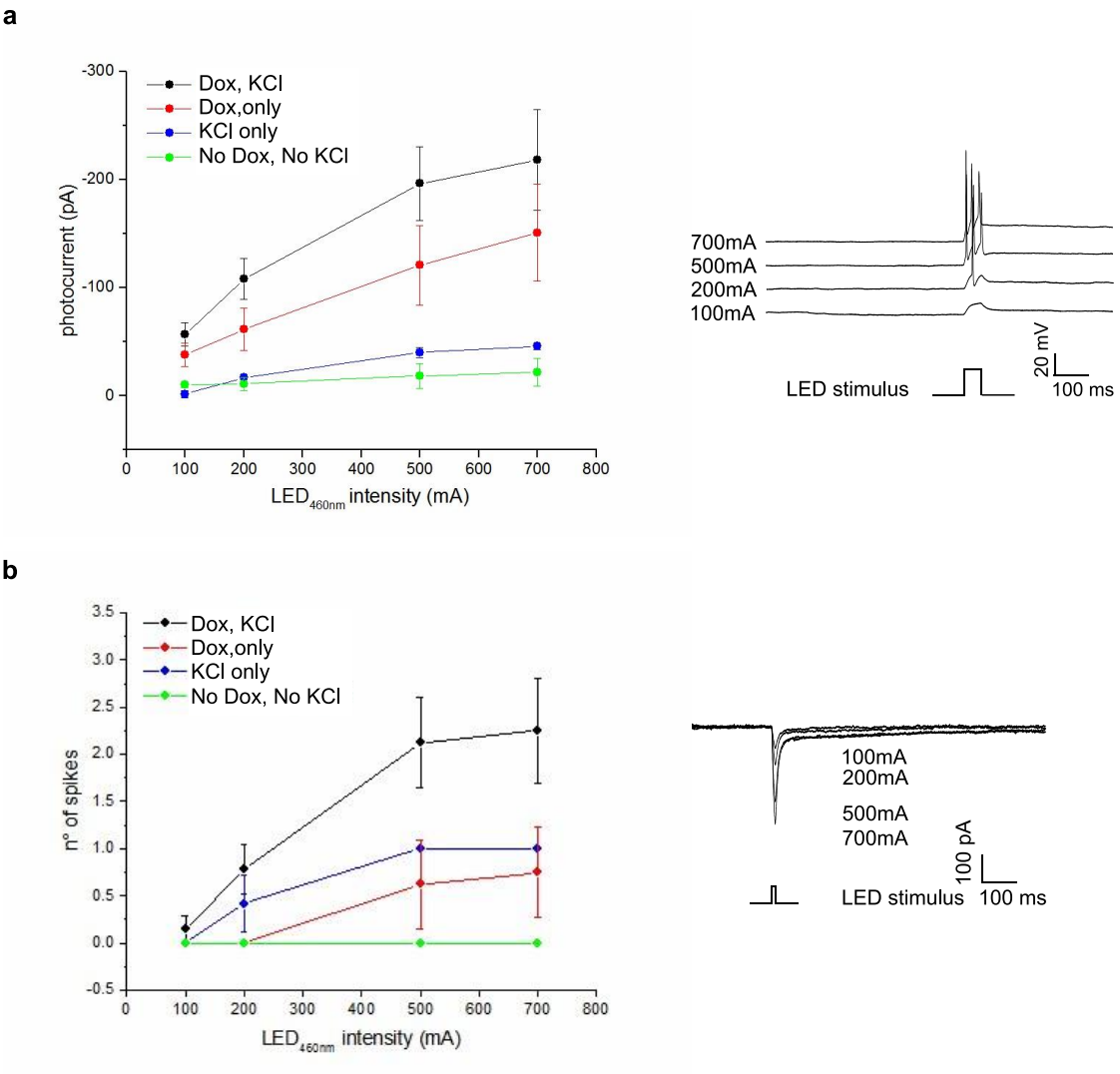


**Figure 4.28 Activation of SynActive-ChR2XXM-mVenus induces photocurrents and spikes in primary neuronal cultures.**

(**a**, **b**) Quantification of photocurrents (**a**) and neuronal spikes (**b**) elicited by 470-nm light illumination, in neurons transfected with SynActive-ChR2XXM-mVenus (*right*). Representative photocurrents (**a**) and neuronal spikes (**b**) from a neuron in the Dox, KCl group (*right*).

# 5 DISCUSSION

Learning and memory correlate with activity-dependent synaptic plasticity processes at appropriate synaptic circuits (Takeuchi *et al.,* 2014; Dringenberg 2020). The underlying mechanisms of information storage in the brain are currently investigated at a whole-neuron scale to identify cellular memory engrams i.e., ensembles of neurons whose recruitment and activation are necessary and sufficient for the retrieval of a specific memory (Tonegawa *et al*., 2018; Josselyn and Tonegawa, 2020). Although successful, they are limited with cellular level resolution and cannot identify the subset of synapses that have undergone learning-induced synaptic plasticity. Traditional methods for structural and functional analysis of synapses are not sufficient for investigating which subset of synapses out of the many thousands received by any given neurons is responsible for representing memory elements. To address this fundamental question, new experimental strategies are required. We have developed 'SynActive', a genetic toolbox exploiting regulatory sequences from the *Arc* mRNA and synapse-targeting peptides, that allows the expression of any protein of interest specifically at potentiated synapses (Gobbo *et al.*, 2017). Here I have extended the SynActive toolbox to map, characterize and manipulate potentiated synapses both *in vitro* and *in vivo*.

## 5.1 SynActive-eGRASP labels potentiated synapses *in vitro*

Although SynActive has been used by Gobbo et al. to label spines potentiated in response to LTP induction *in vitro* and novel context exposure *in vivo*, these experiments did not differentiate among the different hippocampal circuits that could take part in this process (Gobbo *et al.*, 2017). To address this point via circuit-specific labeling of potentiated synapses, I developed SynActive-eGRASP, by adapting the split-GFP (Feinberg *et al.*, 2008; Kim *et al.*, 2011; Choi *et al.*, 2018). In primary hippocampal neurons, I found that 65% of the synapses were labelled with SynActive-eGRASP when long-term potentiation was chemically induced by the established Gly-cLTP protocol (Figure 4.3c) (Lu *et al.*, 2001; Molnár, 2011). The value was closer to the reported percentage of potentiated spines labelled by SynActive-Channelrhodopsin (SA-Ch) in primary cortical cultures after BDNF-, KCl- or NMDA-mediated LTP induction and by activated synapse targeting photoactivatable Rac1 (AS-PaRac1) in primary hippocampal cultures after bicuculline treatment (Hayashi-Takagi *et al.*, 2015; Gobbo *et al.*, 2017). SynActive-eGRASP expression relied on NMDAR activation, as the number of positive synapses was drastically reduced in neurons

cultured in the presence of the NMDAR antagonist D-AP5 (Figure 4.3; Figure 4.8). A good proportion of synapses expressed SynActive-eGRASP even in the absence of any LTP-inducing stimulation (Figure 4.3; Figure 4.8). This might be associated with a consistent fraction of synapses undergoing stimulation-independent LTP as a result of high network activity, which is often found in primary neuronal cultures (Cohen *et al.*, 2008; Biffi *et al.*, 2013). In agreement, I saw almost zero SynActive-eGRASP expression when neurons were treated with both TTX and D-AP5, that inhibit neuronal activity and potentiation, respectively (Figure 4.8).

High-frequency optical stimulation can induce LTP at synapses receiving input from Channelrhodopsin-expressing presynaptic neurons. In brain slices, CA3-CA1 synapses were potentiated by 150 light pulses delivered at 5 Hz or by four repeats of 50 pulses delivered at 20 Hz paired with a long postsynaptic depolarization (3 min, 0 mV) (Choi *et al.*, 2018; Wiegert *et al.*, 2018). In an *in vivo* study, Nabavi *et al.* induced LTP in the synapses from medial geniculate nucleus and auditory cortex to lateral amygdala with optical stimulation of 100 pulses delivered at 100Hz, repeated 5 times with a 3min interval (Nabavi *et al.*, 2014). To optically induce LTP (optoLTP) in primary hippocampal neurons, I expressed channelrhodopsin Chronos in presynaptic neurons and delivered blue light (470-nm) pulses by adapting a conventional theta-burst stimulation (TBS) protocol (Figure 4.7) (Klapoetke *et al.*, 2014; Testa *et al.*, 2019). In neurons receiving direct inputs from Chronos-expressing presynaptic neurons, a gradual increase in the amplitude of optically evoked excitatory postsynaptic potentials (EPSCs) were observed following optoLTP stimulation, reflecting potentiation (Figure 4.7c). Similar to Gly-cLTP, the majority of synapses expressed SynActive-eGRASP after optoLTP (Figure 4.8). LTP induction by optoLTP protocol was more effective and reliable than the Gly-cLTP protocol, as indicated by the number of mTurquoise2 neuron expressing activity dependent mScarlet-I and SynActive-eGRASP being higher after opto-LTP than after Gly-cLTP.

Although genetic methods like SEP-GluA1(AMPAR GluA1 subunit tagged with Super Ecliptic pHluorin (SEP)), SA-Ch and AS-PaRac1 label potentiated spines, they suffer from a pretty low signal enrichment at spines with respect to the dendritic shaft (Makino and Malinow, 2009, 2011; Hayashi-Takagi *et al.*, 2015; Gobbo *et al.*, 2017). SynActive-eGRASP appeared as clear puncta at spine heads and more than 90% of them colocalized with the synaptic proteins PSD95 and Synaptophysin (Figure 4.9). In contrast to the SynActive reporter (SA-ChR) described in Gobbo et al., SynActive-eGRASP did not show any somatic expression *in vitro*.

LTP is associated with increase in synaptic transmission efficiency, initially mediated by exposure of the AMPAR subunit GluA1 on the spine head, correlating with increased spine volume (Kopec *et al.*, 2006; Makino and Malinow, 2009). I found upregulation of GluA1 and structural enlargement in SynActive-eGRASP-positive synapses following induction of Gly-cLTP, indicating them as potentiated synapses (Figure 4.10). These results were in line with previous reports that show co-expression of SynActive and GluA1in stimulated spines following LTP induction using glutamate uncaging (Hayashi-Takagi *et al.*, 2015; Gobbo *et al.*, 2017).

The greatest advantage of SynActive-eGRASP is that the identity of both presynaptic and postsynaptic neurons can be identified and characterized, and that it allows to visualize the potentiated synapses between these two neuronal populations. To achieve expression of individual SynActive-eGRASP components in two separate neuronal populations, I simultaneously transfected neuronal cultures with two separate transfection mix containing pre-GRASP and post-GRASP (please see section 3.3 and Figure 4.2). To study the synaptic potentiation between two genetically defined population, SynActive-eGRASP components could be expressed under the control of neuronal sub-type specific promoters instead of the pan-neuronal human synapsin (hSyn) or CaMKII promoters (Nagai *et al.*, 2019). An alternative approach ach for *in vitro* studies would be to use compartmentalized microfluidics chambers to get two physically separated neuronal population with synaptic connectivity (Taylor *et al.*, 2010). Microfluidics provides more flexibility, allowing chemical or optical manipulation of neurons in one compartment without affecting the other. Combining two or three compartment microfluidics with SynActive-eGRASP in multicolor, experiments can be designed to study the distribution of potentiated synapses from different presynaptic partners and/or potentiated at different time-points.

## 5.2 Structured connectivity of synapses potentiated by encoding of fear memory

With recent technical advancements, spines potentiated in response to whisker stimulation, motor task learning and novel context exposure have been identified in the mouse barrel cortex, motor cortex and hippocampus, respectively (Makino and Malinow, 2011; Hayashi-Takagi *et al.*, 2015; Gobbo *et al.*, 2017). CA3 synapses on CA1 pyramidal neurons (CA3-CA1 synapses) were reported to be potentiated following the learning of behavioral tasks such as contextual fear conditioning (CFC), inhibitory avoidance, eyelid conditioning and Morris water maze (Gruart, Muñoz and Delgado-García, 2006; Whitlock *et al.*, 2006; Habib *et al.*, 2014; Pavlowsky *et al.*,

2017; Choi *et al.,* 2018). Exploiting the ability of SynActive-eGRASP to label input-specific potentiated synapses, I used this method to visualize the CA3-CA1 synapses that had undergone potentiation during learning of contextual fear conditioning task. The average number of potentiated CA3-CA1 synapses was almost double in fear-conditioned mice in comparison to animals kept in their home cage (Figure 4.18a). This was in line with the recent report that identified increased synaptic connectivity between putative CA3 and CA1 engram neurons 2 days after CFC using dual-eGRASP (i.e., labelling synapses from two distinct presynaptic neuronal populations with GRASP in two different colors) (Choi *et al.,* 2018). LTP occlusion experiments showed that theses synapses had undergone learning induced potentiation (Choi *et al.,* 2018). Similarly, in a recent study that employed synaptic proximity ligation assay (SYNPLA) with recombinantly expressed presynaptic myc tagged neurexin 1b (myc-NRXN) and endogenous postsynaptic GluA1, a threefold increase in potentiated synapses from auditory cortex (and/or medial geniculate nucleus) to the lateral amygdala was reported after auditory fear conditioning (Dore *et al.,* 2020). I observed intraindividual variability in the density of SynActive-eGRASP-positive potentiated synapses among dendritic segments (Figure 4.18c), which suggests individual dendritic segments contribute differentially to the encoding and storage of a memory. This is in line with the school of thought that identifies the dendritic branch as the functional unit of plasticity (Govindarajan *et al.,* 2006; Branco and Häusser, 2010; Govindarajan *et al.,* 2011).

The size of SynActive-eGRASP puncta can be a proxy of spine volume and synaptic strength. A correspondence between mGRASP puncta size and postsynaptic conductance has been observed in the synapses between auditory cortex and inferior colliculus (Song *et al.,* 2018). I found increased SynActive-eGRASP-positive puncta volume in CFC compared to HC (Figure 4.18d). This suggests that structural (and possibly functional) potentiation associated with learning (CFC) is more likely to be stronger or retained for longer periods (24 h in the current study) than baseline synaptic potentiation (HC). In the motor cortex, spines potentiated during learning in the rotarod task maintained structural enlargement for at least 48 h (Hayashi-Takagi *et al.,* 2015). In putative CA1engram neurons, spines that received inputs from putative CA3 engram neurons were larger than spines that synapsed with CA3 non-engram neurons, even 2 days after CFC (Choi *et al.,* 2018). Persistence of the increased synaptic efficiency achieved during the learning, either by spine enlargement or number increase, is crucial for the effective storage and recall of the memory (Xu

*et al.*, 2009; Yang, Pan and Gan, 2009; Takeuchi, Duszkiewicz and Morris, 2014; Ryan *et al.*, 2015; Roy *et al.*, 2016; Kitamura *et al.*, 2017).

CA1 neurons receive multimodal sensory information from the entorhinal cortex (EC) directly through temporoammonic or perforant pathway (EC layer III-CA1), and indirectly, through trisynaptic pathway (EC layer II-DG-CA3-CA1) (Basu and Siegelbaum, 2015). In addition to CA3-CA1 synapses, EC-CA1 synapses are also crucial for the encoding of episodic memories, as mice expressing tetanus toxin light chain (TeTX; inhibits synaptic transmission) in the EC layer III displayed severe deficits in temporal association memory task and trace fear conditioning (Suh *et al.*, 2011). Although EC-CA1 synapses are weaker and cannot elicit spiking of CA1 neurons, they can induce heterosynaptic potentiation at CA3-CA1 synapses (Jarsky *et al.*, 2005; Dudman *et al.*, 2007). Paired activation of EC and CA3 inputs at a 20 ms delay (EC before CA3) in brain slices induced large (100-300%) potentiation in CA3-CA1 synapses without altering the EC-CA1 synaptic strength (Dudman *et al.*, 2007). This predicts that during the encoding phase of a memory, CA3-CA1 synapses in the distal *stratum radiatum* which are closer to the EC-CA1 synapses in the *stratum lacunosum moleculare*, are more likely to be potentiated than proximal synapses. Consistently, I found an increasing trend in the percentage of SynActive-eGRASP-labelled potentiated CA3-CA1 synapses in the distal *stratum radiatum* compared to its proximal part (Figure 4.19c). Moreover, in the CFC mice SynActive-eGRASP volume increased from proximal to distal (Figure 4.19d). These results are in line with the studies that suggest distal synapses should be stronger to compensate the distance-dependent signal attenuation and thus to have influence on the somatic output (Magee and Cook, 2000; Katz *et al.*, 2009).

Theoretical models predict that the clustered synapses can have many computational and memory-related advantages, resulting from the supra-linear synaptic integration and induction of dendritic spikes (Poirazi and Mel, 2001; Poirazi *et al.*, 2003; Kastellakis *et al.*, 2016; Kastellakis and Poirazi, 2019). Recent studies report learning-associated anatomical and/or functional clustering of synapses in brain areas such as motor cortex, retrosplenial cortex and hippocampus (Makino and Malinow, 2011; Fu *et al.*, 2012; Gobbo *et al.*, 2017; Frank *et al.*, 2018). In agreement, I observed clustering of potentiated CA3-CA1 synapses in fear conditioned mice (Figure 4.20). The distribution of the distance between two adjacent SynActive-eGRASP puncta (nearest neighbor distance, d) was shifted to shorter values in CFC mice compared to HC animals (Figure 4.20a). Moreover, the total number of clusters and proportion of clustered potentiated CA3-CA1

synapses were significantly higher in the CFC (Figure 4.20c, d). Multiple mechanisms can lead to synapse clustering. Since compound synapses (multiple synapses formed between by a single axon on the same dendrite) are not commonly found in the *stratum radiatum*, clustering might have occurred here by cooperative plasticity on nearby CA1 synapses that received inputs from multiple CA3 axons with synchronous activity (Govindarajan *et al.*, 2006; Govindarajan *et al.*, 2011; Bloss *et al.*, 2018; Kastellakis and Poirazi, 2019).

I analyzed the SynActive-eGRASP expression 24 h after LTP induction (*in vitro*) or fear conditioning (*in vivo*), that provided enough time for the expression, reconstitution, and fluorescence maturation of the proteins, while in Choi *et al*. eGRASP expression was analyzed 2 days after CFC. A time course experiment will provide information on how early the SynActive-eGRASP appears after LTP induction or fear conditioning and how long does it last. This information is crucial while designing experiments with multiple rounds of LTP inducing stimulations or with encoding and recall. Postsynaptic neurons receive input from multiple presynaptic neurons of distinct cell types or origin, eg: CA3 and EC synapses on CA1 pyramidal neurons (Kajiwara *et al.*, 2008). Multicolor SynActive-eGRASP (Figure 4.11) opens the possibility to study learning associated synapse potentiation in multiple neuronal circuits within the same animal. After learning, new spines are found to be formed closer to the stable spines, thus increasing spine density locally (Fu *et al.*, 2012; Frank *et al.*, 2018). Impact of circuit specific potentiation on the nearby spine structure and distribution can be analyzed by combining SynActive-eGRASP with a bright postsynaptic filler. Recently dual-eGRASP has been employed to examine the connection between astrocytes and putative engram neurons (Kim *et al.*, 2023). As an extension, the role of astrocytic connections on learning-induced synaptic potentiation can be studied by expressing pre-eGRASP in astrocytes and SynActive-post-eGRASP in potentiated spines. Literature suggests that the influence of a brain region on the expression of memory can change over time by a process termed ‘systems consolidation’ (see section 1.5). SynActive-eGRASP can be employed to investigate how the potentiation in different compartments of the same circuit, or in different circuits, can support different phases of memory.

### 5.3 Spatial precision of the SynActive reporters.

The subcellular spatial precision of the reporters expressed with the SynActive approach depends on (and is limited by) the precision of the underlying biological process of local synaptic

translation and on the diffusion of the locally translated proteins. Briefly, it depends on the following factors:

i) activity-dependent targeting of neo-transcribed *Arc* mRNAs from the nucleus to soma to dendrites under nominally translationally repressed conditions (because of the 5' and 3' UTR from *Arc* mRNA in the SynActive vector).

What proportion of Arc mRNA molecules undergoes dendritic transport (versus residency in the soma or proximal dendritic compartment), how precise is the translational repression during the transport to the dendritic compartment, and if on route-translation occurs are all factors that could (and do) limit the spatial precision of "potentiated-synapse localization of the SynActive reporter protein. Also, the 5' UTR and 3' UTR of *Arc* mRNA may not recapitulate the full stringency of *Arc* mRNA regulation.

ii) activity-dependent and translation-dependent local expression of reporters/actuator proteins at excitatory potentiated synapses, based on the RNA component of the SynActive vector.

iii) targeting of *de novo* translated protein into the dendritic spine, based on the synaptic protein tag moiety of the SynActive vector, and diffusion of the SynActive reporter out of the potentiated synapse.

What is the spatial spread of the nascent locally translated proteins? And what influences the spatial limit of their actions? What is the spatial extent of the neuronal postsynaptic translation compartment? The spatial precision of synaptically translated proteins, and their limits with respect to single synapse precision, have been discussed (Rangaraju *et al*., 2017). Local translation and synaptic proteome remodelling is a complex phenomenon carried out in several phases. Each phase (mRNA redistribution, signalling events, translation of proteins) occupies its own spatial compartment ultimately operating towards a coordinated functional outcome. Translational hot spots of 5–20 μm in size have been observed in dendrites following global or local stimulation, although what defines this size remains to be determined. In particular, it should be underlined that the measured size of the translation compartment is driven by the biology, or the methodology used (Rangaraju *et al*., 2017). Finally, the diffusional limits of synaptic-plasticity proteins modified, activated, or translated in the course of long-term potentiation have been measured for several proteins and found to vary for different proteins (Yasuda, 2017). This limits the single synaptic precision but forms the basis of clustered plasticity phenomena.

Altogether, for all these reasons the first generation of SynActive reporters, based on the direct expression show, in addition to the prevalent predicted localization at potentiated postsynaptic dendritic spines, also a certain degree of staining in the dendritic shaft and, in some cases in the soma (for reasons that we do not yet fully understand, in cultured neurons more than *in vivo*). While this "spurious" non-synaptic localization can be limited by carefully titrating the expression level and the experimental conditions, it reduces the signal to ratio of the first generation, direct, SynActive imaging method.

The GRASP method for imaging learning-related potentiated synapses *in vivo*, that I have developed and validated in my thesis, has a remarkably precise synaptic localization precision, with an optimal signal-to-noise ratio. The superior precision of the GRASP method is due to the inbuilt, intrinsic two-tier approach, that makes the "potentiated-synapse-specific" signal conditional also on the presence of the presynaptic component that provides a necessary element of the signaling event. Thus, SynActive-eGRASP reporter is an AND logic gate that only reconstitutes a signal if a presynaptic partner is apposed to the potentiated postsynaptic element. In this format, all spurious SynActive signals deriving from the SynActive component (dendritic shaft or soma) are automatically neglected, unless there is a pre-synaptic component.

In summary, the SynActive-eGRASP appears to be the best solution to identify and map learning-related potentiated spines *in vivo*. Its advantages are a very favourable signal-to-noise ratio, intrinsically overcoming technical and biological limitations of the strategy with an inbuilt noise-reducing mechanism. The SynActive-eGRASP method lends itself to build cartography and atlases of the *in vivo* distributions of potentiated excitatory synapses in response to a variety of learning paradigms. It is not of minor practical importance that the signal is viewed directly as a fluorescence signal, with no indirect immunohistochemistry amplification. Thus, the method lends itself also for *in vivo* longitudinal imaging in living behaving mice, with two-photon microscopy (ongoing work). Indeed, dual-eGRASP has been recently employed for the longitudinal imaging of the synaptic connections between CA3 and CA1. (Lee *et al.*, 2023).

To facilitate the anatomical localization of the soma of the presynaptic inputs responsible for postsynaptic potentiation, future developments will combine the SynActive-eGRASP principle with the release, in the presynaptic terminal, of a retrograde signal that triggers an "imaging "event on the soma of the presynaptic neuron. During my PhD I have started working on this principle,

exploiting the synthetic Notch signalling system (Morsut *et al.*, 2016). In this approach, the ligand is expressed in an activity-dependent manner at the postsynaptic potentiated spines and the synthetic notch receptor is expressed constitutively at the presynaptic terminal. Ligand-receptor interaction at the potentiated synapses induces the cytosolic release of transcription factor (e.g., tTA) from the C-terminus of the receptor, which in turn binds to its cognate binding sites in the DNA and drives the expression of the fluorescent reporter in presynaptic neurons.

One main limitation of SynActive-eGRASP is related to the need to ensure the avoidance of co-expression of pre-and post-synaptic partner vectors in the same neuron. This would give an artefactual positive signal (see Figure 4.6). For this reason, we must ensure that the two vectors are injected in spatially well-distant locations (in my case this is why I injected the two vectors contralaterally). This may not always be possible for specific applications of interest. Adding an additional level of regulation, such as cell-type-specific transcriptional control might provide a solution to this limitation, in some cases.

In any case, the SynActive GRASP appears to be the best solution to identify and map learning-related potentiated spines *in vivo* and provides a significant and unprecedented advantage over current tools to visualize learning-task-related synaptic plasticity *in vivo*.

## 5.4 Mapping, characterizing and manipulating potentiated spines using SynActive.

Memory engrams are likely to be distributed among multiple brain regions (Wheeler *et al.*, 2013; Roy *et al.*, 2022). Recent studies exploiting the IEGs have mapped neurons activated during contextual fear memory in more than a hundred brain regions, including hippocampus and amygdala (Wheeler *et al.*, 2013; Roy *et al.*, 2022). To examine the learning-induced change in synaptic strength among multiple brain regions, I developed SynActive constructs that express fluorescent proteins in all potentiated spines of neuron. These constructs, SynActive-PSD95Δ-mVenus and SynActive-DsRED-E5 labelled the potentiated spines in primary neuron cultures (Figure 4.21; Figure 4.22). Brain-wide mapping of memory associated potentiated spines can be achieved by packaging these constructs in blood-brain barrier-permeable AAV serotypes like PHP.eB and delivered systemically (Chan *et al.*, 2017). Although the SA-ChR construct introduced in Gobbo *et al.* labelled potentiated spines *in vivo*, dependence on *in utero* electroporation limited its ease of use and could label only brain regions accessible to this delivery

route (i.e., the hippocampus, the cerebellum, and the visual, motor and prefrontal cortices) (Szczurkowska *et al.*, 2016; Gobbo *et al.*, 2017).

### 5.4.1 Employing SynActive to label two rounds of synaptic potentiation.

In primary hippocampal neurons, potentiated spines expressed green (immature) and red (mature) forms of SynActive-DsRED-E5 after the induction of Gly-cLTP (Figure 4.22). As a *in vivo* application, this construct can be used to address whether spines potentiated during the encoding of a specific memory are also reactivated during recall. Photoconvertible proteins that change the emission spectra after external illumination is an alternative to DsRED-E5 (Pham *et al.*, 2012; Paez-Segala *et al.*, 2015). A recent study employed CaMPARI which includes photoconvertible protein mEos, to map a subset of synapses active during illumination both *in vitro* and *in vivo* (Perez-Alvarez *et al.*, 2020).

### 5.4.2 Characterization of the potentiation-specific protein content of synapses.

Learning induces long-lasting changes in the synaptic strength that depend on the rearrangement of existing proteins followed by *de novo* protein synthesis (Mayford *et al.*, 2012). I developed SynActive-PSD95-FLAG, to identify the proteins up- or down-regulated at potentiated synapses following learning. Western blot images confirmed the *in vivo* expression of SynActive-PSD95-FLAG after contextual fear conditioning and co-immunoprecipitation of synaptic proteins along with Const- or SynActive-PSD95-FLAG. Preliminary analysis indicates an enrichment of known PSD95 interactors in potentiated spines (**Error! Reference source not found.**). The amount of proteins affinity purified with SynActive-PSD95-FLAG was lower as it was expected to be expressed at the potentiated spines, which is only a small proportion of the whole synapses present at a time. High-throughput analysis of the SynActive-PSD95-FLAG affinity purified proteins by mass spectrometry should yield a proteomic fingerprint of potentiated spines, in contrast to the proteomic data reported in previous studies that purified proteins from a mixed pool of potentiated and non-potentiated synapses (Fernández *et al.*, 2009; Rao-Ruiz *et al.*, 2015).

This part of the study provides the first important proof of principle of the possibility to achieve a remarkable selectivity and specificity in the molecular characterization of potentiated excitatory synapses in physiology and pathology. The study also shows the way ahead on how to improve on the current approach, towards increasingly greater precision, by combining the expression of the

SynActive proteomic bait with its cell-type specific Cre-dependent expression. Also, one might conceive to have the proteomic bait constructed in a manner similar to the SynActive-eGRASP vector used for imaging, having a reconstitution of the proteomic bait conditional upon the presence of a presynaptic afferent apposed to the potentiated post-synaptic spine.

### 5.4.3 Identifying and manipulating potentiated spines.

To prove that SynActive labelled potentiated spines are indeed the synaptic engrams supporting the memory, it should be shown that they are necessary and sufficient for the memory retrieval. SynActive-ChR2XXM-mVenus was an improvement over the SA-Ch previously reported in Gobbo *et al*. (2017). I found enrichment of SynActive-ChR2XXM-mVenus at dendritic spines following KCl-induced depolarization in the presence of doxycycline. Substantiating the imaging data, patch clamp recordings showed intensity dependent photocurrents and photoinduced action potentials in SynActive-ChR2XXM-mVenus expressing neurons. In addition to the synaptic signal, clear somatic expression of SynActive-ChR2XXM-mVenus was visible and was in line with the reported SA-Ch expression *in vitro* (Gobbo *et al.*, 2017). This might be due to the overexpression of the construct in primary cultures after transfection, as SA-Ch somatic signal was not detectable *in vivo* (Gobbo *et al.*, 2017). SynActive-eGRASP signal was found to be solely synaptic without any somatic expression, owing to the split expression from the pre- and postsynaptic compartments. Theoretically, by expressing a split channelrhodopsin at the potentiated synapses, one can selectively photoactivate them at later timepoints to induce neuronal firing and memory retrieval, and thus proving the existence of synaptic engram. Since, Channelrhodopsin are transmembrane ion channels, creating a split version and expressing them from two synaptic compartments is challenging. An alternate approach is to use trans-synaptic photoactivable ligand receptor system. In such a system, receptor (a ligand gated ion channel or a GPCR) will be expressed from the potentiated spines and the ligand, accessible to the receptors only during the photo stimulation (controlled using LOV domains), will be expressed constitutively at the presynaptic terminals. Photo stimulation should induce the binding of ligand to the receptor and activate a photo current than can induce neuronal activation and subsequent memory retrieval.

# 6 CONCLUSION

Taking advantage of the SynActive toolbox based on Arc mRNA regulatory sequences, I was able to express the protein of interest, including fluorescent reporters, an affinity purification tag, and an optogenetic actuator specifically at in vitro and in vivo potentiated spines. SynActive-eGRASP allows circuit-specific labeling of potentiated synapses. Employing SynActive-eGRASP I mapped the CA3-CA1 synapses potentiated during an associative memory task – contextual fear conditioning. Semi-automated analysis using a custom-made algorithm revealed a spatially nonuniform and clustered distribution of SynActive-eGRASP-positive synapses. SynActive controlled expression of fluorescent reporters- mVenus, and DsRED-E5 labeled dendritic spines undergoing potentiation in primary neuronal cultures. SynActive-PSD95Δ-mVenus is currently used in our lab to map the location of dendritic spines undergoing potentiation in response to contextual fear conditioning in the CA1 and dentate gyrus. By expressing FLAG-tagged PSD95 under SynActive control, I was able to immunoprecipitate PSD95 and its interactors from in vivo potentiated spines. Mass spectrometry and comparative bioinformatics analysis of the affinity-purified proteins will provide the molecular fingerprint of potentiated spines. In primary neuronal cultures, reactivation of potentiated spines expressing channelrhodopsin induces neuronal spiking. In vivo, SynActive-ChR2XXM-mVenus can be used to tag memory-specific synapses, and optically activating them at later time points might induce memory retrieval.

These novel tools and the initial results they produced provide the first step towards a shift in the study of memory engrams from a cellular to a synaptic resolution. In addition, our quantitative maps of synaptic potentiation in whole brain areas or in specific synaptic circuits can be used to refine computational models of neural plasticity. Ongoing experiments are aimed at performing a comparative analysis of synaptic maps obtained in different phases of memory encoding and recall, in both physiological conditions and in models of neurodegenerative and neurodevelopmental diseases.

## REFERENCES


Abdou, K. *et al.* (2018) 'Synapse-specific representation of the identity of overlapping memory engrams', *Science*, 360(6394), pp. 1227–1231. Available at: https://doi.org/10.1126/science.aat3810.

Abel, T. *et al.* (1997) 'Genetic demonstration of a role for PKA in the late phase of LTP and in hippocampus-based long-term memory.', *Cell*, 88(5), pp. 615–26. Available at: https://doi.org/10.1016/s0092-8674(00)81904-2.

Ahmari, S.E. and Smith, S.J. (2002) 'Knowing a Nascent Synapse When You See It', *Neuron*, 34(3), pp. 333–336. Available at: https://doi.org/10.1016/S0896-6273(02)00685-2.

Amaral, D. and Lavenex, P. (2007) 'Hippocampal neuroanatomy.', in *The hippocampus book*. New York, NY, US: Oxford University Press, pp. 37–114.

Arsic, N. *et al.* (2003) 'Induction of functional neovascularization by combined VEGF and angiopoietin-1 gene transfer using AAV vectors', *Molecular Therapy*, 7(4), pp. 450–459. Available at: https://doi.org/10.1016/S1525-0016(03)00034-0.

Ascher, P. and Nowak, L. (1988) 'The role of divalent cations in the N-methyl-D-aspartate responses of mouse central neurones in culture.', *The Journal of Physiology*, 399(1), pp. 247–266. Available at: https://doi.org/10.1113/jphysiol.1988.sp017078.

Bailey, C.H., Kandel, E.R. and Harris, K.M. (2015) 'Structural Components of Synaptic Plasticity and Memory Consolidation.', *Cold Spring Harbor perspectives in biology*, 7(7), p. a021758. Available at: https://doi.org/10.1101/cshperspect.a021758.

Baltaci, S.B., Mogulkoc, R. and Baltaci, A.K. (2019) 'Molecular Mechanisms of Early and Late LTP', *Neurochemical Research*, 44(2), pp. 281–296. Available at: https://doi.org/10.1007/s11064-018-2695-4.

Barnes, C.A. and McNaughton, B.L. (1985) 'An age comparison of the rates of acquisition and forgetting of spatial information in relation to long-term enhancement of hippocampal synapses.', *Behavioral Neuroscience*, 99(6), pp. 1040–1048. Available at: https://doi.org/10.1037/0735-7044.99.6.1040.

Basu, J. and Siegelbaum, S.A. (2015) ‘The corticohippocampal circuit, synaptic plasticity, and memory’, *Cold Spring Harbor Perspectives in Biology*. Cold Spring Harbor Laboratory Press. Available at: https://doi.org/10.1101/cshperspect.a021733.

Biffi, E. *et al.* (2013) ‘The influence of neuronal density and maturation on network activity of hippocampal cell cultures: a methodological study.’, *PloS one*, 8(12), p. e83899. Available at: https://doi.org/10.1371/journal.pone.0083899.

Binzegger, T., Douglas, R.J. and C Martin, K.A. (2004) ‘Behavioral/Systems/Cognitive A Quantitative Map of the Circuit of Cat Primary Visual Cortex’. Available at: https://doi.org/10.1523/JNEUROSCI.1400-04.2004.

Bliss, T.V.P. and Collingridge, G.L. (1993) ‘A synaptic model of memory: long-term potentiation in the hippocampus’, *Nature*, 361(6407), pp. 31–39. Available at: https://doi.org/10.1038/361031a0.

Bliss, T.V.P. and Gardner-Medwin, A.R. (1973) ‘Long-lasting potentiation of synaptic transmission in the dentate area of the unanaesthetized rabbit following stimulation of the perforant path’, *The Journal of Physiology*, 232(2), pp. 357–374. Available at: https://doi.org/https://doi.org/10.1113/jphysiol.1973.sp010274.

Bliss, T.V.P. and Lømo, T. (1973) ‘Long-lasting potentiation of synaptic transmission in the dentate area of the anaesthetized rabbit following stimulation of the perforant path’, *The Journal of Physiology*, 232(2), pp. 331–356. Available at: https://doi.org/10.1113/jphysiol.1973.sp010273.

Bloss, E.B. *et al.* (2018) ‘Single excitatory axons form clustered synapses onto CA1 pyramidal cell dendrites’, *Nature Neuroscience*, 21(3), pp. 353–363. Available at: https://doi.org/10.1038/s41593-018-0084-6.

Bourne, J.N., Chirillo, M.A. and Harris, K.M. (2013) ‘Presynaptic ultrastructural plasticity along CA3→CA1 axons during long-term potentiation in mature hippocampus.’, *The Journal of comparative neurology*, 521(17), pp. 3898–912. Available at: https://doi.org/10.1002/cne.23384.

Bourne, J.N. and Harris, K.M. (2011) ‘Coordination of size and number of excitatory and inhibitory synapses results in a balanced structural plasticity along mature hippocampal CA1 dendrites during LTP’, *Hippocampus*, 21(4), pp. 354–373. Available at: https://doi.org/10.1002/hipo.20768.

Bourtchuladze, R. *et al.* (1994) 'Deficient long-term memory in mice with a targeted mutation of the cAMP-responsive element-binding protein.', *Cell*, 79(1), pp. 59–68. Available at: https://doi.org/10.1016/0092-8674(94)90400-6.

Bramham, C.R. *et al.* (2010) 'The Arc of synaptic memory.', *Experimental brain research*, 200(2), pp. 125–40. Available at: https://doi.org/10.1007/s00221-009-1959-2.

Branco, T. and Häusser, M. (2010) 'The single dendritic branch as a fundamental functional unit in the nervous system', *Current Opinion in Neurobiology*, 20(4), pp. 494–502. Available at: https://doi.org/10.1016/J.CONB.2010.07.009.

Brun, V.H. *et al.* (2001) 'Retrograde amnesia for spatial memory induced by NMDA receptor-mediated long-term potentiation.', *The Journal of neuroscience : the official journal of the Society for Neuroscience*, 21(1), pp. 356–62. Available at: http://www.ncbi.nlm.nih.gov/pubmed/11150353.

Cabantous, S., Terwilliger, T.C. and Waldo, G.S. (2005) 'Protein tagging and detection with engineered self-assembling fragments of green fluorescent protein', *Nature Biotechnology*, 23(1), pp. 102–107. Available at: https://doi.org/10.1038/nbt1044.

Cajal, S.R.Y. (1894) 'The Croonian Lecture: La Fine Structure des Centres Nerveux', *Proceedings of the Royal Society of London Series I*, 55, pp. 444–468.

Cammalleri, M. *et al.* (2003) 'Time-restricted role for dendritic activation of the mTOR-p70S6K pathway in the induction of late-phase long-term potentiation in the CA1.', *Proceedings of the National Academy of Sciences of the United States of America*, 100(24), pp. 14368–73. Available at: https://doi.org/10.1073/pnas.2336098100.

Cannon, R.C. *et al.* (1998) 'An on-line archive of reconstructed hippocampal neurons', *Journal of Neuroscience Methods*, 84(1–2), pp. 49–54. Available at: https://doi.org/10.1016/S0165-0270(98)00091-0.

Castro, C.A. *et al.* (1989) 'Recovery of spatial learning deficits after decay of electrically induced synaptic enhancement in the hippocampus.', *Nature*, 342(6249), pp. 545–8. Available at: https://doi.org/10.1038/342545a0.

Chan, K.Y. *et al.* (2017) 'Engineered AAVs for efficient noninvasive gene delivery to the central and peripheral nervous systems', *Nature Neuroscience*, 20(8), pp. 1172–1179. Available at: https://doi.org/10.1038/nn.4593.

Chen, T.-W. *et al.* (2013) 'Ultrasensitive fluorescent proteins for imaging neuronal activity.', *Nature*, 499(7458), pp. 295–300. Available at: https://doi.org/10.1038/nature12354.

Chen, X. *et al.* (2011) 'Functional mapping of single spines in cortical neurons in vivo.', *Nature*, 475(7357), pp. 501–5. Available at: https://doi.org/10.1038/nature10193.

Choi, J.-H. *et al.* (2018) 'Interregional synaptic maps among engram cells underlie memory formation.', *Science (New York, N.Y.)*, 360(6387), pp. 430–435. Available at: https://doi.org/10.1126/science.aas9204.

Cohen, E. *et al.* (2008) 'Determinants of spontaneous activity in networks of cultured hippocampus.', *Brain research*, 1235, pp. 21–30. Available at: https://doi.org/10.1016/j.brainres.2008.06.022.

Collingridge, G.L. *et al.* (2010) 'Long-term depression in the CNS', *Nature Reviews Neuroscience*, 11(7), pp. 459–473. Available at: https://doi.org/10.1038/nrn2867.

Collingridge, G.L., Kehl, S.J. and McLennan, H. (1983) 'Excitatory amino acids in synaptic transmission in the Schaffer collateral-commissural pathway of the rat hippocampus.', *The Journal of Physiology*, 334(1), pp. 33–46. Available at: https://doi.org/10.1113/jphysiol.1983.sp014478.

Denny, C.A. *et al.* (2014) 'Hippocampal memory traces are differentially modulated by experience, time, and adult neurogenesis', *Neuron*, 83(1), pp. 189–201. Available at: https://doi.org/10.1016/j.neuron.2014.05.018.

Derkach, V., Barria, A. and Soderling, T.R. (1999) 'Ca2+/calmodulin-kinase II enhances channel conductance of alpha-amino-3-hydroxy-5-methyl-4-isoxazolepropionate type glutamate receptors.', *Proceedings of the National Academy of Sciences of the United States of America*, 96(6), pp. 3269–74. Available at: https://doi.org/10.1073/pnas.96.6.3269.

Dieterich, D.C. and Kreutz, M.R. (2016) 'Proteomics of the Synapse – A Quantitative Approach to Neuronal Plasticity', *Molecular & Cellular Proteomics*, 15(2), pp. 368–381. Available at: https://doi.org/10.1074/mcp.R115.051482.

Dore, K. *et al.* (2020) 'SYNPLA, a method to identify synapses displaying plasticity after learning', *Proceedings of the National Academy of Sciences*, 117(6), pp. 3214–3219. Available at: https://doi.org/10.1073/pnas.1919911117.

Dragunow, M. and Robertson, H.A. (1987) 'Kindling stimulation induces c-fos protein(s) in granule cells of the rat dentate gyrus', *Nature*, 329(6138), pp. 441–442. Available at: https://doi.org/10.1038/329441a0.

Druckmann, S. *et al.* (2014) 'Structured Synaptic Connectivity between Hippocampal Regions', *Neuron*, 81(3), pp. 629–640. Available at: https://doi.org/10.1016/j.neuron.2013.11.026.

Dudek, S.M. and Bear, M.F. (1992) 'Homosynaptic long-term depression in area CA1 of hippocampus and effects of N-methyl-D-aspartate receptor blockade.', *Proceedings of the National Academy of Sciences of the United States of America*, 89(10), pp. 4363–7. Available at: https://doi.org/10.1073/pnas.89.10.4363.

Dudman, J.T., Tsay, D. and Siegelbaum, S.A. (2007) 'A role for synaptic inputs at distal dendrites: instructive signals for hippocampal long-term plasticity.', *Neuron*, 56(5), pp. 866–79. Available at: https://doi.org/10.1016/j.neuron.2007.10.020.

Economo, M.N. *et al.* (2016) 'A platform for brain-wide imaging and reconstruction of individual neurons.', *eLife*, 5, p. e10566. Available at: https://doi.org/10.7554/eLife.10566.

Emptage, N.J. *et al.* (2003) 'Optical Quantal Analysis Reveals a Presynaptic Component of LTP at Hippocampal Schaffer-Associational Synapses', *Neuron*, 38(5), pp. 797–804. Available at: https://doi.org/10.1016/S0896-6273(03)00325-8.

Engert, F. and Bonhoeffer, T. (1999) 'Dendritic spine changes associated with hippocampal long-term synaptic plasticity', *Nature*, 399(6731), pp. 66–70. Available at: https://doi.org/10.1038/19978.

Ester, M. *et al.* (1996) 'A Density-Based Algorithm for Discovering Clusters in Large Spatial Databases with Noise', in *Proceedings of the Second International Conference on Knowledge Discovery and Data Mining*. AAAI Press (KDD'96), pp. 226–231.

Farris, S. *et al.* (2014) 'Selective localization of arc mRNA in dendrites involves activity- and translation-dependent mRNA degradation.', *The Journal of neuroscience : the official journal of*

*the Society for Neuroscience*, 34(13), pp. 4481–93. Available at: https://doi.org/10.1523/JNEUROSCI.4944-13.2014.

Feinberg, E.H. *et al.* (2008) 'GFP Reconstitution Across Synaptic Partners (GRASP) Defines Cell Contacts and Synapses in Living Nervous Systems', *Neuron*, 57(3), pp. 353–363. Available at: https://doi.org/10.1016/j.neuron.2007.11.030.

Feng, L., Zhao, T. and Kim, J. (2012) 'Improved synapse detection for mGRASP-assisted brain connectivity mapping', *Bioinformatics*, 28(12), pp. i25–i31. Available at: https://doi.org/10.1093/bioinformatics/bts221.

Feng, L., Zhao, T. and Kim, J. (2015) 'neuTube 1.0: A New Design for Efficient Neuron Reconstruction Software Based on the SWC Format.', *eNeuro*, 2(1), p. ENEURO.0049-14.2014. Available at: https://doi.org/10.1523/ENEURO.0049-14.2014.

Feng, S. *et al.* (2019) 'Bright split red fluorescent proteins for the visualization of endogenous proteins and synapses', *Communications Biology*, 2(1). Available at: https://doi.org/10.1038/s42003-019-0589-x.

Fernández, E. *et al.* (2009) 'Targeted tandem affinity purification of PSD-95 recovers core postsynaptic complexes and schizophrenia susceptibility proteins', *Molecular Systems Biology*, 5(1), p. 269. Available at: https://doi.org/10.1038/msb.2009.27.

Fifková, E. and van Harreveld, A. (1977) 'Long-lasting morphological changes in dendritic spines of dentate granular cells following stimulation of the entorhinal area', *Journal of Neurocytology*, 6(2), pp. 211–230. Available at: https://doi.org/10.1007/BF01261506.

Finnerty, G.T. and Jefferys, J.G.R. (1993) 'Functional connectivity from ca3 to the ipsilateral and contralateral ca1 in the rat dorsal hippocampus', *Neuroscience*, 56(1), pp. 101–108. Available at: https://doi.org/10.1016/0306-4522(93)90566-X.

Fleischmann, A. *et al.* (2003) 'Impaired long-term memory and NR2A-type NMDA receptor-dependent synaptic plasticity in mice lacking c-Fos in the CNS.', *The Journal of neuroscience : the official journal of the Society for Neuroscience*, 23(27), pp. 9116–22. Available at: https://doi.org/10.1523/JNEUROSCI.23-27-09116.2003.

Fosque, B.F. *et al.* (2015) 'Labeling of active neural circuits in vivo with designed calcium integrators', *Science*, 347(6223), pp. 755–760. Available at: https://doi.org/10.1126/science.1260922.

Frank, A.C. *et al.* (2018) 'Hotspots of dendritic spine turnover facilitate clustered spine addition and learning and memory.', *Nature communications*, 9(1), p. 422. Available at: https://doi.org/10.1038/s41467-017-02751-2.

Frankland, P.W. and Bontempi, B. (2005) 'The organization of recent and remote memories.', *Nature reviews. Neuroscience*, 6(2), pp. 119–30. Available at: https://doi.org/10.1038/nrn1607.

Frey, U. *et al.* (1989) 'Long-term potentiation induced in dendrites separated from rat's CA1 pyramidal somata does not establish a late phase', *Neuroscience Letters*, 97(1), pp. 135–139. Available at: https://doi.org/https://doi.org/10.1016/0304-3940(89)90152-3.

Frey, U. *et al.* (1996) 'Influence of actinomycin D, a RNA synthesis inhibitor, on long-term potentiation in rat hippocampal neurons in vivo and in vitro.', *The Journal of Physiology*, 490(3), pp. 703–711. Available at: https://doi.org/10.1113/jphysiol.1996.sp021179.

Frey, U. and Morris, R.G.M. (1997) 'Synaptic tagging and long-term potentiation', *Nature*, 385(6616), pp. 533–536. Available at: https://doi.org/10.1038/385533a0.

Frey, U. and Morris, R.G.M. (1998) 'Synaptic tagging: implications for late maintenance of hippocampal long-term potentiation', *Trends in Neurosciences*, 21(5), pp. 181–188. Available at: https://doi.org/10.1016/S0166-2236(97)01189-2.

Fu, M. *et al.* (2012) 'Repetitive motor learning induces coordinated formation of clustered dendritic spines in vivo', *Nature*, 483(7387), pp. 92–95. Available at: https://doi.org/10.1038/nature10844.

Fukazawa, Y. *et al.* (2003) 'Hippocampal LTP is accompanied by enhanced F-actin content within the dendritic spine that is essential for late LTP maintenance in vivo.', *Neuron*, 38(3), pp. 447–60. Available at: https://doi.org/10.1016/s0896-6273(03)00206-x.

Ghandour, K. *et al.* (2019) 'Orchestrated ensemble activities constitute a hippocampal memory engram', *Nature Communications*, 10(1), p. 2637. Available at: https://doi.org/10.1038/s41467-019-10683-2.

Gobbo, F. *et al.* (2017) 'Activity-dependent expression of Channelrhodopsin at neuronal synapses', *Nature Communications*, 8(1). Available at: https://doi.org/10.1038/s41467-017-01699-7.

Gobbo, F. and Cattaneo, A. (2020) 'Neuronal Activity at Synapse Resolution: Reporters and Effectors for Synaptic Neuroscience', *Frontiers in Molecular Neuroscience*, 13. Available at: https://doi.org/10.3389/fnmol.2020.572312.

Gold, P.E. (1986) 'The use of avoidance training in studies of modulation of memory storage', *Behavioral and Neural Biology*, 46(1), pp. 87–98. Available at: https://doi.org/10.1016/S0163-1047(86)90927-1.

Gordon, M.D. and Scott, K. (2009) 'Motor Control in a Drosophila Taste Circuit', *Neuron*, 61(3), pp. 373–384. Available at: https://doi.org/10.1016/j.neuron.2008.12.033.

Goto, A. *et al.* (2021) 'Stepwise synaptic plasticity events drive the early phase of memory consolidation.', *Science (New York, N.Y.)*, 374(6569), pp. 857–863. Available at: https://doi.org/10.1126/science.abj9195.

Govindarajan, A. *et al.* (2011) 'The Dendritic Branch Is the Preferred Integrative Unit for Protein Synthesis-Dependent LTP', *Neuron*, 69(1), pp. 132–146. Available at: https://doi.org/10.1016/j.neuron.2010.12.008.

Govindarajan, A., Kelleher, R.J. and Tonegawa, S. (2006) 'A clustered plasticity model of long-term memory engrams', *Nature Reviews Neuroscience*, 7(7), pp. 575–583. Available at: https://doi.org/10.1038/nrn1937.

Graves, A.R. *et al.* (2021) 'Visualizing synaptic plasticity in vivo by large-scale imaging of endogenous AMPA receptors', *eLife*, 10, p. 66809. Available at: https://doi.org/10.7554/eLife.66809.

Gruart, A., Muñoz, M.D. and Delgado-García, J.M. (2006) 'Involvement of the CA3-CA1 synapse in the acquisition of associative learning in behaving mice.', *The Journal of neuroscience : the official journal of the Society for Neuroscience*, 26(4), pp. 1077–87. Available at: https://doi.org/10.1523/JNEUROSCI.2834-05.2006.

Guenthner, C.J. *et al.* (2013) 'Permanent genetic access to transiently active neurons via TRAP: Targeted recombination in active populations', *Neuron*, 78(5), pp. 773–784. Available at: https://doi.org/10.1016/j.neuron.2013.03.025.

Guzowski, J.F. *et al.* (1999) 'Environment-specific expression of the immediate-early gene Arc in hippocampal neuronal ensembles', *Nature Neuroscience*, 2(12), pp. 1120–1124. Available at: https://doi.org/10.1038/16046.

Guzowski, J.F. *et al.* (2001) 'Experience-dependent gene expression in the rat hippocampus after spatial learning: a comparison of the immediate-early genes Arc, c-fos, and zif268', *The Journal of Neuroscience*, 21(14), pp. 5089–5098. Available at: https://doi.org/10.1523/JNEUROSCI.21-14-05089.2001.

Guzowski, J.F. (2002) 'Insights into immediate-early gene function in hippocampal memory consolidation using antisense oligonucleotide and fluorescent imaging approaches', *Hippocampus*, 12(1), pp. 86–104. Available at: https://doi.org/10.1002/hipo.10010.

Guzowski, J.F. *et al.* (2005) 'Mapping behaviorally relevant neural circuits with immediate-early gene expression', *Current Opinion in Neurobiology*, 15(5), pp. 599–606. Available at: https://doi.org/10.1016/j.conb.2005.08.018.

Habib, D. *et al.* (2014) 'Occlusion of low-frequency-induced, heterosynaptic long-term potentiation in the rat hippocampus in vivo following spatial training.', *Cerebral cortex (New York, N.Y. : 1991)*, 24(11), pp. 3090–6. Available at: https://doi.org/10.1093/cercor/bht174.

Han, J.-H. *et al.* (2007) 'Neuronal Competition and Selection During Memory Formation', *Science*, 316(5823), pp. 457–460. Available at: https://doi.org/10.1126/science.1139438.

Han, J.-H. *et al.* (2009) 'Selective Erasure of a Fear Memory', *Science*, 323(5920), pp. 1492–1496. Available at: https://doi.org/10.1126/science.1164139.

Han, X. *et al.* (2011) 'A High-Light Sensitivity Optical Neural Silencer: Development and Application to Optogenetic Control of Non-Human Primate Cortex', *Frontiers in Systems Neuroscience*, 5. Available at: https://doi.org/10.3389/fnsys.2011.00018.

Harris, K.M. (2020) 'Structural LTP: from synaptogenesis to regulated synapse enlargement and clustering', *Current Opinion in Neurobiology*, 63, pp. 189–197. Available at: https://doi.org/10.1016/j.conb.2020.04.009.

Hayashi-Takagi, A. *et al.* (2015) 'Labelling and optical erasure of synaptic memory traces in the motor cortex', *Nature*, 525(7569), pp. 333–338. Available at: https://doi.org/10.1038/nature15257.

Hebb, D.O. (1949) *The organization of behavior: A neuropsychological theory*. New York: Wiley.

Hörl, D. *et al.* (2019) 'BigStitcher: reconstructing high-resolution image datasets of cleared and expanded samples.', *Nature methods*, 16(9), pp. 870–874. Available at: https://doi.org/10.1038/s41592-019-0501-0.

Huganir, R.L. and Nicoll, R.A. (2013) 'AMPARs and Synaptic Plasticity: The Last 25 Years', *Neuron*, 80(3), pp. 704–717. Available at: https://doi.org/10.1016/j.neuron.2013.10.025.

Iascone, D.M. *et al.* (2020) 'Whole-Neuron Synaptic Mapping Reveals Spatially Precise Excitatory/Inhibitory Balance Limiting Dendritic and Somatic Spiking.', *Neuron*, 106(4), pp. 566-578.e8. Available at: https://doi.org/10.1016/j.neuron.2020.02.015.

Isaac, J.T.R., Nicoll, R.A. and Malenka, R.C. (1995) 'Evidence for silent synapses: Implications for the expression of LTP', *Neuron*, 15(2), pp. 427–434. Available at: https://doi.org/10.1016/0896-6273(95)90046-2.

Jarsky, T. *et al.* (2005) 'Conditional dendritic spike propagation following distal synaptic activation of hippocampal CA1 pyramidal neurons', *Nature Neuroscience*, 8(12), pp. 1667–1676. Available at: https://doi.org/10.1038/nn1599.

Jia, H. *et al.* (2010) 'Dendritic organization of sensory input to cortical neurons in vivo.', *Nature*, 464(7293), pp. 1307–12. Available at: https://doi.org/10.1038/nature08947.

Josselyn, S.A., Köhler, S. and Frankland, P.W. (2017) 'Heroes of the engram', *Journal of Neuroscience*, 37(18), pp. 4647–4657. Available at: https://doi.org/10.1523/JNEUROSCI.0056-17.2017.

Josselyn, S.A. and Tonegawa, S. (2020) 'Memory engrams: Recalling the past and imagining the future', *Science*, 367(6473). Available at: https://doi.org/10.1126/science.aaw4325.

Kähne, T. *et al.* (2012) 'Synaptic proteome changes in mouse brain regions upon auditory discrimination learning', *Proteomics*, 12(15–16), pp. 2433–2444. Available at: https://doi.org/10.1002/pmic.201100669.

Kajiwara, R. *et al.* (2008) 'Convergence of entorhinal and CA3 inputs onto pyramidal neurons and interneurons in hippocampal area CA1--an anatomical study in the rat.', *Hippocampus*, 18(3), pp. 266–80. Available at: https://doi.org/10.1002/hipo.20385.

Kastellakis, G. and Poirazi, P. (2019) 'Synaptic Clustering and Memory Formation', *Frontiers in Molecular Neuroscience*, 12. Available at: https://doi.org/10.3389/FNMOL.2019.00300/FULL.

Kastellakis, G., Silva, A.J. and Poirazi, P. (2016) 'Linking Memories across Time via Neuronal and Dendritic Overlaps in Model Neurons with Active Dendrites', *Cell Reports*, 17(6), pp. 1491–1504. Available at: https://doi.org/10.1016/j.celrep.2016.10.015.

Katz, Y. *et al.* (2009) 'Synapse Distribution Suggests a Two-Stage Model of Dendritic Integration in CA1 Pyramidal Neurons', *Neuron*, 63(2), pp. 171–177. Available at: https://doi.org/10.1016/j.neuron.2009.06.023.

Kauer, J.A., Malenka, R.C. and Nicoll, R.A. (1988) 'A persistent postsynaptic modification mediates long-term potentiation in the hippocampus.', *Neuron*, 1(10), pp. 911–7. Available at: https://doi.org/10.1016/0896-6273(88)90148-1.

Kawashima, T. *et al.* (2013) 'Functional labeling of neurons and their projections using the synthetic activity-dependent promoter E-SARE.', *Nature methods*, 10(9), pp. 889–95. Available at: https://doi.org/10.1038/nmeth.2559.

Kim, J. *et al.* (2011) 'mGRASP enables mapping mammalian synaptic connectivity with light microscopy.', *Nature methods*, 9(1), pp. 96–102. Available at: https://doi.org/10.1038/nmeth.1784.

Kim, Jooyoung *et al.* (2023) 'Astrocytic connection to engram neurons Increased after learning', *bioRxiv* [Preprint]. Available at: https://doi.org/10.1101/2023.01.25.525617.

Kitamura, T. *et al.* (2017) 'Engrams and circuits crucial for systems consolidation of a memory.', *Science (New York, N.Y.)*, 356(6333), pp. 73–78. Available at: https://doi.org/10.1126/science.aam6808.

Klapoetke, N.C. *et al.* (2014) ‘Independent optical excitation of distinct neural populations’, *Nature Methods*, 11(3), pp. 338–346. Available at: https://doi.org/10.1038/nmeth.2836.

Kleindienst, T. *et al.* (2011) ‘Activity-dependent clustering of functional synaptic inputs on developing hippocampal dendrites’, *Neuron*, 72(6), pp. 1012–1024. Available at: https://doi.org/10.1016/j.neuron.2011.10.015.

Kopec, C.D. *et al.* (2006) ‘Glutamate receptor exocytosis and spine enlargement during chemically induced long-term potentiation.’, *The Journal of neuroscience : the official journal of the Society for Neuroscience*, 26(7), pp. 2000–9. Available at: https://doi.org/10.1523/JNEUROSCI.3918-05.2006.

Krug, M., Lössner, B. and Ott, T. (1984) ‘Anisomycin blocks the late phase of long-term potentiation in the dentate gyrus of freely moving rats.’, *Brain research bulletin*, 13(1), pp. 39–42. Available at: https://doi.org/10.1016/0361-9230(84)90005-4.

Kwon, H.-B. and Sabatini, B.L. (2011) ‘Glutamate induces de novo growth of functional spines in developing cortex’, *Nature*, 474(7349), pp. 100–104. Available at: https://doi.org/10.1038/nature09986.

Lanahan, A. and Worley, P. (1998) ‘Immediate-Early Genes and Synaptic Function’, *Neurobiology of Learning and Memory*, 70(1–2), pp. 37–43. Available at: https://doi.org/10.1006/nlme.1998.3836.

Lang, C. *et al.* (2004) ‘Transient expansion of synaptically connected dendritic spines upon induction of hippocampal long-term potentiation’, *Proceedings of the National Academy of Sciences*, 101(47), pp. 16665–16670. Available at: https://doi.org/10.1073/pnas.0407581101.

Larson, J. and Munkácsy, E. (2015) ‘Theta-burst LTP.’, *Brain research*, 1621, pp. 38–50. Available at: https://doi.org/10.1016/j.brainres.2014.10.034.

Lashley (1963) *Brain Mechanisms and Intelligence:A Quantitative Study of Injuries to the Brain*. Dover Publications.

Lee, Chaery *et al.* (2023) ‘Hippocampal engram networks for fear memory recruit new synapses and modify pre-existing synapses in vivo’, *Current Biology* [Preprint]. Available at: https://doi.org/10.1016/j.cub.2022.12.038.

Lee, S.-J.R. *et al.* (2009) 'Activation of CaMKII in single dendritic spines during long-term potentiation.', *Nature*, 458(7236), pp. 299–304. Available at: https://doi.org/10.1038/nature07842.

Levy, W.B. and Steward, O. (1979) 'Synapses as associative memory elements in the hippocampal formation.', *Brain research*, 175(2), pp. 233–45. Available at: https://doi.org/10.1016/0006-8993(79)91003-5.

Liao, D., Hessler, N.A. and Malinow, R. (1995) 'Activation of postsynaptically silent synapses during pairing-induced LTP in CA1 region of hippocampal slice', *Nature*, 375(6530), pp. 400–404. Available at: https://doi.org/10.1038/375400a0.

Lisman, J., Yasuda, R. and Raghavachari, S. (2012) 'Mechanisms of CaMKII action in long-term potentiation.', *Nature reviews. Neuroscience*, 13(3), pp. 169–82. Available at: https://doi.org/10.1038/nrn3192.

Liu, X. *et al.* (2012) 'Optogenetic stimulation of a hippocampal engram activates fear memory recall', *Nature*, 484(7394), pp. 381–385. Available at: https://doi.org/10.1038/nature11028.

Liu, Z. *et al.* (2017) 'Systematic comparison of 2A peptides for cloning multi-genes in a polycistronic vector', *Scientific Reports*, 7(1), p. 2193. Available at: https://doi.org/10.1038/s41598-017-02460-2.

Lu, W.-Y. *et al.* (2001) 'Activation of Synaptic NMDA Receptors Induces Membrane Insertion of New AMPA Receptors and LTP in Cultured Hippocampal Neurons', *Neuron*, 29(1), pp. 243–254. Available at: https://doi.org/10.1016/S0896-6273(01)00194-5.

Luo, U. *et al.* (1996) *Differential effects of the Rae GTPase on Purkinje cell axons and dendritic trunks and spines*.

Luscher, C. and Malenka, R.C. (2012) 'NMDA Receptor-Dependent Long-Term Potentiation and Long-Term Depression (LTP/LTD)', *Cold Spring Harbor Perspectives in Biology*, 4(6), pp. a005710–a005710. Available at: https://doi.org/10.1101/cshperspect.a005710.

Lynch, G. *et al.* (1983) 'Intracellular injections of EGTA block induction of hippocampal long-term potentiation', *Nature*, 305(5936), pp. 719–721. Available at: https://doi.org/10.1038/305719a0.

MacDermott, A.B. *et al.* (1986) 'NMDA-receptor activation increases cytoplasmic calcium concentration in cultured spinal cord neurones', *Nature*, 321(6069), pp. 519–522. Available at: https://doi.org/10.1038/321519a0.

Macpherson, L.J. *et al.* (2015) 'Dynamic labelling of neural connections in multiple colours by trans-synaptic fluorescence complementation', *Nature Communications*, 6. Available at: https://doi.org/10.1038/ncomms10024.

Magee, J.C. and Cook, E.P. (2000) 'Somatic EPSP amplitude is independent of synapse location in hippocampal pyramidal neurons.', *Nature neuroscience*, 3(9), pp. 895–903. Available at: https://doi.org/10.1038/78800.

Makino, H. and Malinow, R. (2009) 'AMPA Receptor Incorporation into Synapses during LTP: The Role of Lateral Movement and Exocytosis', *Neuron*, 64(3), pp. 381–390. Available at: https://doi.org/10.1016/j.neuron.2009.08.035.

Makino, H. and Malinow, R. (2011) 'Compartmentalized versus Global Synaptic Plasticity on Dendrites Controlled by Experience', *Neuron*, 72(6), pp. 1001–1011. Available at: https://doi.org/10.1016/j.neuron.2011.09.036.

Maletic-Savatic, M. (1999) 'Rapid Dendritic Morphogenesis in CA1 Hippocampal Dendrites Induced by Synaptic Activity', *Science*, 283(5409), pp. 1923–1927. Available at: https://doi.org/10.1126/science.283.5409.1923.

Maletic-Savatic, M., Malinow, R. and Svoboda, K. (1999) 'Rapid Dendritic Morphogenesis in CA1 Hippocampal Dendrites Induced by Synaptic Activity', *Science*, 283(5409), pp. 1923–1927. Available at: https://doi.org/10.1126/science.283.5409.1923.

Manahan-Vaughan, D., Kulla, A. and Frey, J.U. (2000) 'Requirement of translation but not transcription for the maintenance of long-term depression in the CA1 region of freely moving rats', *Journal of Neuroscience*, 20(22), pp. 8572–8576. Available at: https://doi.org/10.1523/jneurosci.20-22-08572.2000.

Maren, S. and Fanselow, M.S. (1996) 'The Amygdala and Fear Conditioning: Has the Nut Been Cracked?', *Neuron*, 16(2), pp. 237–240. Available at: https://doi.org/10.1016/S0896-6273(00)80041-0.

Marr D (1971) *Simple memory: a theory for archicortex*. London : Proceedings of the Royal Society of London.

Matsuo, N., Reijmers, L. and Mayford, M. (2008) 'Spine-Type-Specific Recruitment of Newly Synthesized AMPA Receptors with Learning', *Science*, 319(5866), pp. 1104–1107. Available at: https://doi.org/10.1126/science.1149967.

Matsuzaki, M. *et al.* (2004) 'Structural basis of long-term potentiation in single dendritic spines', *Nature*, 429(6993), pp. 761–766. Available at: https://doi.org/10.1038/nature02617.

Mayer, M.L., Westbrook, G.L. and Guthrie, P.B. (1984) 'Voltage-dependent block by Mg2+ of NMDA responses in spinal cord neurones', *Nature*, 309(5965), pp. 261–263. Available at: https://doi.org/10.1038/309261a0.

Mayford, M. and Reijmers, L. (2015) 'Exploring Memory Representations with Activity-Based Genetics.', *Cold Spring Harbor perspectives in biology*, 8(3), p. a021832. Available at: https://doi.org/10.1101/cshperspect.a021832.

Mayford, M., Siegelbaum, S.A. and Kandel, E.R. (2012) 'Synapses and Memory Storage', *Cold Spring Harbor Perspectives in Biology*, 4(6), pp. a005751–a005751. Available at: https://doi.org/10.1101/cshperspect.a005751.

McGaugh, J.L. and Roozendaal, B. (2009) 'Drug enhancement of memory consolidation: historical perspective and neurobiological implications', *Psychopharmacology*, 202(1), pp. 3–14. Available at: https://doi.org/10.1007/s00213-008-1285-6.

McHugh, T.J. *et al.* (2007) 'Dentate Gyrus NMDA Receptors Mediate Rapid Pattern Separation in the Hippocampal Network', *Science*, 317(5834), pp. 94–99. Available at: https://doi.org/10.1126/science.1140263.

McKernan, M.G. and Shinnick-Gallagher, P. (1997) 'Fear conditioning induces a lasting potentiation of synaptic currents in vitro.', *Nature*, 390(6660), pp. 607–11. Available at: https://doi.org/10.1038/37605.

McNaughton, B.L. *et al.* (1986) 'Long-term enhancement of hippocampal synaptic transmission and the acquisition of spatial information.', *The Journal of neuroscience : the official journal of the Society for Neuroscience*, 6(2), pp. 563–71. Available at: http://www.ncbi.nlm.nih.gov/pubmed/3005525.

McNaughton, B.L., Douglas, R.M. and Goddard, G.V. (1978) ‘Synaptic enhancement in fascia dentata: Cooperativity among coactive afferents’, *Brain Research*, 157(2), pp. 277–293. Available at: https://doi.org/10.1016/0006-8993(78)90030-6.

McNaughton, B.L. and Morris, R.G.M. (1987) ‘Hippocampal synaptic enhancement and information storage within a distributed memory system’, *Trends in Neurosciences*, 10(10), pp. 408–415. Available at: https://doi.org/10.1016/0166-2236(87)90011-7.

Megías, M. *et al.* (2001) ‘Total number and distribution of inhibitory and excitatory synapses on hippocampal CA1 pyramidal cells’, *Neuroscience*, 102(3), pp. 527–540. Available at: https://doi.org/10.1016/S0306-4522(00)00496-6.

Messaoudi, E. *et al.* (2007) ‘Sustained Arc/Arg3.1 synthesis controls long-term potentiation consolidation through regulation of local actin polymerization in the dentate gyrus in vivo’, *Journal of Neuroscience*, 27(39), pp. 10445–10455. Available at: https://doi.org/10.1523/JNEUROSCI.2883-07.2007.

Miesenböck, G., de Angelis, D.A. and Rothman, J.E. (1998) ‘Visualizing secretion and synaptic transmission with pH-sensitive green fluorescent proteins’, *Nature*, 394(6689), pp. 192–195. Available at: https://doi.org/10.1038/28190.

Milanovic, S. *et al.* (1998) ‘Production of the Fos protein after contextual fear conditioning of C57BL/6N mice’, *Brain Research*, 784(1–2), pp. 37–47. Available at: https://doi.org/10.1016/S0006-8993(97)01266-3.

Minatohara, K., Akiyoshi, M. and Okuno, H. (2016) ‘Role of Immediate-Early Genes in Synaptic Plasticity and Neuronal Ensembles Underlying the Memory Trace’, *Frontiers in Molecular Neuroscience*, 8(JAN2016). Available at: https://doi.org/10.3389/fnmol.2015.00078.

Mishchenko, Y. *et al.* (2010) ‘Ultrastructural Analysis of Hippocampal Neuropil from the Connectomics Perspective’, *Neuron*, 67(6), pp. 1009–1020. Available at: https://doi.org/10.1016/j.neuron.2010.08.014.

Miura, K., Cordelières, F.P. and Klemm, A.H. (2020) ‘Bleach correction ImageJ plugin for compensating the photobleaching of time-lapse sequences [version 1; peer review: 4 approved, 1 approved with reservations] report report report report report’. Available at: https://doi.org/10.12688/f1000research.27171.1.

Molnár, E. (2011) ‘Long-term potentiation in cultured hippocampal neurons’, *Seminars in Cell and Developmental Biology*. Elsevier Ltd, pp. 506–513. Available at: https://doi.org/10.1016/j.semcdb.2011.07.017.

Morgan, J.I. *et al.* (1987) ‘Mapping patterns of c-fos expression in the central nervous system after seizure’, *Science*, 237(4811), pp. 192–197. Available at: https://doi.org/10.1126/science.3037702.

Morris, R.G.M. *et al.* (1982) ‘Place navigation impaired in rats with hippocampal lesions’, *Nature*, 297(5868), pp. 681–683. Available at: https://doi.org/10.1038/297681a0.

Morris, R.G.M. *et al.* (1986) ‘Selective impairment of learning and blockade of long-term potentiation by an N-methyl-D-aspartate receptor antagonist, AP5’, *Nature*, 319(6056), pp. 774–776. Available at: https://doi.org/10.1038/319774a0.

Morsut, L. *et al.* (2016) ‘Engineering Customized Cell Sensing and Response Behaviors Using Synthetic Notch Receptors.’, *Cell*, 164(4), pp. 780–91. Available at: https://doi.org/10.1016/j.cell.2016.01.012.

Moser, E.I. *et al.* (1998) ‘Impaired Spatial Learning after Saturation of Long-Term Potentiation’, *Science*, 281(5385), pp. 2038–2042. Available at: https://doi.org/10.1126/science.281.5385.2038.

Moser, M.B., Trommald, M. and Andersen, P. (1994) ‘An increase in dendritic spine density on hippocampal CA1 pyramidal cells following spatial learning in adult rats suggests the formation of new synapses’, *Proceedings of the National Academy of Sciences of the United States of America*, 91(26), pp. 12673–12675. Available at: https://doi.org/10.1073/pnas.91.26.12673.

Mulkey, R.M., Herron, C.E. and Malenka, R.C. (1993) ‘An Essential Role for Protein Phosphatases in Hippocampal Long-Term Depression’, *Science*, 261(5124), pp. 1051–1055. Available at: https://doi.org/10.1126/science.8394601.

Muller, D., Joly, M. and Lynch, G. (1988) ‘Contributions of Quisqualate and NMDA Receptors to the Induction and Expression of LTP’, *Science*, 242(4886), pp. 1694–1697. Available at: https://doi.org/10.1126/science.2904701.

Nabavi, S. *et al.* (2014) ‘Engineering a memory with LTD and LTP’, *Nature*, 511(7509), pp. 348–352. Available at: https://doi.org/10.1038/nature13294.

Nagai, Y. *et al.* (2019) ‘Identification of neuron-type specific promoters in monkey genome and their functional validation in mice’, *Biochemical and Biophysical Research Communications*, 518(4), pp. 619–624. Available at: https://doi.org/https://doi.org/10.1016/j.bbrc.2019.08.101.

Nägerl, U.V. *et al.* (2004) ‘Bidirectional activity-dependent morphological plasticity in hippocampal neurons’, *Neuron*, 44(5), pp. 759–767. Available at: https://doi.org/10.1016/j.neuron.2004.11.016.

Nakai, J., Ohkura, M. and Imoto, K. (2001) ‘A high signal-to-noise Ca2+ probe composed of a single green fluorescent protein’, *Nature Biotechnology*, 19(2), pp. 137–141. Available at: https://doi.org/10.1038/84397.

Nakazawa, K. *et al.* (2002) ‘Requirement for Hippocampal CA3 NMDA Receptors in Associative Memory Recall’, *Science*, 297(5579), pp. 211–218. Available at: https://doi.org/10.1126/science.1071795.

Nicoll, R.A. (2017) ‘A Brief History of Long-Term Potentiation’, *Neuron*, 93(2), pp. 281–290. Available at: https://doi.org/10.1016/j.neuron.2016.12.015.

Nowak, L. *et al.* (1984) ‘Magnesium gates glutamate-activated channels in mouse central neurones’, *Nature*, 307(5950), pp. 462–465. Available at: https://doi.org/10.1038/307462a0.

Ohkawa, N. *et al.* (2015) ‘Artificial association of pre-stored information to generate a qualitatively new memory’, *Cell Reports*, 11(2), pp. 261–269. Available at: https://doi.org/10.1016/j.celrep.2015.03.017.

Okuno, H. (2011) ‘Regulation and function of immediate-early genes in the brain: beyond neuronal activity markers.’, *Neuroscience research*, 69(3), pp. 175–86. Available at: https://doi.org/10.1016/j.neures.2010.12.007.

Okuno, H. *et al.* (2012) ‘Inverse synaptic tagging of inactive synapses via dynamic interaction of Arc/Arg3.1 with CaMKIIβ.’, *Cell*, 149(4), pp. 886–98. Available at: https://doi.org/10.1016/j.cell.2012.02.062.

Opazo, P. *et al.* (2010) ‘CaMKII triggers the diffusional trapping of surface AMPARs through phosphorylation of stargazin.’, *Neuron*, 67(2), pp. 239–52. Available at: https://doi.org/10.1016/j.neuron.2010.06.007.

Ostroff, L.E. *et al.* (2010) 'Fear and safety learning differentially affect synapse size and dendritic translation in the lateral amygdala', *Proceedings of the National Academy of Sciences of the United States of America*, 107(20), pp. 9418–9423. Available at: https://doi.org/10.1073/pnas.0913384107.

Otani, S. and Abraham, W.C. (1989) 'Inhibition of protein synthesis in the dentate gyrus, but not the entorhinal cortex, blocks maintenance of long-term potentiation in rats', *Neuroscience Letters*, 106(1–2), pp. 175–180. Available at: https://doi.org/10.1016/0304-3940(89)90222-X.

Otto, T. *et al.* (1991) 'Learning-related patterns of CA1 spike trains parallel stimulation parameters optimal for inducing hippocampal long-term potentiation', *Hippocampus*, 1(2), pp. 181–192. Available at: https://doi.org/https://doi.org/10.1002/hipo.450010206.

Paez-Segala, M.G. *et al.* (2015) 'Fixation-resistant photoactivatable fluorescent proteins for CLEM', *Nature Methods*, 12(3), pp. 215–218. Available at: https://doi.org/10.1038/nmeth.3225.

Pastuzyn, E.D. *et al.* (2018) 'The Neuronal Gene Arc Encodes a Repurposed Retrotransposon Gag Protein that Mediates Intercellular RNA Transfer', *Cell*, 172(1–2), pp. 275-288.e18. Available at: https://doi.org/10.1016/j.cell.2017.12.024.

Patterson, M.A., Szatmari, E.M. and Yasuda, R. (2010) 'AMPA receptors are exocytosed in stimulated spines and adjacent dendrites in a Ras-ERK–dependent manner during long-term potentiation', *Proceedings of the National Academy of Sciences*, 107(36), pp. 15951–15956. Available at: https://doi.org/10.1073/pnas.0913875107.

Pavlowsky, A. *et al.* (2017) 'Persistent modifications of hippocampal synaptic function during remote spatial memory.', *Neurobiology of learning and memory*, 138, pp. 182–197. Available at: https://doi.org/10.1016/j.nlm.2016.08.015.

Penfield, W. and Perot, P. (1963) 'The brain's record of auditory and visual experience', *Brain*, 86(4), pp. 595–696. Available at: https://doi.org/10.1093/brain/86.4.595.

Peng, H. *et al.* (2014) 'Extensible visualization and analysis for multidimensional images using Vaa3D', *Nature Protocols*, 9(1), pp. 193–208. Available at: https://doi.org/10.1038/nprot.2014.011.

Perez-Alvarez, A. *et al.* (2020) ‘Freeze-frame imaging of synaptic activity using SynTagMA.’, *Nature communications*, 11(1), p. 2464. Available at: https://doi.org/10.1038/s41467-020-16315-4.

Peter M. Milner (1999) ‘CELL ASSEMBLIES: WHOSE IDEA?’, *Psycoloquy*, 10(053), p. 4. Available at: https://www.cogsci.ecs.soton.ac.uk/cgi/psyc/newpsy?10.053 (Accessed: 26 September 2022).

Pham, A.H., McCaffery, J.M. and Chan, D.C. (2012) ‘Mouse lines with photo-activatable mitochondria to study mitochondrial dynamics’, *genesis*, 50(11), pp. 833–843. Available at: https://doi.org/10.1002/dvg.22050.

Pintchovski, S.A. *et al.* (2009) ‘The serum response factor and a putative novel transcription factor regulate expression of the immediate-early gene Arc/Arg3.1 in neurons.’, *The Journal of neuroscience : the official journal of the Society for Neuroscience*, 29(5), pp. 1525–37. Available at: https://doi.org/10.1523/JNEUROSCI.5575-08.2009.

Plath, N. *et al.* (2006) ‘Arc/Arg3.1 is essential for the consolidation of synaptic plasticity and memories.’, *Neuron*, 52(3), pp. 437–44. Available at: https://doi.org/10.1016/j.neuron.2006.08.024.

Poirazi, P., Brannon, T. and Mel, B.W. (2003) ‘Pyramidal Neuron as Two-Layer Neural Network’, *Neuron*, 37(6), pp. 989–999. Available at: https://doi.org/10.1016/S0896-6273(03)00149-1.

Poirazi, P. and Mel, B.W. (2001) ‘Impact of Active Dendrites and Structural Plasticity on the Memory Capacity of Neural Tissue’, *Neuron*, 29(3), pp. 779–796. Available at: https://doi.org/10.1016/S0896-6273(01)00252-5.

Ramirez, S. *et al.* (2013) ‘Creating a False Memory in the Hippocampus’, *Science*, 341(6144), pp. 387–391. Available at: https://doi.org/10.1126/science.1239073.

Rampon, C. *et al.* (2000) ‘Enrichment induces structural changes and recovery from nonspatial memory deficits in CA1 NMDAR1-knockout mice’, *Nature Neuroscience*, 3(3), pp. 238–244. Available at: https://doi.org/10.1038/72945.

Rangaraju, V., tom Dieck, S. and Schuman, E.M. (2017) ‘Local translation in neuronal compartments: how local is local?’, *EMBO reports*, 18(5), pp. 693–711. Available at: https://doi.org/10.15252/embr.201744045.

Rao-Ruiz, P. *et al.* (2015) ‘Time-dependent changes in the mouse hippocampal synaptic membrane proteome after contextual fear conditioning’, *Hippocampus*, 25(11), pp. 1250–1261. Available at: https://doi.org/10.1002/hipo.22432.

Redondo, R.L. and Morris, R.G.M. (2011) ‘Making memories last: The synaptic tagging and capture hypothesis’, *Nature Reviews Neuroscience*, 12(1), pp. 17–30. Available at: https://doi.org/10.1038/nrn2963.

Reijmers, L.G. *et al.* (2007) ‘Localization of a stable neural correlate of associative memory’, *Science*, 317(5842), pp. 1230–1233. Available at: https://doi.org/10.1126/science.1143839.

Reisel, D. *et al.* (2002) ‘Spatial memory dissociations in mice lacking GluR1.’, *Nature neuroscience*, 5(9), pp. 868–73. Available at: https://doi.org/10.1038/nn910.

Reymann, K.G. and Frey, J.U. (2007) ‘The late maintenance of hippocampal LTP: Requirements, phases, “synaptic tagging”, “late-associativity” and implications’, *Neuropharmacology*, 52(1), pp. 24–40. Available at: https://doi.org/10.1016/j.neuropharm.2006.07.026.

Robertson, L.M. *et al.* (1995) ‘Regulation of c-fos expression in transgenic mice requires multiple interdependent transcription control elements.’, *Neuron*, 14(2), pp. 241–52. Available at: https://doi.org/10.1016/0896-6273(95)90282-1.

Rogan, M.T., Stäubli, U. v. and LeDoux, J.E. (1997) ‘Fear conditioning induces associative long-term potentiation in the amygdala’, *Nature*, 390(6660), pp. 604–607. Available at: https://doi.org/10.1038/37601.

Romanski, L.M. and LeDoux, J.E. (1992) ‘Equipotentiality of thalamo-amygdala and thalamo-cortico-amygdala circuits in auditory fear conditioning’, *The Journal of Neuroscience*, 12(11), p. 4501. Available at: https://doi.org/10.1523/JNEUROSCI.12-11-04501.1992.

Ronzitti, E. *et al.* (2017) ‘Submillisecond Optogenetic Control of Neuronal Firing with Two-Photon Holographic Photoactivation of Chronos’, *The Journal of Neuroscience*, 37(44), pp. 10679–10689. Available at: https://doi.org/10.1523/JNEUROSCI.1246-17.2017.

De Roo, M., Klauser, P. and Muller, D. (2008) ‘LTP Promotes a Selective Long-Term Stabilization and Clustering of Dendritic Spines’, *PLoS Biology*. Edited by M. Sheng, 6(9), p. e219. Available at: https://doi.org/10.1371/journal.pbio.0060219.

Ross, W.N. (2012) ‘Understanding calcium waves and sparks in central neurons.’, *Nature reviews. Neuroscience*, 13(3), pp. 157–68. Available at: https://doi.org/10.1038/nrn3168.

Roy, D.S. *et al.* (2016) ‘Memory retrieval by activating engram cells in mouse models of early Alzheimer’s disease’, *Nature*, 531(7595), pp. 508–512. Available at: https://doi.org/10.1038/nature17172.

Roy, D.S. *et al.* (2022) ‘Brain-wide mapping reveals that engrams for a single memory are distributed across multiple brain regions’, *Nature Communications*, 13(1). Available at: https://doi.org/10.1038/s41467-022-29384-4.

Ryan, T.J. *et al.* (2015) ‘Engram cells retain memory under retrograde amnesia’, *Science*, 348(6238), pp. 1007–1013. Available at: https://doi.org/10.1126/science.aaa5542.

Sajikumar, S. and Frey, J.U. (2003) ‘Anisomycin inhibits the late maintenance of long-term depression in rat hippocampal slices in vitro’, *Neuroscience Letters*, 338(2), pp. 147–150. Available at: https://doi.org/10.1016/S0304-3940(02)01400-3.

Scholz, N. *et al.* (2017) ‘Mechano-dependent signaling by Latrophilin/CIRL quenches cAMP in proprioceptive neurons’, *eLife*, 6. Available at: https://doi.org/10.7554/eLife.28360.

Scoville, W.B. and Milner, B. (1957) ‘Loss of recent memory after bilateral hippocampal lesions’, *Journal of Neurology, Neurosurgery & Psychiatry*, 20(1), pp. 11–21. Available at: https://doi.org/10.1136/jnnp.20.1.11.

Semon (1904) *Die Mneme als erhaltendes Prinzip im Wechsel desorganischen Geschehens*. Leipzig: W. Engelmann.

Semon (1921) *The mneme*. London, New York: Allen & Unwin; First British Edition.

Shepherd, G.M. and Harris, K.M. (1998) ‘Three-dimensional structure and composition of CA3-->CA1 axons in rat hippocampal slices: implications for presynaptic connectivity and compartmentalization.’, *The Journal of neuroscience : the official journal of the Society for Neuroscience*, 18(20), pp. 8300–10. Available at: http://www.ncbi.nlm.nih.gov/pubmed/9763474.

Shi, S.-H. *et al.* (1999) ‘Rapid Spine Delivery and Redistribution of AMPA Receptors After Synaptic NMDA Receptor Activation’, *Science*, 284(5421), pp. 1811–1816. Available at: https://doi.org/10.1126/science.284.5421.1811.

Siano, G. *et al.* (2019) ‘Tau Modulates VGluT1 Expression’, *Journal of Molecular Biology*, 431(4), pp. 873–884. Available at: https://doi.org/https://doi.org/10.1016/j.jmb.2019.01.023.

Silva, A.J., Stevens, C.F., *et al.* (1992) ‘Deficient Hippocampal Long-Term Potentiation in α-Calcium-Calmodulin Kinase II Mutant Mice’, *Science*, 257(5067), pp. 201–206. Available at: https://doi.org/10.1126/science.1378648.

Silva, A.J., Paylor, R., *et al.* (1992) ‘Impaired Spatial Learning in α-Calcium-Calmodulin Kinase II Mutant Mice’, *Science*, 257(5067), pp. 206–211. Available at: https://doi.org/10.1126/science.1321493.

Song, J.H. *et al.* (2018) ‘Combining mGRASP and Optogenetics Enables High-Resolution Functional Mapping of Descending Cortical Projections’, *Cell Reports*, 24(4), pp. 1071–1080. Available at: https://doi.org/10.1016/j.celrep.2018.06.076.

Sorra, K.E. and Harris, K.M. (1998) ‘Stability in synapse number and size at 2 Hr after long-term potentiation in hippocampal area CA1’, *Journal of Neuroscience*, 18(2), pp. 658–671. Available at: https://doi.org/10.1523/jneurosci.18-02-00658.1998.

Spalletti, C. *et al.* (2017) ‘Combining robotic training and inactivation of the healthy hemisphere restores pre-stroke motor patterns in mice’, *eLife*, 6. Available at: https://doi.org/10.7554/eLife.28662.

Sternberg (1983) ‘Biomedical Image Processing’, *Computer*, 16(1), pp. 22–34. Available at: https://doi.org/10.1109/MC.1983.1654163.

Steward, O. *et al.* (1998) ‘Synaptic activation causes the mRNA for the IEG Arc to localize selectively near activated postsynaptic sites on dendrites.’, *Neuron*, 21(4), pp. 741–51. Available at: https://doi.org/10.1016/s0896-6273(00)80591-7.

Steward, O. *et al.* (2015) ‘Localization and local translation of Arc/Arg3.1 mRNA at synapses: some observations and paradoxes’, *Frontiers in Molecular Neuroscience*, 7(JAN), pp. 1–15. Available at: https://doi.org/10.3389/fnmol.2014.00101.

Steward, O. and Levy, W.B. (1982) ‘Preferential localization of polyribosomes under the base of dendritic spines in granule cells of the dentate gyrus.’, *The Journal of neuroscience : the official journal of the Society for Neuroscience*, 2(3), pp. 284–91. Available at: https://doi.org/10.1523/JNEUROSCI.02-03-00284.1982.

Steward, O. and Schuman, E.M. (2003) ‘Compartmentalized synthesis and degradation of proteins in neurons.’, *Neuron*, 40(2), pp. 347–59. Available at: https://doi.org/10.1016/s0896-6273(03)00635-4.

Suh, J. *et al.* (2011) ‘Entorhinal Cortex Layer III Input to the Hippocampus Is Crucial for Temporal Association Memory’, *Science*, 334(6061), pp. 1415–1420. Available at: https://doi.org/10.1126/science.1210125.

Sun, X. *et al.* (2020) ‘Functionally Distinct Neuronal Ensembles within the Memory Engram.’, *Cell*, 181(2), pp. 410-423.e17. Available at: https://doi.org/10.1016/j.cell.2020.02.055.

Sutton, M.A. and Schuman, E.M. (2005) ‘Local translational control in dendrites and its role in long-term synaptic plasticity’, *Journal of Neurobiology*, pp. 116–131. Available at: https://doi.org/10.1002/neu.20152.

Szczurkowska, J. *et al.* (2016) ‘Targeted in vivo genetic manipulation of the mouse or rat brain by in utero electroporation with a triple-electrode probe’, *Nature Protocols*, 11(3), pp. 399–412. Available at: https://doi.org/10.1038/nprot.2016.014.

Takahashi, N. *et al.* (2012) ‘Locally Synchronized Synaptic Inputs’, *Science*, 335(6066), pp. 353–356. Available at: https://doi.org/10.1126/science.1210362.

Takeuchi, T., Duszkiewicz, A.J. and Morris, R.G.M. (2014) ‘The synaptic plasticity and memory hypothesis: encoding, storage and persistence.’, *Philosophical transactions of the Royal Society of London. Series B, Biological sciences*, 369(1633), p. 20130288. Available at: https://doi.org/10.1098/rstb.2013.0288.

Tanaka, K.Z. *et al.* (2014) ‘Cortical Representations Are Reinstated by the Hippocampus during Memory Retrieval’, *Neuron*, 84(2), pp. 347–354. Available at: https://doi.org/10.1016/j.neuron.2014.09.037.

Tayler, K.K. *et al.* (2013) 'Reactivation of Neural Ensembles during the Retrieval of Recent and Remote Memory', *Current Biology*, 23(2), pp. 99–106. Available at: https://doi.org/10.1016/j.cub.2012.11.019.

Taylor, A.M. *et al.* (2010) 'Microfluidic local perfusion chambers for the visualization and manipulation of synapses.', *Neuron*, 66(1), pp. 57–68. Available at: https://doi.org/10.1016/j.neuron.2010.03.022.

Terskikh, A. *et al.* (2000) '"Fluorescent Timer": Protein That Changes Color with Time', *Science*, 290(5496), pp. 1585–1588. Available at: https://doi.org/10.1126/science.290.5496.1585.

Testa, G. *et al.* (2019) 'The NGFR100W Mutation Specifically Impairs Nociception without Affecting Cognitive Performance in a Mouse Model of Hereditary Sensory and Autonomic Neuropathy Type V.', *The Journal of neuroscience : the official journal of the Society for Neuroscience*, 39(49), pp. 9702–9715. Available at: https://doi.org/10.1523/JNEUROSCI.0688-19.2019.

Tonegawa, S. *et al.* (2015) 'Memory Engram Cells Have Come of Age', *Neuron*, 87(5), pp. 918–931. Available at: https://doi.org/10.1016/j.neuron.2015.08.002.

Tonegawa, S., Morrissey, M.D. and Kitamura, T. (2018) 'The role of engram cells in the systems consolidation of memory.', *Nature reviews. Neuroscience*, 19(8), pp. 485–498. Available at: https://doi.org/10.1038/s41583-018-0031-2.

Tongiorgi, E., Righi, M. and Cattaneo, A. (1997) 'Activity-dependent dendritic targeting of BDNF and TrkB mRNAs in hippocampal neurons.', *The Journal of neuroscience : the official journal of the Society for Neuroscience*, 17(24), pp. 9492–505. Available at: https://doi.org/10.1523/JNEUROSCI.17-24-09492.1997.

Toni, N. *et al.* (1999) 'LTP promotes formation of multiple spine synapses between a single axon terminal and a dendrite', *Nature*, 402(6760), pp. 421–425. Available at: https://doi.org/10.1038/46574.

Trommald, M. and Jensen, V. (1995) *Analysis Pyramidal of Dendritic Spines in Rat CAI Cells Intracellularly Filled With a Fluorescent Dye*, *THE JOURNAL OF COMPARATIVE NEUROLOGY*.

Tsien, J.Z., Huerta, P.T. and Tonegawa, S. (1996) 'The Essential Role of Hippocampal CA1 NMDA Receptor–Dependent Synaptic Plasticity in Spatial Memory', *Cell*, 87(7), pp. 1327–1338. Available at: https://doi.org/10.1016/S0092-8674(00)81827-9.

Varga, Z. *et al.* (2011) 'Dendritic coding of multiple sensory inputs in single cortical neurons in vivo.', *Proceedings of the National Academy of Sciences of the United States of America*, 108(37), pp. 15420–5. Available at: https://doi.org/10.1073/pnas.1112355108.

Vlasov, K., van Dort, C.J. and Solt, K. (2018) 'Optogenetics and Chemogenetics', in R.G. Eckenhoff and I.J. Dmochowski (eds) *Methods in Enzymology*. Academic Press, pp. 181–196. Available at: https://doi.org/10.1016/bs.mie.2018.01.022.

Wheeler, A.L. *et al.* (2013) 'Identification of a Functional Connectome for Long-Term Fear Memory in Mice', *PLoS Computational Biology*, 9(1). Available at: https://doi.org/10.1371/journal.pcbi.1002853.

Whitlock, J.R. *et al.* (2006) 'Learning induces long-term potentiation in the hippocampus', *Science*, 313(5790), pp. 1093–1097. Available at: https://doi.org/10.1126/science.1128134.

Wiegert, J.S. *et al.* (2018) 'The fate of hippocampal synapses depends on the sequence of plasticity-inducing events', *eLife*, 7. Available at: https://doi.org/10.7554/eLife.39151.

Xu, T. *et al.* (2009) 'Rapid formation and selective stabilization of synapses for enduring motor memories', *Nature*, 462(7275), pp. 915–919. Available at: https://doi.org/10.1038/nature08389.

Xu, W. *et al.* (2008) 'Molecular Dissociation of the Role of PSD-95 in Regulating Synaptic Strength and LTD', *Neuron*, 57(2), pp. 248–262. Available at: https://doi.org/10.1016/j.neuron.2007.11.027.

Yang, G., Pan, F. and Gan, W.-B. (2009) 'Stably maintained dendritic spines are associated with lifelong memories', *Nature*, 462(7275), pp. 920–924. Available at: https://doi.org/10.1038/nature08577.

Yasuda, R. (2017) 'Biophysics of Biochemical Signaling in Dendritic Spines: Implications in Synaptic Plasticity.', *Biophysical journal*, 113(10), pp. 2152–2159. Available at: https://doi.org/10.1016/j.bpj.2017.07.029.

Yiu, A.P. *et al.* (2014) 'Neurons Are Recruited to a Memory Trace Based on Relative Neuronal Excitability Immediately before Training', *Neuron*, 83(3), pp. 722–735. Available at: https://doi.org/10.1016/j.neuron.2014.07.017.

Zhang, Y. *et al.* (2015) 'Visualization of NMDA receptor–dependent AMPA receptor synaptic plasticity in vivo', *Nature Neuroscience*, 18(3), pp. 402–407. Available at: https://doi.org/10.1038/nn.3936.

Zhou, Q., Homma, K.J. and Poo, M.M. (2004) 'Shrinkage of dendritic spines associated with long-term depression of hippocampal synapses', *Neuron*, 44(5), pp. 749–757. Available at: https://doi.org/10.1016/j.neuron.2004.11.011.

Zhou, Y. *et al.* (2009) 'CREB regulates excitability and the allocation of memory to subsets of neurons in the amygdala', *Nature Neuroscience*, 12(11), pp. 1438–1443. Available at: https://doi.org/10.1038/nn.2405.

## APPENDIX

Sequences of constructs generated in this thesis (5’ to 3’)

### 1) Const-pre-eGRASP (5883 bp)

CATGTCCTGCAGGCAGCTGCGCGCTCGCTCGCTCACTGAGGCCGCCCGGGCGTCGGGCGACCTTTGGTCGCCCGGCCTCA
GTGAGCGAGCGAGCGCGCAGAGAGGGAGTGGCCAACTCCATCACTAGGGGTTCCTGCGGCCGCACGCGTGTGTCTAGACT
GCAGACCATGGGCCCTTGACGTCCGGTCCGTTTACTCCCTATCAGTGATAGAGAACGTATGAAGAGTTTACTCCCTATCA
GTGATAGAGAACGTATGCAGACTTTACTCCCTATCAGTGATAGAGAACGTATAAGGAGTTTACTCCCTATCAGTGATAGA
GAACGTATGACCAGTTTACTCCCTATCAGTGATAGAGAACGTATCTACAGTTTACTCCCTATCAGTGATAGAGAACGTAT
ATCCAGTTTACTCCCTATCAGTGATAGAGAACGTATAAGCTTTAGGCGTGTACGGTGGGCGCCTATAAAAGCAGAGCTCG
TTTAGTGAACCGTCAGATCGCCTGGAGCAATTCCACAACACTTTTGTCTTATACCAACTTTCCGTACCACTTCCTACCCT
CGTAAAAGCCTCCGCGGCCCCGAATTCGAGCTCGGTACCCGGGGATCCTCTAGTCAGCTGACGCGTGCCGCCACTAGCCA
CCATGGAGACCGACACCCTCCTGCTATGGGTGCTGCTGCTCTGGGTGCCCGGCAGCACCGGCGACGCACCGGTCGGAGGC
AGCAAGGGCGAGGAGCTGTTCACCGGGGTGGTGCCCATCCTGGTCGAGCTGGACGGCGACGTAAACGGCCACAAGTTCAG
CGTGAGGGGCGAGGGCGAGGGCGATGCCACCATCGGCAAGCTGACCCTGAAGTTCATCTGCACCACCGGCAAGCTGCCCG
TGCCCTGGCCCACCCTCGTGACCACCCTGACCTACGGCGTGCAGTGCTTCGCCCGCTACCCCGACCACATGAAGCGGCAC
GACTTCTTCAAGTCCGCCATGCCCGAAGGCTACGTCCAGGAGCGCACCATCTCCTTCAAGGACGACGGCAAGTACAAGAC
CCGCGCCGTGGTGAAGTTCGAGGGCGACACCCTGGTGAACCGCATCGAGCTGAAGGGCACCGACTTCAAGGAGGACGGCA
ACATCCTGGGGCACAAGCTGGAGTACAACTTCAACAGCCACAACGTCTATATCACCGCCGACAAGCAGAAGAACGGCATC
AAGGCCAACTTCACCGTGCGCCACAACGTGGAGGACGGCAGCGTGCAGCTCGCCGACCACTACCAGCAGAACACCCCCAT
CGGCGACGGCCCCGTGCTGCTGCCCGACAACCACTACCTGAGCACCCAGACCGTGCTGAGCAAAGACCCCAACGAGAAGA
CCGGTGGATCTGGAGGCAGTGGCGGATCTAGATCTCCTAGCTACTCTCCACCACCTCCACCTGGAGGAGGTTCCGGAGGC
GGAAGCGGTACCGAAGTGCCTTCCTCTATGACAACTGAGTCGACAGCCACTGCCATGCAGTCCGAGATGTCCACCTCAAT
CATGGAGACCACCACAACCCTGGCTACCAGCACAGCTCGACGAGGAAAGCCCCCCACAAAGGAGCCTATCAGCCAGACCA
CGGATGATATCCTTGTGGCCTCGGCAGAGTGTCCCAGCGACGATGAGGACATTGACCCCTGTGAGCCGAGCTCAGGTGGG
TTAGCCAACCCCACCCGAGTGGGCGGCCGCGAACCATACCCAGGCTCGGCAGAGGTGATCCGGGAGTCTAGCAGTACCAC
TGGCATGGTGGTGGGGATTGTCGCAGCAGCAGCTCTGTGCATCCTCATCCTCCTCTATGCCATGTACAAGTACAGAAACC
GGGATGAAGGCTCATATCACGTGGATGAGAGTCGAAACTACATCAGTAACTCAGCACAGTCCAATGGGGCTGTGGTCAAG
GAGAAGCAGCCCAGCAGTGCGAAAAGCGCCAACAAAAACAAGAAGAACAAGGATAAGGAGTATTATGTCTGAATTCGATA
TCAAGCTTATCGATAATCAACCTCTGGATTACAAAATTTGTGAAAGATTGACTGGTATTCTTAACTATGTTGCTCCTTTT
ACGCTATGTGGATACGCTGCTTTAATGCCTTTGTATCATGCTATTGCTTCCCGTATGGCTTTCATTTTCTCCTCCTTGTA
TAAATCCTGGTTGCTGTCTCTTTATGAGGAGTTGTGGCCCGTTGTCAGGCAACGTGGCGTGGTGTGCACTGTGTTTGCTG
ACGCAACCCCCACTGGTTGGGGCATTGCCACCACCTGTCAGCTCCTTTCCGGGACTTTCGCTTTCCCCCTCCCTATTGCC
ACGGCGGAACTCATCGCCGCCTGCCTTGCCCGCTGCTGGACAGGGGCTCGGCTGTTGGGCACTGACAATTCCGTGGTGTT
GTCGGGGAAATCATCGTCCTTTCCTTGGCTGCTCGCCTATGTTGCCACCTGGATTCTGCGCGGGACGTCCTTCTGCTACG
TCCCTTCGGCCCTCAATCCAGCGGACCTTCCTTCCCGCGGCCTGCTGCCGGCTCTGCGGCCTCTTCCGCGTCTTCGCCTT
CGCCCTCAGACGAGTCGGATCTCCCTTTGGGCCGCCTCCCCGCATCGATACCGAGCGCTGCTCGAGAGATCTACGGGTGG
CATCCCTGTGACCCCTCCCCAGTGCCTCTCCTGGCCCTGGAAGTTGCCACTCCAGTGCCCACCAGCCTTGTCCTAATAAA
ATTAAGTTGCATCATTTTGTCTGACTAGGTGTCCTTCTATAATATTATGGGGTGGAGGGGGGTGGTATGGAGCAAGGGGC
AAGTTGGGAAGACAACCTGTAGGGCCTGCGGGGTCTATTGGGAACCAAGCTGGAGTGCAGTGGCACAATCTTGGCTCACT
GCAATCTCCGCCTCCTGGGTTCAAGCGATTCTCCTGCCTCAGCCTCCCGAGTTGTTGGGATTCCAGGCATGCATGACCAG
GCTCAGCTAATTTTTGTTTTTTTGGTAGAGACGGGGTTTCACCATATTGGCCAGGCTGGTCTCCAACTCCTAATCTCAGG
TGATCTACCCACCTTGGCCTCCCAAATTGCTGGGATTACAGGCGTGAACCACTGCTCCCTTCCCTGTCCTTCTGATTTTG
TAGGTAACCACGTGCGGACCGAGCGGCCGCAGGAACCCCTAGTGATGGAGTTGGCCACTCCCTCTCTGCGCGCTCGCTCG
CTCACTGAGGCCGGGCGACCAAAGGTCGCCCGACGCCCGGGCTTTGCCCGGGCGGCCTCAGTGAGCGAGCGAGCGCGCAG
CTGCCTGCAGGGGCGCCTGATGCGGTATTTTCTCCTTACGCATCTGTGCGGTATTTCACACCGCATACGTCAAAGCAACC
ATAGTACGCGCCCTGTAGCGGCGCATTAAGCGCGGCGGGTGTGGTGGTTACGCGCAGCGTGACCGCTACACTTGCCAGCG
CCTTAGCGCCCGCTCCTTTCGCTTTCTTCCCTTCCTTTCTCGCCACGTTCGCCGGCTTTCCCCGTCAAGCTCTAAATCGG
GGGCTCCCTTTAGGGTTCCGATTTAGTGCTTTACGGCACCTCGACCCCAAAAAACTTGATTTGGGTGATGGTTCACGTAG
TGGGCCATCGCCCTGATAGACGGTTTTTCGCCCTTTGACGTTGGAGTCCACGTTCTTTAATAGTGGACTCTTGTTCCAAA
CTGGAACAACACTCAACTCTATCTCGGGCTATTCTTTTGATTTATAAGGGATTTTGCCGATTTCGGTCTATTGGTTAAAA
AATGAGCTGATTTAACAAAAATTTAACGCGAATTTTAACAAAATATTAACGTTTACAATTTTATGGTGCACTCTCAGTAC
AATCTGCTCTGATGCCGCATAGTTAAGCCAGCCCCGACACCCGCCAACACCCGCTGACGCGCCCTGACGGGCTTGTCTGC
TCCCGGCATCCGCTTACAGACAAGCTGTGACCGTCTCCGGGAGCTGCATGTGTCAGAGGTTTTCACCGTCATCACCGAAA
CGCGCGAGACGAAAGGGCCTCGTGATACGCCTATTTTTATAGGTTAATGTCATGATAATAATGGTTTCTTAGACGTCAGG
TGGCACTTTTCGGGGAAATGTGCGCGGAACCCCTATTTGTTTATTTTTCTAAATACATTCAAATATGTATCCGCTCATGA
GACAATAACCCTGATAAATGCTTCAATAATATTGAAAAAGGAAGAGTATGAGTATTCAACATTTCCGTGTCGCCCTTATT
CCCTTTTTTGCGGCATTTTGCCTTCCTGTTTTTGCTCACCCAGAAACGCTGGTGAAAGTAAAAGATGCTGAAGATCAGTT

GGGTGCACGAGTGGGTTACATCGAACTGGATCTCAACAGCGGTAAGATCCTTGAGAGTTTTCGCCCCGAAGAACGTTTTC
CAATGATGAGCACTTTTAAAGTTCTGCTATGTGGCGCGGTATTATCCCGTATTGACGCCGGGCAAGAGCAACTCGGTCGC
CGCATACACTATTCTCAGAATGACTTGGTTGAGTACTCACCAGTCACAGAAAAGCATCTTACGGATGGCATGACAGTAAG
AGAATTATGCAGTGCTGCCATAACCATGAGTGATAACACTGCGGCCAACTTACTTCTGACAACGATCGGAGGACCGAAGG
AGCTAACCGCTTTTTTGCACAACATGGGGGATCATGTAACTCGCCTTGATCGTTGGGAACCGGAGCTGAATGAAGCCATA
CCAAACGACGAGCGTGACACCACGATGCCTGTAGCAATGGCAACAACGTTGCGCAAACTATTAACTGGCGAACTACTTAC
TCTAGCTTCCCGGCAACAATTAATAGACTGGATGGAGGCGGATAAAGTTGCAGGACCACTTCTGCGCTCGGCCCTTCCGG
CTGGCTGGTTTATTGCTGATAAATCTGGAGCCGGTGAGCGTGGGTCTCGCGGTATCATTGCAGCACTGGGGCCAGATGGT
AAGCCCTCCCGTATCGTAGTTATCTACACGACGGGGAGTCAGGCAACTATGGATGAACGAAATAGACAGATCGCTGAGAT
AGGTGCCTCACTGATTAAGCATTGGTAACTGTCAGACCAAGTTTACTCATATATACTTTAGATTGATTTAAAACTTCATT
TTTAATTTAAAAGGATCTAGGTGAAGATCCTTTTTGATAATCTCATGACCAAAATCCCTTAACGTGAGTTTTCGTTCCAC
TGAGCGTCAGACCCCGTAGAAAAGATCAAAGGATCTTCTTGAGATCCTTTTTTTCTGCGCGTAATCTGCTGCTTGCAAAC
AAAAAAACCACCGCTACCAGCGGTGGTTTGTTTGCCGGATCAAGAGCTACCAACTCTTTTTCCGAAGGTAACTGGCTTCA
GCAGAGCGCAGATACCAAATACTGTTCTTCTAGTGTAGCCGTAGTTAGGCCACCACTTCAAGAACTCTGTAGCACCGCCT
ACATACCTCGCTCTGCTAATCCTGTTACCAGTGGCTGCTGCCAGTGGCGATAAGTCGTGTCTTACCGGGTTGGACTCAAG
ACGATAGTTACCGGATAAGGCGCAGCGGTCGGGCTGAACGGGGGGTTCGTGCACACAGCCCAGCTTGGAGCGAACGACCT
ACACCGAACTGAGATACCTACAGCGTGAGCTATGAGAAAGCGCCACGCTTCCCGAAGGGAGAAAGGCGGACAGGTATCCG
GTAAGCGGCAGGGTCGGAACAGGAGAGCGCACGAGGGAGCTTCCAGGGGGAAACGCCTGGTATCTTTATAGTCCTGTCGG
GTTTCGCCACCTCTGACTTGAGCGTCGATTTTTGTGATGCTCGTCAGGGGGGCGGAGCCTATGGAAAAACGCCAGCAACG
CGGCCTTTTTACGGTTCCTGGCCTTTTGCTGGCCTTTTGCTCA

Features :

| | |
|---|---|
| ColE1 origin | : [5217 : 5845 - CW] |
| AmpR | : [4406 : 5065 - CW] |
| Amp prom | : [4138 : 4166 - CW] |
| AAV2 ITR | : [6 : 135 - CW] |
| TRE3g | : [172 : 632 - CW] |
| CDS | : [643 : 1992 - CW] |
| IgG kappa signal peptide | : [643 : 714 - CW] |
| GFP1-10 | : [721 : 1359 - CW] |
| p32 | : [1393 : 1422 - CW] |
| truncated Neurexin 1b | : [1453 : 1989 - CW] |
| WPRE | : [2016 : 2603 - CW] |
| AAV2 ITR | : [3151 : 3291 - CW] |

For Const-cyan-pre-eGRASP, GFP1-10 is,

AGCAAGGGCGAGGAGCTGTTCACCGGGGTGGTGCCCATCCTGGTCGAGCTGGACGGCGACGTAAACGGCCACAAGTTCAG
CGTGAGGGGCGAGGGCGAGGGCGATGCCACCATCGGCAAGCTGACCCTGAAGTTCATCTGCACCACCGGCAAGCTGCCCG
TGCCCTGGCCCACCCTCGTGACCACCCTGAGCTGGGGCGTGCAGTGCTTCGCCCGCTACCCCGACCACATGAAGCGGCAC
GACTTCTTCAAGTCCGCCATGCCCGAAGGCTACGTCCAGGAGCGCACCATCTCCTTCAAGGACGACGGCAAGTACAAGAC
CCGCGCCGTGGTGAAGTTCGAGGGCGACACCCTGGTGAACCGCATCGAGCTGAAGGGCACCGACTTCAAGGAGGACGGCA
ACATCCTGGGGCACAAGCTGGAGTACAACTTCAACAGCGGCAACGTCTATATCACCGCCGACAAGCAGAAGAACGGCATC
AAGGCCAACTTCACCGTGCGCCACAACGTGGAGGACGGCAGCGTGCAGCTCGCCGACCACTACCAGCAGAACACCCCCAT
CGGCGACGGCCCCGTGCTGCTGCCCGACAACCACTACCTGAGCACCCAGAGCGTGCTGAGCAAAGACCCCAACGAGAAG

For Const-yellow-pre-eGRASP, GFP1-10 is,

AGCAAGGGCGAGGAGCTGTTCACCGGGGTGGTGCCCATCCTGGTCGAGCTGGACGGCGACGTAAACGGCCACAAGTTCAG
CGTGAGGGGCGAGGGCGAGGGCGATGCCACCATCGGCAAGCTGACCCTGAAGTTCATCTGCACCACCGGCAAGCTGCCCG
TGCCCTGGCCCACCCTCGTGACCACCCTGACCTACGGCGTGCAGTGCTTCGCCCGCTACCCCGACCACATGAAGCGGCAC
GACTTCTTCAAGTCCGCCATGCCCGAAGGCTACGTCCAGGAGCGCACCATCTCCTTCAAGGACGACGGCAAGTACAAGAC
CCGCGCCGTGGTGAAGTTCGAGGGCGACACCCTGGTGAACCGCATCGAGCTGAAGGGCACCGACTTCAAGGAGGACGGCA
ACATCCTGGGGCACAAGCTGGAGTACAACTTCAACAGCCACAACGTCTATATCACCGCCGACAAGCAGAAGAACGGCATC
AAGGCCAACTTCACCGTGCGCCACAACGTGGAGGACGGCAGCGTGCAGCTCGCCGACCACTACCAGCAGAACACCCCCAT
CGGCGACGGCCCCGTGCTGCTGCCCGACAACCACTACCTGAGCTACCAGACCGTGCTGAGCAAAGACCCCAACGAGAAG

## 2) SynActive-post-eGRASP (7241 bp)

CATGTCCTGCAGGCAGCTGCGCGCTCGCTCGCTCACTGAGGCCGCCCGGGCGTCGGGCGACCTTTGGTCGCCCGGCCTCA
GTGAGCGAGCGAGCGCGCAGAGAGGGAGTGGCCAACTCCATCACTAGGGGTTCCTGCGGCCGCACGCGTGTGTCTAGACT
GCAGACCATGGGCCCTTGACGTCCGGTCCGTTTACTCCCTATCAGTGATAGAGAACGTATGAAGAGTTTACTCCCTATCA
GTGATAGAGAACGTATGCAGACTTTACTCCCTATCAGTGATAGAGAACGTATAAGGAGTTTACTCCCTATCAGTGATAGA
GAACGTATGACCAGTTTACTCCCTATCAGTGATAGAGAACGTATCTACAGTTTACTCCCTATCAGTGATAGAGAACGTAT
ATCCAGTTTACTCCCTATCAGTGATAGAGAACGTATAAGCTTTAGGCGTGTACGGTGGGCGCCTATAAAAGCAGAGCTCG
TTTAGTGAACCGTCAGATCGCCTGGAGCAATTCCACAACACTTTTGTCTTATACCAACTTTCCGTACCACTTCCTACCCT
CGTAAAAGCCTCCGCGGCCCCGAATTCGAGCTCGGTACCCGGGGATCCTCTAGTCAGCTGACGCGTGCCGCCACTAGCAG
TGCTCTGGCGAGTAGTCCTCCCTCAGCCGCAGTCTCTGGGCCTCTTCAGCTTGAGCGGCGGCGAGCCTGCCACACTCGCT
AAGCTCCTCCGGCACCGCGCACTTGCCACTGCCACTGCCGCTTCGCGCCCGCTGCAGCCGCCGGCTCTGAATCCTTCTGG
CTTCCGCCTCAGAGGAGTTCTTAGCCTGTCCCGAACCGTAACCCCGGCGAGCAGACGGAGCTGGACCATCTAGCCACCAT
GGGCTGTGTGCAGTGTAAGGACAAGGAGGCTACCAAGCTGACAGGAGGCGTGAGCAAGGGCGAGGCAGTGATCAAGGAGT
TCATGCGGTTCAAGGTGCACATGGAGGGCTCCATGAACGGCCACGAGTTCGAGATCGAGGGCGAGGGCGAGGGCCGCCCC
TACGAGGGCACCCAGACCGCCAAGCTGAAGGTGACCAAGGGTGGCCCCCTGCCCTTCTCCTGGGACATCCTGTCCCCTCA
GTTCATGTACGGCTCCAGGGCCTTCATCAAGCACCCCGCCGACATCCCCGACTACTATAAGCAGTCCTTCCCCGAGGGCT
TCAAGTGGGAGCGCGTGATGAACTTCGAGGACGGCGGCGCCGTGACCGTGACCCAGGACACCTCCCTGGAGGACGGCACC
CTGATCTACAAGGTGAAGCTCCGCGGCACCAACTTCCCTCCTGACGGCCCCGTAATGCAGAAGAAGACAATGGGCTGGGA
AGCGTCCACCGAGCGGTTGTACCCCGAGGACGGCGTGCTGAAGGGCGACATTAAGATGGCCCTGCGCCTGAAGGACGGCG
GCCGCTACCTGGCGGACTTCAAGACCACCTACAAGGCCAAGAAGCCCGTGCAGATGCCCGGCGCCTACAACGTCGACCGC
AAGTTGGACATCACCTCCCACAACGAGGACTACACCGTGGTGGAACAGTACGAACGCTCCGAGGGCCGCCACTCCACCGG
CGGCATGGACGAGCTGTACAAGGGAAGCGGAGCTACTAACTTCAGCCTGCTGAAGCAGGCTGGAGACGTGGAGGAGAACC
CTGGACCTGAGACCGACACCCTCCTGCTATGGGTGCTGCTGCTCTGGGTGCCCGGCAGCACCGGCGACGCACCGGTCGGA
GGCAACGACCCTAACCTGTTCGTCGCCCTGTACGACTTCGTCGCCTCTGGCGACAACACCCTGAGCATCACCAAGGGCGA
GAAGCTGAGAGTCCTGGGCTACAACCACAACGGCGAGTGGTGCGAGGCCCAGACCAAGAACGGCCAGGGCTGGGTCCCTA
GCAACTACATCACACCTGTCAACAGCACCGGTGGAGGCAGCGGAGGAGGCTCCGGAAGAGACCACATGGTGCTGCACGAG
TACGTGAACGCTGCTGGAATCACAGGAGGAGGCTCCGGAGGCGGAAGCGGTACCCTCGAGCTGGTGCCCCACTTGCATAA
CCTCAATGACATCAGCCAATACACAAGTACAACCACCAAGGTCCCAAGCACTGACATCACCCTTCGACCAACTCGGAAAA
ACTCAACCCCTGTGACCAGCGCATTTCCAACCGCTAAGCAAGACGACCCCAAACAACAGCCTAGTCCATTTAGCGTAGAC
CAAAGGGACTACAGCACAGAGCTGTCCGTGACCATAGCTGTAGGAGCTTCCCTGCTTTTCCTGAACATTCTGGCTTTCGC
GGCCCTCTATTACAAGAAGGACAAAAGGCGCCACGACGTACATAGGAGATGTAGTCCGCAACGAACTACAACCAATGATC
TTACGCACGCACCTGAGGAGGAGATCATGAGTCTTCAGATGAAACACACAGACCTGGACCACGAGTGTGAATCCATCCAT
CCCCATGAGGTGGTGCTGAGGACAGCATGCCCTCCGGACTATACCCTGGCAATGCGCCGAAGCCCAGACGACATTCCCCT
GATGACACCCAATACCATAACCATGATTCCCAACACTATTCCAGGAATCCAGCCTCTCCACACTTTCAACACATTCACTG
GTGGACAGAATAATACTCTCCCTCATCCGCATCCACACCCCCACTCCCACAGCTAAGAATTCAGGGGCCAGCCCAGGGTC
CCCAGCCTGCCTGCCACACCCAGTCTGTGGCTTTTGTCAACTAGGACTTGATTGAGCTGGGGCTGACACCCAAGGGGATG
CCCTGTCCAGCCAGACACCTTCTCACCCACTGGCCTGACTCACAACTGCCACACAACCATGATTCATGGACATCAAGAAG
CCCCTCTCCCATAGGGCTCCCACCTGCCACCTACCCCTCACCTGTCTGCCCTAGTCCTGGCCCTGTCTCCAGTGGCCTCA
CCCTCTACACTCTCAGACCATCACAGAACACCTTTGGCTTCCTCATTCTGCATCAGTGTCCAGGGCCCTTTGGGTAGTCA
AGAAATCAAGTGTCTGAAAGGCAATGAAAAGTAGGCACCAAACCCAAGGGGCATCCCAGGGCAGATGCTAAAGCAGAATC
AGAGATGGCCGAAGGAACCTCTACTTCCGGGGATGCAGCCCGCTCCTACAGACACAGCAGATCCAGCTGGTGCCCTACCT
GCCTCCCAGAGCAACTGGCCAGTCTTGGGCAGCATAGCTCCCCTCTCAGGGTGAGCTGAAGCAGCAGACCTGACGCGCTG
GCGCCTCCTGGCCCCCAGCAGTGATTCATACCAGTGAAGAAAAGCAGACTTCGGCTCCATGACTCAGCCATGCCAGGCGG
AGGGTCCCAGAGGGGCTGAGTCCTCAGCCCCAGCTGAGGCAGCAGCTGGAGTCTTCAGAGCCAGGTGAATGACACCAGGT
CTCAAGCTGCTGAGAAGTCTTTCCGGCCATGTCTGGAAGGGGTACCACCCCAGCACCAGCACCGTCCCCTCCTCTCTTGA
AGCTGCCTGCACAGAGGTTCCAAGACACTTTCAAGGCAGAGAAAATAGGATTACAAAGAGGAGGTGCCTGGCAGAGGGCA
GCACCCAGCTCAGCCTCAGAGCTGAAGGTGAAGACAAGCCAGCGTGAAACCCCGGGTCTGCCACGAATGCCCGCTCCGCT
GGCCACTCACCAGCTGCCTGCCACAAGCCACTGCAGCTTGAGCAGGGTCTGTGCCCTCTCAGCACAGAGCCCAGTTCGCT
GCGTGGCCTTTGGCCCCCGCCAGAACCTTGCAGGAGCCTTAAGGTTCGGGCCCTAGCCCAGCCTGACCTTACCTGCTGTG
CCCTGCCTGCTGGTCAAGTCCAGTCCCAGGAGACCCCATGCCTTGGCTCCTAGGCTGTTCCAGGCACTTCCCTGACCTGC
CGGGTGATTGCCCAGCTGGAACCTCATCCACACCCCAGCACCAACCACCTCGTGTTGGTAACTGCTCGTGTCTGTAGTCT

GAGTAGGCCATGTTGAGGTTCCTCCATCTGCCTGGTCCATTGGTGTTCTGAGACCAGTTCCACTGCTGTTCTGACAGATC
CCCCACCCTGTGCCCCTGCCAGCCCCCACAGGTTTATTTTTGCACATAAACCATGACCCATACTAATTTGGCTAGCTCTG
GGGACTAGGGAGACCCTGGAGATCTCAAGAGTGTGGCTATCCCCTATTTTCACCAAGCCTTCAATATCCAGCCAGGCCAT
CTGCCCACACCATCTTACCTCAAAGACAGACATATATATATATACATATATATGATTTTGTTAATAAAACTATGAAAT
TTAAACTCGAGGTGAAATTTGTGATGCTATTGCTTTATTTGTAACCATCTAGCTTTATTTGTGAAATTTGTGATGCTATT
GCTTTATTTGTAACCATTATAAGCTGCAATAAACAAGTTAACAACAACAATTGCATTCATTTTATGTTTCAGGTTCCGGT
CCGTTGGCCGTGCGGACCGAGCGGCCGCAGGAACCCCTAGTGATGGAGTTGGCCACTCCCTCTCTGCGCGCTCGCTCGCT
CACTGAGGCCGGGCGACCAAAGGTCGCCCGACGCCCGGGCTTTGCCCGGGCGGCCTCAGTGAGCGAGCGAGCGCGCAGCT
GCCTGCAGGGGCGCCTGATGCGGTATTTTCTCCTTACGCATCTGTGCGGTATTTCACACCGCATACGTCAAAGCAACCAT
AGTACGCGCCCTGTAGCGGCGCATTAAGCGCGGCGGGTGTGGTGGTTACGCGCAGCGTGACCGCTACACTTGCCAGCGCC
TTAGCGCCCGCTCCTTTCGCTTTCTTCCCTTCCTTTCTCGCCACGTTCGCCGGCTTTCCCCGTCAAGCTCTAAATCGGGG
GCTCCCTTTAGGGTTCCGATTTAGTGCTTTACGGCACCTCGACCCCAAAAAACTTGATTTGGGTGATGGTTCACGTAGTG
GGCCATCGCCCTGATAGACGGTTTTTCGCCCTTTGACGTTGGAGTCCACGTTCTTTAATAGTGGACTCTTGTTCCAAACT
GGAACAACACTCAACTCTATCTCGGGCTATTCTTTTGATTTATAAGGGATTTTGCCGATTTCGGTCTATTGGTTAAAAAA
TGAGCTGATTTAACAAAAATTTAACGCGAATTTTAACAAAATATTAACGTTTACAATTTTATGGTGCACTCTCAGTACAA
TCTGCTCTGATGCCGCATAGTTAAGCCAGCCCCGACACCCGCCAACACCCGCTGACGCGCCCTGACGGGCTTGTCTGCTC
CCGGCATCCGCTTACAGACAAGCTGTGACCGTCTCCGGGAGCTGCATGTGTCAGAGGTTTTCACCGTCATCACCGAAACG
CGCGAGACGAAAGGGCCTCGTGATACGCCTATTTTTATAGGTTAATGTCATGATAATAATGGTTTCTTAGACGTCAGGTG
GCACTTTTCGGGGAAATGTGCGCGGAACCCCTATTTGTTTATTTTTCTAAATACATTCAAATATGTATCCGCTCATGAGA
CAATAACCCTGATAAATGCTTCAATAATATTGAAAAAGGAAGAGTATGAGTATTCAACATTTCCGTGTCGCCCTTATTCC
CTTTTTTGCGGCATTTTGCCTTCCTGTTTTTGCTCACCCAGAAACGCTGGTGAAAGTAAAAGATGCTGAAGATCAGTTGG
GTGCACGAGTGGGTTACATCGAACTGGATCTCAACAGCGGTAAGATCCTTGAGAGTTTTCGCCCCGAAGAACGTTTTCCA
ATGATGAGCACTTTTAAAGTTCTGCTATGTGGCGCGGTATTATCCCGTATTGACGCCGGGCAAGAGCAACTCGGTCGCCG
CATACACTATTCTCAGAATGACTTGGTTGAGTACTCACCAGTCACAGAAAAGCATCTTACGGATGGCATGACAGTAAGAG
AATTATGCAGTGCTGCCATAACCATGAGTGATAACACTGCGGCCAACTTACTTCTGACAACGATCGGAGGACCGAAGGAG
CTAACCGCTTTTTTGCACAACATGGGGGATCATGTAACTCGCCTTGATCGTTGGGAACCGGAGCTGAATGAAGCCATACC
AAACGACGAGCGTGACACCACGATGCCTGTAGCAATGGCAACAACGTTGCGCAAACTATTAACTGGCGAACTACTTACTC
TAGCTTCCCGGCAACAATTAATAGACTGGATGGAGGCGGATAAAGTTGCAGGACCACTTCTGCGCTCGGCCCTTCCGGCT
GGCTGGTTTATTGCTGATAAATCTGGAGCCGGTGAGCGTGGGTCTCGCGGTATCATTGCAGCACTGGGGCCAGATGGTAA
GCCCTCCCGTATCGTAGTTATCTACACGACGGGGAGTCAGGCAACTATGGATGAACGAAATAGACAGATCGCTGAGATAG
GTGCCTCACTGATTAAGCATTGGTAACTGTCAGACCAAGTTTACTCATATATACTTTAGATTGATTTAAAACTTCATTTT
TAATTTAAAAGGATCTAGGTGAAGATCCTTTTTGATAATCTCATGACCAAAATCCCTTAACGTGAGTTTTCGTTCCACTG
AGCGTCAGACCCCGTAGAAAAGATCAAAGGATCTTCTTGAGATCCTTTTTTTCTGCGCGTAATCTGCTGCTTGCAAACAA
AAAAACCACCGCTACCAGCGGTGGTTTGTTTGCCGGATCAAGAGCTACCAACTCTTTTTCCGAAGGTAACTGGCTTCAGC
AGAGCGCAGATACCAAATACTGTTCTTCTAGTGTAGCCGTAGTTAGGCCACCACTTCAAGAACTCTGTAGCACCGCCTAC
ATACCTCGCTCTGCTAATCCTGTTACCAGTGGCTGCTGCCAGTGGCGATAAGTCGTGTCTTACCGGGTTGGACTCAAGAC
GATAGTTACCGGATAAGGCGCAGCGGTCGGGCTGAACGGGGGGTTCGTGCACACAGCCCAGCTTGGAGCGAACGACCTAC
ACCGAACTGAGATACCTACAGCGTGAGCTATGAGAAAGCGCCACGCTTCCCGAAGGGAGAAAGGCGGACAGGTATCCGGT
AAGCGGCAGGGTCGGAACAGGAGAGCGCACGAGGGAGCTTCCAGGGGGAAACGCCTGGTATCTTTATAGTCCTGTCGGGT
TTCGCCACCTCTGACTTGAGCGTCGATTTTTGTGATGCTCGTCAGGGGGGCGGAGCCTATGGAAAAACGCCAGCAACGCG
GCCTTTTTACGGTTCCTGGCCTTTTGCTGGCCTTTTGCTCA

Features :

| | | |
|---|---|---|
| ColE1 origin | : [6575 : 7203 - CW] | |
| AmpR | : [5764 : 6423 - CW] | |
| Amp prom | : [5496 : 5524 - CW] | |
| AAV2 ITR | : [6 : 135 - CW] | |
| TRE3g | : [172 : 632 - CW] | |
| 5' Arc UTR | : [639 : 868 - CW] | |
| CDS | : [879 : 2696 - CW] | |
| IgG kappa signal peptide | : [1689 : 1757 - CW] | |
| Myristoylation tag | : [879 : 929 - CW] | |
| mScarlet_1 | : [930 : 1622 - CW] | |

P2A : [1632 : 1688 - CW]

Abl SH3 : [1764 : 1946 - CW]

GFP11 : [1977 : 2024 - CW]

truncated Neuroligin1 : [2055 : 2693 - CW]

3' Arc UTR : [2719 : 4325 - CW]

short pA : [4332 : 4476 - CW]

AAV2 ITR : [4509 : 4648 - CW]

## 3) SynActive -PSD95Δ-Venus (7659 bp)

CATGTCCTGCAGGCAGCTGCGCGCTCGCTCGCTCACTGAGGCCGCCCGGGCGTCGGGCGACCTTTGGTCGCCCGGCCTCA
GTGAGCGAGCGAGCGCGCAGAGAGGGAGTGGCCAACTCCATCACTAGGGGTTCCTGCGGCCGCACGCGTGTGTCTAGACT
GCAGACCATGGGCCCTTGACGTCCGGTCCGTTTACTCCCTATCAGTGATAGAGAACGTATGAAGAGTTTACTCCCTATCA
GTGATAGAGAACGTATGCAGACTTTACTCCCTATCAGTGATAGAGAACGTATAAGGAGTTTACTCCCTATCAGTGATAGA
GAACGTATGACCAGTTTACTCCCTATCAGTGATAGAGAACGTATCTACAGTTTACTCCCTATCAGTGATAGAGAACGTAT
ATCCAGTTTACTCCCTATCAGTGATAGAGAACGTATAAGCTTTAGGCGTGTACGGTGGGCGCCTATAAAAGCAGAGCTCG
TTTAGTGAACCGTCAGATCGCCTGGAGCAATTCCACAACACTTTTGTCTTATACCAACTTTCCGTACCACTTCCTACCCT
CGTAAAAGCCTCCGCGGCCCCGAATTCGAGCTCGGTACCCGGGGATCCTCTAGTCAGCTGACGCGTGCCGCCACTAGTAG
TGCTCTGGCGAGTAGTCCTCCCTCAGCCGCAGTCTCTGGGCCTCTTCAGCTTGAGCGGCGGCGAGCCTGCCACACTCGCT
AAGCTCCTCCGGCACCGCGCACTTGCCACTGCCACTGCCGCTTCGCGCCCGCTGCAGCCGCCGGCTCTGAATCCTTCTGG
CTTCCGCCTCAGAGGAGTTCTTAGCCTGTCCCGAACCGTAACCCCGGCGAGCAGACGGAGCTGGACCATCTAGAATGGAC
TGTCTCTGTATAGTGACAACCAAGAAATACCGCTACCAAGATGAAGACACGCCCCCTCTGGAACACAGCCCGGCCCACCT
CCCCAACCAGGCCAATTCTCCCCCCTGTGATTGTCAACACGGACACCCTAGAAGCCCCAGGATATGAGTTGCAGGTGAATG
GAACAGAGGGGGAGATGGAGTATGAGCGGATCGTGATCCATCGGGGCTCCACCGGCCTGGGCTTCAACATCGTGGGCGGC
GAGGATGGTGAAGGCATCTTCATCTCCTTCATCCTTGCTGGGGGTCCAGCCGACCTCAGTGGGGAGCTACGGAAGGGGA
CCAGATCCTGTCGGTCAATGGTGTTGACCTCCGCAATGCCAGTCACGAACAGGCTGCCATTGCCCTGAAGAATGCGGGTC
AGACGGTCACGATCATCGCTCAGTATAAACCAGAAGAGTATAGTCGATTCGAGGCCAAGATCCATGATCTTCGGGAACAG
CTCATGAATAGTAGCCTAGGCTCAGGGACTGCATCCTTGCGAAGCAACCCCAAGAGGGGCTTCTACATTAGGGCCCTGTT
TGATTACGACAAGACCAAGGACTGCGGTTTCTTGAGCCAGGCCCTGAGCTTCCGCTTCGGGGATGTGCTTCATGTCATTG
ACGCTGGTGACGAAGAGTGGTGGCAAGCACGGCGGGTCCACTCCGACAGTGAGACCGACGACATTGGCTTCATTCCCAGC
AAACGGCGGGTCGAGCGACGAGAGTGGTCAAGGTTAAAGGCCAAGGACTGGGGCTCCAGCTCTGGATCACAGGGTCGAGA
AGACTCGGTTCTGAGCTATGAGACGGTGACCCAGATGGAAGTGCACTATGCTCGTCCCATCATCATCCTTGGACCCACCA
AAGACCGTGCCAACGATGATCTTCTCTCCGAGTTCCCCGACAAGTTTGGATCCTGTGTCCCTCATACGACACGTCCTAAG
CGGGAATATGAGATAGACGGCCGGGATTACCACTTTGTCTCCTCCCGGGAGAAAATGGAGAAGGACATCCAGGCACACAA
GTTCATTGAGGCTGGCCAGTACAACAGCCACCTCTATGGGACCAGCGTCCAGTCTGTGCGAGAGGTAGCAGAGCAGGGGA
AGCACTGCATCCTCGATGTCTCGGCCAATGCCGTGCGGCGGCTGCAGGCGGCCCACCTGCACCCCATCGCCATCTTCATC
CGTCCCCGCTCCCTGGAGAATGTGCTAGAGATCAATAAGCGGATCACAGAGGAGCAAGCCCGGAAAGCCTTCGACAGAGC
CACGAAGCTGGAGCAGGAGTTCACAGAGTGCTTCTCAGCCATCGTAGAGGGCGACAGCTTTGAAGAGATCTATCACAAAG
TGAAACGTGTCATTGAAGACCTCTCAGGCCCCTACATCTGGGTCCCAGCCCGAGAGAGACTCGGTGGCGGCGGTGGCACG
CGTGTGAGCAAGGGCGAGGAGCTGTTCACCGGGGTGGTGCCCATCCTGGTCGAGCTGGACGGCGACGTAAACGGCCACAA
GTTCAGCGTGTCCGGCGAGGGCGAGGGCGATGCCACCTACGGCAAGCTGACCCTGAAGCTGATCTGCACCACCGGCAAGC
TGCCCGTGCCCTGGCCCACCCTCGTGACCACCCTGGGCTACGGCCTGCAGTGCTTCGCCCGCTACCCCGACCACATGAAG
CAGCACGACTTCTTCAAGTCCGCCATGCCCGAAGGCTACGTCCAGGAGCGCACCATCTTCTTCAAGGACGACGGCAACTA
CAAGACCCGCGCCGAGGTGAAGTTCGAGGGCGACACCCTGGTGAACCGCATCGAGCTGAAGGGCATCGACTTCAAGGAGG
ACGGCAACATCCTGGGGCACAAGCTGGAGTACAACTACAACAGCCACAACGTCTATATCACCGCCGACAAGCAGAAGAAC
GGCATCAAGGCCAACTTCAAGATCCGCCACAACATCGAGGACGGCGGCGTGCAGCTCGCCGACCACTACCAGCAGAACAC
CCCCATCGGCGACGGCCCCGTGCTGCTGCCCGACAACCACTACCTGAGCTACCAGTCCGCCCTGAGCAAAGACCCCAACG
AGAAGCGCGATCACATGGTCCTGCTGGAGTTCGTGACCGCCGCCGGGATCACTCTCGGCATGGACGAGCTGTACCCCTAC
GACGTGCCCGACTACGCCGGTGGCTATCCATATGATGTTCCAGATTATGCTTAATAAGTACAAGTAAGGCGCGTCAATTC
AGGGGCCAGCCCAGGGTCCCCAGCCTGCCTGCCACACCCAGTCTGTGGCTTTTGTCAACTAGGACTTGATTGAGCTGGGG
CTGACACCCAAGGGGATGCCCTGTCCAGCCAGACACCTTCTCACCCACTGGCCTGACTCACAACTGCCACACAACCATGA
TTCATGGACATCAAGAAGCCCCTCTCCCATAGGGCTCCCACCTGCCACCTACCCCTCACCTGTCTGCCCTAGTCCTGGCC
CTGTCTCCAGTGGCCTCACCCTCTACACTCTCAGACCATCACAGAACACCTTTGGCTTCCTCATTCTGCATCAGTGTCCA
GGGCCCTTTGGGTAGTCAAGAAATCAAGTGTCTGAAAGGCAATGAAAAGTAGGCACCAAACCCAAGGGGCATCCCAGGGC

AGATGCTAAAGCAGAATCAGAGATGGCCGAAGGAACCTCTACTTCCGGGGATGCAGCCCGCTCCTACAGACACAGCAGAT
CCAGCTGGTGCCCTACCTGCCTCCCAGAGCAACTGGCCAGTCTTGGGCAGCATAGCTCCCCTCTCAGGGTGAGCTGAAGC
AGCAGACCTGACGCGCTGGCGCCTCCTGGCCCCCAGCAGTGATTCATACCAGTGAAGAAAAGCAGACTTCGGCTCCATGA
CTCAGCCATGCCAGGCGGAGGGTCCCAGAGGGGCTGAGTCCTCAGCCCCAGCTGAGGCAGCAGCTGGAGTCTTCAGAGCC
AGGTGAATGACACCAGGTCTCAAGCTGCTGAGAAGTCTTTCCGGCCATGTCTGGAAGGGGTACCACCCCAGCACCAGCAC
CGTCCCCTCCTCTCTTGAAGCTGCCTGCACAGAGGTTCCAAGACACTTTCAAGGCAGAGAAAATAGGATTACAAAGAGGA
GGTGCCTGGCAGAGGGCAGCACCCAGCTCAGCCTCAGAGCTGAAGGTGAAGACAAGCCAGCGTGAAACCCCGGGTCTGCC
ACGAATGCCCGCTCCGCTGGCCACTCACCAGCTGCCTGCCACAAGCCACTGCAGCTTGAGCAGGGTCTGTGCCCTCTCAG
CACAGAGCCCAGTTCGCTGCGTGGCCTTTGGCCCCCGCCAGAACCTTGCAGGAGCCTTAAGGTTCGGGCCCTAGCCCAGC
CTGACCTTACCTGCTGTGCCCTGCCTGCTGGTCAAGTCCAGTCCCAGGAGACCCCATGCCTTGGCTCCTAGGCTGTTCCA
GGCACTTCCCTGACCTGCCGGGTGATTGCCCAGCTGGAACCTCATCCACACCCCAGCACCAACCACCTCGTGTTGGTAAC
TGCTCGTGTCTGTAGTCTGAGTAGGCCATGTTGAGGTTCCTCCATCTGCCTGGTCCATTGGTGTTCTGAGACCAGTTCCA
CTGCTGTTCTGACAGATCCCCCACCCTGTGCCCCTGCCAGCCCCCACAGGTTTATTTTTGCACATAAACCATGACCCATA
CTAATTTGGCTAGCTCTGGGGACTAGGGAGACCCTGGAGATCTCAAGAGTGTGGCTATCCCCTATTTTCACCAAGCCTTC
AATATCCAGCCAGGCCATCTGCCCACACCATCTTACCTCAAAGACAGACATATATATATATATACATATATATGATTTTG
TTAATAAAACTATGAAATTTAAACTCGAGGTGAAATTTGTGATGCTATTGCTTTATTTGTAACCATCTAGCTTTATTTGT
GAAATTTGTGATGCTATTGCTTTATTTGTAACCATTATAAGCTGCAATAAACAAGTTAACAACAACAATTGCATTCATTT
TATGTTTCAGGTTCCGGTCCGTTGGCCGTGCGGACCGAGCGGCCGCAGGAACCCCTAGTGATGGAGTTGGCCACTCCCTC
TCTGCGCGCTCGCTCGCTCACTGAGGCCGGGCGACCAAAGGTCGCCCGACGCCCGGGCTTTGCCCGGGCGGCCTCAGTGA
GCGAGCGAGCGCGCAGCTGCCTGCAGGGGCGCCTGATGCGGTATTTTCTCCTTACGCATCTGTGCGGTATTTCACACCGC
ATACGTCAAAGCAACCATAGTACGCGCCCTGTAGCGGCGCATTAAGCGCGGCGGGTGTGGTGGTTACGCGCAGCGTGACC
GCTACACTTGCCAGCGCCTTAGCGCCCGCTCCTTTCGCTTTCTTCCCTTCCTTTCTCGCCACGTTCGCCGGCTTTCCCCG
TCAAGCTCTAAATCGGGGGCTCCCTTTAGGGTTCCGATTTAGTGCTTTACGGCACCTCGACCCCAAAAAACTTGATTTGG
GTGATGGTTCACGTAGTGGGCCATCGCCCTGATAGACGGTTTTTCGCCCTTTGACGTTGGAGTCCACGTTCTTTAATAGT
GGACTCTTGTTCCAAACTGGAACAACACTCAACTCTATCTCGGGCTATTCTTTTGATTTATAAGGGATTTTGCCGATTTC
GGTCTATTGGTTAAAAAATGAGCTGATTTAACAAAAATTTAACGCGAATTTTAACAAAATATTAACGTTTACAATTTTAT
GGTGCACTCTCAGTACAATCTGCTCTGATGCCGCATAGTTAAGCCAGCCCCGACACCCGCCAACACCCGCTGACGCGCCC
TGACGGGCTTGTCTGCTCCCGGCATCCGCTTACAGACAAGCTGTGACCGTCTCCGGGAGCTGCATGTGTCAGAGGTTTTC
ACCGTCATCACCGAAACGCGCGAGACGAAAGGGCCTCGTGATACGCCTATTTTTATAGGTTAATGTCATGATAATAATGG
TTTCTTAGACGTCAGGTGGCACTTTTCGGGGAAATGTGCGCGGAACCCCTATTTGTTTATTTTTCTAAATACATTCAAAT
ATGTATCCGCTCATGAGACAATAACCCTGATAAATGCTTCAATAATATTGAAAAAGGAAGAGTATGAGTATTCAACATTT
CCGTGTCGCCCTTATTCCCTTTTTTGCGGCATTTTGCCTTCCTGTTTTTGCTCACCCAGAAACGCTGGTGAAAGTAAAAG
ATGCTGAAGATCAGTTGGGTGCACGAGTGGGTTACATCGAACTGGATCTCAACAGCGGTAAGATCCTTGAGAGTTTTCGC
CCCGAAGAACGTTTTCCAATGATGAGCACTTTTAAAGTTCTGCTATGTGGCGCGGTATTATCCCGTATTGACGCCGGGCA
AGAGCAACTCGGTCGCCGCATACACTATTCTCAGAATGACTTGGTTGAGTACTCACCAGTCACAGAAAAGCATCTTACGG
ATGGCATGACAGTAAGAGAATTATGCAGTGCTGCCATAACCATGAGTGATAACACTGCGGCCAACTTACTTCTGACAACG
ATCGGAGGACCGAAGGAGCTAACCGCTTTTTTGCACAACATGGGGGATCATGTAACTCGCCTTGATCGTTGGGAACCGGA
GCTGAATGAAGCCATACCAAACGACGAGCGTGACACCACGATGCCTGTAGCAATGGCAACAACGTTGCGCAAACTATTAA
CTGGCGAACTACTTACTCTAGCTTCCCGGCAACAATTAATAGACTGGATGGAGGCGGATAAAGTTGCAGGACCACTTCTG
CGCTCGGCCCTTCCGGCTGGCTGGTTTATTGCTGATAAATCTGGAGCCGGTGAGCGTGGGTCTCGCGGTATCATTGCAGC
ACTGGGGCCAGATGGTAAGCCCTCCCGTATCGTAGTTATCTACACGACGGGGAGTCAGGCAACTATGGATGAACGAAATA
GACAGATCGCTGAGATAGGTGCCTCACTGATTAAGCATTGGTAACTGTCAGACCAAGTTTACTCATATATACTTTAGATT
GATTTAAAACTTCATTTTTAATTTAAAAGGATCTAGGTGAAGATCCTTTTTGATAATCTCATGACCAAAATCCCTTAACG
TGAGTTTTCGTTCCACTGAGCGTCAGACCCCGTAGAAAAGATCAAAGGATCTTCTTGAGATCCTTTTTTTCTGCGCGTAA
TCTGCTGCTTGCAAACAAAAAAACCACCGCTACCAGCGGTGGTTTGTTTGCCGGATCAAGAGCTACCAACTCTTTTTCCG
AAGGTAACTGGCTTCAGCAGAGCGCAGATACCAAATACTGTTCTTCTAGTGTAGCCGTAGTTAGGCCACCACTTCAAGAA
CTCTGTAGCACCGCCTACATACCTCGCTCTGCTAATCCTGTTACCAGTGGCTGCTGCCAGTGGCGATAAGTCGTGTCTTA
CCGGGTTGGACTCAAGACGATAGTTACCGGATAAGGCGCAGCGGTCGGGCTGAACGGGGGGTTCGTGCACACAGCCCAGC
TTGGAGCGAACGACCTACACCGAACTGAGATACCTACAGCGTGAGCTATGAGAAAGCGCCACGCTTCCCGAAGGGAGAAA
GGCGGACAGGTATCCGGTAAGCGGCAGGGTCGGAACAGGAGAGCGCACGAGGGAGCTTCCAGGGGGAAACGCCTGGTATC
TTTATAGTCCTGTCGGGTTTCGCCACCTCTGACTTGAGCGTCGATTTTTGTGATGCTCGTCAGGGGGGCGGAGCCTATGG
AAAAACGCCAGCAACGCGGCCTTTTTACGGTTCCTGGCCTTTTGCTGGCCTTTTGCTCA

Features :

ColE1 origin : [6993 : 7621 - CW]

AmpR : [6182 : 6841 - CW]

Amp prom : [5914 : 5942 - CW]

AAV2 ITR : [6 : 135 - CW]

TRE3g : [172 : 632 - CW]

5' Arc UTR : [639 : 868 - CW]

CDS : [875 : 3094 - CW]

rPSD95Δ : [875 : 2302 - CW]

mVenus : [2324 : 3031 - CW]

HA tag : [3065 : 3091 - CW]

HA tag : [3032 : 3058 - CW]

3' Arc UTR : [3137 : 4743 - CW]

short polyA : [4750 : 4894 - CW]

AAV2 ITR : [4927 : 5066 - CW]

## 4) SynActive-DsRED-E5 (6178 bp)

```
CATGTCCTGCAGGCAGCTGCGCGCTCGCTCGCTCACTGAGGCCGCCCGGGCGTCGGGCGACCTTTGGTCGCCCGGCCTCA
GTGAGCGAGCGAGCGCGCAGAGAGGGAGTGGCCAACTCCATCACTAGGGGTTCCTGCGGCCGCACGCGTGTGTCTAGACT
GCAGACCATGGGCCCTTGACGTCCGGTCCGTTTACTCCCTATCAGTGATAGAGAACGTATGAAGAGTTTACTCCCTATCA
GTGATAGAGAACGTATGCAGACTTTACTCCCTATCAGTGATAGAGAACGTATAAGGAGTTTACTCCCTATCAGTGATAGA
GAACGTATGACCAGTTTACTCCCTATCAGTGATAGAGAACGTATCTACAGTTTACTCCCTATCAGTGATAGAGAACGTAT
ATCCAGTTTACTCCCTATCAGTGATAGAGAACGTATAAGCTTTAGGCGTGTACGGTGGGCGCCTATAAAAGCAGAGCTCG
TTTAGTGAACCGTCAGATCGCCTGGAGCAATTCCACAACACTTTTGTCTTATACCAACTTTCCGTACCACTTCCTACCCT
CGTAAAAGCCTCCGCGGCCCCGAATTCGAGCTCGGTACCCGGGGATCCTCTAGTCAGCTGACGCGTGCCGCCACTAGTAG
TGCTCTGGCGAGTAGTCCTCCCTCAGCCGCAGTCTCTGGGCCTCTTCAGCTTGAGCGGCGGCGAGCCTGCCACACTCGCT
AAGCTCCTCCGGCACCGCGCACTTGCCACTGCCACTGCCGCTTCGCGCCCGCTGCAGCCGCCGGCTCTGAATCCTTCTGG
CTTCCGCCTCAGAGGAGTTCTTAGCCTGTCCCGAACCGTAACCCCGGCGAGCAGACGGAGCTGGACCATCTAGAGCCACC
ATGGTGCGCTCCTCCAAGAACGTCATCAAGGAGTTCATGCGCTTCAAGGTGCGCATGGAGGGCACCGTGAACGGCCACGA
GTTCGAGATCGAGGGCGAGGGCGAGGGCCGCCCCTACGAGGGCCACAACACCGTGAAGCTGAAGGTGACCAAGGGCGGCC
CCCTGCCCTTCGCCTGGGACATCCTGTCCCCCCAGTTCCAGTACGGCTCCAAGGTGTACGTGAAGCACCCCGCCGACATC
CCCGACTACAAGAAGCTGTCCTTCCCCGAGGGCTTCAAGTGGGAGCGCGTGATGAACTTCGAGGACGGCGGCGTGGCGAC
CGTGACCCAGGACTCCTCCCTGCAGGACGGCTGCTTCATCTACAAGGTGAAGTTCATCGGCGTGAACTTCCCCTCCGACG
GCCCCGTGATGCAGAAGAAGACCATGGGCTGGGAGGCCTCCACCGAGCGCCTGTACCCCCGCGACGGCGTGCTGAAGGGC
GAGATCCACAAGGCCCTGAAGCTGAAGGACGGCGGCCACTACCTGGTGGAGTTCAAGTCCATCTACATGGCCAAGAAGCC
CGTGCAGCTGCCCGGCTACTACTACGTGGACACCAAGCTGGACATCACCTCCCACAACGAGGACTACACCATCGTGGAGC
AGTACGAGCGCACCGAGGGCCGCCACCACCTGTTCCTGGGCGGCGGAGGCGGAGCCGCTGCTTCAATCGAAAGTGACGTG
GCCGCAGCCGAAACCCAGGTGTAATAAACGCGTCAATTCAGGGGCCAGCCCAGGGTCCCCAGCCTGCCTGCCACACCCAG
TCTGTGGCTTTTGTCAACTAGGACTTGATTGAGCTGGGGCTGACACCCAAGGGGATGCCCTGTCCAGCCAGACACCTTCT
CACCCACTGGCCTGACTCACAACTGCCACACAACCATGATTCATGGACATCAAGAAGCCCCTCTCCCATAGGGCTCCCAC
CTGCCACCTACCCCTCACCTGTCTGCCCTAGTCCTGGCCCTGTCTCCAGTGGCCTCACCCTCTACACTCTCAGACCATCA
CAGAACACCTTTGGCTTCCTCATTCTGCATCAGTGTCCAGGGCCCTTTGGGTAGTCAAGAAATCAAGTGTCTGAAAGGCA
ATGAAAAGTAGGCACCAAACCCAAGGGGCATCCCAGGGCAGATGCTAAAGCAGAATCAGAGATGGCCGAAGGAACCTCTA
CTTCCGGGGATGCAGCCCGCTCCTACAGACACAGCAGATCCAGCTGGTGCCCTACCTGCCTCCCAGAGCAACTGGCCAGT
CTTGGGCAGCATAGCTCCCCTCTCAGGGTGAGCTGAAGCAGCAGACCTGACGCGCTGGCGCCTCCTGGCCCCCAGCAGTG
ATTCATACCAGTGAAGAAAAGCAGACTTCGGCTCCATGACTCAGCCATGCCAGGCGGAGGGTCCCAGAGGGGCTGAGTCC
TCAGCCCCAGCTGAGGCAGCAGCTGGAGTCTTCAGAGCCAGGTGAATGACACCAGGTCTCAAGCTGCTGAGAAGTCTTTC
CGGCCATGTCTGGAAGGGGTACCACCCCAGCACCAGCACCGTCCCCTCCTCTCTTGAAGCTGCCTGCACAGAGGTTCCAA
GACACTTTCAAGGCAGAGAAAATAGGATTACAAAGAGGAGGTGCCTGGCAGAGGGCAGCACCCAGCTCAGCCTCAGAGCT
GAAGGTGAAGACAAGCCAGCGTGAAACCCCGGGTCTGCCACGAATGCCCGCTCCGCTGGCCACTCACCAGCTGCCTGCCA
CAAGCCACTGCAGCTTGAGCAGGGTCTGTGCCCTCTCAGCACAGAGCCCAGTTCGCTGCGTGGCCTTTGGCCCCCGCCAG
AACCTTGCAGGAGCCTTAAGGTTCGGGCCCTAGCCCAGCCTGACCTTACCTGCTGTGCCCTGCCTGCTGGTCAAGTCCAG
TCCCAGGAGACCCCATGCCTTGGCTCCTAGGCTGTTCCAGGCACTTCCCTGACCTGCCGGGTGATTGCCCAGCTGGAACC
TCATCCACACCCCAGCACCAACCACCTCGTGTTGGTAACTGCTCGTGTCTGTAGTCTGAGTAGGCCATGTTGAGGTTCCT
CCATCTGCCTGGTCCATTGGTGTTCTGAGACCAGTTCCACTGCTGTTCTGACAGATCCCCCACCCTGTGCCCCTGCCAGC
```

CCCCACAGGTTTATTTTTGCACATAAACCATGACCCATACTAATTTGGCTAGCTCTGGGGACTAGGGAGACCCTGGAGAT
CTCAAGAGTGTGGCTATCCCCTATTTTCACCAAGCCTTCAATATCCAGCCAGGCCATCTGCCCACACCATCTTACCTCAA
AGACAGACATATATATATATATACATATATATGATTTTGTTAATAAAACTATGAAATTTAAACTCGAGGTGAAATTTGTG
ATGCTATTGCTTTATTTGTAACCATCTAGCTTTATTTGTGAAATTTGTGATGCTATTGCTTTATTTGTAACCATTATAAG
CTGCAATAAACAAGTTAACAACAACAATTGCATTCATTTTATGTTTCAGGTTCCGGTCCGTTGGCCGTGCGGACCGAGCG
GCCGCAGGAACCCCTAGTGATGGAGTTGGCCACTCCCTCTCTGCGCGCTCGCTCGCTCACTGAGGCCGGGCGACCAAAGG
TCGCCCGACGCCCGGGCTTTGCCCGGGCGGCCTCAGTGAGCGAGCGAGCGCGCAGCTGCCTGCAGGGGCGCCTGATGCGG
TATTTTCTCCTTACGCATCTGTGCGGTATTTCACACCGCATACGTCAAAGCAACCATAGTACGCGCCCTGTAGCGGCGCA
TTAAGCGCGGCGGGTGTGGTGGTTACGCGCAGCGTGACCGCTACACTTGCCAGCGCCTTAGCGCCCGCTCCTTTCGCTTT
CTTCCCTTCCTTTCTCGCCACGTTCGCCGGCTTTCCCCGTCAAGCTCTAAATCGGGGGCTCCCTTTAGGGTTCCGATTTA
GTGCTTTACGGCACCTCGACCCCAAAAAACTTGATTTGGGTGATGGTTCACGTAGTGGGCCATCGCCCTGATAGACGGTT
TTTCGCCCTTTGACGTTGGAGTCCACGTTCTTTAATAGTGGACTCTTGTTCCAAACTGGAACAACACTCAACTCTATCTC
GGGCTATTCTTTTGATTTATAAGGGATTTTGCCGATTTCGGTCTATTGGTTAAAAAATGAGCTGATTTAACAAAAATTTA
ACGCGAATTTTAACAAAATATTAACGTTTACAATTTTATGGTGCACTCTCAGTACAATCTGCTCTGATGCCGCATAGTTA
AGCCAGCCCCGACACCCGCCAACACCCGCTGACGCGCCCTGACGGGCTTGTCTGCTCCCGGCATCCGCTTACAGACAAGC
TGTGACCGTCTCCGGGAGCTGCATGTGTCAGAGGTTTTCACCGTCATCACCGAAACGCGCGAGACGAAAGGGCCTCGTGA
TACGCCTATTTTTATAGGTTAATGTCATGATAATAATGGTTTCTTAGACGTCAGGTGGCACTTTTCGGGGAAATGTGCGC
GGAACCCCTATTTGTTTATTTTTCTAAATACATTCAAATATGTATCCGCTCATGAGACAATAACCCTGATAAATGCTTCA
ATAATATTGAAAAAGGAAGAGTATGAGTATTCAACATTTCCGTGTCGCCCTTATTCCCTTTTTTGCGGCATTTTGCCTTC
CTGTTTTTGCTCACCCAGAAACGCTGGTGAAAGTAAAAGATGCTGAAGATCAGTTGGGTGCACGAGTGGGTTACATCGAA
CTGGATCTCAACAGCGGTAAGATCCTTGAGAGTTTTCGCCCCGAAGAACGTTTTCCAATGATGAGCACTTTTAAAGTTCT
GCTATGTGGCGCGGTATTATCCCGTATTGACGCCGGGCAAGAGCAACTCGGTCGCCGCATACACTATTCTCAGAATGACT
TGGTTGAGTACTCACCAGTCACAGAAAAGCATCTTACGGATGGCATGACAGTAAGAGAATTATGCAGTGCTGCCATAACC
ATGAGTGATAACACTGCGGCCAACTTACTTCTGACAACGATCGGAGGACCGAAGGAGCTAACCGCTTTTTTGCACAACAT
GGGGGATCATGTAACTCGCCTTGATCGTTGGGAACCGGAGCTGAATGAAGCCATACCAAACGACGAGCGTGACACCACGA
TGCCTGTAGCAATGGCAACAACGTTGCGCAAACTATTAACTGGCGAACTACTTACTCTAGCTTCCCGGCAACAATTAATA
GACTGGATGGAGGCGGATAAAGTTGCAGGACCACTTCTGCGCTCGGCCCTTCCGGCTGGCTGGTTTATTGCTGATAAATC
TGGAGCCGGTGAGCGTGGGTCTCGCGGTATCATTGCAGCACTGGGGCCAGATGGTAAGCCCTCCCGTATCGTAGTTATCT
ACACGACGGGGAGTCAGGCAACTATGGATGAACGAAATAGACAGATCGCTGAGATAGGTGCCTCACTGATTAAGCATTGG
TAACTGTCAGACCAAGTTTACTCATATATACTTTAGATTGATTTAAAACTTCATTTTTAATTTAAAAGGATCTAGGTGAA
GATCCTTTTTGATAATCTCATGACCAAAATCCCTTAACGTGAGTTTTCGTTCCACTGAGCGTCAGACCCCGTAGAAAAGA
TCAAAGGATCTTCTTGAGATCCTTTTTTTTCTGCGCGTAATCTGCTGCTTGCAAACAAAAAAACCACCGCTACCAGCGGTG
GTTTGTTTGCCGGATCAAGAGCTACCAACTCTTTTTCCGAAGGTAACTGGCTTCAGCAGAGCGCAGATACCAAATACTGT
TCTTCTAGTGTAGCCGTAGTTAGGCCACCACTTCAAGAACTCTGTAGCACCGCCTACATACCTCGCTCTGCTAATCCTGT
TACCAGTGGCTGCTGCCAGTGGCGATAAGTCGTGTCTTACCGGGTTGGACTCAAGACGATAGTTACCGGATAAGGCGCAG
CGGTCGGGCTGAACGGGGGGTTCGTGCACACAGCCCAGCTTGGAGCGAACGACCTACACCGAACTGAGATACCTACAGCG
TGAGCTATGAGAAAGCGCCACGCTTCCCGAAGGGAGAAAGGCGGACAGGTATCCGGTAAGCGGCAGGGTCGGAACAGGAG
AGCGCACGAGGGAGCTTCCAGGGGGAAACGCCTGGTATCTTTATAGTCCTGTCGGGTTTCGCCACCTCTGACTTGAGCGT
CGATTTTTGTGATGCTCGTCAGGGGGGCGGAGCCTATGGAAAAACGCCAGCAACGCGGCCTTTTTACGGTTCCTGGCCTT
TTGCTGGCCTTTTGCTCA

Features :

| | | |
|---|---|---|
| ColE1 origin | : [5512 : 6140 - CW] | |
| AmpR | : [4701 : 5360 - CW] | |
| Amp prom | : [4433 : 4461 - CW] | |
| AAV2 ITR | : [6 : 135 - CW] | |
| TRE3g | : [172 : 632 - CW] | |
| CDS | : [881 : 1627 - CW] | |
| 5' Arc UTR | : [639 : 868 - CW] | |
| DsRED-E5 | : [881 : 1558 - CW] | |
| SYNtag | : [1574 : 1627 - CW] | |
| 3' Arc UTR | : [1656 : 3262 - CW] | |

shortPA : [3269 : 3413 - CW]

AAV2 ITR : [3446 : 3585 - CW]

## 5) SynActive-PSD95-FLAG (8042 bp)

CATGTCCTGCAGGCAGCTGCGCGCTCGCTCGCTCACTGAGGCCGCCCGGGCGTCGGGCGACCTTTGGTCGCCCGGCCTCA
GTGAGCGAGCGAGCGCGCAGAGAGGGAGTGGCCAACTCCATCACTAGGGGTTCCTGCGGCCGCACGCGTGTGTCTAGACT
GCAGACCATGGGGATCCAGCGCACAGAGCCTTCCTGCGTGGGGAAGCTCCTTGCTGCGTCATGGCTCAGCTATTCTCAGC
CTCTCTCCTTTTATGGTGCCGGAAGCAGGCAGGCTGCTGCTAGATCCAGCGCACAGAGCCTTCCTGCGTGGGGAAGCTCC
TTGCTGCGTCATGGCTCAGCTATTCTCAGCCTCTCTCCTTTTATGGTGCCGGAAGCAGGCAGGCTGCTGCTAGATCCAGC
GCACAGAGCCTTCCTGCGTGGGGAAGCTCCTTGCTGCGTCATGGCTCAGCTATTCTCAGCCTCTCTCCTTTTATGGTGCC
GGAAGCAGGCAGGCTGCTGCTAGATCCAGCGCACAGAGCCTTCCTGCGTGGGGAAGCTCCTTGCTGCGTCATGGCTCAGC
TATTCTCAGCCTCTCTCCTTTTATGGTGCCGGAAGCAGGCAGGCTGCTGCTAGATCCAGCGCACAGAGCCTTCCTGCGTG
GGGAAGCTCCTTGCTGCGTCATGGCTCAGCTATTCTCAGCCTCTCTCCTTTTATGGTGCCGGAAGCAGGCAGGCTGCTGC
TCGCGCAGCAGAGCACATTAGTCACTCGGGGCTGTGAAGGGGCGGGTCCTTGAGGGCACCCACGGGAGGGGAGCGAGTAG
GCGCGGAAGGCGGGGCCTGCGGCAGGAGAGGGCGCGGGCGGGCTCTGGCGCGGAGCCTGGGCGCCGCCAATGGGAGCCAG
GGCTCCACGAGCTGCCGCCCACGGGCCCCGCGCAGCATAAATAGCCGCTGGTGGCGGTTTCGGTGCAGAGCTCAAGCGAG
TTCTCCCGCAGCCGCAGTCTCTGGGCCTCTCTAGCTTCAGCGGCGACGAGCCTGCCACACTCGCTAAGCTCCTCCGGCAC
CGCACACCTGCCACTGCCGCTGCAGCCGCCGGCTCTGCTCCCTTCCGGCTTCTGCCTCAGAGGAGTTCTTAGCCTGTTCG
GAGCCGCAGCACCGACGACCAGGCTAGAATGGACTGTCTCTGTATAGTGACAACCAAGAAATACCGCTACCAAGATGAAG
ACACGCCCCCTCTGGAACACAGCCCGGCCCACCTCCCCAACCAGGCCAATTCTCCCCCTGTGATTGTCAACACGGACACC
CTAGAAGCCCCAGGATATGTGAACGGAACAGAGGGGGAGATGGAGTATGAGGAGATCACATTGGAAAGGGGTAACTCAGG
TCTGGGCTTCAGCATCGCAGGTGGCACCGACAACCCACACATCGGTGACGACCCATCCATCTTTATCACCAAGATCATTC
CTGGTGGGGCTGCAGCCCAGGATGGCCGCCTCAGGGTCAACGACAGCATCCTGTTTGTCAATGAAGTGGATGTCCGGGAG
GTGACCCATTCAGCTGCAGTGGAGGCCCTCAAAGAGGCGGGTTCCATCGTTCGCCTCTACGTCATGCGCCGGAAACCCCC
AGCTGAGAAGATCATAGAGATCAAGCTTATCAAAGGGCCTAAAGGACTTGGCTTCAGCATCGCAGGGGGCGTTGGGAACC
AGCACATCCCTGGAGATAATAGCATCTACGTAACCAAGATCATCGAAGGAGGCGCTGCCCACAAGGATGGCAGGTTGCAG
ATCGGAGACAAGATCCTGGCGGTCAACAGTGTGGGGCTAGAGGATGTCATGCATGAGGACGCCGTGGCAGCCCTGAAGAA
CACATATGACGTTGTGTACCTAAAGGTGGCCAAGCCCAGCAATGCCTACCTGAGTGACAGCTATGCTCCCCCAGACATCA
CAACCTCATATTCTCAGCACCTGGACAATGAGATCAGTCATAGCAGCTACTTGGGCACCGACTACCCCACAGCCATGACC
CCCACTTCCCCTCGGCGCTACTCCCCCGTGGCCAAGGACCTGCTAGGGGAGGAAGATATTCCCCGGGAACCAAGGCGGAT
CGTGATCCATCGGGGCTCCACCGGCCTGGGCTTCAACATTGTGGGCGGCGAGGACGGTGAAGGCATCTTCATCTCCTTCA
TCCTTGCTGGGGGTCCAGCTGACCTCAGTGGGGAGCTACGGAAGGGGGACCAGATCCTGTCGGTCAATGGTGTTGACCTC
CGCAATGCCAGTCATGAACAGGCTGCCATTGCCCTGAAGAACGCGGGTCAGACGGTCACGATCATCGCTCAGTATAAACC
AGAAGAGTATAGCCGATTCGAGGCCAAGATCCATGATCTTCGGGAACAGCTTATGAATAGTAGCCTGGGCTCAGGGACTG
CATCTCTGCGAAGCAACCCCAAGCGGGGCTTCTATATCAGGGCCCTGTTTGACTACGACAAGACCAAGGACTGCGGTTTC
TTGAGCCAGGCCCTGAGCTTCCACTTTGGGGATGTGCTTCATGTAATTGACGCCAGCGACGAAGAGTGGTGGCAAGCGCG
GCGGGTCCACTCTGACAGTGAGACCGATGACATTGGCTTCATTCCCAGCAAACGGCGGGTCGAGCGACGAGAGTGGTCAA
GGTTAAAGGCCAAGGACTGGGGCTCCAGCTCTGGATCACAGGGTCGAGAAGACTCGGTTCTGAGCTATGAGACGGTGACG
CAGATGGAAGTGCACTACGCTCGCCCCATCATCATCCTTGGGCCTACCAAAGACCGTGCCAACGATGATCTTCTCTCCGA
GTTCCCCGACAAGTTTGGATCCTGTGTCCCTCATACGACACGTCCTAAGCGGGAATATGAGATAGACGGCCGCGATTACC
ACTTTGTCTCCTCCCGGGAGAAAATGGAGAAGGACATTCAGGCGCACAAGTTCATTGAGGCTGGCCAGTACAACAGCCAC
CTCTACGGGACCAGCGTCCAGTCTGTGCGAGAGGTAGCAGAGCAGGGGAAGCACTGCATCCTTGATGTCTCAGCCAATGC
CGTGCGGCGGCTGCAGGCGGCCCACCTGCACCCTATCGCCATCTTCATCCGTCCCCGCTCCCTGGAGAATGTGCTAGAGA
TCAATAAGCGGATCACAGAGGAGCAAGCCCGGAAAGCCTTCGACAGGGCCACGAAGCTGGAGCAGGAGTTCACGGAGTGC
TTCTCAGCCATCGTAGAGGGCGACAGCTTTGAAGAGATCTATCACAAAGTGAAACGTGTCATCGAAGACCTCTCAGGCCC
CTACATCTGGGTCCCAGCCCGAGAGAGACTCGGTACCAGCCGCAAAGATCATCTGATTCATAACGTGCATAAAGAAGAAC
ATGCGCATGCGCATAACAAAATTGAAAACCTGTATTTTCAGGGCGAACTGCCGACCGCGGCGGATTATAAAGATCATGAT
GGCGATTATAAAGATCATGATATTGATTATAAAGATGATGATGATAAATAGACGCGTCAATTCAGGGGCCAGCCCAGGGT
CCCCAGCCTGCCTGCCACACCCAGTCTGTGGCTTTTGTCAACTAGGACTTGATTGAGCTGGGGCTGACACCCAAGGGGAT
GCCCTGTCCAGCCAGACACCTTCTCACCCACTGGCCTGACTCACAACTGCCACACAACCATGATTCATGGACATCAAGAA
GCCCCTCTCCCATAGGGCTCCCACCTGCCACCTACCCCTCACCTGTCTGCCCTAGTCCTGGCCCTGTCTCCAGTGGCCTC
ACCCTCTACACTCTCAGACCATCACAGAACACCTTTGGCTTCCTCATTCTGCATCAGTGTCCAGGGCCCTTTGGGTAGTC
AAGAAATCAAGTGTCTGAAAGGCAATGAAAAGTAGGCACCAAACCCAAGGGGCATCCCAGGGCAGATGCTAAAGCAGAAT
CAGAGATGGCCGAAGGAACCTCTACTTCCGGGGATGCAGCCCGCTCCTACAGACACAGCAGATCCAGCTGGTGCCCTACC
TGCCTCCCAGAGCAACTGGCCAGTCTTGGGCAGCATAGCTCCCCTCTCAGGGTGAGCTGAAGCAGCAGACCTGACGCGCT
GGCGCCTCCTGGCCCCCAGCAGTGATTCATACCAGTGAAGAAAAGCAGACTTCGGCTCCATGACTCAGCCATGCCAGGCG
GAGGGTCCCAGAGGGGCTGAGTCCTCAGCCCCAGCTGAGGCAGCAGCTGGAGTCTTCAGAGCCAGGTGAATGACACCAGG
TCTCAAGCTGCTGAGAAGTCTTTCCGGCCATGTCTGGAAGGGGTACCACCCCAGCACCAGCACCGTCCCCTCCTCTCTTG
AAGCTGCCTGCACAGAGGTTCCAAGACACTTTCAAGGCAGAGAAAATAGGATTACAAAGAGGAGGTGCCTGGCAGAGGGC

AGCACCCAGCTCAGCCTCAGAGCTGAAGGTGAAGACAAGCCAGCGTGAAACCCCGGGTCTGCCACGAATGCCCGCTCCGC
TGGCCACTCACCAGCTGCCTGCCACAAGCCACTGCAGCTTGAGCAGGGTCTGTGCCCTCTCAGCACAGAGCCCAGTTCGC
TGCGTGGCCTTTGGCCCCCGCCAGAACCTTGCAGGAGCCTTAAGGTTCGGGCCCTAGCCCAGCCTGACCTTACCTGCTGT
GCCCTGCCTGCTGGTCAAGTCCAGTCCCAGGAGACCCCATGCCTTGGCTCCTAGGCTGTTCCAGGCACTTCCCTGACCTG
CCGGGTGATTGCCCAGCTGGAACCTCATCCACACCCCAGCACCAACCACCTCGTGTTGGTAACTGCTCGTGTCTGTAGTC
TGAGTAGGCCATGTTGAGGTTCCTCCATCTGCCTGGTCCATTGGTGTTCTGAGACCAGTTCCACTGCTGTTCTGACAGAT
CCCCCACCCTGTGCCCCTGCCAGCCCCCACAGGTTTATTTTTGCACATAAACCATGACCCATACTAATTTGGCTAGCTCT
GGGGACTAGGGAGACCCTGGAGATCTCAAGAGTGTGGCTATCCCCTATTTTCACCAAGCCTTCAATATCCAGCCAGGCCA
TCTGCCCACACCATCTTACCTCAAAGACAGACATATATATATATATACATATATATGATTTTGTTAATAAAACTATGAAA
TTTAAACTCGAGGTGAAATTTGTGATGCTATTGCTTTATTTGTAACCATCTAGCTTTATTTGTGAAATTTGTGATGCTAT
TGCTTTATTTGTAACCATTATAAGCTGCAATAAACAAGTTAACAACAACAATTGCATTCATTTTATGTTTCAGGTTCCGG
TCCGTTGGCCGTGCGGACCGAGCGGCCGCAGGAACCCCTAGTGATGGAGTTGGCCACTCCCTCTCTGCGCGCTCGCTCGC
TCACTGAGGCCGGGCGACCAAAGGTCGCCCGACGCCCGGGCTTTGCCCGGGCGGCCTCAGTGAGCGAGCGAGCGCGCAGC
TGCCTGCAGGGGCGCCTGATGCGGTATTTTCTCCTTACGCATCTGTGCGGTATTTCACACCGCATACGTCAAAGCAACCA
TAGTACGCGCCCTGTAGCGGCGCATTAAGCGCGGCGGGTGTGGTGGTTACGCGCAGCGTGACCGCTACACTTGCCAGCGC
CTTAGCGCCCGCTCCTTTCGCTTTCTTCCCTTCCTTTCTCGCCACGTTCGCCGGCTTTCCCCGTCAAGCTCTAAATCGGG
GGCTCCCTTTAGGGTTCCGATTTAGTGCTTTACGGCACCTCGACCCCAAAAAACTTGATTTGGGTGATGGTTCACGTAGT
GGGCCATCGCCCTGATAGACGGTTTTTCGCCCTTTGACGTTGGAGTCCACGTTCTTTAATAGTGGACTCTTGTTCCAAAC
TGGAACAACACTCAACTCTATCTCGGGCTATTCTTTTGATTTATAAGGGATTTTGCCGATTTCGGTCTATTGGTTAAAAA
ATGAGCTGATTTAACAAAAATTTAACGCGAATTTTAACAAAATATTAACGTTTACAATTTTATGGTGCACTCTCAGTACA
ATCTGCTCTGATGCCGCATAGTTAAGCCAGCCCCGACACCCGCCAACACCCGCTGACGCGCCCTGACGGGCTTGTCTGCT
CCCGGCATCCGCTTACAGACAAGCTGTGACCGTCTCCGGGAGCTGCATGTGTCAGAGGTTTTCACCGTCATCACCGAAAC
GCGCGAGACGAAAGGGCCTCGTGATACGCCTATTTTTATAGGTTAATGTCATGATAATAATGGTTTCTTAGACGTCAGGT
GGCACTTTTCGGGGAAATGTGCGCGGAACCCCTATTTGTTTATTTTTCTAAATACATTCAAATATGTATCCGCTCATGAG
ACAATAACCCTGATAAATGCTTCAATAATATTGAAAAAGGAAGAGTATGAGTATTCAACATTTCCGTGTCGCCCTTATTC
CCTTTTTTGCGGCATTTTGCCTTCCTGTTTTTGCTCACCCAGAAACGCTGGTGAAAGTAAAAGATGCTGAAGATCAGTTG
GGTGCACGAGTGGGTTACATCGAACTGGATCTCAACAGCGGTAAGATCCTTGAGAGTTTTCGCCCCGAAGAACGTTTTCC
AATGATGAGCACTTTTAAAGTTCTGCTATGTGGCGCGGTATTATCCCGTATTGACGCCGGGCAAGAGCAACTCGGTCGCC
GCATACACTATTCTCAGAATGACTTGGTTGAGTACTCACCAGTCACAGAAAAGCATCTTACGGATGGCATGACAGTAAGA
GAATTATGCAGTGCTGCCATAACCATGAGTGATAACACTGCGGCCAACTTACTTCTGACAACGATCGGAGGACCGAAGGA
GCTAACCGCTTTTTTGCACAACATGGGGGATCATGTAACTCGCCTTGATCGTTGGGAACCGGAGCTGAATGAAGCCATAC
CAAACGACGAGCGTGACACCACGATGCCTGTAGCAATGGCAACAACGTTGCGCAAACTATTAACTGGCGAACTACTTACT
CTAGCTTCCCGGCAACAATTAATAGACTGGATGGAGGCGGATAAAGTTGCAGGACCACTTCTGCGCTCGGCCCTTCCGGC
TGGCTGGTTTATTGCTGATAAATCTGGAGCCGGTGAGCGTGGGTCTCGCGGTATCATTGCAGCACTGGGGCCAGATGGTA
AGCCCTCCCGTATCGTAGTTATCTACACGACGGGGAGTCAGGCAACTATGGATGAACGAAATAGACAGATCGCTGAGATA
GGTGCCTCACTGATTAAGCATTGGTAACTGTCAGACCAAGTTTACTCATATATACTTTAGATTGATTTAAAACTTCATTT
TTAATTTAAAAGGATCTAGGTGAAGATCCTTTTTGATAATCTCATGACCAAAATCCCTTAACGTGAGTTTTCGTTCCACT
GAGCGTCAGACCCCGTAGAAAAGATCAAAGGATCTTCTTGAGATCCTTTTTTTCTGCGCGTAATCTGCTGCTTGCAAACA
AAAAAACCACCGCTACCAGCGGTGGTTTGTTTGCCGGATCAAGAGCTACCAACTCTTTTTCCGAAGGTAACTGGCTTCAG
CAGAGCGCAGATACCAAATACTGTTCTTCTAGTGTAGCCGTAGTTAGGCCACCACTTCAAGAACTCTGTAGCACCGCCTA
CATACCTCGCTCTGCTAATCCTGTTACCAGTGGCTGCTGCCAGTGGCGATAAGTCGTGTCTTACCGGGTTGGACTCAAGA
CGATAGTTACCGGATAAGGCGCAGCGGTCGGGCTGAACGGGGGGTTCGTGCACACAGCCCAGCTTGGAGCGAACGACCTA
CACCGAACTGAGATACCTACAGCGTGAGCTATGAGAAAGCGCCACGCTTCCCGAAGGGAGAAAGGCGGACAGGTATCCGG
TAAGCGGCAGGGTCGGAACAGGAGAGCGCACGAGGGAGCTTCCAGGGGGAAACGCCTGGTATCTTTATAGTCCTGTCGGG
TTTCGCCACCTCTGACTTGAGCGTCGATTTTTGTGATGCTCGTCAGGGGGGCGGAGCCTATGGAAAAACGCCAGCAACGC
GGCCTTTTTACGGTTCCTGGCCTTTTGCTGGCCTTTTGCTCA

Features :

| | | |
|---|---|---|
| ColE1 origin | : | [7376 : 8004 - CW] |
| AmpR | : | [6565 : 7224 - CW] |
| Amp prom | : | [6297 : 6325 - CW] |
| AAV2 ITR | : | [6 : 135 - CW] |
| ESARE | : | [178 : 721 - CW] |
| miniArc promoter | : | [722 : 1142 - CW] |
| CDS | : | [1149 : 3491 - CW] |

mPSD95 : [1149 : 3311 - CW]

TAP : [3318 : 3488 - CW]

TEV site : [3384 : 3404 - CW]

3' Arc UTR : [3520 : 5126 - CW]

short polyA : [5133 : 5277 - CW]

AAV2 ITR : [5310 : 5449 - CW]

## 6) Const-PSD95-FLAG (6897 bp)

CATGTCCTGCAGGCAGCTGCGCGCTCGCTCGCTCACTGAGGCCGCCCGGGCGTCGGGCGACCTTTGGTCGCCCGGCCTCA
GTGAGCGAGCGAGCGCGCAGAGAGGGAGTGGCCAACTCCATCACTAGGGGTTCCTGCGGCCGCACGCGTGTGTCTAGACT
GCAGAGGGCCCTGCGTATGAGTGCAAGTGGGTTTTAGGACCAGGATGAGGCGGGGTGGGGGTGCCTACCTGACGACCGAC
CCCGACCCACTGGACAAGCACCCAACCCCCATTCCCCAAATTGCGCATCCCCTATCAGAGAGGGGGAGGGGAAACAGGAT
GCGGCGAGGCGCGTGCGCACTGCCAGCTTCAGCACCGCGGACAGTGCCTTCGCCCCCGCCTGGCGGCGCGCGCCACCGCC
GCCTCAGCACTGAAGGCGCGCTGACGTCACTCGCCGGTCCCCCGCAAACTCCCCTTCCCGGCCACCTTGGTCGCGTCCGC
GCCGCCGCCGGCCCAGCCGGACCGCACCACGCGAGGCGCGAGATAGGGGGGCACGGGCGCGACCATCTGCGCTGCGGCGC
CGGCGACTCAGCGCTGCCTCAGTCTGCGGTGGGCAGCGGAGGAGTCGTGTCGTGCCTGAGAGCGCAGTCGAGAAGGTACC
GGATCCGCCACCATGGCCAACATGGACTGTCTCTGTATAGTGACAACCAAGAAATACCGCTACCAAGATGAAGACACGCC
CCCTCTGGAACACAGCCCGGCCCACCTCCCCAACCAGGCCAATTCTCCCCCTGTGATTGTCAACACGGACACCCTAGAAG
CCCCAGGATATGTGAACGGAACAGAGGGGGAGATGGAGTATGAGGAGATCACATTGGAAAGGGGTAACTCAGGTCTGGGC
TTCAGCATCGCAGGTGGCACCGACAACCCACACATCGGTGACGACCCATCCATCTTTATCACCAAGATCATTCCTGGTGG
GGCTGCAGCCCAGGATGGCCGCCTCAGGGTCAACGACAGCATCCTGTTTGTCAATGAAGTGGATGTCCGGGAGGTGACCC
ATTCAGCTGCAGTGGAGGCCCTCAAAGAGGCGGGTTCCATCGTTCGCCTCTACGTCATGCGCCGGAAACCCCCAGCTGAG
AAGATCATAGAGATCAAGCTTATCAAAGGGCCTAAAGGACTTGGCTTCAGCATCGCAGGGGGCGTTGGGAACCAGCACAT
CCCTGGAGATAATAGCATCTACGTAACCAAGATCATCGAAGGAGGCGCTGCCCACAAGGATGGCAGGTTGCAGATCGGAG
ACAAGATCCTGGCGGTCAACAGTGTGGGGCTAGAGGATGTCATGCATGAGGACGCCGTGGCAGCCCTGAAGAACACATAT
GACGTTGTGTACCTAAAGGTGGCCAAGCCCAGCAATGCCTACCTGAGTGACAGCTATGCTCCCCCAGACATCACAACCTC
ATATTCTCAGCACCTGGACAATGAGATCAGTCATAGCAGCTACTTGGGCACCGACTACCCCACAGCCATGACCCCCACTT
CCCCTCGGCGCTACTCCCCCGTGGCCAAGGACCTGCTAGGGGAGGAAGATATTCCCCGGGAACCAAGGCGGATCGTGATC
CATCGGGGCTCCACCGGCCTGGGCTTCAACATTGTGGGCGGCGAGGACGGTGAAGGCATCTTCATCTCCTTCATCCTTGC
TGGGGGTCCAGCTGACCTCAGTGGGGAGCTACGGAAGGGGGACCAGATCCTGTCGGTCAATGGTGTTGACCTCCGCAATG
CCAGTCATGAACAGGCTGCCATTGCCCTGAAGAACGCGGGTCAGACGGTCACGATCATCGCTCAGTATAAACCAGAAGAG
TATAGCCGATTCGAGGCCAAGATCCATGATCTTCGGGAACAGCTTATGAATAGTAGCCTGGGCTCAGGGACTGCATCTCT
GCGAAGCAACCCCAAGCGGGGCTTCTATATCAGGGCCCTGTTTGACTACGACAAGACCAAGGACTGCGGTTTCTTGAGCC
AGGCCCTGAGCTTCCACTTTGGGGATGTGCTTCATGTAATTGACGCCAGCGACGAAGAGTGGTGGCAAGCGCGGCGGGTC
CACTCTGACAGTGAGACCGATGACATTGGCTTCATTCCCAGCAAACGGCGGGTCGAGCGACGAGAGTGGTCAAGGTTAAA
GGCCAAGGACTGGGGCTCCAGCTCTGGATCACAGGGTCGAGAAGACTCGGTTCTGAGCTATGAGACGGTGACGCAGATGG
AAGTGCACTACGCTCGCCCCATCATCATCCTTGGGCCTACCAAAGACCGTGCCAACGATGATCTTCTCTCCGAGTTCCCC
GACAAGTTTGGATCCTGTGTCCCTCATACGACACGTCCTAAGCGGGAATATGAGATAGACGGCCGCGATTACCACTTTGT
CTCCTCCCGGGAGAAAATGGAGAAGGACATTCAGGCGCACAAGTTCATTGAGGCTGGCCAGTACAACAGCCACCTCTACG
GGACCAGCGTCCAGTCTGTGCGAGAGGTAGCAGAGCAGGGGAAGCACTGCATCCTTGATGTCTCAGCCAATGCCGTGCGG
CGGCTGCAGGCGGCCCACCTGCACCCTATCGCCATCTTCATCCGTCCCCGCTCCCTGGAGAATGTGCTAGAGATCAATAA
GCGGATCACAGAGGAGCAAGCCCGGAAAGCCTTCGACAGGGCCACGAAGCTGGAGCAGGAGTTCACGGAGTGCTTCTCAG
CCATCGTAGAGGGCGACAGCTTTGAAGAGATCTATCACAAAGTGAAACGTGTCATCGAAGACCTCTCAGGCCCCTACATC
TGGGTCCCAGCCCGAGAGAGACTCGGTACCAGCCGCAAAGATCATCTGATTCATAACGTGCATAAAGAAGAACATGCGCA
TGCGCATAACAAAATTGAAAACCTGTATTTTCAGGGCGAACTGCCGACCGCGGCGGATTATAAAGATCATGATGGCGATT
ATAAAGATCATGATATTGATTATAAAGATGATGATGATAAATAGGAATTCGATATCAAGCTTATCGATAATCAACCTCTG
GATTACAAAATTTGTGAAAGATTGACTGGTATTCTTAACTATGTTGCTCCTTTTACGCTATGTGGATACGCTGCTTTAAT
GCCTTTGTATCATGCTATTGCTTCCCGTATGGCTTTCATTTTCTCCTCCTTGTATAAATCCTGGTTGCTGTCTCTTTATG
AGGAGTTGTGGCCCGTTGTCAGGCAACGTGGCGTGGTGTGCACTGTGTTTGCTGACGCAACCCCCACTGGTTGGGGCATT
GCCACCACCTGTCAGCTCCTTTCCGGGACTTTCGCTTTCCCCCTCCCTATTGCCACGGCGGAACTCATCGCCGCCTGCCT
TGCCCGCTGCTGGACAGGGGCTCGGCTGTTGGGCACTGACAATTCCGTGGTGTTGTCGGGGAAATCATCGTCCTTTCCTT
GGCTGCTCGCCTATGTTGCCACCTGGATTCTGCGCGGGACGTCCTTCTGCTACGTCCCTTCGGCCCTCAATCCAGCGGAC
CTTCCTTCCCGCGGCCTGCTGCCGGCTCTGCGGCCTCTTCCGCGTCTTCGCCTTCGCCCTCAGACGAGTCGGATCTCCCT
TTGGGCCGCCTCCCCGCATCGATACCGAGCGCTGCTCGAGAGATCTACGGGTGGCATCCCTGTGACCCCTCCCCAGTGCC
TCTCCTGGCCCTGGAAGTTGCCACTCCAGTGCCCACCAGCCTTGTCCTAATAAAATTAAGTTGCATCATTTTGTCTGACT

AGGTGTCCTTCTATAATATTATGGGGTGGAGGGGGGTGGTATGGAGCAAGGGGCAAGTTGGGAAGACAACCTGTAGGGCC
TGCGGGGTCTATTGGGAACCAAGCTGGAGTGCAGTGGCACAATCTTGGCTCACTGCAATCTCCGCCTCCTGGGTTCAAGC
GATTCTCCTGCCTCAGCCTCCCGAGTTGTTGGGATTCCAGGCATGCATGACCAGGCTCAGCTAATTTTTGTTTTTTTGGT
AGAGACGGGGTTTCACCATATTGGCCAGGCTGGTCTCCAACTCCTAATCTCAGGTGATCTACCCACCTTGGCCTCCCAAA
TTGCTGGGATTACAGGCGTGAACCACTGCTCCCTTCCCTGTCCTTCTGATTTTGTAGGTAACCACGTGCGGACCGAGCGG
CCGCAGGAACCCCTAGTGATGGAGTTGGCCACTCCCTCTCTGCGCGCTCGCTCGCTCACTGAGGCCGGGCGACCAAAGGT
CGCCCGACGCCCGGGCTTTGCCCGGGCGGCCTCAGTGAGCGAGCGAGCGCGCAGCTGCCTGCAGGGGCGCCTGATGCGGT
ATTTTCTCCTTACGCATCTGTGCGGTATTTCACACCGCATACGTCAAAGCAACCATAGTACGCGCCCTGTAGCGGCGCAT
TAAGCGCGGCGGGTGTGGTGGTTACGCGCAGCGTGACCGCTACACTTGCCAGCGCCTTAGCGCCCGCTCCTTTCGCTTTC
TTCCCTTCCTTTCTCGCCACGTTCGCCGGCTTTCCCCGTCAAGCTCTAAATCGGGGGCTCCCTTTAGGGTTCCGATTTAG
TGCTTTACGGCACCTCGACCCCAAAAAACTTGATTTGGGTGATGGTTCACGTAGTGGGCCATCGCCCTGATAGACGGTTT
TTCGCCCTTTGACGTTGGAGTCCACGTTCTTTAATAGTGGACTCTTGTTCCAAACTGGAACAACACTCAACTCTATCTCG
GGCTATTCTTTTGATTTATAAGGGATTTTGCCGATTTCGGTCTATTGGTTAAAAAATGAGCTGATTTAACAAAAATTTAA
CGCGAATTTTAACAAAATATTAACGTTTACAATTTTATGGTGCACTCTCAGTACAATCTGCTCTGATGCCGCATAGTTAA
GCCAGCCCCGACACCCGCCAACACCCGCTGACGCGCCCTGACGGGCTTGTCTGCTCCCGGCATCCGCTTACAGACAAGCT
GTGACCGTCTccgggagctgcatgtgtcagaggttttcaccgtcatcaccgaaacgcgcgagACGAAAGGGCCTCGTGAT
ACGCCTATTTTTATAGGTTAATGTCATGATAATAATGGTTTCTTAGACGTCAGGTGGCACTTTTCGGGGAAATGTGCGCG
GAACCCCTATTTGTTTATTTTTCTAAATACATTCAAATATGTATCCGCTCATGAGACAATAACCCTGATAAATGCTTCAA
TAATATTGAAAAAGGAAGAGTATGAGTATTCAACATTTCCGTGTCGCCCTTATTCCCTTTTTTGCGGCATTTTGCCTTCC
TGTTTTTGCTCACCCAGAAACGCTGGTGAAAGTAAAAGATGCTGAAGATCAGTTGGGTGCACGAGTGGGTTACATCGAAC
TGGATCTCAACAGCGGTAAGATCCTTGAGAGTTTTCGCCCCGAAGAACGTTTTCCAATGATGAGCACTTTTAAAGTTCTG
CTATGTGGCGCGGTATTATCCCGTATTGACGCCGGGCAAGAGCAACTCGGTCGCCGCATACACTATTCTCAGAATGACTT
GGTTGAGTACTCACCAGTCACAGAAAAGCATCTTACGGATGGCATGACAGTAAGAGAATTATGCAGTGCTGCCATAACCA
TGAGTGATAACACTGCGGCCAACTTACTTCTGACAACGATCGGAGGACCGAAGGAGCTAACCGCTTTTTTGCACAACATG
GGGGATCATGTAACTCGCCTTGATCGTTGGGAACCGGAGCTGAATGAAGCCATACCAAACGACGAGCGTGACACCACGAT
GCCTGTAGCAATGGCAACAACGTTGCGCAAACTATTAACTGGCGAACTACTTACTCTAGCTTCCCGGCAACAATTAATAG
ACTGGATGGAGGCGGATAAAGTTGCAGGACCACTTCTGCGCTCGGCCCTTCCGGCTGGCTGGTTTATTGCTGATAAATCT
GGAGCCGGTGAGCGTGGGTCTCGCGGTATCATTGCAGCACTGGGGCCAGATGGTAAGCCCTCCCGTATCGTAGTTATCTA
CACGACGGGGAGTCAGGCAACTATGGATGAACGAAATAGACAGATCGCTGAGATAGGTGCCTCACTGATTAAGCATTGGT
AACTGTCAGACCAAGTTTACTCATATATACTTTAGATTGATTTAAAACTTCATTTTTAATTTAAAAGGATCTAGGTGAAG
ATCCTTTTTGATAATCTCATGACCAAAATCCCTTAACGTGAGTTTTCGTTCCACTGAGCGTCAGACCCCGTAGAAAAGAT
CAAAGGATCTTCTTGAGATCCTTTTTTTTCTGCGCGTAATCTGCTGCTTGCAAACAAAAAAACCACCGCTACCAGCGGTGG
TTTGTTTGCCGGATCAAGAGCTACCAACTCTTTTTCCGAAGGTAACTGGCTTCAGCAGAGCGCAGATACCAAATACTGTT
CTTCTAGTGTAGCCGTAGTTAGGCCACCACTTCAAGAACTCTGTAGCACCGCCTACATACCTCGCTCTGCTAATCCTGTT
ACCAGTGGCTGCTGCCAGTGGCGATAAGTCGTGTCTTACCGGGTTGGACTCAAGACGATAGTTACCGGATAAGGCGCAGC
GGTCGGGCTGAACGGGGGGTTCGTGCACACAGCCCAGCTTGGAGCGAACGACCTACACCGAACTGAGATACCTACAGCGT
GAGCTATGAGAAAGCGCCACGCTTCCCGAAGGGAGAAAGGCGGACAGGTATCCGGTAAGCGGCAGGGTCGGAACAGGAGA
GCGCACGAGGGAGCTTCCAGGGGGAAACGCCTGGTATCTTTATAGTCCTGTCGGGTTTCGCCACCTCTGACTTGAGCGTC
GATTTTTGTGATGCTCGTCAGGGGGGCGGAGCCTATGGAAAAACGCCAGCAACGCGGCCTTTTTACGGTTCCTGGCCTTT
TGCTGGCCTTTTGCTCA

Features :

| | | |
|---|---|---|
| ColE1 origin | : [6231 : 6859 - CW] | |
| AmpR | : [5420 : 6079 - CW] | |
| Amp prom | : [5152 : 5180 - CW] | |
| AAV2 ITR | : [6 : 135 - CW] | |
| hSyn promoter | : [164 : 633 - CW] | |
| CDS | : [662 : 3004 - CW] | |
| mPSD95 | : [662 : 2824 - CW] | |
| TAP | : [2831 : 3001 - CW] | |
| TEV site | : [2897 : 2917 - CW] | |
| hGH polyA signal | : [3648 : 4128 - CW] | |

AAV2 ITR : [4165 : 4304 - CW]

## 7) SynActive-ChR2XXM-mVenus (7159 bp)

CATGTCCTGCAGGCAGCTGCGCGCTCGCTCGCTCACTGAGGCCGCCCGGGCGTCGGGCGACCTTTGGTCGCCCGGCCTCA
GTGAGCGAGCGAGCGCGCAGAGAGGGAGTGGCCAACTCCATCACTAGGGGTTCCTGCGGCCGCACGCGTGTGTCTAGACT
GCAGACCATGGGCCCTTGACGTCCGGTCCGTTTACTCCCTATCAGTGATAGAGAACGTATGAAGAGTTTACTCCCTATCA
GTGATAGAGAACGTATGCAGACTTTACTCCCTATCAGTGATAGAGAACGTATAAGGAGTTTACTCCCTATCAGTGATAGA
GAACGTATGACCAGTTTACTCCCTATCAGTGATAGAGAACGTATCTACAGTTTACTCCCTATCAGTGATAGAGAACGTAT
ATCCAGTTTACTCCCTATCAGTGATAGAGAACGTATAAGCTTTAGGCGTGTACGGTGGGCGCCTATAAAAGCAGAGCTCG
TTTAGTGAACCGTCAGATCGCCTGGAGCAATTCCACAACACTTTTGTCTTATACCAACTTTCCGTACCACTTCCTACCCT
CGTAAAAGCCTCCGCGGCCCCGAATTCGAGCTCGGTACCCGGGGATCCTCTAGTCAGCTGACGCGTGCCGCCACTAGCAG
TGCTCTGGCGAGTAGTCCTCCCTCAGCCGCAGTCTCTGGGCCTCTTCAGCTTGAGCGGCGGCGAGCCTGCCACACTCGCT
AAGCTCCTCCGGCACCGCGCACTTGCCACTGCCACTGCCGCTTCGCGCCCGCTGCAGCCGCCGGCTCTGAATCCTTCTGG
CTTCCGCCTCAGAGGAGTTCTTAGCCTGTCCCGAACCGTAACCCCGGCGAGCAGACGGAGCTGGACCATCTAGAGCCACC
ATGGATTATGGAGGCGCCCTGAGTGCCGTTGGGCGCGAGCTGCTATTTGTAACGAACCCAGTAGTCGTCAATGGCTCTGT
ACTTGTGCCTGAGGACCAGTGTTACTGCGCGGGCTGGATTGAGTCGCGTGGCACAAACGGTGCCCAAACGGCGTCGAACG
TGCTGCAATGGCTTGCTGCTGGCTTCTCCATCCTACTGCTTATGTTTTACGCCTACCAAACATGGAAGTCAACCTGCGGC
TGGGAGGAGATCTATGTGTGCGCTATCGAGATGGTCAAGGTGATTCTCGAGTTCTTCTTCGAGTTTAAGAACCCGTCCAT
GCTGTATCTAGCCACAGGCCACCGCGTCCAGTGGTTGCGTTACGCCGAGTGGCTTCTCACCTGCCCGGTCATTCTCATTC
ACCTGTCAAACCTGACGGGCTTGTCCAACGACTACAGCAGGCGCACCATGGGTCTGCTTGTGTCTCATATTGGCACAATT
GTGTGGGGCGCCACTTCCGCCATGGCCACCGGATACGTCAAGGTCATCTTCTTCTGCCTGGGTCTGTGTTATGGTGCTAA
CACGTTCTTTCACGCTGCCAAGGCCTACATCGAGGGTTACCACACCGTGCCGAAGGGCCGGTGTCGCCAGGTGGTGACTG
GCATGGCTTGGCTCTTCTTCGTATCATGGGGTATGTTCCCCATCCTGTTCATCCTCGGCCCCGAGGGCTTCGGCGTCCTG
AGCGTGTACGGCTCCACCGTCGGCCACACCATCATTGACCTGATGTCGAAGAACTGCTGGGGTCTGCTCGGCCACTACCT
GCGCGTGCTGATCCACGAGCATATCCTCATCCACGGCGACATTCGCAAGACCACCAAATTGAACATTGGTGGCACTGAGA
TTGAGGTCGAGACGCTGGTGGAGGACGAGGCCGAGGCTGGCGCGGTACCCGCGGCCGCCACCATGGTGAGCAAGGGCGAG
GAGCTGTTCACCGGGGTGGTGCCCATCCTGGTCGAGCTGGACGGCGACGTAAACGGCCACAAGTTCAGCGTGTCCGGCGA
GGGCGAGGGCGATGCCACCTACGGCAAGCTGACCCTGAAGCTGATCTGCACCACCGGCAAGCTGCCCGTGCCCTGGCCCA
CCCTCGTGACCACCCTGGGCTACGGCCTGCAGTGCTTCGCCCGCTACCCCGACCACATGAAGCAGCACGACTTCTTCAAG
TCCGCCATGCCCGAAGGCTACGTCCAGGAGCGCACCATCTTCTTCAAGGACGACGGCAACTACAAGACCCGCGCCGAGGT
GAAGTTCGAGGGCGACACCCTGGTGAACCGCATCGAGCTGAAGGGCATCGACTTCAAGGAGGACGGCAACATCCTGGGGC
ACAAGCTGGAGTACAACTACAACAGCCACAACGTCTATATCACCGCCGACAAGCAGAAGAACGGCATCAAGGCCAACTTC
AAGATCCGCCACAACATCGAGGACGGCGGCGTGCAGCTCGCCGACCACTACCAGCAGAACACCCCCATCGGCGACGGCCC
CGTGCTGCTGCCCGACAACCACTACCTGAGCTACCAGTCCGCCCTGAGCAAAGACCCCAACGAGAAGCGCGATCACATGG
TCCTGCTGGAGTTCGTGACCGCCGCCGGGATCACTCTCGGCATGGACGAGCTGTACAAGGGCGGCGGAGGCGGAGCCGCT
GCTTCAATCGAAAGTGACGTGGCCGCAGCCGAAACCCAGGTGTAATAAACGCGTCAATTCAGGGGCCAGCCCAGGGTCCC
CAGCCTGCCTGCCACACCCAGTCTGTGGCTTTTGTCAACTAGGACTTGATTGAGCTGGGGCTGACACCCAAGGGGATGCC
CTGTCCAGCCAGACACCTTCTCACCCACTGGCCTGACTCACAACTGCCACACAACCATGATTCATGGACATCAAGAAGCC
CCTCTCCCATAGGGCTCCCACCTGCCACCTACCCCTCACCTGTCTGCCCTAGTCCTGGCCCTGTCTCCAGTGGCCTCACC
CTCTACACTCTCAGACCATCACAGAACACCTTTGGCTTCCTCATTCTGCATCAGTGTCCAGGGCCCTTTGGGTAGTCAAG
AAATCAAGTGTCTGAAAGGCAATGAAAAGTAGGCACCAAACCCAAGGGGCATCCCAGGGCAGATGCTAAAGCAGAATCAG
AGATGGCCGAAGGAACCTCTACTTCCGGGGATGCAGCCCGCTCCTACAGACACAGCAGATCCAGCTGGTGCCCTACCTGC
CTCCCAGAGCAACTGGCCAGTCTTGGGCAGCATAGCTCCCCTCTCAGGGTGAGCTGAAGCAGCAGACCTGACGCGCTGGC
GCCTCCTGGCCCCCAGCAGTGATTCATACCAGTGAAGAAAAGCAGACTTCGGCTCCATGACTCAGCCATGCCAGGCGGAG
GGTCCCAGAGGGGCTGAGTCCTCAGCCCCAGCTGAGGCAGCAGCTGGAGTCTTCAGAGCCAGGTGAATGACACCAGGTCT
CAAGCTGCTGAGAAGTCTTTCCGGCCATGTCTGGAAGGGGTACCACCCCAGCACCAGCACCGTCCCCTCCTCTCTTGAAG
CTGCCTGCACAGAGGTTCCAAGACACTTTCAAGGCAGAGAAAATAGGATTACAAAGAGGAGGTGCCTGGCAGAGGGCAGC
ACCCAGCTCAGCCTCAGAGCTGAAGGTGAAGACAAGCCAGCGTGAAACCCCGGGTCTGCCACGAATGCCCGCTCCGCTGG
CCACTCACCAGCTGCCTGCCACAAGCCACTGCAGCTTGAGCAGGGTCTGTGCCCTCTCAGCACAGAGCCCAGTTCGCTGC
GTGGCCTTTGGCCCCCGCCAGAACCTTGCAGGAGCCTTAAGGTTCGGGCCCTAGCCCAGCCTGACCTTACCTGCTGTGCC
CTGCCTGCTGGTCAAGTCCAGTCCCAGGAGACCCCATGCCTTGGCTCCTAGGCTGTTCCAGGCACTTCCCTGACCTGCCG
GGTGATTGCCCAGCTGGAACCTCATCCACACCCCAGCACCAACCACCTCGTGTTGGTAACTGCTCGTGTCTGTAGTCTGA
GTAGGCCATGTTGAGGTTCCTCCATCTGCCTGGTCCATTGGTGTTCTGAGACCAGTTCCACTGCTGTTCTGACAGATCCC
CCACCCTGTGCCCCTGCCAGCCCCCACAGGTTTATTTTTGCACATAAACCATGACCCATACTAATTTGGCTAGCTCTGGG
GACTAGGGAGACCCTGGAGATCTCAAGAGTGTGGCTATCCCCTATTTTCACCAAGCCTTCAATATCCAGCCAGGCCATCT
GCCCACACCATCTTACCTCAAAGACAGACATATATATATATATACATATATATGATTTTGTTAATAAAACTATGAAATTT
AAACTCGAGGTGAAATTTGTGATGCTATTGCTTTATTTGTAACCATCTAGCTTTATTTGTGAAATTTGTGATGCTATTGC
TTTATTTGTAACCATTATAAGCTGCAATAAACAAGTTAACAACAACAATTGCATTCATTTTATGTTTCAGGTTCCGGTCC
GTTGGCCGTGCGGACCGAGCGGCCGCAGGAACCCCTAGTGATGGAGTTGGCCACTCCCTCTCTGCGCGCTCGCTCGCTCA
CTGAGGCCGGGCGACCAAAGGTCGCCCGACGCCCGGGCTTTGCCCGGGCGGCCTCAGTGAGCGAGCGAGCGCGCAGCTGC

CTGCAGGGGCGCCTGATGCGGTATTTTCTCCTTACGCATCTGTGCGGTATTTCACACCGCATACGTCAAAGCAACCATAG
TACGCGCCCTGTAGCGGCGCATTAAGCGCGGCGGGTGTGGTGGTTACGCGCAGCGTGACCGCTACACTTGCCAGCGCCTT
AGCGCCCGCTCCTTTCGCTTTCTTCCCTTCCTTTCTCGCCACGTTCGCCGGCTTTCCCCGTCAAGCTCTAAATCGGGGGC
TCCCTTTAGGGTTCCGATTTAGTGCTTTACGGCACCTCGACCCCAAAAAACTTGATTTGGGTGATGGTTCACGTAGTGGG
CCATCGCCCTGATAGACGGTTTTTCGCCCTTTGACGTTGGAGTCCACGTTCTTTAATAGTGGACTCTTGTTCCAAACTGG
AACAACACTCAACTCTATCTCGGGCTATTCTTTTGATTTATAAGGGATTTTGCCGATTTCGGTCTATTGGTTAAAAAATG
AGCTGATTTAACAAAAATTTAACGCGAATTTTAACAAAATATTAACGTTTACAATTTTATGGTGCACTCTCAGTACAATC
TGCTCTGATGCCGCATAGTTAAGCCAGCCCCGACACCCGCCAACACCCGCTGACGCGCCCTGACGGGCTTGTCTGCTCCC
GGCATCCGCTTACAGACAAGCTGTGACCGTCTCCGGGAGCTGCATGTGTCAGAGGTTTTCACCGTCATCACCGAAACGCG
CGAGACGAAAGGGCCTCGTGATACGCCTATTTTTATAGGTTAATGTCATGATAATAATGGTTTCTTAGACGTCAGGTGGC
ACTTTTCGGGGAAATGTGCGCGGAACCCCTATTTGTTTATTTTTCTAAATACATTCAAATATGTATCCGCTCATGAGACA
ATAACCCTGATAAATGCTTCAATAATATTGAAAAAGGAAGAGTATGAGTATTCAACATTTCCGTGTCGCCCTTATTCCCT
TTTTTGCGGCATTTTGCCTTCCTGTTTTTGCTCACCCAGAAACGCTGGTGAAAGTAAAAGATGCTGAAGATCAGTTGGGT
GCACGAGTGGGTTACATCGAACTGGATCTCAACAGCGGTAAGATCCTTGAGAGTTTTCGCCCCGAAGAACGTTTTCCAAT
GATGAGCACTTTTAAAGTTCTGCTATGTGGCGCGGTATTATCCCGTATTGACGCCGGGCAAGAGCAACTCGGTCGCCGCA
TACACTATTCTCAGAATGACTTGGTTGAGTACTCACCAGTCACAGAAAAGCATCTTACGGATGGCATGACAGTAAGAGAA
TTATGCAGTGCTGCCATAACCATGAGTGATAACACTGCGGCCAACTTACTTCTGACAACGATCGGAGGACCGAAGGAGCT
AACCGCTTTTTTGCACAACATGGGGGATCATGTAACTCGCCTTGATCGTTGGGAACCGGAGCTGAATGAAGCCATACCAA
ACGACGAGCGTGACACCACGATGCCTGTAGCAATGGCAACAACGTTGCGCAAACTATTAACTGGCGAACTACTTACTCTA
GCTTCCCGGCAACAATTAATAGACTGGATGGAGGCGGATAAAGTTGCAGGACCACTTCTGCGCTCGGCCCTTCCGGCTGG
CTGGTTTATTGCTGATAAATCTGGAGCCGGTGAGCGTGGGTCTCGCGGTATCATTGCAGCACTGGGGCCAGATGGTAAGC
CCTCCCGTATCGTAGTTATCTACACGACGGGGAGTCAGGCAACTATGGATGAACGAAATAGACAGATCGCTGAGATAGGT
GCCTCACTGATTAAGCATTGGTAACTGTCAGACCAAGTTTACTCATATATACTTTAGATTGATTTAAAACTTCATTTTTA
ATTTAAAAGGATCTAGGTGAAGATCCTTTTTGATAATCTCATGACCAAAATCCCTTAACGTGAGTTTTCGTTCCACTGAG
CGTCAGACCCCGTAGAAAAGATCAAAGGATCTTCTTGAGATCCTTTTTTTCTGCGCGTAATCTGCTGCTTGCAAACAAAA
AAACCACCGCTACCAGCGGTGGTTTGTTTGCCGGATCAAGAGCTACCAACTCTTTTTCCGAAGGTAACTGGCTTCAGCAG
AGCGCAGATACCAAATACTGTTCTTCTAGTGTAGCCGTAGTTAGGCCACCACTTCAAGAACTCTGTAGCACCGCCTACAT
ACCTCGCTCTGCTAATCCTGTTACCAGTGGCTGCTGCCAGTGGCGATAAGTCGTGTCTTACCGGGTTGGACTCAAGACGA
TAGTTACCGGATAAGGCGCAGCGGTCGGGCTGAACGGGGGGTTCGTGCACACAGCCCAGCTTGGAGCGAACGACCTACAC
CGAACTGAGATACCTACAGCGTGAGCTATGAGAAAGCGCCACGCTTCCCGAAGGGAGAAAGGCGGACAGGTATCCGGTAA
GCGGCAGGGTCGGAACAGGAGAGCGCACGAGGGAGCTTCCAGGGGGAAACGCCTGGTATCTTTATAGTCCTGTCGGGTTT
CGCCACCTCTGACTTGAGCGTCGATTTTTGTGATGCTCGTCAGGGGGGCGGAGCCTATGGAAAAACGCCAGCAACGCGGC
CTTTTTACGGTTCCTGGCCTTTTGCTGGCCTTTTGCTCA

Features :

| | | |
|---|---|---|
| ColE1 origin | : [6493 : 7121 - CW] | |
| AmpR | : [5682 : 6341 - CW] | |
| Amp prom | : [5414 : 5442 - CW] | |
| AAV2 ITR | : [6 : 135 - CW] | |
| TRE3g | : [172 : 632 - CW] | |
| 5' Arc UTR | : [639 : 868 - CW] | |
| CDS | : [881 : 2608 - CW] | |
| ChR2-XXM | : [884 : 1807 - CW] | |
| mVenus | : [1826 : 2539 - CW] | |
| SYNtag | : [2555 : 2608 - CW] | |
| 3' Arc UTR | : [2637 : 4243 - CW] | |
| short pA | : [4250 : 4394 - CW] | |
| AAV2 ITR | : [4427 : 4566 - CW] | |

8) tdTomato filler (6786 bp)

CATGTCCTGCAGGCAGCTGCGCGCTCGCTCGCTCACTGAGGCCGCCCGGGCGTCGGGCGACCTTTGGTCGCCCGGCCTCA
GTGAGCGAGCGAGCGCGCAGAGAGGGAGTGGCCAACTCCATCACTAGGGGTTCCTGCGGCCGCACGCGTGTGTCTAGACT
GCAGAGGGCCCTGCGTATGAGTGCAAGTGGGTTTTAGGACCAGGATGAGGCGGGGTGGGGGTGCCTACCTGACGACCGAC
CCCGACCCACTGGACAAGCACCCAACCCCCATTCCCCAAATTGCGCATCCCCTATCAGAGAGGGGGAGGGGAAACAGGAT
GCGGCGAGGCGCGTGCGCACTGCCAGCTTCAGCACCGCGGACAGTGCCTTCGCCCCCGCCTGGCGGCGCGCGCCACCGCC
GCCTCAGCACTGAAGGCGCGCTGACGTCACTCGCCGGTCCCCCGCAAACTCCCCTTCCCGGCCACCTTGGTCGCGTCCGC
GCCGCCGCCGGCCCAGCCGGACCGCACCACGCGAGGCGCGAGATAGGGGGGCACGGGCGCGACCATCTGCGCTGCGGCGC
CGGCGACTCAGCGCTGCCTCAGTCTGCGGTGGGCAGCGGAGGAGTCGTGTCGTGCCTGAGAGCGCAGTCGAGAAGGTACC
GGATCCGCCACCATGTCTAGACTGGACAAGAGCAAAGTCATAAACGGCGCTCTGGAATTACTCAATGGAGTCGGTATCGA
AGGCCTGACGACAAGGAAACTCGCTCAAAAGCTGGGAGTTGAGCAGCCTACCCTGTACTGGCACGTGAAGAACAAGCGGG
CCCTGCTCGATGCCCTGCCAATCGAGATGCTGGACAGGCATCATACCCACTTCTGCCCCCTGGAAGGCGAGTCATGGCAA
GACTTTCTGCGGAACAACGCCAAGTCATTCCGCTGTGCTCTCCTCTCACATCGCGACGGGGCTAAAGTGCATCTCGGCAC
CCGCCCAACAGAGAAACAGTACGAAACCCTGGAAAATCAGCTCGCGTTCCTGTGTCAGCAAGGCTTCTCCCTGGAGAACG
CACTGTACGCTCTGTCCGCCGTGGGCCACTTTACACTGGGCTGCGTATTGGAGGAACAGGAGCATCAAGTAGCAAAAGAG
GAAAGAGAGACACCTACCACCGATTCTATGCCCCCACTTCTGAGACAAGCAATTGAGCTGTTCGACCGGCAGGGAGCCGA
ACCTGCCTTCCTTTTCGGCCTGGAACTAATCATATGTGGCCTGGAGAAACAGCTAAAGTGCGAAAGCGGCGGGCCGGCCG
ACGCCCTTGACGATTTTGACTTAGACATGCTCCCAGCCGATGCCCTTGACGACTTTGACCTTGATATGCTGCCTGCTGAC
GCTCTTGACGATTTTGACCTTGACATGCTCCCCGGGGGAAGCGGAGCTACTAACTTCAGCCTGCTGAAGCAGGCTGGAGA
CGTGGAGGAGAACCCTGGACCTATGGTGAGCAAGGGCGAGGAGGTCATCAAAGAGTTCATGCGCTTCAAGGTGCGCATGG
AGGGCTCCATGAACGGCCACGAGTTCGAGATCGAGGGCGAGGGCGAGGGCCGCCCCTACGAGGGCACCCAGACCGCCAAG
CTGAAGGTGACCAAGGGCGGCCCCCTGCCCTTCGCCTGGGACATCCTGTCCCCCCAGTTCATGTACGGCTCCAAGGCGTA
CGTGAAGCACCCCGCCGACATCCCCGATTACAAGAAGCTGTCCTTCCCCGAGGGCTTCAAGTGGGAGCGCGTGATGAACT
TCGAGGACGGCGGTCTGGTGACCGTGACCCAGGACTCCTCCCTGCAGGACGGCACGCTGATCTACAAGGTGAAGATGCGC
GGCACCAACTTCCCCCCCGACGGCCCCGTAATGCAGAAGAAGACCATGGGCTGGGAGGCCTCCACCGAGCGCCTGTACCC
CCGCGACGGCGTGCTGAAGGGCGAGATCCACCAGGCCCTGAAGCTGAAGGACGGCGGCCACTACCTGGTGGAGTTCAAGA
CCATCTACATGGCCAAGAAGCCCGTGCAACTGCCCGGCTACTACTACGTGGACACCAAGCTGGACATCACCTCCCACAAC
GAGGACTACACCATCGTGGAACAGTACGAGCGCTCCGAGGGCCGCCACCACCTGTTCCTGGGGCATGGCACCGGCAGCAC
CGGCAGCGGCAGCTCCGGCACCGCCTCCTCCGAGGACAACAACATGGCCGTCATCAAAGAGTTCATGCGCTTCAAGGTGC
GCATGGAGGGCTCCATGAACGGCCACGAGTTCGAGATCGAGGGCGAGGGCGAGGGCCGCCCCTACGAGGGCACCCAGACC
GCCAAGCTGAAGGTGACCAAGGGCGGCCCCCTGCCCTTCGCCTGGGACATCCTGTCCCCCCAGTTCATGTACGGCTCCAA
GGCGTACGTGAAGCACCCCGCCGACATCCCCGATTACAAGAAGCTGTCCTTCCCCGAGGGCTTCAAGTGGGAGCGCGTGA
TGAACTTCGAGGACGGCGGTCTGGTGACCGTGACCCAGGACTCCTCCCTGCAGGACGGCACGCTGATCTACAAGGTGAAG
ATGCGCGGCACCAACTTCCCCCCCGACGGCCCCGTAATGCAGAAGAAGACCATGGGCTGGGAGGCCTCCACCGAGCGCCT
GTACCCCCGCGACGGCGTGCTGAAGGGCGAGATCCACCAGGCCCTGAAGCTGAAGGACGGCGGCCACTACCTGGTGGAGT
TCAAGACCATCTACATGGCCAAGAAGCCCGTGCAACTGCCCGGCTACTACTACGTGGACACCAAGCTGGACATCACCTCC
CACAACGAGGACTACACCATCGTGGAACAGTACGAGCGCTCCGAGGGCCGCCACCACCTGTTCCTGTACGGCATGGACGA
GCTGTACAAGTAGGAATTCGATATCAAGCTTATCGATAATCAACCTCTGGATTACAAAATTTGTGAAAGATTGACTGGTA
TTCTTAACTATGTTGCTCCTTTTACGCTATGTGGATACGCTGCTTTAATGCCTTTGTATCATGCTATTGCTTCCCGTATG
GCTTTCATTTTCTCCTCCTTGTATAAATCCTGGTTGCTGTCTCTTTATGAGGAGTTGTGGCCCGTTGTCAGGCAACGTGG
CGTGGTGTGCACTGTGTTTGCTGACGCAACCCCCACTGGTTGGGGCATTGCCACCACCTGTCAGCTCCTTTCCGGGACTT
TCGCTTTCCCCCTCCCTATTGCCACGGCGGAACTCATCGCCGCCTGCCTTGCCCGCTGCTGGACAGGGGCTCGGCTGTTG
GGCACTGACAATTCCGTGGTGTTGTCGGGGAAATCATCGTCCTTTCCTTGGCTGCTCGCCTATGTTGCCACCTGGATTCT
GCGCGGGACGTCCTTCTGCTACGTCCCTTCGGCCCTCAATCCAGCGGACCTTCCTTCCCGCGGCCTGCTGCCGGCTCTGC
GGCCTCTTCCGCGTCTTCGCCTTCGCCCTCAGACGAGTCGGATCTCCCTTTGGGCCGCCTCCCCGCATCGATACCGAGCG
CTGCTCGAGAGATCTACGGGTGGCATCCCTGTGACCCCTCCCCAGTGCCTCTCCTGGCCCTGGAAGTTGCCACTCCAGTG
CCCACCAGCCTTGTCCTAATAAAATTAAGTTGCATCATTTTGTCTGACTAGGTGTCCTTCTATAATATTATGGGGTGGAG
GGGGGTGGTATGGAGCAAGGGGCAAGTTGGGAAGACAACCTGTAGGGCCTGCGGGGTCTATTGGGAACCAAGCTGGAGTG
CAGTGGCACAATCTTGGCTCACTGCAATCTCCGCCTCCTGGGTTCAAGCGATTCTCCTGCCTCAGCCTCCCGAGTTGTTG
GGATTCCAGGCATGCATGACCAGGCTCAGCTAATTTTTGTTTTTTTGGTAGAGACGGGGTTTCACCATATTGGCCAGGCT
GGTCTCCAACTCCTAATCTCAGGTGATCTACCCACCTTGGCCTCCCAAATTGCTGGGATTACAGGCGTGAACCACTGCTC
CCTTCCCTGTCCTTCTGATTTTGTAGGTAACCACGTGCGGACCGAGCGGCCGCAGGAACCCCTAGTGATGGAGTTGGCCA
CTCCCTCTCTGCGCGCTCGCTCGCTCACTGAGGCCGGGCGACCAAAGGTCGCCCGACGCCCGGGCTTTGCCCGGGCGGCC
TCAGTGAGCGAGCGAGCGCGCAGCTGCCTGCAGGGGCGCCTGATGCGGTATTTTCTCCTTACGCATCTGTGCGGTATTTC
ACACCGCATACGTCAAAGCAACCATAGTACGCGCCCTGTAGCGGCGCATTAAGCGCGGCGGGTGTGGTGGTTACGCGCAG
CGTGACCGCTACACTTGCCAGCGCCTTAGCGCCCGCTCCTTTCGCTTTCTTCCCTTCCTTTCTCGCCACGTTCGCCGGCT
TTCCCCGTCAAGCTCTAAATCGGGGGCTCCCTTTAGGGTTCCGATTTAGTGCTTTACGGCACCTCGACCCCAAAAAACTT
GATTTGGGTGATGGTTCACGTAGTGGGCCATCGCCCTGATAGACGGTTTTTCGCCCTTTGACGTTGGAGTCCACGTTCTT
TAATAGTGGACTCTTGTTCCAAACTGGAACAACACTCAACTCTATCTCGGGCTATTCTTTTGATTTATAAGGGATTTTGC
CGATTTCGGTCTATTGGTTAAAAAATGAGCTGATTTAACAAAAATTTAACGCGAATTTTAACAAAATATTAACGTTTACA
ATTTTATGGTGCACTCTCAGTACAATCTGCTCTGATGCCGCATAGTTAAGCCAGCCCCGACACCCGCCAACACCCGCTGA

CGCGCCCTGACGGGCTTGTCTGCTCCCGGCATCCGCTTACAGACAAGCTGTGACCGTCTCCGGGAGCTGCATGTGTCAGA
GGTTTTCACCGTCATCACCGAAACGCGCGAGACGAAAGGGCCTCGTGATACGCCTATTTTTATAGGTTAATGTCATGATA
ATAATGGTTTCTTAGACGTCAGGTGGCACTTTTCGGGGAAATGTGCGCGGAACCCCTATTTGTTTATTTTTCTAAATACA
TTCAAATATGTATCCGCTCATGAGACAATAACCCTGATAAATGCTTCAATAATATTGAAAAAGGAAGAGTATGAGTATTC
AACATTTCCGTGTCGCCCTTATTCCCTTTTTTGCGGCATTTTGCCTTCCTGTTTTTGCTCACCCAGAAACGCTGGTGAAA
GTAAAAGATGCTGAAGATCAGTTGGGTGCACGAGTGGGTTACATCGAACTGGATCTCAACAGCGGTAAGATCCTTGAGAG
TTTTCGCCCCGAAGAACGTTTTCCAATGATGAGCACTTTTAAAGTTCTGCTATGTGGCGCGGTATTATCCCGTATTGACG
CCGGGCAAGAGCAACTCGGTCGCCGCATACACTATTCTCAGAATGACTTGGTTGAGTACTCACCAGTCACAGAAAAGCAT
CTTACGGATGGCATGACAGTAAGAGAATTATGCAGTGCTGCCATAACCATGAGTGATAACACTGCGGCCAACTTACTTCT
GACAACGATCGGAGGACCGAAGGAGCTAACCGCTTTTTTGCACAACATGGGGGATCATGTAACTCGCCTTGATCGTTGGG
AACCGGAGCTGAATGAAGCCATACCAAACGACGAGCGTGACACCACGATGCCTGTAGCAATGGCAACAACGTTGCGCAAA
CTATTAACTGGCGAACTACTTACTCTAGCTTCCCGGCAACAATTAATAGACTGGATGGAGGCGGATAAAGTTGCAGGACC
ACTTCTGCGCTCGGCCCTTCCGGCTGGCTGGTTTATTGCTGATAAATCTGGAGCCGGTGAGCGTGGGTCTCGCGGTATCA
TTGCAGCACTGGGGCCAGATGGTAAGCCCTCCCGTATCGTAGTTATCTACACGACGGGGAGTCAGGCAACTATGGATGAA
CGAAATAGACAGATCGCTGAGATAGGTGCCTCACTGATTAAGCATTGGTAACTGTCAGACCAAGTTTACTCATATATACT
TTAGATTGATTTAAAACTTCATTTTTAATTTAAAAGGATCTAGGTGAAGATCCTTTTTGATAATCTCATGACCAAAATCC
CTTAACGTGAGTTTTCGTTCCACTGAGCGTCAGACCCCGTAGAAAAGATCAAAGGATCTTCTTGAGATCCTTTTTTTCTG
CGCGTAATCTGCTGCTTGCAAACAAAAAAACCACCGCTACCAGCGGTGGTTTGTTTGCCGGATCAAGAGCTACCAACTCT
TTTTCCGAAGGTAACTGGCTTCAGCAGAGCGCAGATACCAAATACTGTTCTTCTAGTGTAGCCGTAGTTAGGCCACCACT
TCAAGAACTCTGTAGCACCGCCTACATACCTCGCTCTGCTAATCCTGTTACCAGTGGCTGCTGCCAGTGGCGATAAGTCG
TGTCTTACCGGGTTGGACTCAAGACGATAGTTACCGGATAAGGCGCAGCGGTCGGGCTGAACGGGGGGTTCGTGCACACA
GCCCAGCTTGGAGCGAACGACCTACACCGAACTGAGATACCTACAGCGTGAGCTATGAGAAAGCGCCACGCTTCCCGAAG
GGAGAAAGGCGGACAGGTATCCGGTAAGCGGCAGGGTCGGAACAGGAGAGCGCACGAGGGAGCTTCCAGGGGGAAACGCC
TGGTATCTTTATAGTCCTGTCGGGTTTCGCCACCTCTGACTTGAGCGTCGATTTTTGTGATGCTCGTCAGGGGGGCGGAG
CCTATGGAAAAACGCCAGCAACGCGGCCTTTTTACGGTTCCTGGCCTTTTGCTGGCCTTTTGCTCA

Features :

| | | |
|---|---|---|
| ColE1 origin | : [6120 : 6748 - CW] | |
| AmpR | : [5309 : 5968 - CW] | |
| Amp prom | : [5041 : 5069 - CW] | |
| AAV2 ITR | : [6 : 135 - CW] | |
| hSyn | : [164 : 633 - CW] | |
| CDS | : [653 : 2893 - CW] | |
| rtTA | : [653 : 1396 - CW] | |
| P2A | : [1406 : 1462 - CW] | |
| tdTomato | : [1463 : 2890 - CW] | |
| WPRE | : [2919 : 3506 - CW] | |
| hGH polyA signal | : [3537 : 4017 - CW] | |
| AAV2 ITR | : [4054 : 4193 - CW] | |

## 9) mTurquoise2-filler (6075 bp)

CATGTCCTGCAGGCAGCTGCGCGCTCGCTCGCTCACTGAGGCCGCCCGGGCGTCGGGCGACCTTTGGTCGCCCGGCCTCA
GTGAGCGAGCGAGCGCGCAGAGAGGGAGTGGCCAACTCCATCACTAGGGGTTCCTGCGGCCGCACGCGTGTGTCTAGACT
GCAGAGGGCCCTGCGTATGAGTGCAAGTGGGTTTTAGGACCAGGATGAGGCGGGGTGGGGGTGCCTACCTGACGACCGAC
CCCGACCCACTGGACAAGCACCCAACCCCCATTCCCCAAATTGCGCATCCCCTATCAGAGAGGGGGAGGGGAAACAGGAT
GCGGCGAGGCGCGTGCGCACTGCCAGCTTCAGCACCGCGGACAGTGCCTTCGCCCCCGCCTGGCGGCGCGCGCCACCGCC
GCCTCAGCACTGAAGGCGCGCTGACGTCACTCGCCGGTCCCCCGCAAACTCCCCTTCCCGGCCACCTTGGTCGCGTCCGC
GCCGCCGCCGGCCCAGCCGGACCGCACCACGCGAGGCGCGAGATAGGGGGGCACGGGCGCGACCATCTGCGCTGCGGCGC

CGGCGACTCAGCGCTGCCTCAGTCTGCGGTGGGCAGCGGAGGAGTCGTGTCGTGCCTGAGAGCGCAGTCGAGAAGGTACC
GGATCCGCCACCATGTCTAGACTGGACAAGAGCAAAGTCATAAACGGCGCTCTGGAATTACTCAATGGAGTCGGTATCGA
AGGCCTGACGACAAGGAAACTCGCTCAAAAGCTGGGAGTTGAGCAGCCTACCCTGTACTGGCACGTGAAGAACAAGCGGG
CCCTGCTCGATGCCCTGCCAATCGAGATGCTGGACAGGCATCATACCCACTTCTGCCCCCTGGAAGGCGAGTCATGGCAA
GACTTTCTGCGGAACAACGCCAAGTCATTCCGCTGTGCTCTCCTCTCACATCGCGACGGGGCTAAAGTGCATCTCGGCAC
CCGCCCAACAGAGAAACAGTACGAAACCCTGGAAAATCAGCTCGCGTTCCTGTGTCAGCAAGGCTTCTCCCTGGAGAACG
CACTGTACGCTCTGTCCGCCGTGGGCCACTTTACACTGGGCTGCGTATTGGAGGAACAGGAGCATCAAGTAGCAAAAGAG
GAAAGAGAGACACCTACCACCGATTCTATGCCCCCACTTCTGAGACAAGCAATTGAGCTGTTCGACCGGCAGGGAGCCGA
ACCTGCCTTCCTTTTCGGCCTGGAACTAATCATATGTGGCCTGGAGAAACAGCTAAAGTGCGAAAGCGGCGGGCCGGCCG
ACGCCCTTGACGATTTTGACTTAGACATGCTCCCAGCCGATGCCCTTGACGACTTTGACCTTGATATGCTGCCTGCTGAC
GCTCTTGACGATTTTGACCTTGACATGCTCCCCGGGGGAAGCGGAGCTACTAACTTCAGCCTGCTGAAGCAGGCTGGAGA
CGTGGAGGAGAACCCTGGACCTATGGTGAGCAAGGGCGAGGAGCTGTTCACCGGGGTGGTGCCCATCCTGGTCGAGCTGG
ACGGCGACGTAAACGGCCACAAGTTCAGCGTGTCCGGCGAGGGCGAGGGCGATGCCACCTACGGCAAGCTGACCCTGAAG
TTCATCTGCACCACCGGCAAGCTGCCCGTGCCCTGGCCCACCCTCGTGACCACCCTGTCCTGGGGCGTGCAGTGCTTCGC
CCGCTACCCCGACCACATGAAGCAGCACGACTTCTTCAAGTCCGCCATGCCCGAAGGCTACGTCCAGGAGCGCACCATCT
TCTTCAAGGACGACGGCAACTACAAGACCCGCGCCGAGGTGAAGTTCGAGGGCGACACCCTGGTGAACCGCATCGAGCTG
AAGGGCATCGACTTCAAGGAGGACGGCAACATCCTGGGGCACAAGCTGGAGTACAACTACTTTAGCGACAACGTCTATAT
CACCGCCGACAAGCAGAAGAACGGCATCAAGGCCAACTTCAAGATCCGCCACAACATCGAGGACGGCGGCGTGCAGCTCG
CCGACCACTACCAGCAGAACACCCCCATCGGCGACGGCCCCGTGCTGCTGCCCGACAACCACTACCTGAGCACCCAGTCC
AAGCTGAGCAAAGACCCCAACGAGAAGCGCGATCACATGGTCCTGCTGGAGTTCGTGACCGCCGCCGGGATCACTCTCGG
CATGGACGAGCTGTACAAGTAGGAATTCGATATCAAGCTTATCGATAATCAACCTCTGGATTACAAAATTTGTGAAAGAT
TGACTGGTATTCTTAACTATGTTGCTCCTTTTACGCTATGTGGATACGCTGCTTTAATGCCTTTGTATCATGCTATTGCT
TCCCGTATGGCTTTCATTTTCTCCTCCTTGTATAAATCCTGGTTGCTGTCTCTTTATGAGGAGTTGTGGCCCGTTGTCAG
GCAACGTGGCGTGGTGTGCACTGTGTTTGCTGACGCAACCCCCACTGGTTGGGGCATTGCCACCACCTGTCAGCTCCTTT
CCGGGACTTTCGCTTTCCCCCTCCCTATTGCCACGGCGGAACTCATCGCCGCCTGCCTTGCCCGCTGCTGGACAGGGGCT
CGGCTGTTGGGCACTGACAATTCCGTGGTGTTGTCGGGGAAATCATCGTCCTTTCCTTGGCTGCTCGCCTATGTTGCCAC
CTGGATTCTGCGCGGGACGTCCTTCTGCTACGTCCCTTCGGCCCTCAATCCAGCGGACCTTCCTTCCCGCGGCCTGCTGC
CGGCTCTGCGGCCTCTTCCGCGTCTTCGCCTTCGCCCTCAGACGAGTCGGATCTCCCTTTGGGCCGCCTCCCCGCATCGA
TACCGAGCGCTGCTCGAGAGATCTACGGGTGGCATCCCTGTGACCCCTCCCCAGTGCCTCTCCTGGCCCTGGAAGTTGCC
ACTCCAGTGCCCACCAGCCTTGTCCTAATAAAATTAAGTTGCATCATTTTGTCTGACTAGGTGTCCTTCTATAATATTAT
GGGGTGGAGGGGGGTGGTATGGAGCAAGGGGCAAGTTGGGAAGACAACCTGTAGGGCCTGCGGGGTCTATTGGGAACCAA
GCTGGAGTGCAGTGGCACAATCTTGGCTCACTGCAATCTCCGCCTCCTGGGTTCAAGCGATTCTCCTGCCTCAGCCTCCC
GAGTTGTTGGGATTCCAGGCATGCATGACCAGGCTCAGCTAATTTTTGTTTTTTTGGTAGAGACGGGGTTTCACCATATT
GGCCAGGCTGGTCTCCAACTCCTAATCTCAGGTGATCTACCCACCTTGGCCTCCCAAATTGCTGGGATTACAGGCGTGAA
CCACTGCTCCCTTCCCTGTCCTTCTGATTTTGTAGGTAACCACGTGCGGACCGAGCGGCCGCAGGAACCCCTAGTGATGG
AGTTGGCCACTCCCTCTCTGCGCGCTCGCTCGCTCACTGAGGCCGGGCGACCAAAGGTCGCCCGACGCCCGGGCTTTGCC
CGGGCGGCCTCAGTGAGCGAGCGAGCGCGCAGCTGCCTGCAGGGGCGCCTGATGCGGTATTTTCTCCTTACGCATCTGTG
CGGTATTTCACACCGCATACGTCAAAGCAACCATAGTACGCGCCCTGTAGCGGCGCATTAAGCGCGGCGGGTGTGGTGGT
TACGCGCAGCGTGACCGCTACACTTGCCAGCGCCTTAGCGCCCGCTCCTTTCGCTTTCTTCCCTTCCTTTCTCGCCACGT
TCGCCGGCTTTCCCCGTCAAGCTCTAAATCGGGGGCTCCCTTTAGGGTTCCGATTTAGTGCTTTACGGCACCTCGACCCC
AAAAAACTTGATTTGGGTGATGGTTCACGTAGTGGGCCATCGCCCTGATAGACGGTTTTTCGCCCTTTGACGTTGGAGTC
CACGTTCTTTAATAGTGGACTCTTGTTCCAAACTGGAACAACACTCAACTCTATCTCGGGCTATTCTTTTGATTTATAAG
GGATTTTGCCGATTTCGGTCTATTGGTTAAAAAATGAGCTGATTTAACAAAAATTTAACGCGAATTTTAACAAAATATTA
ACGTTTACAATTTTATGGTGCACTCTCAGTACAATCTGCTCTGATGCCGCATAGTTAAGCCAGCCCCGACACCCGCCAAC
ACCCGCTGACGCGCCCTGACGGGCTTGTCTGCTCCCGGCATCCGCTTACAGACAAGCTGTGACCGTCTCCGGGAGCTGCA
TGTGTCAGAGGTTTTCACCGTCATCACCGAAACGCGCGAGACGAAAGGGCCTCGTGATACGCCTATTTTTATAGGTTAAT
GTCATGATAATAATGGTTTCTTAGACGTCAGGTGGCACTTTTCGGGGAAATGTGCGCGGAACCCCTATTTGTTTATTTTT
CTAAATACATTCAAATATGTATCCGCTCATGAGACAATAACCCTGATAAATGCTTCAATAATATTGAAAAAGGAAGAGTA
TGAGTATTCAACATTTCCGTGTCGCCCTTATTCCCTTTTTTGCGGCATTTTGCCTTCCTGTTTTTGCTCACCCAGAAACG
CTGGTGAAAGTAAAAGATGCTGAAGATCAGTTGGGTGCACGAGTGGGTTACATCGAACTGGATCTCAACAGCGGTAAGAT
CCTTGAGAGTTTTCGCCCCGAAGAACGTTTTCCAATGATGAGCACTTTTAAAGTTCTGCTATGTGGCGCGGTATTATCCC
GTATTGACGCCGGGCAAGAGCAACTCGGTCGCCGCATACACTATTCTCAGAATGACTTGGTTGAGTACTCACCAGTCACA
GAAAAGCATCTTACGGATGGCATGACAGTAAGAGAATTATGCAGTGCTGCCATAACCATGAGTGATAACACTGCGGCCAA
CTTACTTCTGACAACGATCGGAGGACCGAAGGAGCTAACCGCTTTTTTGCACAACATGGGGGATCATGTAACTCGCCTTG
ATCGTTGGGAACCGGAGCTGAATGAAGCCATACCAAACGACGAGCGTGACACCACGATGCCTGTAGCAATGGCAACAACG
TTGCGCAAACTATTAACTGGCGAACTACTTACTCTAGCTTCCCGGCAACAATTAATAGACTGGATGGAGGCGGATAAAGT
TGCAGGACCACTTCTGCGCTCGGCCCTTCCGGCTGGCTGGTTTATTGCTGATAAATCTGGAGCCGGTGAGCGTGGGTCTC
GCGGTATCATTGCAGCACTGGGGCCAGATGGTAAGCCCTCCCGTATCGTAGTTATCTACACGACGGGGAGTCAGGCAACT
ATGGATGAACGAAATAGACAGATCGCTGAGATAGGTGCCTCACTGATTAAGCATTGGTAACTGTCAGACCAAGTTTACTC
ATATATACTTTAGATTGATTTAAAACTTCATTTTTAATTTAAAAGGATCTAGGTGAAGATCCTTTTTGATAATCTCATGA
CCAAAATCCCTTAACGTGAGTTTTCGTTCCACTGAGCGTCAGACCCCGTAGAAAAGATCAAAGGATCTTCTTGAGATCCT
TTTTTTCTGCGCGTAATCTGCTGCTTGCAAACAAAAAAACCACCGCTACCAGCGGTGGTTTGTTTGCCGGATCAAGAGCT
ACCAACTCTTTTTCCGAAGGTAACTGGCTTCAGCAGAGCGCAGATACCAAATACTGTTCTTCTAGTGTAGCCGTAGTTAG

GCCACCACTTCAAGAACTCTGTAGCACCGCCTACATACCTCGCTCTGCTAATCCTGTTACCAGTGGCTGCTGCCAGTGGC
GATAAGTCGTGTCTTACCGGGTTGGACTCAAGACGATAGTTACCGGATAAGGCGCAGCGGTCGGGCTGAACGGGGGGTTC
GTGCACACAGCCCAGCTTGGAGCGAACGACCTACACCGAACTGAGATACCTACAGCGTGAGCTATGAGAAAGCGCCACGC
TTCCCGAAGGGAGAAAGGCGGACAGGTATCCGGTAAGCGGCAGGGTCGGAACAGGAGAGCGCACGAGGGAGCTTCCAGGG
GGAAACGCCTGGTATCTTTATAGTCCTGTCGGGTTTCGCCACCTCTGACTTGAGCGTCGATTTTTGTGATGCTCGTCAGG
GGGGCGGAGCCTATGGAAAAACGCCAGCAACGCGGCCTTTTTACGGTTCCTGGCCTTTTGCTGGCCTTTTGCTCA

Features :

| | | |
|---|---|---|
| ColE1 origin | : | [5409 : 6037 - CW] |
| AmpR | : | [4598 : 5257 - CW] |
| Amp prom | : | [4330 : 4358 - CW] |
| AAV2 ITR | : | [6 : 135 - CW] |
| hSyn | : | [164 : 633 - CW] |
| CDS | : | [653 : 2182 - CW] |
| rtTA | : | [653 : 1396 - CW] |
| P2A | : | [1406 : 1462 - CW] |
| mTurquoise2 | : | [1463 : 2179 - CW] |
| WPRE | : | [2208 : 2795 - CW] |
| hGH polyA signal | : | [2826 : 3306 - CW] |
| AAV2 ITR | : | [3343 : 3482 - CW] |

**ACKNOWLEDGEMENT**

I take this opportunity to thank Antonino Cattaneo for his valuable, inspiring, and encouraging guidance and for providing me with scientific freedom that enabled me to work enthusiastically and molded my scientific development. I thank all members of the SynActive lab for discussion and support throughout this Ph.D. thesis work – especially Marco Mainardi for guiding and providing feedback with the daily experiments, and teaching techniques including immunoprecipitation, and western blotting. I sincerely thank Francesca Chiara Latini for helping with the in vivo part of the SynActive-eGRASP project, by performing stereotaxic surgery, behavior assays, histology, and helping with confocal imaging and analysis. I wish to thank Mariachiara Di Caprio for helping with primary neuronal cultures and optogenetics, and Andrea Faraone for performing stereotaxic surgery and behavior assays for the proteomics project. Thanks to Mariantonietta Calvello and Vania Liverani for the technical help with molecular biology. I would like to thank Francesco Gobbo, Laura Marchetti, Simona Capsoni, Giovanna Testa, Paola Pacifico, Keagen Dunville, Manuella Martins, and all the people that supported me during these years.

I thank collaborators of the proteomics project, especially Lorena Zentilin (ICGEB, Trieste) for AAV preparation, Alessandro Ori (Franz-Lipmann Institut, Jena, Germany) for Mass Spectrometry, Ivan Arisi (EBRI, Rome) for proteomic analysis and Silvia Marinelli (EBRI, Rome).

I thank my family and friends for showing faith and providing confidence during my entire Ph.D. journey.